Nasal mucus: friend or foe?

The effect of mucus on mucosal barrier dysfunction in chronic rhinosinusitis

THE UNIVERSITY of ADELAIDE

STEPHEN SHIH-TENG KAO

MBBS MClinSc

Submitted for the degree of Doctor of Philosophy

Adelaide Medical School, Discipline of Surgical Specialities

Faculty of Health and Medical Sciences, The University of Adelaide

August 2020

Dedicated to my amazing parents

Wen-I and Lin Huei-Jong

He who knows all the answers has not

been asked all the questions

- Confucius

TABLE OF CONTENTS

ABSTRACT

Chronic rhinosinusitis (CRS) is a complex and heterogenous disease characterised by nasal obstruction, facial pressure, rhinorrhoea, postnasal drip and reduction in smell. The pathophysiology of CRS is multifaceted with an interplay between host, environmental and microbial factors. Numerous hypothesise have been proposed to elucidate this complicated disease process, however, the jury is still out. Recently, the dysfunction in the mucosal barrier with associated pathogen invasion is described as a potential basis for the development of CRS. Studies have identified the overactivation of inflammatory cells with superfluous secretion of proinflammatory proteases and cytokines associated with the chronic inflammatory environment observed in CRS. Therefore, it is vital to understand the interactions between the host immunity with the mucosal barrier.

Nasal mucus overproduction is a hallmark symptom of CRS and thus it is paramount to investigate its interaction with the mucosal barrier function in both healthy and CRS patients. Classically, nasal mucus from CRS patients are more viscous and contain increased levels of inflammatory cytokines. Previous research has found *Pseudomonas aeruginosa* elastase, an exoprotein, present in CRS nasal mucus associated with increased barrier dysfunction and worse symptom-scores. Furthermore, neutrophil infiltration is observed in CRS mucosa secondary to the persistent inflammation and bacterial activation. The collateral damage to host tissues secondary to the release of neutrophil-associated proteases against infections must be elucidated.

Advances in mass spectrometry techniques allow for detailed analysis of differentially expressed proteins in nasal mucus. A systemic review of the nasal proteome will be conducted to determine the current progress and deficiencies within the literature. Based on these findings,

the direct comparison of healthy and CRS mucus proteomes will be performed. By analysing the different proteins and cellular processes present in nasal mucus may assist in understanding the downstream manifestations of CRS.

This thesis examines the interaction of nasal mucus with the nasal mucosal barrier function. Secondly, to ascertain the effects of neutrophil serine proteases on the mucosa barrier function. Lastly, to investigate and understand the differing mucus composition between healthy and CRS patients. Ultimately, through understanding the pathophysiology and various endotypes of CRS, we aim to direct future research to develop treatment regimens for numerous patients.

DECLARATION

I certify that this work contains no material which has been accepted for the award of any other degree or diploma in my name, in any university or other tertiary institution and, to the best of my knowledge and belief, contains no material previously published or written by another person, except where due reference has been made in the text. In addition, I certify that no part of this work will, in the future, be used in a submission in my name, for any other degree or diploma in any university or other tertiary institution without the prior approval of the University of Adelaide and where applicable, any partner institution responsible for the joint-award of this degree.

I acknowledge that copyright of published works contained within this thesis resides with the copyright holder(s) of those works.

I also give permission for the digital version of my thesis to be made available on the web, via the University's digital research repository, the Library Search and also through web search engines, unless permission has been granted by the University to restrict access for a period of time.

I acknowledge the support I have received for my research through the provision of an Australian Government Research Training Program Scholarship.

Stephen Shih-Teng Kao

ACKNOWLEDGEMENTS

I would like to thank and acknowledge the “big three” for taking me on as their PhD student. Professor Peter-John Wormald, I admire the passion you have for research and teaching, with successes evidenced by the long line of surgeon-scientists before me and the ever-growing ENT research family. Thank you for your teachings in both the research and clinical setting. Associate Professor Alkis Psaltis, thank you for your kind ongoing support throughout my PhD. You have been a great mentor with your positive attitude inspiring me to work harder. Associate Professor Sarah Vreugde, thank you for your enthusiastic guidance and direction in improving my understanding of research, and progressing my scientific progress. All of you have pushed me to become a better student, researcher and surgeon by providing me with the knowledge and skills to last me a lifetime.

I would like to thank Mahnaz Ramezanpour for being such a supportive supervisor, teaching me everything I needed to know to function independently in the lab. I hope I have made you proud as your first PhD student! Thank you to the ENT scientists Catherine Bennett, Clare Cooksley and Shari Javadiyan for your teachings, assistance and all-round banter in the lab. Your patience and hard work keep the lab running at peak efficiency.

I would like to thank Professor Tim Chataway, Alex Colella and Nusha Chegeni for your guidance in the proteomic component of my project. From day one in your lab, you have been able to show me the complex world of mass spectrometry and proteomics. Prof Chataway, thank you for your patience in troubleshooting my various proteomic issues and providing me with guidance in running my experiments and reviewing my manuscripts.

Thank you to the Garnett Passe and Rodney Williams Memorial Foundation, Bertha Sudholz Foundation and Adelaide University for providing me with a scholarship to pursue my goals in pursuing this PhD.

Thank you to the previous and current surgeon-scientists Rachel Goggin, Saththish Paramasivan, Jae Murphy, Giri Krishnan, Michael Gouzos and Anna Megow for your support, laughs and friendship during my PhD. A special thanks to Ahmed Bassiouni for your outstanding help with all the statistical analysis. Thank you to the ENT secretary, Annette Kreutner, for your help processing my paperwork and ensuring everything runs smoothly in the department.

I would like to thank my sisters Jennifer, Alice, Rebecca and Vanessa for your support over the years. It is fantastic having an additional four mothers to take care for me. All of you have been my idol and inspired me to work harder and to be a better person. Doris Tang, thank you for being my best friend for the past 10 years. Your support through thick and thin over this time will never be forgotten.

Lastly, I would like to thank my parents, Dr Wen-I and Lin Huei-Jong Kao, for your unconditional love and support. I appreciate the sacrifices you have made and everything you have done throughout my life to get me to where I am today. I doctor doctor now!

PUBLICATIONS ARISING FROM THESIS

1. **Kao SS**, Ramezanpour M, Bassiouni A, Finnie J, Wormald PJ, Vreugde S, Psaltis AJ. Barrier disruptive effects of mucus isolated from chronic rhinosinusitis patients. Allergy 2019.

2. **Kao SS**, Ramezanpour M, Bassiouni A, Wormald PJ, Psaltis AJ, Vreugde S. The effect of neutrophil serine proteases on human nasal epithelial cell barrier function. Int Forum Allergy Rhinol 2019.

3. **Kao SS**, Bassiouni A, Ramezanpour M, Chegeni N, Colella AD, Chataway TK, Wormald PJ, Vreugde S, Psaltis AJ, Scoping review of chronic rhinosinusitis. Rhinology 2020.

4. **Kao SS**, Bassiouni A, Ramezanpour M, Chegeni N, Colella AD, Chataway TK, Wormald PJ, Vreugde S, Psaltis AJ, Proteomic analysis of nasal mucus samples of healthy patients and patients with chronic rhinosinusitis. J Allergy Clin Immunol 2020.

PRESENTATIONS ARISING FROM THESIS

1. Nasal mucus. Friend or foe? The Queen Elizabeth Hospital Research Day Expo 2018. Adelaide, Australia.
2. Barrier disruptive effects of mucus isolated from chronic rhinosinusitis patients. American Rhinologic Society (ARS) Annual Meeting, September 2019. New Orleans USA.
3. Barrier disruptive effects of mucus isolated from chronic rhinosinusitis patients. Australian New Zealand Rhinologic Society (ANZRS) Annual Meeting, September 2019. Melbourne, Australia.
4. Nasal mucus: Friend or foe? The effect of barrier dysfunction on mucosal inflammation in chronic rhinosinusitis. Florey Research Symposium, September 2019. Adelaide, Australia.
5. Barrier disruptive effects of mucus isolated from chronic rhinosinusitis patients. The Queen Elizabeth Research Day Expo, October 2019. Adelaide, Australia.
6. Barrier disruptive effects of mucus isolated from chronic rhinosinusitis patients. Ronald Gristwood ENT Registrar Meeting, October 2019. Adelaide, Australia.

ABBREVIATIONS

1D	One-dimensional
1-DE	One-dimensional gel electrophoresis
2D	Two-dimensional
2-DE	Two-dimensional gel electrophoresis
2DLC	Two-dimensional liquid chromatography
3D	Three-dimensional
A1M	Alpha-1-microglobulin
AC	Alternating current
ADIP	Afadin DIL domain-interacting protein
AERD	Aspirin exacerbated respiratory disease
AFRS	Acute fungal rhinosinusitis
AJ	Adherens Junction
ALI	Air-liquid-interface
AMBP	Alpha-1-microglobulin/bikunin
ANCA	Anti-neutrophil cytoplasmic autoantibodies
aPKC	Atypical protein kinase C
APO	Apolipoprotein
ASL	Airway surface liquid
ATP	Adenosine triphosphate
BAFF	B cell activating factor
BCR	B cell receptors
CAPG	Macrophage capping protein
CBF	Ciliary beat frequency
CF	Cystic fibrosis
CFTR	Cystic fibrosis transmembrane conductance regulator
CG	Cathepsin G
CID	Collision-induced dissociation
COX	Cyclooxygenase
CP110	Centriolar coiled-coil protein of 110 kDa
CRS	Chronic rhinosinusitis
CRSsNP	Chronic rhinosinusitis without nasal polyposis
CRSwNP	Chronic rhinosinusitis with nasal polyposis
CT	Computed tomography
DBMT1	Deleted in brain malignant tumours 1
DC	Direct current
DHC	Dynein heavy chain
DIFC	Desmosome-intermediate filament complex
DIL	Dilute domain
DNA	Deoxyribonucleic acid
DPPI	Dipeptidyl peptidase I
Dsc	Desmocollins
Dsg	Desmoglein
DTD	Glycine rich desmoglein terminal domain
ELISA	Enzyme-linked immunosorbent assay
emPAI	Exponentially modified abundance index

EMT	Epithelial-mesenchymal transition
EPLIN	Epithelial protein list in neoplasm
ESI	Electrospray ionisation
FOXJ1	Forkhead box protein J1
FOXP3	Forkhead box protein 3
FT-ICR	Fourier transform ion cyclotron resonance
GJ	Gap junction
GSEA	Gene set enrichment analysis
GUK	Guanylate kinase
H2O2	Hydrogen Peroxide
HLA	Human leukocyte antigen
HMWK	High-molecular-weight kininogen
HNEC	Human nasal epithelial cells
IDA	Inner dynein arm
IEC	Ion exchange chromatography
Ig	Immunoglobin
IL	Interleukin
ILC2	Type-2 innate lymphoid cells
INF	Interferon
IPL	Intracellular proline-rich linker
JNK	c-Jun N-terminal kinase
KNG1	Kininogen-1
LC	Liquid chromatography
LDH	Lactate dehydrogenase
LMWK	Low-molecular-weight kininogen
LPO	Lactoperoxidase
LPO/H2O2	Lactoperoxidase system
LPS	Lipopolysaccharide
LSR	Lipolysis-stimulated lipoprotein receptor
LT	Leukotriene
m/z	Mass to charge ratio
MAGI	Membrane-associated guanylate kinase with inverted domain structure
MAGUK	Membrane-associated guanylate kinase family
MAL	Myelin and lymphocyte protein
MALDI	Matrix-assisted laser desorption/ionisation
MALT	Mucosal associated lymphoid organs
MARVEL	MAR and related proteins for vesicle trafficking and membrane link
MCC	Mucociliary clearance
MS	Mass spectrometry
MS/MS	Tandem mass spectrometry
MUC5AC	Mucin 5AC
MUPP1	Multi-PDZ domain protein 1
NADPH	Nicotinamide adenine dinucleotide phosphate
N-DRC	Nexin-dynein regulatory complex
NE	Neutrophil elastase
NET	Neutrophil extracellular traps
NLF	Nasal lavage fluid
NO	Nitric oxide
NSPs	Neutrophil serine proteases
ODA	Outer dynein arm
PAMPs	Pathogen-associated molecular patterns

PAR-3	Partitioning-defective protein 3
PAR-6	Partitioning-defective protein 6
PATJ	Pals1-associated tight junction protein
PBS	Phosphate buffered saline
PC1/3	Proconvertase-1
PCL	Periciliary layer
PDGF	Platelet-derived growth factor
PE	Pseudomonas aeruginosa elastase
PG	Prostaglandin
PGI2	Prostacyclin
PI3	Elafin
PIR	Polymeric immunoglobulin
PKP	Plakophilin
PLUNC	Palate, lung, nasal epithelium clone
PMF	Peptide mass fingerprinting
PR3	Proteinase 3
PRR	Pattern recognition receptors
PSMA1	Proteasome subunit alpha type-1
PSMB2	Proteasome subunit beta type-2
RF	Radiofrequency
RFX	Regulatory factor X
RNA	Ribonucleic acid
RNH1	Ribonuclease inhibitor
ROS	Reactive oxygen species
RP-HPLC	Reversed-phase high-pressure liquid chromatography
RPSA	40S ribosome protein SA
RUD	Variable number of repeat unit domain
S100A7	Psoriasin
SAGE	Serial analysis of gene expression
SDS	Sodium dodecyl sulphate
SEC	Size exclusion chromatography
SEM	Standard error of the mean
SH3	Src homology 3
SLO	Secondary lymphoid organ
SP	Surfactant protein
spp.	Species
T2R	Bitter taste receptor
TER	Transepithelial electrical resistance
TGF	Transforming growth factor
TJ	Tight junction
TLO	Tertiary lymphoid organ
TLR	Toll-like receptors
TNF	Tissue necrosis factor
TOF	Time-of-flight
TPM3	Tropomyosin alpha-3 chains
Treg	Regulatory T cells
TSLP	Thymic stromal lymphopoietin
TxA2	Thromboxane
ZO	Zonula occludens

LIST OF TABLES

SUPPLEMENTARY TABLES

LIST OF FIGURES

SUPPLEMENTARY FIGURES

CHAPTER 1: CHRONIC RHINOSINUSITIS

DEFINITION

Chronic rhinosinusitis (CRS) is a clinical syndrome characterised by persisting symptomatic mucosal inflammation within the nasal cavity and paranasal sinuses. In adults, CRS is defined as greater than two or more of the following symptoms for greater than 12 weeks in duration: nasal blockage, congestion, rhinorrhoea, facial pain or alteration in smell.[1]

Nasal endoscopic examination is a vital component in the assessment and management of CRS patients (Figure 1.1A). Invariably, the sinonasal mucosa becomes erythematous and inflamed with variable amounts of secretions, including mucus and pus. Some patients will exhibit space occupying nasal polyps which commonly lead to nasal obstruction or reduced sense of smell. Polyps are pale, oedematous and pedunculated inflammatory outgrowths of sinonasal mucosa (Figure 1.1B). Commonly, they are bilateral and originate from the middle meatus projecting into the nasal cavity.[2] The Lund-Kennedy endoscopic score is a commonly utilised tool by clinicians and researchers to quantify the severity of sinus disease.[3] Each nostril is scored separately. The five parameters are scored from 0 to 2 and comprise of polyps, oedema, scarring, discharge and crusting.

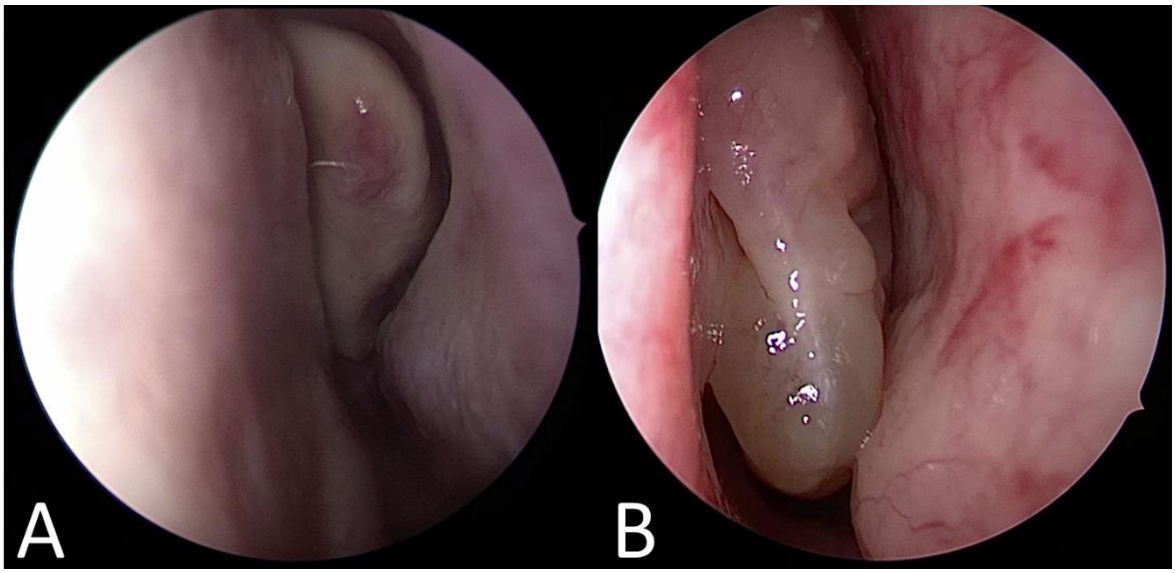

Figure 1.1. Rigid nasoendoscopic view of the nasal cavity.

(A) Healthy patient with healthy nasal mucosa **(B)** CRS patient with erythematous mucosa and nasal polyp.

Computed tomography (CT) scan is an important adjunct in the assessment of CRS patients. It provides clinicians with additional information regarding disease severity and bony anatomy required for surgical planning. Anatomical variability detected on radiological imaging will allow surgeons to identify patients with unfavourable anatomy that may place them at higher risk of disease recurrence or complications. The Lund-Mackay CT Score is a commonly employed standardised scoring system to quantify the severity of radiological disease.[4] Each sinus is given a score of 0 (No abnormality), 1 (Partial opacification) or 2 (Complete opacification) and the osteomeatal complex is given 0 (Not obstructed) or 2 (Obstructed). Below are CT sinus scans from a healthy and CRS patient (Figure 1.2).

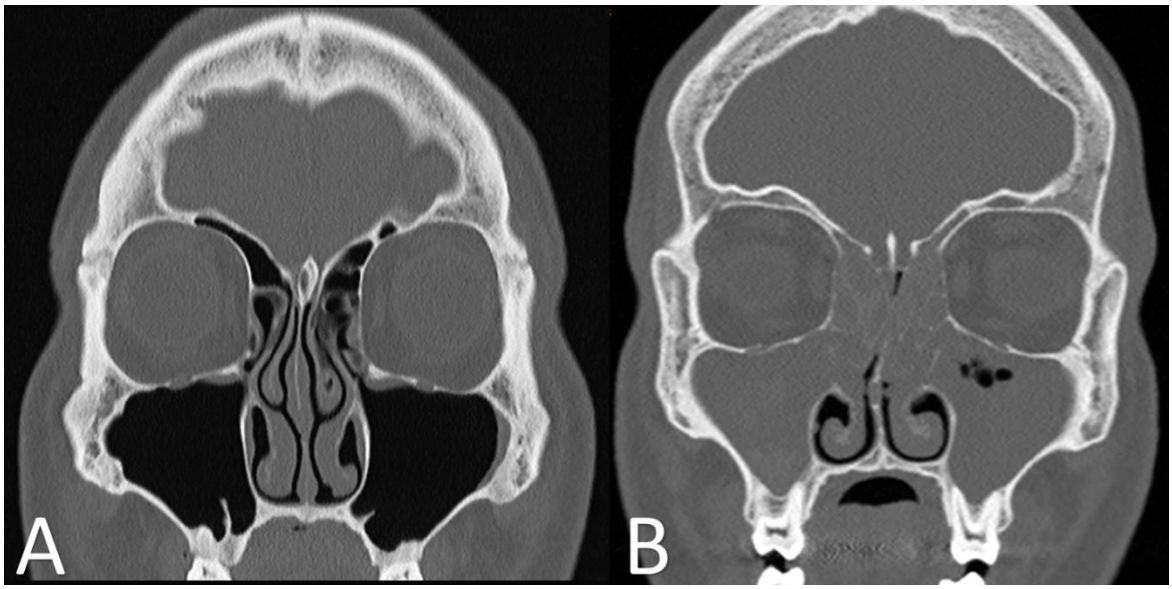

Figure 1.2. CT Sinuses (Coronal view).

(A) *Healthy patient with clear sinuses.* **(B)** *CRS patient with opacification within the maxillary and ethmoid sinuses.*

CLASSIFICATION

Phenotypically, CRS is classified into two subtypes: chronic rhinosinusitis with nasal polys (CRSwNP) or without polyps (CRSsNP). This distinction is made through endoscopic visualisation of nasal polyps present within the sinonasal cavity.[1] This is the commonly utilised classification tool by clinicians and researchers within the literature. This classification system is limited as it does not sufficiently encompass the pathogenesis of CRS and its course. Furthermore, the classification becomes ambiguous once CRSwNP patients return for revision surgery and no polyps are identified. Thus, the evolving literature has aimed to formulate new classification systems to better define CRS.

There have been attempts at reclassifying CRS according to histopathological parameters. The term "endotypes" was coined to group CRS into biological subtypes based on their inflammatory profiles or pathophysiological mechanisms.[5] The goal of the endotypes was to

better understand the clinical course of the disease with improvements in treatment regimes. Research into CRS endotyping is growing with various classifications described in the literature.[6] For instance, CRSwNP patients with high levels of IL-5 and IgE antibodies to *Staphylococcal* antigens were associated with comorbid asthma.[7] Furthermore, the inflammatory profiles of CRS nasal mucus is described as another potential endotyping tool.[8]

Allergic fungal rhinosinusitis (AFRS) has been described as an immunologically distinct subset of CRS.[9] It is characterised by fungal growth, commonly *Aspergillus* or *Alternaria*, with associated eosinophilia and thick mucin. Bent and Kuhn in 1994 proposed this type of CRS secondary to a Type I hypersensitivity reaction.[10] Patients with AFRS secreted Th2 cytokines in response to fungal antigens with fungal specific IgE in the eosinophilic mucin and mucosa.[11-13] This process is further described in the fungal hypothesis section.

Aspirin-exacerbated respiratory disease (AERD) in conjunction with CRS is a particularly severe form characterised by nasal polyposis, aspirin hypersensitivity and asthma.[14] Approximately 15% of CRS patients have AERD.[15] The pathogenesis remains unclear; however, dysregulation of the arachidonic acid metabolism has been implicated. Patients have elevated inflammatory mediators, such as cysteinyl leukotrienes, and reduced inflammatory suppressors, such as prostaglandin E_2.[16-18] Patients with AERD have a significant quality of life and financial detriment.[19] This is described further under the eicosanoid hypothesis section.

Due to the heterogenous nature of CRS, there is not one classification system that is capable of covering the whole disease process. The phenotypical classification, CRSsNP and CRSwNP, is commonly employed due to the simple and practical application clinically. However, its use in prognostication is limited. Thus, further research is required to better understand the disease

pathogenesis to devise a more insightful classification system capable of accurate prognostication. Developing an increased understanding of CRS endotypes will ultimately guide improved medical and surgical management options for these patients.

EPIDEMIOLOGY

There is geographical variation in the incidence of CRS, however, it has been estimated to be the second most prevalent chronic condition.[1] The national self-reported health survey conducted by the Australian Bureau of Statistics in 2017-2018 demonstrated an estimated two million Australians, or 8.4%, are affected with CRS.[20] It is estimated to affect up to 12.5% of the population in the United States.[21] The Global Allergy and Asthma European Network (GA^2LEN) found 10.9% of adults in Europe were affected by CRS.[22] More men suffer from CRSwNP compared to women, however, more women have AERD than men.[23] Notably, women have more severe disease on radiological imaging than males and are more likely to be taking corticosteroids at the time of surgery.[23] Overall, the prevalence is speculative as diagnostic guidelines are not always utilised. The diagnosis is commonly made by primary care physicians through symptoms of nasal congestion or facial pain. As most primary care physicians do not have the training and equipment to perform nasal endoscopy, this leads to the over diagnosis of CRS.[24, 25]

The chronic recurrent symptoms associated with CRS create a significant burden on the healthcare system. In Australia, CRS is one of the most common primary care presentations occurring 1.4 in every 100 general practice appointments.[26] Studies have shown CRS to have a greater impact on social functioning than other chronic diseases such as heart failure, angina or back pain.[27] The estimated annual cost of CRS in the Unites States is $8.6 billion, consisting of emergency department presentations, specialist clinic reviews and medications.[28] The indirect

cost of CRS-related losses in work productivity is estimated to be over $20 billion per year.[29] Up to 33% of patients with CRS require multiple revision surgeries due relapsing symptoms secondary to polyp recurrence or adhesions.[1, 30] The chronic relapsing and remitting nature of CRS has significant impacts on the quality of life of many sufferers with a significant cost to the healthcare system globally.

PATHOGENESIS

The pathogenesis of CRS is a complex and multifactorial process which remains under much debate. Historically, CRS was believed to be secondary to undertreated acute rhinosinusitis (CRSsNP) or severe atopy (CRSwNP). However, as our understanding of CRS has improved, there have been a number of hypothesise suggested. The fungal hypothesis was the first to be considered as the inciting cause for CRS. Bacterial involvement through the superantigen and biofilm hypothesis have been considered. The dysbiosis of the sinonasal microbiome have been investigated in recent times. The impairment in the eicosanoid pathway has been considered due to the association with CRSwNP and aspirin intolerance. Finally, the dysfunction of the host immune response and barrier disruption theories have recently been proposed.[1] These hypothesise are described in detail below.

FUNGAL HYPOTHESIS

Airborne fungal elements were initially hypothesised to be a cause for CRS by investigators in the Mayo clinic.[31, 32] Fungal microorganisms were identified in both CRS and healthy sinonasal cavities, however, hyperactivity of peripheral blood mononuclear cells to *Alternaria* antigens was only present in CRS patients.[33, 34] This absent response in healthy patients was proposed to reflect the immunological sensitisation to fungal antigens. Increased cytokine release with induction of Th2 responses were observed following exposure to *Aspergillus* and *Alternaria*.[35, 36] Additional studies demonstrated eosinophil migration and degranulation following exposure

to CRS mucus.[37, 38] It was hypothesised, *Alternaria* and possibly other fungi, were presented to sensitised T cells triggering cytokine release with the activation and migration of eosinophils to the mucosal surface. The degranulation of the activated eosinophils against these fungi as an aberrant host defence response then lead to collateral tissue damage manifesting as symptoms of CRS. Follow up studies demonstrated the clustering of eosinophils within CRS mucus with associated release of cytotoxic major basic protein and deposition on the epithelium. It was estimated the levels of major basic protein far exceeded the amount required to cause epithelial injury, thus predisposing CRS patients to secondary bacterial infections.[39]

Despite these original findings and interest in *Alternaria* as the aetiologic factor in CRS, there has been a shift away from fungal hypothesis due to new findings in the literature. The sensitisation of peripheral blood mononuclear cells to fungal antigens has not been able to be replicated, indicating a non-universal response compared to the original study.[36, 40] Furthermore, antifungal agents have been used in double-blind, placebo-controlled trials with no evidence of disease improvement in CRS.[41] Although not the primary aetiologic factor in CRS, the degree of fungal colonisation is regarded as an important disease modifier.

BACTERIAL-BASED HYPOTHESIS

Historical studies have suggested the important role of bacteria, particularly *Staphylococcus aureus*, in CRS. *Staphylococcus aureus* is capable of both extracellular and intracellular infections, residing within epithelial cells and macrophages of CRS patients. The superantigen and biofilm hypothesises have been proposed in the pathogenesis of CRS.

The superantigen theory suggests superantigenic exotoxins (Enterotoxin A and B) secreted by *Staphylococcus aureus* augment non-specific, polyclonal activation of T cells.[42] These superantigens bind to T cell receptors outside the human leukocyte antigen (HLA) class II

antigen presentation receptors and antigen-binding groove.[43, 44] This bypassing of normal antigen presentation and recognition leads to polyclonal T lymphocyte proliferation, triggering a cascade of immunologic events leading to a massive release of cytokines and inflammatory cell migration.[45] Additional events include polyclonal B cell responses resulting in local polyclonal IgE responses and eosinophilic inflammation in polyp tissue. Studies have found higher percentages of CRSwNP patients having *Staphylococcus aureus* within their tissues with superantigens identified in 55-73% of CRSwNP mucus samples.[43, 46] It has been found *Staphylococcal* superantigen B has a potent synergistic response with fungal infections in eosinophilic polyps, demonstrating a clinically severe endotype.[36] As the superantigen effect is not present in all patients, it has been deemed not a causative role in CRS. Thus, similar to the fungal hypothesis, bacterial superantigens are viewed as disease modifiers rather than primary aetiologic agents.

Bacterial biofilms have been implicated as a predictor of disease severity and recalcitrance to treatment paradigms. These biofilms are irreversibly adherent to sinonasal mucosa and composed of bacteria encapsulated in a protective matrix of polysaccharides, nucleic acids and proteins. Bacteria contained within these biofilms have a dramatically reduced metabolic rate further protecting them from the host's immune system and antibiotics. Studies have demonstrated the culmination of these protective features contribute to a 10 to 1000-fold decrease in antibiotic susceptibility compared to free-floating planktonic bacteria.[47] Furthermore, bacteria within biofilms are capable of releasing planktonic bacteria and exotoxins, potentially contributing to the persisiting inflammation in CRS. Several species of bacteria are capable of biofilm production, including *Staphylococcus aureus, Pseudomonas aeruginosa, Streptococcus pneumoniae, Moraxella catarrhalis and Haemophilus influenza. Staphylococcus aureus* biofilms with superantigen production is thought to enhance the Th2

response commonly observed in recalcitrant CRS.[48] However, other studies have identified sinonasal mucosa with biofilms inducing a Th1 response. Thus, further studies are required to understand factors contributing to the potential switch from a Th1 to Th2 response in CRS.[49]

Numerous studies have investigated the properties of bacterial biofilms and prognosis of CRS. Biofilms were associated with more severe sinus disease evidenced by higher CT and nasoendoscopy scores.[50, 51] Furthermore, the presence of biofilm postoperatively was associated with worse nasoendoscopy scores, subjective symptoms scores and more outpatient visits.[52] Reduced lactoferrin, an antimicrobial protein, has been found in bacterial biofilm mucosa.[53] However, it remains unclear if this is secondary to reduced production by the innate immune system or due to bacterial biofilm colonisation. Furthermore, the presence of surface *Staphylococcus aureus* biofilm was associated with intracellular *Staphylococcus aureus* infections. Patients with both biofilms and intracellular infections were also more likely to have re-infections compared to only the presence of biofilms alone.[54] There is vast evidence demonstrating the importance bacterial biofilms as a disease severity predictor in CRS.

Pseudomonas aeruginosa is an opportunistic Gram-negative bacterium originating from the family *Pseudomonadaceae*. It commonly infects patients with immunosuppression, cystic fibrosis, chronic non-healing wounds and CRS. *P. aeruginosa* has several extracellular and cell-associated virulence factors such as proteases, exotoxins and lipopolysaccharides that enable it to evade the immune system.[55] This is evidenced by the release of *P. aeruginosa* elastase (PE), resembling neutrophil elastase, leading to reduced inflammatory cytokine production in vivo and consequent host defence evasion.[56] Nomura et al demonstrated transiently disrupted epithelial barrier evidenced by down regulation of transmembrane tight junction proteins and protease-activated receptor-2 expression following PE exposure.[55] Further studies support these

findings with reduction in TER and paracellular permeability following PE exposure, in addition to higher Lund-Mackay CT scores of CRS patients with *P. aeruginosa* positive cultures.[57] These findings implicate PE an important virulence factor in patients were severe and recalcitrant CRS.

Overall, it is apparent bacteria play a pivotal role in the disease course of CRS. Bacteria are considered important disease modifiers as secondary bacterial infections or recalcitrant disease are common causes for morbidity in CRS patients. More studies are required to understand factors in play that contribute to complex host-bacterium interaction to ultimately develop targeted therapies for these patients.

EICOSANOID PATHWAY HYPOTHESIS

Eicosanoids are signalling molecules involved in the arachidonic acid metabolic pathway.[58, 59] Dysfunctions in this pathway are associated with inflammation observed in both aspirin-tolerant and intolerant CRSwNP.[60] Eicosanoids of particular interest include leukotrienes (LT), prostaglandins (PGD_2, PGE_2, PGF_2), prostacyclin (PGI_2) and thromboxane (TxA2).[61-64] All these eicosanoids have proinflammatory effects, except PGE_2 which is anti-inflammatory.

Leukotrienes are formed from the lipoxygenase pathway, giving rise to leukotriene A4 (LTA4) precursor. Further enzymic activity results in the production of LTB4, LTC4, LTD4 and LTE4, where the latter three are classified as cysteinyl leukotrienes. These cysteinyl leukotrienes require leukotriene C4 synthase (LTC4 synthase) for activation, where polymorphisms have been associated with CRSwNP.[65] Studies have found elevated levels of cysteinyl leukotrienes and LTC4 synthase in eosinophilic polyps and aspirin sensitive polyps.[66, 67] Activated platelets have been linked to the stimulation of AERD through the formation of circulating leukocyte

aggregates and recruitment of platelet-adherent leukocytes to extravascular tissue.[68] These elevated levels of platelet-adherent leukocytes induce LTC4 synthase expression in cysteinyl leukotriene-mediated CRS.

Cyclooxygenase enzymes (COX-1, COX-2) are required for the generation of prostaglandins, prostacyclin and thromboxane. COX-1 is produced constantly as rest, whereas COX-2 is inducible and upregulated with tissue inflammation. The binding of PGD_2 to prostanoid receptors results in a proinflammatory response, consisting of eosinophil degranulation, chemotaxis and Th2 lymphocyte migration.[69-72] Alternatively, PGE_2 triggers an anti-inflammatory effect with the inhibition of leukotriene production.[17] Increased levels of PGD_2 synthase and PGD_2 with reduction in PGE_2 synthase and PGE_2 were found in CRSwNP.[67, 73, 74] Furthermore, studies have found superantigens suppressing the PGE_2 pathway, leading to increased proinflammatory mediator production.[75, 76]

Disturbances in the eicosanoid pathway can indeed lead to the proinflammatory environment present in CRS. However, more studies are required to understand the associations with aspirin tolerant and intolerant CRSwNP populations.

MICROBIOME HYPOTHESIS

The microbiome hypothesis proposed a balance of native microbial flora within the sinonasal cavity with the host immune system. An imbalance in the system induced by a precipitating event, such as an infection or antibiotic resistance, induces a dysbiosis of the sinonasal microbiome. This hypothesis follows on from studies of the gastrointestinal tract and skin which have identified externally induced changes to the microbiome mediating chronic inflammation through microbial dysbiosis.[77] The commensal microorganisms maintain

homeostasis through secretion of antimicrobial proteins and lipids interfering with pathogen proliferation. [78, 79] The study of the sinonasal microbiome has rapidly evolved over recent years, made possible through examination of culture independent 16S rRNA gene molecular techniques.[80]

The total amount of bacteria in sinonasal cavities of healthy and CRS patients are similar, commonly consisting of *Staphylococcus*, *Corynebacterium* and *Propionibacterium*. Studies have found pathogenic organisms to be low in abundance or transient in healthy sinuses. Low concentrations of *Staphylococcus aureus* in healthy sinuses induced an anti-inflammatory response through the release of IL-10. Alternatively, high concentrations of *Staphylococcus aureus* caused a reduction in IL-10 leading to a proinflammatory response.[81] *Propionibacterium acnes* present in healthy nasal mucosa produced bacteriocin, an antimicrobial and antifungal compound capable of modulating the immune response against pathogenic microorganisms.[82] A meta-analysis found no significant difference in composition of bacteria between healthy and CRS patients, however, CRS patients had reduced microbial diversity with increased bacterial load.[83, 84]

Molecular studies have identified the mycobiome of sinus mucosa, consisting of *Cryptococcus neoformans*, *Aspergillus spp* and *Malassezia spp* in CRS patients.[85, 86] Reduced levels of *Malassezia* was present in healthy sinus mucosa samples.[87] The virome of the nasal cavity remains an evolving field due to laboratory challenges. DNA, RNA viruses and bacteriophages have been detected in healthy adults with varying abundances in CRS.[88] A recent study demonstrated worse CT and endoscopic scores in virus positive CRSsNP patients. Main viruses identified across all cohorts were *rhinovirus* and *coronavirus*, with increased *influenza* in the CRS group.[89] Viruses are capable of impairing the immune system, reducing mucociliary

clearance and tight junction expression.[89] There is potentially a synergistic action between bacteria, fungi and viruses in the pathogenesis of CRS.[90] Further research is required to investigate the relationship between these microorganisms and the pathogenesis of CRS. Advances in laboratory techniques will enable further insights into the sinonasal microbiome to direct management in CRS.

IMPAIRED INNATE IMMUNE RESPONSE

The mucosal immune system is capable of protecting the host from environmental and pathogen-induced injury, where the innate immune system is the first line. The complement system is a vital aspect of the innate immune system, particularly against inhaled pathogens within the airway. Studies have demonstrated the upregulation of complement components in tissues of CRS patients and the deposition of complement factors along the basement membrane in nasal polyp tissue.[91, 92] Furthermore, C5a has been found to induce production of oncostatin M, a potent cytokine, known to disrupt epithelial barrier integrity in CRSwNP.[93] The presence of these pathways in CRS mucus indicates a link between complement and barrier dysfunction associated with the sinonasal inflammatory response.

Neutrophils play a paramount role in the innate immunity against invading pathogens in addition to being a mediator of the inflammatory response. In acute inflammation, they are the first cells to leave the vasculature and migrate to sites of inflammation.[94] Neutrophil serine proteases (NSPs) are key enzymes in this process, consisting of neutrophil elastase (NE), cathepsin C (CG) and proteinase 3 (PR3). Contained within neutrophil azurophil granules, these NSPs are central to the nonoxidative pathway of intracellular and extracellular pathogen destruction. Furthermore, the secretion and accumulation of NSPs has been implicated in the pathogenesis of numerous chronic inflammatory airways conditions. The superfluous

secretions of the NSPs in these conditions is associated with chronic inflammation with consequent barrier dysfunction.[94] Therefore, it is vital to understand the balances between the physiological functions of NSPs and the potential cause of collateral damage to the host tissues.

All three NSPs belong to the chymotrypsin superfamily of serine proteases, evolving from a common ancestor via gene duplication.[94] Gene expression for NE, CG and PR3 are found in granulocytes, monocytes and mast cells.[95] The NSPs are synthesised as inactive prepro-protein with a signal peptide and amino-terminal prodipeptide. They are regulated at both the transcriptional and post-transcriptional levels. At the transcriptional level, it occurs during granulocyte development, and post-transcriptionally it occurs prior to storage in its proteolytically active form within neutrophil azurophilic granules.[94] The activation of NSPs are induced by the cleavage of the amino-terminal peptide and dipeptide by a signal peptidase and dipeptidyl peptidase I (DPPI).[94, 96] Azurophil granules are the primary storage site for all NSPs, however, NE is also present in the nuclear envelope and PR3 has been identified in secretory vesicles.[97, 98] Neutrophil exposure to cytokines (TNF-α), chemoattractants (PAF, IL-8) or bacterial lipopolysaccharides at inflammatory sites leads to activation and subsequent translocation of intracytoplasmic granules.[94]

All NSPs are implicated in various biological functions including pathogenic killing of microbes and regulation of inflammatory processes.[96] Intracellular killing of phagocytosed bacteria is mediated by activated NSPs contained within phagolysosomes. Furthermore, myeloperoxidase and the generation of reactive oxygen species (ROS) by the NADPH oxidase complex facilitates this process.[99] Extracellularly, neutrophil extracellular traps (NET) are secreted by neutrophils and are composed of chromatin bound to positively charged molecules, such as NSPs and histones. This web-like structure of DNA serves as a physical barrier, killing

extracellular pathogens and preventing dissemination. Additionally, NET-associated NSPs kill extracellular pathogens through degradation of bacterial virulence factors.[100] The positive surface charges on the NSPs facilitate bacterial membrane binding with protein synthesis inhibition and subsequent membrane depolarisation and disruption.[101] Studies have demonstrated these antimicrobial properties of NSPs with effective killing of both Gram-positive and Gram-negative bacteria.[94] Furthermore, murine models deficient in NE and CG have increased susceptibility to both Gram-positive and -negative bacterial infections.[102] These findings demonstrate the pivotal role NSPs have in the innate immunity against the ongoing battle against invading pathogens.

Extracellular secretion of NSPs during acute inflammation have various implications to the local environment. The activated NSPs are secreted extracellularly in two forms: membrane bound on the extracellular surface of the neutrophil or in soluble form. Both forms are capable of regulating the function of cytokines, growth factors, cell surface receptors, apoptotic and adhesion molecules.[96] Proinflammatory cytokines TNF-α and IL-1β are synthesised as inactive membrane-bound pro-forms.[103, 104] Studies have demonstrated mixed findings with cleavage of pro-TNF-α and pro-IL-1β by NE and PR3 with consequent activation.[94] Furthermore, IL-8 is a vital chemokine in neutrophil migration and degranulation during acute inflammation. It is able to be activated from its pro-form by PR3.[94, 105] The regulation of NE, CG and PR3 activity is closely monitored in the extracellular space to avoid destruction of connective tissue proteins. Serpins are a superfamily of protease inhibitors vital in the regulation of proteolytic events, with deficiencies contributing to emphysema and angioedema.[106] Therefore, it is vital to understand the dynamic interactions between NSPs and protease regulators in the pathogenesis of chronic inflammatory diseases.

The inappropriate activation and proliferation of inflammatory cells, and subsequent secretion of proteases play a role in the cellular changes observed in chronic inflammation. Physiologically, inflammation is a protective mechanism against injury or infection, characterised by endothelial activation, leukocyte chemotaxis and activation, and increased vascular permeability.[94] Dysregulation of this process evidenced by the accumulation of neutrophils with secondary tissue injury from the release of cytotoxic products such as ROS and proteases. These histological findings are present in a range of chronic lung diseases including cystic fibrosis, chronic obstructive airways disease and acute respiratory distress syndrome.[94] The exposure to NE is associated with degradation of the airway epithelial host defence protein short palate, lung and nasal epithelial clone 1 (PLUNC1). An increased bacterial load was associated with this reduction in PLUNC1.[107] Furthermore, NE is capable of cleaving E-cadherin, further disrupting cell-cell adhesion and impairing barrier function.[108] Future studies are required to focus on the effect and roles of NSPs in the inflammatory regulation of CRS.

Studies have proposed type-2 innate lymphoid cells (ILC2) responsible in the initiation of the type-2 inflammatory response observed in CRS.[109] These innate effector cells secrete IL-5 and IL-33 upon activation by epithelial-derived cytokines, thymic stromal lymphopoietin (TSLP) and IL-33.[110] Elevated levels of ILC2 has been found in eosinophilic nasal polyps.[111] Although eosinophilia is a hallmark feature of Western nasal polyposis, numerous innate inflammatory cells are also elevated in CRSwNP compared to healthy patients.[112, 113] These innate effector cells are capable to releasing inflammatory mediators and toxic granules leading to chronic type-2 inflammation with collateral damage of host tissue.

The secretions of innate antimicrobials by epithelial cells, innate effector cells and glands are vital to the innate immune system. These antimicrobial proteins are secreted tonically at rest, increasing upon stimulation of pattern recognition receptors (PRR). Toll-like receptors (TLR), a family of transmembrane PRR, stimulate the direct transcription and translation of mucins and antimicrobial peptides, regulating the antimicrobial secretions by the sinonasal mucosa.[114, 115] Changes in expression of TLR have been demonstrated in CRS and thus may play a role in its pathogenesis.[116] Reduced IL-8 production is observed following TLR-2 ligand stimulation in CRS patients, which may account for the impaired immunity.[117] The distribution and expression of these antimicrobial proteins vary throughout the sinonasal cavity, likely a reflection of differences in the microbiome.[118, 119] Further differences in expression between healthy and CRS patients has been documented.

Lactoferrin is an important antimicrobial protein capable of mediating microbial destruction through various pathways. [115] Firstly, lactoferrin chelates and sequesters iron required for bacterial and fungal metabolism. Iron has been implicated in the destruction of the mucosal barrier through the catalysation of mucin degradation by bacteria.[120] Secondly, lactoferrin binds to pathogen-associated molecular patterns (PAMPs), including lipopolysaccharide (LPS), thus inhibiting its proinflammatory receptors. Additionally, Gram-negative bacterial permeabilisation occurs following the binding of lactoferrin to LPS.[121] Lastly, lactoferrin is capable of binding to viruses and host virus receptors, inhibiting the invasion of DNA and RNA viruses.[122] Studies have found reduced levels of lactoferrin in CRSsNP and CRSwNP patients.[53, 123]

The innate immune system antimicrobial enzymes of importance in CRS include lysozyme and peroxidases. Lysozyme is a cationic protein secreted by submucosal glands capable of

disrupting the peptidoglycan wall of bacteria. This is particularly effective against Gram-positive bacteria commonly encountered in the upper respiratory tract.[115, 124] Additional cofactors are required for Gram-negative bacterial killing, to allow the lysozyme access to the peptidoglycan layer.[125] Cofactors include lactoferrin, antibody complement complexes or ascorbic acid, which are capable of disrupting the outer membrane.[126-128] The reduction in submucosal glands in CRSwNP may account for the variability in results whether lysozymes are increased or decreased.[109, 129] The generation of ROS by the sinonasal mucosa is another process employed in the battle against bacteria. Of interest, the lactoperoxidase system (LPO/ H_2O_2) is vital in the innate immune system. Lactoperoxidase (LPO), secreted from mucosa, catalyses the oxidation of substrates by hydrogen peroxide.[130] Hydrogen peroxide (H_2O_2) is produced by ciliated airway epithelial cells through NADPH oxidase isoforms. [131] Thiocyanate, an important substrate in this system, becomes oxidised to hypothiocyanite with potent antimicrobial effects. Studies have found reduced levels of thiocyanate in airway secretions associated with CFTR defects, which may account for the impaired innate immune response in cystic fibrosis (CF).[132]

Collectin proteins including surfactant proteins (SP-A and SP-D) and mannose-binding lectin exhibit antimicrobial activities in addition to activation of the complement pathway.[133] SP-A and SP-D adhere to microbes and inorganic substrates followed by initiation of cell ingestion and destruction. They are capable of recognising and binding to PAMPs, assisting in bacterial clearance.

Permeabilising proteins including cathelicidins and defensins are vital in mucosal immunity. LL-37, a cathelicidin secreted by the human nasal mucosa, demonstrates a range of antibacterial capacities including destruction of LPS.[134, 135] Furthermore, it is synergistic with lactoferrin and

lysozyme having a broad spectrum activity against Gram-positive, Gram-negative bacteria, fungi and viruses.[136] Additional studies have demonstrated its abilities to eradicate *Pseudomonas aeruginosa* biofilms and reduction of bacterial counts in rabbit models.[137] Interestingly, exposure of sinonasal mucosa cells to inactive vitamin D precursors induced both synthesis of active vitamin D and LL-37.[138] These findings suggest a potential role of vitamin D in the sinonasal immunity.[139] The defensin family (α and β) are antimicrobial proteins contained within neutrophil granules and sinonasal mucosa against bacteria, viruses and fungi.[140, 141] Studies have found the up-regulation of defensins in viral and bacterial infections. They are capable of forming pores against bacteria and fungi with the ability to inhibit virus entry into host cells.[117, 142-144] Additionally, defensins induce cytokine release further activating the immune response against pathogen invasion. Interestingly, defensins are inhibited by high ionic concentrations of airway surface liquid (ASL) suggesting ion transport dysfunction may reduce defensin function, as observed in CF.[145]

The PLUNC family have been recognised to have antimicrobial and surfactant activities, secreted in high concentrations at the uncinate process.[129] These PLUNC proteins bind to LPS and bacteria mediating opsonisation, bacterial killing and biofilm degradation.[146] S100, including S100A7 (psoriasin) and S100A8/9 (calprotectin), is a family of proteins important in the wound healing and barrier repair in addition to its antimicrobial effects.[147] Reduced expression of these epithelial defence proteins were found in CRSwNP compared to healthy patients mucosa and nasal mucus.[129, 147] Epithelial cells are capable of innate immune response activation when T cell cytokine IL-22 binds to IL-22R.[148, 149] This process induces the activation of transcription factor STAT3, which further stimulates mucosal defence and epithelial repair, including the S100 family.[150-152] Notably, reduced levels of IL-22R and impairment in the STAT3 pathway have been described in CRSwNP.[153, 154]

Nitric oxide (NO) has a role in the innate immune system through the stimulation of cilia beating in conjunction with antibacterial and antiviral effects.[117, 155] NO is secreted by NO synthase in the sinonasal epithelium, with particularly high expression in the maxillary sinuses.[156, 157] There is heterogeneity in the literature regarding the significance of NO levels and its relation to CRS disease severity and prognostication.[158] Thus, at present, further research is required before NO is considered to be used as a clinical marker in CRS.

The bitter taste receptor (T2R) family, particularly T2R38, has been associated with activation of the local innate immune response through the increase in mucociliary clearance and bactericidal activity.[159, 160] Bitter taste receptors have been identified outside the oral cavity, including the sinonasal epithelium and within solitary chemosensory cells.[161] These solitary chemosensory cells are specialised cells capable of stimulating the rapid release of antimicrobial peptides from surrounding cells.[160] Both solitary chemosensory cells and T2R are regulated by sweet taste receptors (T1R), which is potentially significant due to elevated levels of glucose in ASL of CRS and CF patients.[162-166] There is growing interest in the relationship between taste receptors and mucosal immunity against invading pathogens. Further research is required to better understand this association and the polymorphisms in T2R receptors and the role in sinonasal immunity in CRS.[167]

Constantly growing literature demonstrates the loss of sinonasal mucosa homeostasis occurring from both over and under activity of the normal innate immune system. The imbalance between the host immunity and external environmental factors likely trigger a cascade of events leading to CRS, a process which is not entirely understood. Further research is required to understand

the maintenance of the innate immune barrier in the face of constant microbial exposure and the relationship of how this dysregulated system leads to CRS.

DYSREGULATED ADAPTIVE IMMUNE RESPONSE

Adaptive immune T and B cells are recruited against invading pathogens when the local innate immune system response is insufficient. Both innate and adaptive immune responses are crucial against invading microbes, however, the same mediators produced also contribute to the chronic inflammatory environment manifested in CRS.

T lymphocytes have been classified as two separate subsets based on their surface protein expression, $CD4^+$ T helper cells and $CD8^+$ cytotoxic T cells. $CD8^+$ T cells are capable to cell lysis following intracellular infections, whereas $CD4^+$ T helper cells mediate antibody production from B cells. Moreover, $CD4^+$ cells are further classified into T helper type 1 (Th1) and T helper type 2 (Th2) and T helper 17 (Th17) lymphocytes depending on the cytokines produced. Th1 cells regulate type 1 immunity characterised by intense phagocytosis and a proinflammatory state through the production of INF-γ, IL-2 and lymphotoxin.[168] Type 1 immunity is employed in the clearance of intracellular or phagocytosable pathogens. Conversely, Th2 cells mediate the type 2 immunity characterised by elevated levels of antibody production. This pathway is mediated by the release of IL-4, IL-5, IL-9, IL-10 and IL-13.[168] Type 2 immunity is required for large extracellular microbes that are not phagocytosable. Furthermore, type 2 immunity can develop from prolonged type 1 responses. Th17 cells, a subset of activated $CD4^+$ T cells, have been described as the bridge between the innate and adaptive immune response, a crucial step in the development of inflammation and autoimmunity.[169] This immune response is characterised by the production of IL-17A, IL-17F,

IL-22 and IL-26.[170] Thus, inflammatory cytokines obtained from the sinonasal mucosa have been employed in the classification of CRS endotypes.

Classically, CRSsNP has been described as a Th1 dominated inflammatory process whereas CRSwNP is regarded as a type 2 immune response with the presence of large quantities of eosinophils, basophils and mast cells. Type 2 inflammatory cytokines elevated in CRSwNP compared to healthy patients include: TSLP, IL-5, IL-13, Eoxtaxin-1, Eotaxin-2 and Eotaxin-3.[171-174] Interestingly, Asian patients with CRSwNP appear to have a type 1 immune response with elevated levels of INF-γ and reduced IL-5 levels. Furthermore, the inflammatory patterns are associated with increased neutrophilic infiltrations in contrast to the eosinophilic infiltrations observed in the Caucasian population.[175, 176] These variations are possibly secondary to genetic differences, however, further research is required to determine the cause. Controversy remains regarding the inflammatory environment in CRSsNP. Initially it was thought to be a type 1 response with elevated INF-γ and reduced IL-5 expression compared to CRSwNP,[174, 177] however, further studies have found similar levels between the two groups.[171, 175] From these results, it is difficult to ascertain if differences in protein expression is secondary to regional variances in the sinonasal cavity. Th17 plays a significant role in chronic airway inflammation, promoting neutrophil chemotaxis and antimicrobial peptide secretions.[178] Elevated expression of Th17 cytokines were identified in recalcitrant CRSwNP patients with evidence of increased barrier dysfunction and epithelial permeability.[179, 180] Further studies are required to determine if the inflammatory profile of CRSsNP develops into CRSwNP or if it is a separate entity itself.

T cells encompass a large aspect of the adaptive immune response. Studies have proposed an impairment in regulatory T cells resulting in the imbalance in inflammatory responses observed

in CRS.[181] Reports found a reduction in Forkhead box protein 3 (FOXP3), a master transcription factor for $CD4^+$ regulatory T cells (Treg), with increased inflammatory cells in the airway mucosa.[173, 177, 181, 182] These Treg have a role in the downregulation of immune responses, thus mediating tolerance.[116] Conversely, another study identified elevated levels of Treg with CRSwNP patients.[183] Interestingly, the preservation of quantity and suppression of function of Treg have been identified in autoimmune thyroiditis, ulcerative colitis and sarcoidosis.[184] These findings suggest the importance of determining dysfunctions in the Treg pathways which may lead to autoimmunity.

B cells and their immunoglobulins are vital components of the mucosal barrier defence against invading pathogens. Immunoglobulins bound to B cell receptors (BCR) allow B cells to recognise and respond appropriately to foreign microbes, such as secretion of antibodies, production of cytokines and activation of T cells.[185] Upon recognition of an antigen, B cells become activated in secondary lymphoid organs (SLO) through the germinal centre reaction.[186] Activated B cells then migrate from the SLO to sites of inflammation. Alternatively, B cells have the ability to be activated directly at sites of inflammation, referred to as mucosal associated lymphoid organs (MALT). Well known MALT includes Waldeyer's ring (Palatine, pharyngeal, tubal and lingual tonsils) in the airway and Peyer's patches in the bowel.[187] Tertiary lymphoid organs (TLO) are formed as a response to inflammation in pathogen clearance and malignant processes.[188, 189] Structurally, TLO follicles appear more disorganised compared to SLO.[190] It is proposed this disorganised structure accounts for reduced clonal selection leading to autoreactive B and T cell clones contributing to the chronic inflammation observed in CRS.[191, 192]

Over recent years, there has been advances in the understanding of the pathogenic potential of B cells in CRS. Clustering of B cell infiltrates have been described in CRS but the significance is unclear.[193] A histopathologic study of sinus tissue from CRSwNP and control patients found no difference in frequency of TLO presence between CRSwNP polyp tissue and healthy control uncinate tissue.[194] Despite this finding, research from our department demonstrated 37% of polyp tissue from recalcitrant CRSwNP patients had evidence of TLO formation, compared to none from control patients.[195] The conflicting literature demonstrates promising potential to improve our knowledge of the association between TLOs and CRS pathogenesis. However, more research is required to determine if B cell activation by TLOs indeed leads to the development of nasal polyps in CRS.

Antibody secretion from B cells is another important function in health, but its dysregulation is also implicated in CRS and autoimmunity. Overproduction can progress to inflammation through complement activation or innate effector immune cells with Fc receptor expression. On the other hand, underproduction of antibodies may lead to insufficient adaptive immune response against pathogens.[187] Elevated levels of naïve B cells and activated plasma cells have been identified in CRSwNP tissue compared to CRSsNP and controls.[190, 196, 197] B cell activating factor (BAFF) and IL-6, vital in B cell activation and proliferation, were also elevated in nasal polyps.[154, 190] These B cells within nasal polyp tissue were found to secrete IgA, IgE and IgG in larger quantities at higher frequencies compared to tonsil B cells.[194] Further studies have found CRSwNP polyp tissue accumulating high levels of all antibody isotopes, except IgD, with suggestions of B cell activation within polyp tissue and subsequent antibody secretion.[196, 198, 199] Interestingly, there is no elevation in antibodies within the peripheral blood of CRSwNP patients, indicating a local stimulus inciting this inflammatory response.[197]

Antibody specificity and autoreactivity within nasal polyps and its association with the pathogenesis of CRS is an area of interest. In particularly, IgE antibodies for *Staphylococcus aureus* enterotoxins have been linked to more severe disease.[190, 200] Reports have found polyp-localised polyclonal IgE antibodies inducing histamine release from tissue contributing to chronic inflammation by continuously activating mast cells.[201] Thus, it is clear the accumulation of activated B cells and their respective antibodies within sinonasal mucosa of CRS patients contributes to the chronic inflammation observed.

IMMUNE BARRIER HYPOTHESIS

The ciliated mucosal barrier is composed of mucus, the mucociliary elevator and apical junctional complexes regulating paracellular permeability and limiting stimulation of the immune system by pathogens.[202] This hypothesis proposes dysfunction in both the physical barrier and innate immune response predisposing the development of CRS. This theory originated from CF patients who have mucociliary dysfunction and a higher incidence of CRS. Interestingly, even carriers of the CF mutation without clinical respiratory symptoms had significantly higher prevalence of CRSsNP.[203] Reductions in expression of the tight junction proteins, occludin and zonula occludens-1 (ZO-1) were found in CRSwNP patients compared to healthy controls.[204] Furthermore, there was an associated reduction in transepithelial electrical resistance, a measure of membrane integrity, in both AFRS and CRSwNP compared to healthy patients.[204, 205] It has been proposed that the disrupted epithelial barrier allows for the invasion of the submucosa and deeper tissues by microbial pathogens resulting in recalcitrant CRS.[204]

Changes in epithelial barrier function and morphology have been thoroughly studied in the literature. As discussed previously, CRS patients exhibit reduced expression of tight junction proteins leading to barrier disruption and increased susceptibility to sensitisation and atopy.

Parallels in these findings are observed in atopic diseases of the bowel, skin and lungs.[206-209] Histopathological changes observed in the tissue remodelling process of CRS is manifested as increased collagen deposition, basement membrane thickening, mucosal oedema, inflammatory infiltrates and goblet cell hyperplasia.[210, 211] These patterns of airway remodelling have been associated with asthma, CF and pulmonary fibrosis.[39, 212] The pleotropic cytokine, TGF-β, regulates extracellular matrix deposition in the airway and appears to play a key role in this remodelling process and polyp formation.[213] Reduced levels of TGF-β in CRSwNP have been implicated in decreased tissue repair, collagen and albumin deposition with increased tissue oedema. Alternatively, higher levels found in CRSsNP is associated with increased collagen deposition with fibrosis and basement membrane thickening.[214, 215] Interestingly, low TGF-β and Treg activity is consistent across both Caucasian and Asian polyps, despite differences in inflammatory profiles.[63] Thus, suggesting a role in tissue remodelling and polyp formation in CRS.

Epithelial-mesenchymal transition (EMT) occurs at junctions of mucosal and cutaneous barriers as a result to inflammation and remodelling observed in CRS, asthma and cancer.[216, 217] During this process, epithelial cells lose their normal morphology, polarity and junctional attachments to neighbouring cells becoming spindle-shaped mesenchymal cells, or myofibroblasts.[218] Studies have demonstrated loss of tight junction and adherens junction proteins with associated mucosal changes.[219, 220] The deposition of complement factors in the basement membrane of CRSwNP polyps have been associated with EMT.[221, 222] A range of pathways have demonstrated involvement in EMT induction. Periostin, a matricellular protein expressed in Th2 inflammation by epithelial cells, is capable of inducing EMT through a TGF-β-dependent pathway.[223] Furthermore, proconvertase-1 (PC1/3), a hormone processing enzyme typically expressed in neuroendocrine tissue, was found to have elevated expression in CRS

polyps, but not in healthy control tissue. Profound EMT was induced by this overexpression of PC1/3.[224] The underlying causes of EMT in CRS remains unclear, with potential inducers from the impaired host immune response or external factors.

The dysregulation of the coagulation cascade has been hypothesised to play a role in the pathogenesis of many inflammatory conditions including asthma, rheumatoid arthritis and Crohn's disease.[225] Factor XIII-A in the coagulation cascade, present in platelets and macrophages, is also elevated in nasal polyp tissues of CRSwNP patients.[226] It was hypothesised overproduction of factor XIII-A may lead to accelerated coagulation cascade with subsequent excessive fibrin deposition. In turn, leading to tissue remodelling and oedema of the submucosa of nasal polyp tissue.[225] Elevated expression of platelet-derived growth factor (PDGF) has been identified in nasal polyps suggesting involvement in epithelial proliferation observed in CRS.[227] PDGF is chemotactic and mitogenic for fibroblasts, and involved in the pathogenesis of fibrosis.[228] Activated macrophages are a source of PDGF within the airway, and are commonly present within inflamed epithelium. The dysregulation of the platelet degranulation pathway may have a role in the development of nasal polyposis in CRS.

Microbes have demonstrated abilities to cause barrier dysfunction in the sinonasal epithelium. *Staphylococcus aureus* are capable of secreting toxins that disrupt the mucosal barrier, evidenced by reduced expression of ZO-1 and claudin-1.[229, 230] *Pseudomonas aeruginosa* causes epithelial barrier dysfunction through reductions in occludin and claudin and increased paracellular permeability.[55, 57] Furthermore, there was a significantly strong correlation between *Pseudomonas aeruginosa* elastase activity and CRS severity on radiological imaging.[57] This pathogen-induced sinonasal epithelial disruption can potentially lead to further bacterial infections and biofilm formations leading to disease recalcitrance.

Mucociliary clearance is paramount in the maintenance of sinonasal health, as the increased transit and exposure time to foreign material secondary to mucociliary dysfunction potentially plays a role in CRS.[231, 232] Cystic fibrosis patients have demonstrated diminished tight junction protein expression and increased epithelial permeability.[220, 232, 233] Cilia length from CRS patients were approximately double the length with signs of damage and disorganised structure compared to healthy patients. These findings were further supported by overexpression of forkhead box protein J1 (FOXJ1), centriolar coiled-coil protein of 110 kDa (CP110) and TAp73, all factors present in the initiation and execution of cilia assembly.[234] Increased mucus production and viscosity associated with glandular and goblet cell hyperplasia were common features of airway remodelling.[235, 236] These changes are likely induced by inflammatory cytokines TNF-α, IL-8 and IL-13.[237] Furthermore, a subset of mast cells from CRSwNP tissue was found to secrete chymase, a known mucus production inducer. It has been hypothesised these mast cells may play a role in the overproduction of mucus commonly reported in CRS.[112] Differential expression of mucin genes, MUC5AC and MUC5B, are present in CRS and CF, likely accounting for the varying consistency of the mucus.[235, 238, 239]

The mucus from CRS patients are typically laden with a high burden of pathogenic bacteria including *Streptococcus pneumoniae, Staphylococcus aureus, Haemophilus influenzae and Pseudomonas aeruginosa*. These bacteria are known to produce detrimental toxins targeting cilia motion and structure.[240] It is believed that this is one means by which the bacteria avoid removal by mucociliary clearance, and gain a foothold for biofilm formation as well as cellular and stromal invasion. In addition to pathogens, mucus from CRS patients contain high levels of pro-inflammatory cytokines that can also affect cilia function. IL-8 demonstrated inhibition

of ciliary beat frequency (CBF) in bovine bronchial epithelial cells.[241] Furthermore IL-6 showed similar reduction in CBF in high concentrations in fallopian tube cilia.[242]

Chronic inflammation with recurrent cellular remodelling may account for changes in cytoskeletal structure and barrier dysfunction of CRS cells leading to increased epithelial permeability and polyp formation. However, it remains unclear if these epithelial cells are intrinsically impaired or if exposure to extrinsic factors induce this dysregulation. Irrespective of the order of events, we hypothesise that this perpetual cycle of inflammation and infection may also cause gradual genotypical changes that may result in the development of polyps.

CONCLUSION

There is currently no single hypothesis or molecular pathway that is capable of describing the process from the inciting inflammatory event to tissue remodelling observed in CRS.[243] However, there is growing consensus that the chronic inflammatory response evident in CRS is an imbalance between the host, commensal flora, invading pathogens and exogenous stressors.[1]

CHAPTER 2: MUCOSAL BARRIER

STRUCTURE AND FUNCTION OF THE MUCOSAL BARRIER

Mucosal barrier structure and function is largely maintained by apical junctional complexes. These complexes are located at the apex of polarised epithelial cells, composed of numerous families of transmembrane proteins. This highly organised, dynamic structure is responsible for cell-cell adhesion, cell polarity and paracellular permeability.[244, 245] This junctional complex is composed of tight junctions, adherens junctions, gap junctions and desmosomes which together protect the underlying sinonasal mucosa from the constant insult of pathogens, allergens and irritants (Figure 2.1).

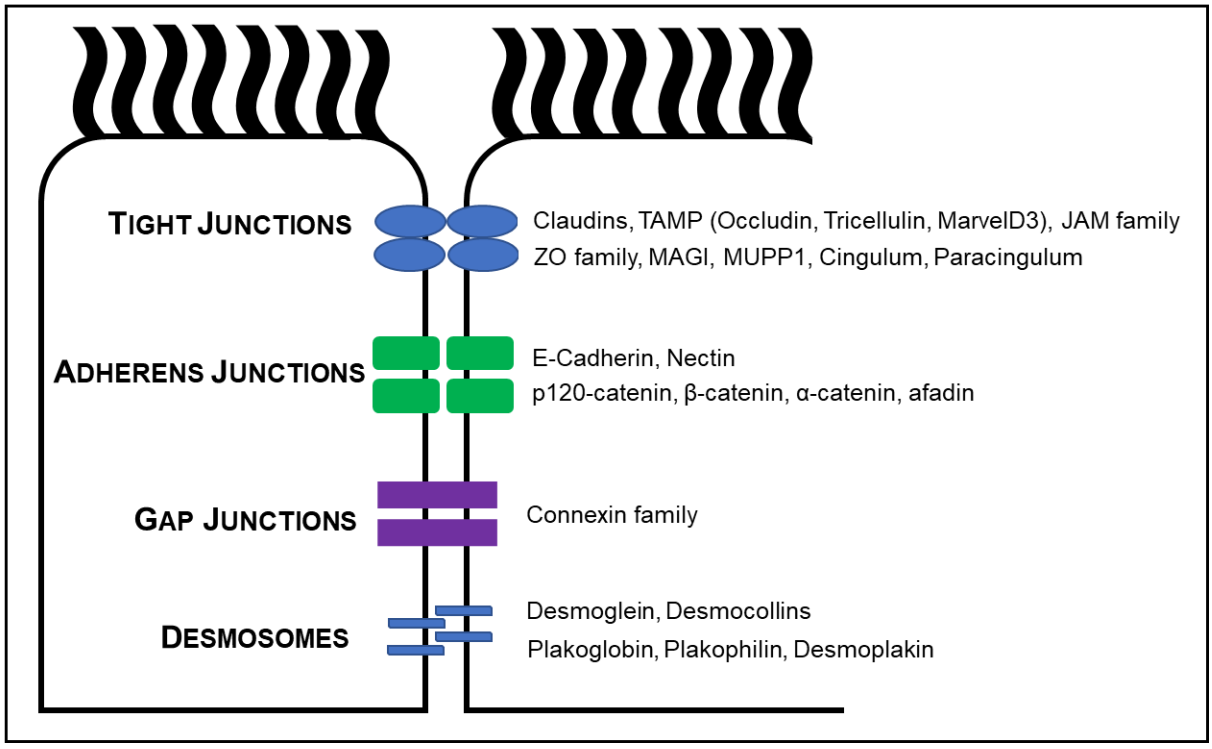

Figure 2.1 Schematic of an intercellular junction.

The configuration of tight junctions, adherens junctions, gap junctions and desmosomes within an intercellular junction.

TIGHT JUNCTIONS

Tight junctions (TJs) form an uninterrupted intercellular barrier between epithelial cells necessary to separate tissue compartments and regulate selective permeability of solutes. Furthermore, they are vital in establishing cellular polarity ensuring both apical and basal surfaces are orientated and aligned, known as the fence function. The structures of TJs are stratified into transmembrane (integral) and scaffolding (peripheral) components. The transmembrane proteins responsible for paracellular permeability and cellular polarity include: the claudin family, tight junction-associated marvel proteins (TAMPs) and the junctional adhesion molecule (JAM) family.[246, 247] The scaffolding components are closely associated with the cellular actin cytoskeleton and adherens junctions. They comprise of cingulin, paracingulin and signalling proteins.

The claudin superfamily of tetraspan proteins are major structural components of TJs, comprising at least 24 members ranging from 20-27 kDa in size.[246] Claudins are composed of four transmembrane helices with two extracellular loops, N- and C- terminal cytoplasmic tails (Figure 2.2).[248] The first extracellular loop contains charged amino acids proposed to influence paracellular ion selectivity.[249] Additionally, highly conserved cysteine residues present in this loop are hypothesised to increase protein stability through the formation of intramolecular disulphide bonds.[250] The second extracellular loop is capable of forming dimers with different claudins on opposing cell membranes through hydrophobic interactions.[251] The C-terminal tail is the region of sequence and size heterogeneity among the claudin proteins. Furthermore, it determines the overall protein stability and function based on post-translational modifications such as phosphorylation or palmitoylation.[251] The PDZ-domain-binding motif located at this tail allows direct interaction with cytoplasmic scaffolding proteins such as zonula occludens (ZO)-1, ZO-2, ZO-3, pals1-associated tight junction protein (PATJ) and multi-PDZ domain

protein 1 (MUPP1).[248 251] Furuse et al discovered claudin overexpression in occludin- and TJ-deficient fibroblasts were capable of forming TJ strand-like structures between adjacent cells.[252] Further studies found claudins to constitute a key role in determining the paracellular permeability of epithelial cells, through the pore pathway.[253] The paracellular barrier regulation is divided into two processes, the pore and leak pathways.[254, 255] The pore pathway is a large capacity and charge selective process which allows the passage of small ions less than 4 Å. Alternatively, macromolecule passage is through the low capacity non-ion selective leak pathway.[256] The claudin type will determine the size and pore charge state. Thus, TJs can become either "leakier" or "tighter" depending on the expression of the type of claudin present. For instance, claudin-1 and claudin-3 increase barrier integrity evidenced by increased transepithelial electrical resistance.[253] Alternatively, claudin-2 is commonly expressed in "leaky" epithelial tissues acting as a cation permeable paracellular pore.[253]

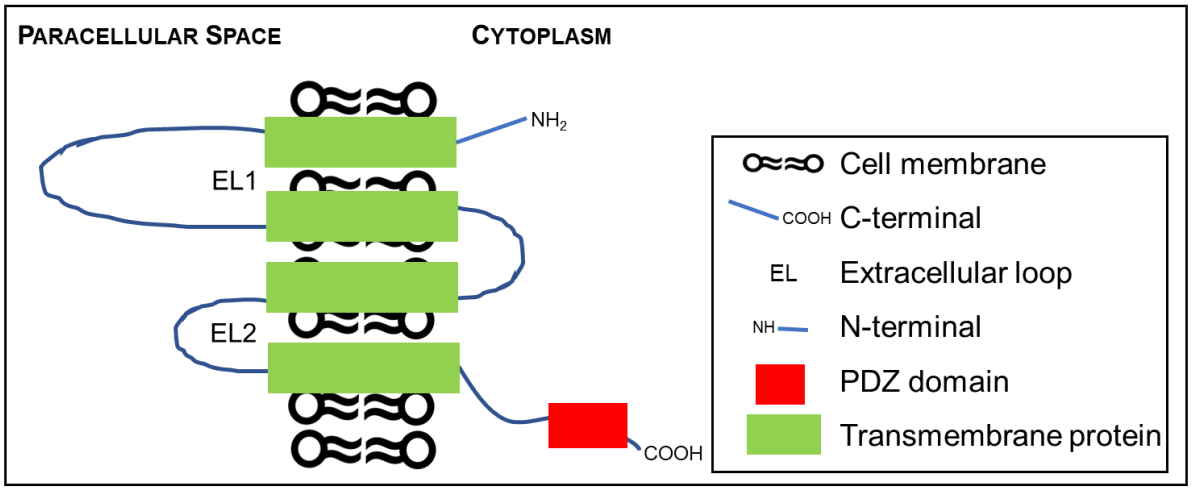

Figure 2.2. Claudin structure.

Schematic diagram of a claudin protein.

The tight junction-associated marvel protein (TAMP) family consists of occludin, tricellulin (MarvelD2) and MarvelD3. They share a conserved myelin and lymphocyte protein (MAL) and related proteins for vesicle trafficking and membrane link (MARVEL) domain with four

transmembrane helices linked by two extracellular and one intracellular loop.[257] TAMPs are proposed to modulate junctional permeability through the regulation of signalling mechanisms between TJs and the cell interior.[258] Occludin is a 60 kDa protein expressed in epithelial cells involved in the regulation of paracellular permeability (Figure 2.3).[259] Multiple phosphorylation sites on occludin are proposed to be linked to its regulation and localisation to TJs. Phosphorylated occludin is localised to TJs, whereas non-phosphorylated occludin is localised to the basolateral membrane and cytoplasmic vesicles.[260] The phosphorylation states of occludin are regulated by various kinases and phosphatases, including protein kinase C, non-receptor tyrosine kinase c-Yes and protein phosphatase 2A.[261-263] The inhibition of occludin phosphorylation leads to loss of TJ localisation and subsequent reduced barrier integrity.[261] Additionally, studies have associated occludin overexpression with increased cell-cell adhesion and improved barrier function.[264] Tricellulin, a transmembrane protein located at tricellular TJs has been demonstrated to have important roles in TJ formation. [265, 266] Tricellulin has been suggested to contribute to the paracellular leak pathway as the tricellular TJs are large enough to allow passage of macromolecules.[265] Furthermore, mouse models have established a role of tricellulin as a functional redundancy in occludin null mice in maintaining barrier function and integrity.[266] The function and expression of TAMPs can be altered by interactions with claudins and tissue necrosis factor.[247, 267] Additionally, IL-13 can induce the downregulation of tricellulin with increased macromolecule permeability.[268] MarvelD3 is the most recently identified TAMP, with studies demonstrating that it is not required for the formation of TJs.[247, 269] Instead, in vitro studies have shown MarvelD3 to be a junctional signalling inhibitor that is capable of regulating epithelial stress response though attenuation of JNK activity ultimately regulating cellular behaviour through gene expression, cell migration, survival and proliferation.[270]

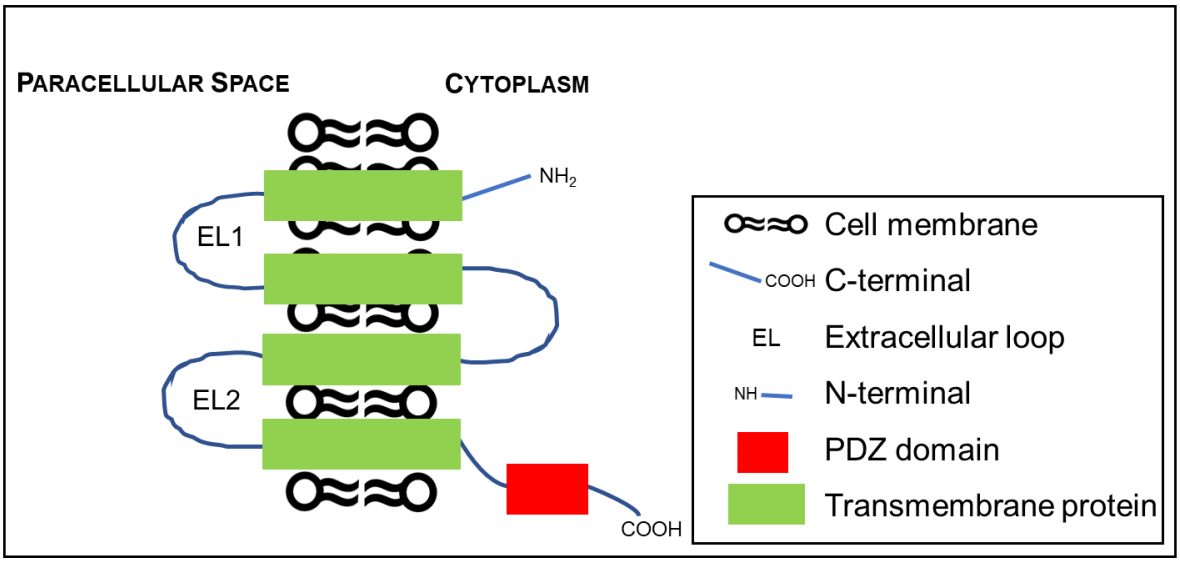

Figure 2.3. Occludin structure.

Schematic diagram of an occludin protein.

Junctional adhesion molecules (JAMs) are members of the immunoglobulin superfamily and consist of the cell-cell adhesion molecules JAM-A, JAM-B and JAM-C with a molecular weight of 40 kDa. They are composed of two extracellular immunoglobulin-like domains, one transmembrane domain and a cytoplasmic tail of variable length containing both the C-terminal domain and PDZ domain (Figure 2.4).[271] Its extracellular domains are capable of interacting with other adhesion receptors on surrounding cells. The cytoplasmic tail is capable of interacting with signalling and scaffolding proteins ZO-1, MAGI-1 and MUPP1.[272-274] Through these interactions, JAMs are capable of regulating cell-cell contact formation, epithelial barrier formation, homeostasis and cell migration.[274] Of all the JAMs, the role of JAM-A in TJs is the most understood. Initially, JAM-A acts as a positional cue for subcellular localisation and site-specific activation of the PAR-aPKC complex. Partitioning-defective protein 3 (PAR-3) is capable of forming complexes with PAR-6 and atypical protein kinase C (aPKC) to establish epithelial cell polarity in TJ assembly.[275] JAM-A then induces the PAR-aPKC complex to promote junctional maturation and apico-basal polarisation and cell-cell contact formation.[276]

JAMs interact directly with cell polarity regulator PAR-3.[277-279] The PAR complex localises to TJs and separates the apical and basolateral membrane domains.[280] Upon establishment of mature cell-cell contacts, continuous Ser285 phosphorylation of JAM-A by the PAR-aPKC complex is required to maintain the TJ epithelial barrier.[281] Furthermore, JAM-A is capable of regulating the expression of various claudins.[281, 282] Observations from murine studies have associated severely compromised intestinal barrier epithelium in JAM-A-deficient mice.[282, 283]

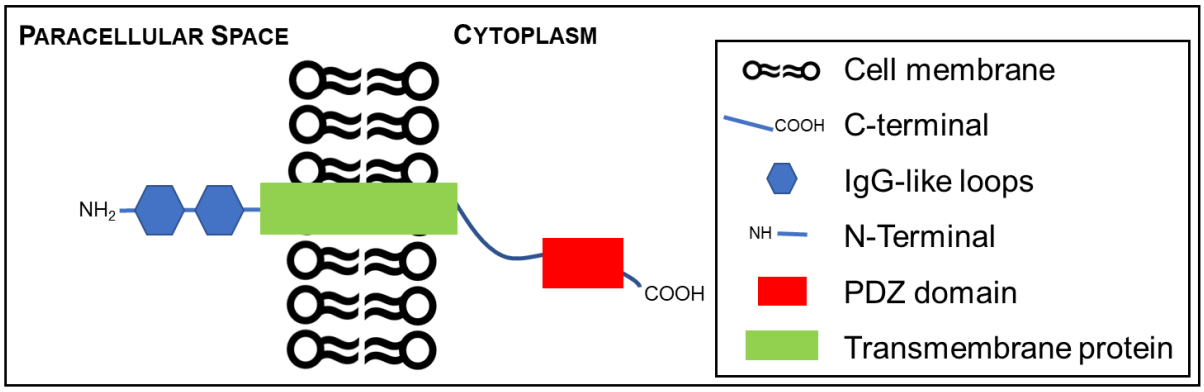

Figure 2.4. Junctional adhesion molecule structure.

Schematic diagram of a junctional adhesion molecule protein.

Scaffolding proteins, or TJ plaques, are proteins located within the cytoplasm underlying the TJs. They are complex dynamic targets and effectors that assist in the development and maintenance of cellular polarity, establishment of TJs and cellular proliferation.[284] The structure of the TJ plaques is formed by proteins with PDZ domains. PDZ is a initialism combining the first three proteins identified sharing the domain: Psd-95 (Post-synaptic density protein 95), DIg (Discs-large, a protein in Drosophila, mutation of which leads to overgrowth of wing imaginal discs), ZO-1 (Zonula occludens 1).[284] PDZ domain-containing proteins interact with other PDZ proteins to assist in anchoring TJ membrane proteins to the cytoskeleton, in addition to signal transduction pathways in numerous biological processes including cell proliferation and polarity.[285] Scaffolding proteins with PDZ domains include the zonula occludens (ZO)

family, membrane-associated guanylate kinase with inverted domain structure (MAGI) family, and the multi-PDZ domain protein 1 (MUPP1). The second, heterogenous group of scaffolding proteins lack PDZ domains and are primarily involved in the regulation of signalling pathways at the TJ rather than the structural TJ components. These include cingulin, paracingulin and signalling proteins (kinases, phosphatases, GTPase regulators and membrane traffic regulators).[284]

The zonula occludens (ZO) family (ZO-1, ZO-2 and ZO-3) belong to the membrane associated guanylate kinase (MAGUK) family of proteins with binding domains to TJs, adherens junctions and the actin cytoskeleton.[286] All three ZO share similar structures with a N-terminal containing three PDZ domains, one Src homology 3 (SH3) domain and one guanylate kinase domain (GUK) and a C-terminal with an acidic domain with a proline-rich region. Their molecular weights range from 130 to 220 kDa.[284] The first PDZ domain from all three ZO proteins binds directly to claudins aiding in the formation and assembly of TJ strands. Studies have demonstrated the deletion of ZO-1 and ZO-2 scaffolding proteins lead to the failure of TJ strand formation with consequent increase in barrier permeability.[287] The second PDZ domain is vital for interactions with other ZO proteins and binding to connexins.[288, 289] The third PDZ domain interacts with JAM-A which in turn interacts with the PDZ of PAR-3, thus, provides connections between ZO-claudin-based TJ strands and PAR-3-aPKC polarity complexes.[279] The SH3, GUK domains have been proposed to aid in recruiting ZO to TJs, where GUK is responsible for occludin interaction.[287, 290] This central region of ZO-1 and ZO-2 has been observed to bind to occludin and α-catenin.[291] The proline-rich C-terminal interacts with actin and cortactin, linking the TJ membrane proteins to the underlying cytoskeleton.[292, 293] ZO-3 has been demonstrated to interact with E-cadherin associated protein p120-catenin.[294]

The membrane-associated guanylate kinase with inverted domain structure (MAGI) proteins are composed of five PDZ domains. Only MAGI-1 and MAGI-2 are TJ-associated proteins.[295] The PDZ domains interact with a range of proteins consisting of integral membrane proteins (including JAMs) and junctional-associated signalling molecules (including β-catenin, K-RAS and Rap1).[296, 297] Reduced expression of MAGI-1 from endothelial cells leads to impaired cadherin-based cell adhesion. [298]

Multi-PDZ domain protein 1 (MUPP1) consists of 13 PDZ domains and localises to TJs to interact with claudins and JAM-A.[273] Despite its similar structure to pals1-associated TJ protein (PATJ), MUPP1's specific role is unclear. Its domain organisation suggests it functions as a scaffold support and regulator of TJs.[284, 299] Alternatively, PATJ is vital in the establishment of epithelial cell polarity.[300] PATJ is capable of binding ZO and claudins at the TJ, where reduction in PATJ expression results in delayed TJ formation and cellular polarity defects.[301]

Cingulin and paracingulin are junction-associated proteins consisting of a globular head domain, coiled-coil rod domain with a small globular tail.[284] Cingulin is a TJ specific protein which interacts with ZO-1, ZO-2, ZO-3, actin and myosin.[302] Furthermore, both cingulin and paracingulin have been demonstrated to play role in the control of claudin-2 expression.[303, 304] The interaction of these two TJ plaques is thought to contribute to the scaffolding through anchoring the TJs with the underlying cytoskeleton.

There have been significant advances in identifying the numerous proteins and their associated interactions in the formation and maintenance of TJs. Numerous studies have observed the paracellular permeability properties of the epithelial barrier secondary to the complex interplay of integral and peripheral TJ proteins. Further improvements in live-imaging technology may

allow for a clearer understanding and visualisation of the abundant dynamic properties of TJs in both physiological and pathological conditions.

ADHERENS JUNCTIONS

Adherens junctions (AJs) are components of the epithelial barrier structure responsible for linking the membrane with cytoskeletal components. It is situated between the luminally located TJs and basally located desmosomes, constituting the apical junction complex.[305] In epithelial cells the AJ regions are parallel to the plasma membranes with an intercellular space of 200 Å. Similar to TJs, transmembrane proteins located within this intercellular space are anchored to numerous microfilaments within the cytoplasm.[306] AJs are responsible for numerous roles in barrier function maintenance including cellular adhesion, polarity, actin skeleton regulation, intracellular signalling and transcriptional regulation.[246] The core structural components of AJs include the cadherin-catenin complex and the nectin-afadin complex.[307]

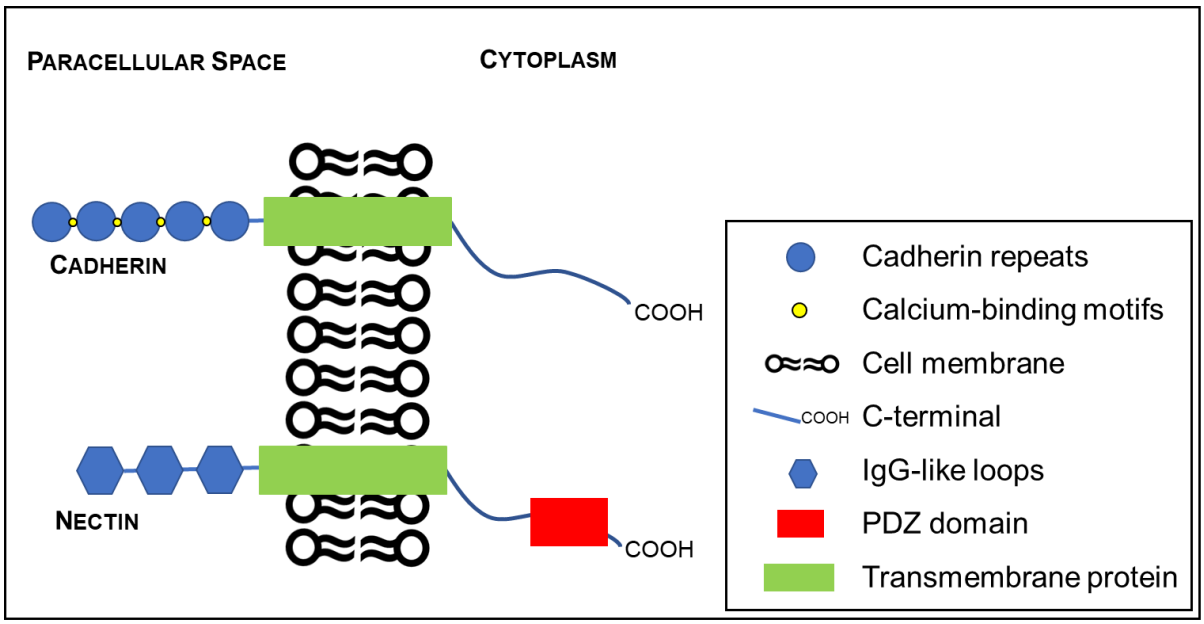

Figure 2.5. Adherens junction protein structures.

Schematic diagrams of cadherin and nectin proteins.

Classic cadherins were the first adhesion molecules identified in the AJs. Since their discovery, the cadherin superfamily has grown to over 80 members.[308] Among the vast types of cadherins, E-cadherin is specifically localised to the AJs of epithelial barriers. Cadherins are type I single-pass transmembrane proteins that facilitate calcium-dependent intercellular adhesion.[307] Their extracellular domains are composed of five repetitive subdomains containing calcium-binding sequences (Figure 2.5).[309] These extracellular domains bind weakly to the homophilic regions of adjacent cadherins. Interaction with calcium ions induces a conformational change of the extracellular domain enhancing the protein's adhesive function.[310] The cadherin cytoplasmic domain facilitates vital structural and signalling pathways for cellular adhesion via cytoplasmic proteins called catenins. The membrane-neighbouring portion of the cytoplasmic tail interacts with p120-catenin, whereas, the C-terminal binds to the β-catenin.[311] These catenins further interact with cytoskeletal proteins and regulators to alter the cell-cell adhesiveness within the AJs. Cadherin-mediated cellular adhesion is a highly dynamic process capable of cellular reorganisation observed during EMT in physiological and pathological conditions. As previously discussed, EMT has been observed in nasal epithelial cells of CRS patients secondary to chronic inflammation.[216, 222] Furthermore, loss of cellular adhesion has been correlated with reduced E-cadherin expression in epithelial tumours.[312]

The catenin family consists of three distinct proteins: p120-catenin, β-catenin and α-catenin. The juxtamembrane domain of E-cadherin has demonstrated a vital role in recruiting p120-catenin to AJs. p120-catenin belongs to a family of armadillo proteins proposed to increase E-cadherin stability and thus cellular adhesiveness.[313, 314] Furthermore, p120-catenin is capable of regulating cell motility via the actin cytoskeleton through interacting with the Rho family GTPases.[315] β-catenin and γ-catenin (plakoglobin), are homologous proteins that bind to the C-terminal of E-cadherin.[316] Specifically, β-catenin is critical in cellular adhesion as it protects

the cytoplasmic domain of cadherin from proteolysis and enhances efficiency of endoplasmic reticulum cell surface transport.[317, 318] Furthermore, β-catenin binding affinity to E-cadherin is strengthened through the phosphorylation of several kinases.[246] As actin filaments are essential to AJ establishment, early studies proposed the connection between the cadherin-β-catenin complex and the actin filaments was via α-catenin as the linking protein.[311] This concept was refuted when studies found α-catenin could not bind to F-actin when already bound to the cadherin-β-catenin complex.[319] Instead a new hypothesis suggested the involvement of other mediators. α-catenin is capable of interacting with a range of actin binding proteins including formin, vinculin and epithelial protein list in neoplasm (EPLIN).[320-322] EPLIN is capable of binding to cadherin-β-catenin-α-catenin complex to F-actin.

Nectin is a calcium-independent adhesion molecule and a member of the IgG superfamily hypothesised to be responsible for the initiation of cell-cell adhesion.[311] Similar to cadherins, nectin is capable of homophilic and heterophilic adhesions with other nectins and nectin-like receptors. Structurally, it contains an extracellular domain with three IgG-like loops and a cytoplasmic domain containing a C-terminal with PDZ-binding motifs (Figure 2.5). Studies have demonstrated nectin's role in recruiting JAM and ZO-1 to TJs, in addition to inducing JAM-associated claudin and occludin recruitment to the apical TJ complex.[323, 324] The cytoplasmic domain of nectin interacts with the actin-binding protein known as afadin. Afadin localises to both TJs and AJs.[325] It consists of one PDZ domain which interacts with both the C-terminals of nectin and JAM immunoglobulin-like adhesion molecules, an N-terminal which binds with ZO-1 and a dilute (DIL) domain which binds to α-catenin via the afadin DIL domain-interacting protein (ADIP).[284] Afadin is capable of linking transmembrane adhesion proteins to the actin cytoskeleton.[326, 327] Murine studies have demonstrated its importance in establishing

epithelial polarity during embryogenesis, as deletion leads to embryo death with loss of apico-basal polarity and ectoderm disorganisation.[328]

Adherens junctions are core components of the epithelial barrier with key adhesive properties of anchoring transmembrane proteins to the underlying cytoskeleton. Similar to TJs, numerous structural proteins and molecular pathways are present to establish and regulate this dynamic structure. The AJ integrity is centred on the interplay of both the cadherin-catenin and nectin-afadin complexes with the underlying actin filaments. Further studies are required to improve the understanding of underlying changes to these proteins and signalling pathways present at AJs during states of chronic inflammation.

GAP JUNCTIONS

Gap junctions (GJs) are specialised membrane channels between neighbouring cells, permitting intercellular communication via the transfer of ions, second messengers and small metabolites.[329] This highly dynamic process of cellular communication is crucial for cellular metabolism, synchronisation, signal transduction and nutrition.[330] Gap junction channels are encoded by a family of genes called connexins.[329] Connexins are composed of four transmembrane domains that form the wall of the channels. They are connected by two extracellular loops that are vital in cell-cell recognition and docking. Each loop contains three uncharged cysteine residues which form intraconnexin disulphide bonds. Furthermore, the cytoplasmic components include N- and C- terminals and a cytoplasmic loop connecting the second and third transmembrane domains (Figure 2.6).[331] The cytoplasmic tail is predisposed to post-translational modifications with proposed regulatory roles.[332] Phosphorylation of connexions are an important feature in the assembly, regulation and physiological properties of these channels.[333] Within the endoplasmic reticulum, six connexins oligomerise into a

connexon (or hemichannel). This connexin hexamer is transported to the cell surface and fuses with the plasma membrane.[329] The hemichannels are capable of interacting with other connexons from adjacent neighbouring cells, completing the formation of intercellular channels (Figure 2.7).[334] Although not typically involved in the paracellular permeability barrier, GJ proteins share the intercellular space and have vital roles in the coordination of ciliary function in the sinonasal mucosa.[335] Studies have demonstrated the interaction of the C-terminal tail of connexin-43 with TJ and AJ proteins including ZO-1, occludin and β-catenin.[289, 336, 337] These findings demonstrate the important relationship between GJ and the tripartite apical junctional complex in the regulation of paracellular barrier integrity and mucociliary clearance in the paranasal sinuses.

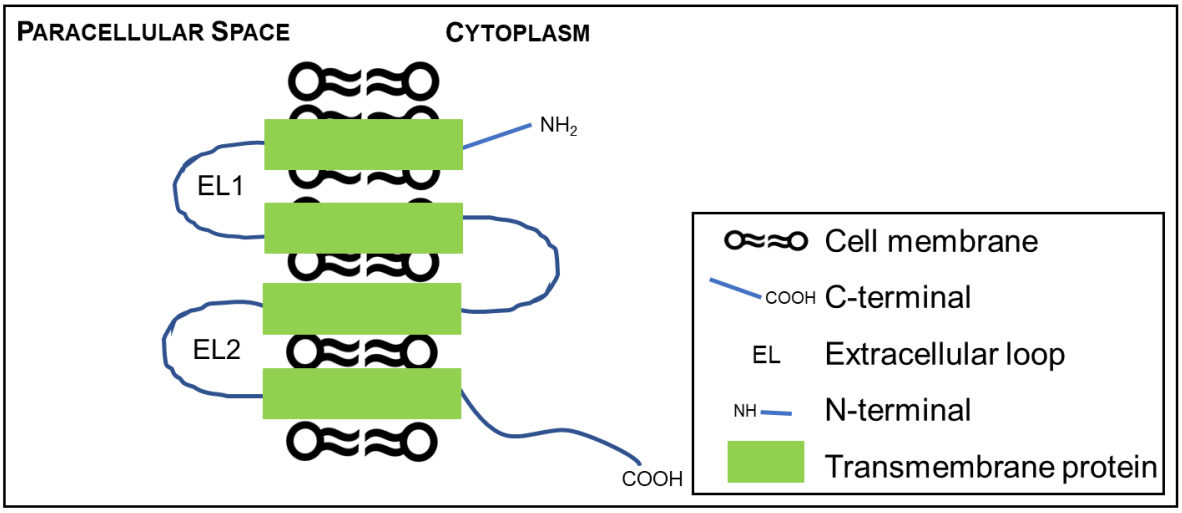

Figure 2.6. Connexin structure.

Schematic diagram of a connexin protein.

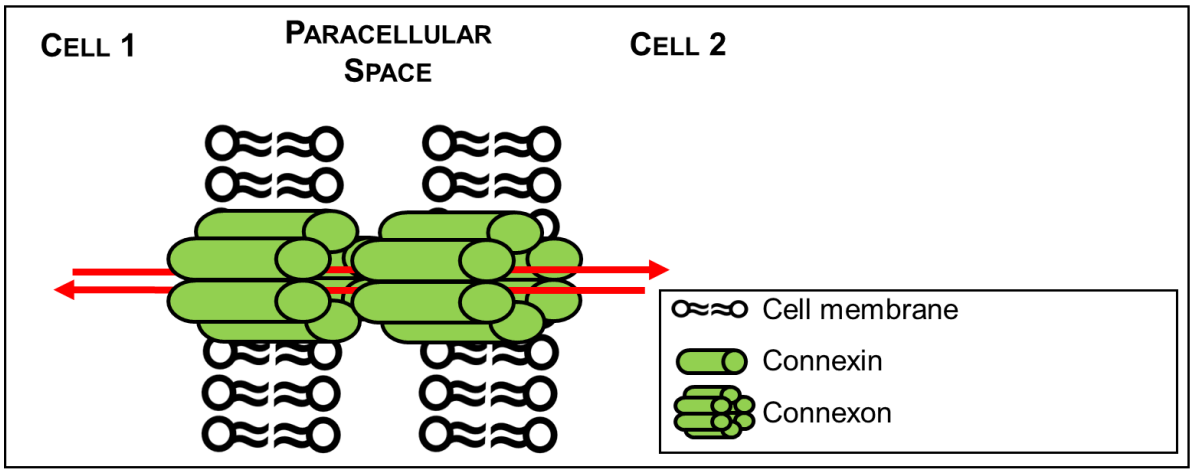

Figure 2.7. Gap junction structure.

Schematic diagram demonstrating the assembly of connexin hexamers into a connexon. Docking of two adjacent connexons establishing an intercellular channel between two neighbouring cells to allow the transfer of solutes.

DESMOSOMES

Desmosomes are intercellular junction complexes responsible for robust cell-cell adhesion and cytoskeletal linkages to resist mechanical stress.[338] Its structural and mechanical properties are emphasised by the distribution of desmosomes throughout tissues subject to regular mechanical forces such as the skin and heart.[339, 340] The desmosome-intermediate filament complex (DIFC) is the scaffold that aids to sustain the integrity of these tissues. Morphologically it can be subdivided into three components: the extracellular core region, the outer dense plaque and the inner dense plaque (Figure 2.8).[341] The extracellular core contains the extracellular domains of desmoglein and desmocollins which facilitate adhesion. The outer dense plaque houses the intracellular cytoplasmic tails of desmoglein and desmocollins which interact with the desmosomal plaques (plakoglobin and plakophilin). Lastly, the inner dense plaque contains desmoplakin and their attachment to keratin intermediate filaments, binding the adhesion complex to the underlying cytoskeletal network.[341]

The desmosomal cadherins, desmoglein (Dsg) and desmocollins (Dsc), facilitate calcium-dependent cell-cell adhesion. Four genes encode desmoglein (Dsg1-4) and three encode desmocollins (Dsc1-3).[341] Dsg2 and Dsc2 are expressed in all desmosomal bearing tissue, whereas the other desmosomal cadherins are expressed in stratified epithelium.[341] These proteins contain five extracellular cadherin repeats each separated by calcium binding motifs.[342] This is followed by a single pass transmembrane domain with an intracellular anchor located juxtamembrane in the cytoplasm.[343] Desmogleins have an intracellular cadherin sequence which interacts with plakoglobin.[344] Furthermore, they also comprise of unique motifs specific to Dsg including intracellular proline-rich linker (IPL) domain, variable number of repeat unit domain (RUD) and glycine rich desmoglein terminal domain (DTD).[345, 346]

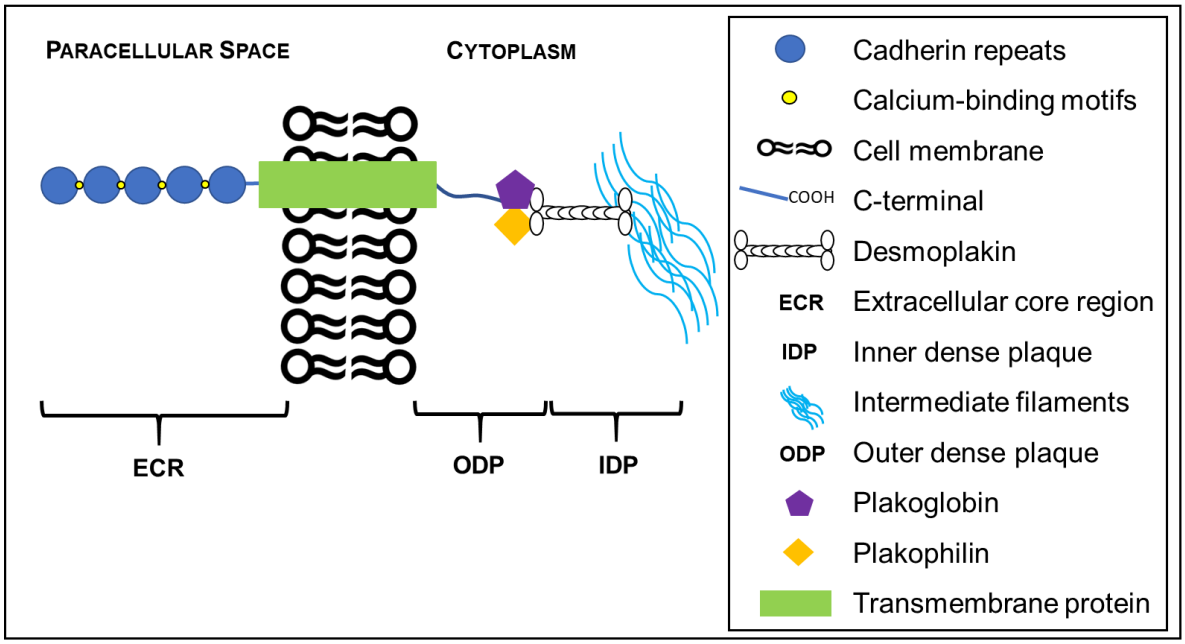

Figure 2.8. Desmosome structure.

Schematic diagram of a desmosome complex.

Armadillo proteins in the desmosome, including plakoglobin and plakophilin, mediate the adhesion of desmosomal cadherins to the underlying cytoskeleton. This relationship is similar to the transmembrane protein linkage with associated plaque proteins present in TJs and AJs.

Armadillo proteins are characterised by a central domain of 42 amino acids with repeating units.[347] Plakoglobin is expressed in both the AJs and desmosomes, however, has a significantly higher affinity for desmosomal cadherins compared to E-cadherin.[348] Plakoglobin binds to the cytoplasmic tails of both desmosomal cadherins which in turn link to desmoplakin, tethering the cytoskeleton to the desmosomal plaque.[341] This process is critical in maintaining cell-cell adhesion integrity, as plakoglobin knockout mice died from fragility of the myocardium.[349] Plakophilin (PKP) plays a crucial role in the highly organised clustering observed in desmosomes, responsible for the desmosomes characteristic adhesive strength. It interacts with Dsg1, desmoplakin and keratin intermediate filaments.[350] Furthermore, the binding between PKP1 and desmoplakin is particularly strong, and induces further recruitment of desmoplakin to cell-cell junctions.[351]

Desmoplakin is the most abundant protein within the desmosome and a member of the plakin family of cytolinkers, key proteins connecting the plasma membrane to the intermediate filaments of the cytoskeleton.[341] Its amino-terminal head binds to plakoglobin and plakophilin, providing the connection of the cadherin-armadillo complex to the desmosome.[346] The C-terminal tail containing three plakin repeat domains and glycine-serine-arginine rich domains bind to the intermediate filaments.[352] Studies have demonstrated the importance of desmoplakin in barrier integrity, where desmosomes in desmoplakin null embryos fail to attach to intermediate filaments and die shortly after implantation.[353, 354] Furthermore, desmoplakin-null mice embryos did not undergo normal cellular proliferation and demonstrated altered actin organisation.[355, 356] Thus, desmoplakin appears to regulate cellular proliferation and organisation in addition to establishing a robust cellular barrier.

Desmosomes are a multifaceted protein complex integral to the strength of apical junctional complexes. In addition to the strong inter- and intra-cellular bonds between proteins, desmosomes are vital in a number of important signalling pathways. Further studies are required to understand how the TJs, AJs, GJs and desmosomes interact and contribute to the overall tissue and epithelial homeostasis.

MUCOCILIARY CLEARANCE

Mucociliary clearance (MCC) is a vital component of the airway's defence system. In conjunction with the paracellular barrier complexes, the coordinated action of beating cilia facilitates the clearance of environmental allergens and pathogens from the airway. The MCC within the paranasal sinuses are orientated toward the natural ostia. Pathogens and particulates bound to the mucus are transported toward the nasopharynx via the semilunar hiatus.[357] The importance of MCC becomes apparent when defects in the system, such as in cystic fibrosis or primary ciliary dyskinesia, present as recurrent infections.[358] Vital components of the MCC system include functioning cilia and well hydrated mucus.

The two primary cell types lining the airway epithelium include ciliated and secretory cells. Secretory cells are capable of releasing mucins, antimicrobial molecules (defensins, lysosome, IgA) and immunomodulatory molecules (cytokines) which are capable of becoming incorporated into mucus.[359] Goblet cells are the principal secretory cells in the superficial epithelium. They are highly polarised with the membrane-bound secretory granules containing mucin located in the apical cytoplasm.[360] Submucosal glands secrete mucins and fluids from the deeper non-ciliated collecting ducts to the superficial ciliated ducts then into the airway lumen. These glands are composed of 60% mucinous cells and 40% serous cells.[359] The volume

of these submucosal glands can fluctuate during various disease processes, such as in cystic fibrosis.[361]

Ciliated pseudostratified columnar epithelium lines the upper and lower airways. These are terminally differentiated cells, that are replaced every 1-4 months by basal cells, functioning as stem cells for ciliated and secretory cells.[362-364] This process of regeneration is accelerated in response to injury, through exposure of the basal cells to luminal air. The transcription factor FOXJ1 in conjunction with regulatory factor X (RFX) direct this formation of ciliated cell formation.[365] Ciliated cells are abundant in mitochondria at the apical regions, ensuring adequate source of ATP to sustain the motor activity of ciliary motion driven by the cytoskeletal protein dynein.[366] Furthermore, ciliated cells exhibit microvilli on its apical surface to increase surface area to maintain moisture and assist in transepithelial movement of fluid and electrolytes.[367]

CILIA

Cilia are specialised hair-like organelles 7 x 0.1 μm in size, present on the surface of cells.[368] The ciliary axoneme is a centriole-derived microtubule core which projects from the plasma membrane.[369] Cilia are classified into motile and immotile based on their ultrastructural axoneme characteristics.[369] Immotile cilia lack the double central tubule and are solitary organelles on most cells functioning as a sensory antenna.[370] Whereas motile cilia are composed of two central singlet microtubules surrounded by nine doublet microtubules (A and B tubules). These outer doublets are connected by the nexin-dynein regulatory complex (N-DRC). Radial spokes projecting from the outer to inner microtubules are vital in the mechanical stability of the axoneme and the regulation of ciliary function (Figure 2.9).[360] Studies have demonstrated the outer dynein arms (ODA) responsible for regulating CBF, whereas the inner dynein arms

(IDA) control cilia bend formation and waveform.[371] Both IDA and ODA are attached to the A microtubule and composed of dynein heavy chains (DHC). The DHC are composed of four separate domains with specific functions. The tail is the cargo binding domain, the stalk region binds to the microtubule, the linker is the mechanical amplifier and the head domain is the site of ATP hydrolysis.[366] ATP activation of DHC induces the doublet microtubules to slide with one another, together with the N-DRC and radial spoke-central pair interaction leads to controlled cilia bending.[360] Proteomic studies have identified over 200 proteins present in motile cilia axonemes.[372]

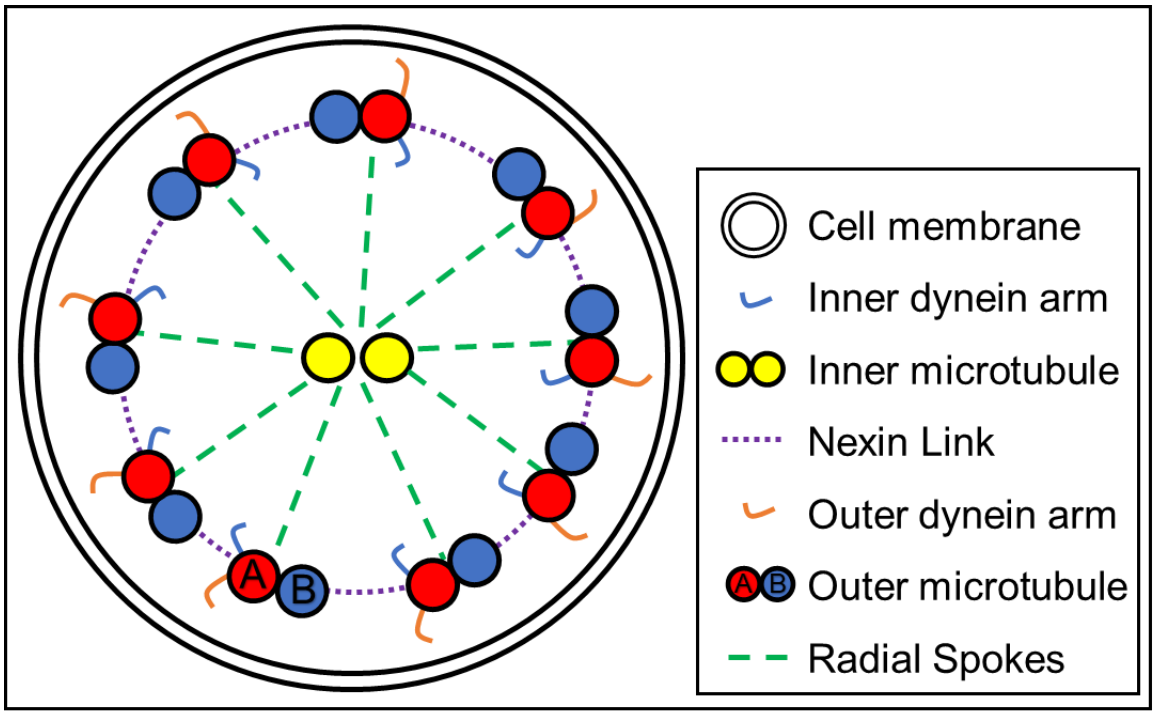

Figure 2.9. Motile cilium axonemal structure.

Microscopic view of a motile cilia axoneme. Adapted from Munkolm et al.[358]

Cilia beat in coordinated metachronal waves in order to transport foreign matter from the airway. Each cilium beats at the same frequency as its neighbours in two phases: the effective stroke, and the recovery stroke. During the effective stroke, the cilia extends an arc

perpendicular to the cell surface, whereas during the recovery stroke the cilia remains bent and parallel to the cell surface prior to returning it its original position.[373] This generates a wave capable of propagating overlying mucus in the cephalad direction. All cilia axonemes must beat in a synchronised and polarised fashion to ensure effective MCC is maintained.[374] Immature MCC demonstrate weak polarisation as axonemes are not orientated. However, as the MCC matures all axonemes progressively re-orientate until they beat in a unidirectional, organised and polarised pattern.[375] Basal CBF varies between 10-20 Hz with a mucociliary clearance rate of 5.5 mm/min.[376, 377]

Numerous exogenous and endogenous factors influence CBF, where dysfunction leads to stagnation of pathogens and allergens leading to infection and inflammation. Human nasal epithelial cells demonstrate increases in CBF following exposure to adenosine and uridine nucleotides. Additionally, ATP induces a rapid increase in CBF, whereas ADP leads to a more protracted response.[378] CBF is temperature-dependent due to the enzymatic hydrolysis of ATP by dynein having an optimal temperature, thus low temperatures reduce CBF.[379] Furthermore, intracellular alkalisation stimulates CBF, whereas intracellular acidification reduces CBF.[380] The bitter taste receptors are expressed on ciliated cells as chemosensory organelles against noxious stimuli, and induce an increased CBF via a calcium-dependent process.[381] Cigarette smoke has been demonstrated to reduce CBF, with reduced numbers of ciliated cells secondary to exposure to ROS.[382, 383]

NASAL MUCUS

The mucus layer plays a vital role in MCC by providing a humidified environment for optimal ciliary function in addition to trapping pathogens and foreign particulates for removal. Nasal

mucus is produced by submucosal glands, seromucous glands, goblet cells and the transudation of blood plasma.[357]

Nasal mucus consists of two layers, the lower periciliary (PCL) and superficial viscous gel layer (Figure 2.10). The PCL is a polyanionic gel approximately 7 μm deep with a similar height to cilia. It has important properties in providing hydration and lubrication for ciliary beating and a physical barrier restricting passage of particles in the airway lumen. [360] Its hydration is maintained by adenosine via A2b receptors on ciliated cells and nucleotides (adenine and uridine) via $P2Y_2$ receptors. Stimulation induces sodium absorption inhibition and chloride release via second messengers, resulting in water diffusion into the airway hydrating the mucus.[384, 385] Further ASL hydration maintenance is through the sodium chloride quantity on the mucosal surface. The sodium chloride content is controlled through epithelial sodium channels, cystic fibrosis transmembrane conductance regulator (CFTR) and calcium-activated chloride channels.[386]

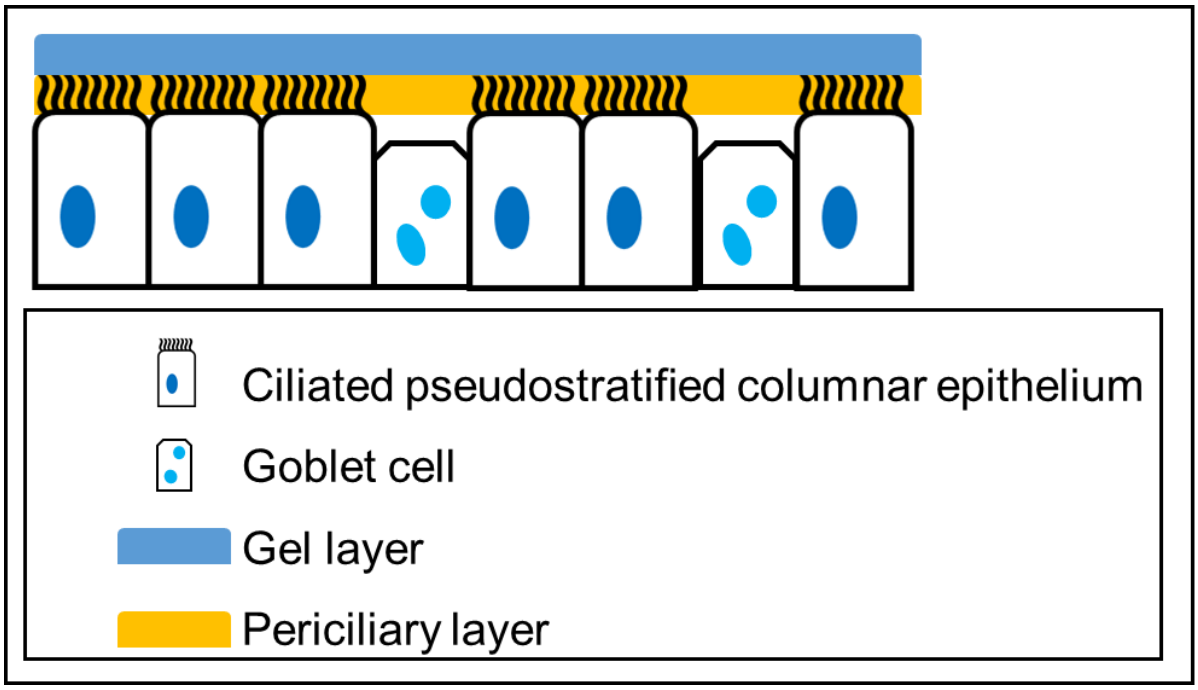

Figure 2.10. Mucus layers.

Nasal mucosa is lined with a thin layer of airway surface liquid. The cilia lie within the periciliary layer with an additional gel layer on the superficial surface. Adapted from Beule et al.[357]

Nasal mucus is a flexible network of linear, hydrated mucin molecules. The viscosity and cohesive properties of nasal mucus is due to the glycoproteins and oligosaccharide chains. Healthy mucus is composed of 97% water and 3% solids (mucins, non-mucin proteins, salts, lipids and cellular debris).[359] Albumin accounts for 15% of total protein, suggesting transudation under physiological conditions. Furthermore, albumin levels rise secondary to increased vascular permeability in inflammatory conditions.[387, 388] Mucins are large glycoproteins, accounting for less than 30% of the solids, and comprise of 50-90% carbohydrates with regions rich in serine and threonine residues bound by hydroxyl groups and sugar chains.[389]

Mucins are encoded by 17 distinct genes, where 7 mucins are secreted and 10 are membrane-bound.[390] Membrane-bound mucins are expressed at the plasma membrane, improving structural integrity of the cilia and extracellular matrix in addition to signal transduction.[391] The secreted mucins are further classified into polymeric (MUC2, MUC5AC, MUC5B, MUC6, MUC19) and non-polymeric glycoconjugates.[391] Polymeric mucins, or gel-forming mucins, have complex multidomain polypeptide structures. They contain cysteine-rich von Willebrand factor-like-domains capable of dimerisation and polymerisation. The capability of polymerisation is paramount for the gel-forming properties of these mucins.[389] MUC5AC and MUC5B are two polymers heavily expressed in the human airway mucus.[389, 390] MUC5AC is secreted constitutively into the airway by surface goblet cells, whereas MUC5B is released by submucosal glands.[392, 393] Numerous factors are implicated in the increased expression of MUC5AC including viruses, cytokines IL-4, IL-9, IL-13, IL-17, IL-23 and IL-25 and acrolein from cigarette smoke.[394-397] Furthermore, increased expression of MUC5AC and MUC5B mRNA were found in CRS mucosa compared to healthy mucosa.[239]

The production and secretion of polymeric mucin is regulated separately.[398] ATP is the key secretagogue acting on the apical membrane via $P2Y_2$ receptors. The constant presence of ATP in ASL induces a basal release of mucins onto the mucosal surface.[399] Submucosal glands also secrete low levels of polymeric mucus constitutively, capable of further stimulation from adrenergic, cholinergic, non-adrenergic and non-cholinergic nerves.[400] Increased mucin production leads to accumulation of intracellular dehydrated mucin contained in secretory granules.[401] When stimulated, the secretory granules are released onto the luminal surface and swell in size secondary to hydration.[402, 403] Therefore, rapid secretion of mucin can lead to depletion of ASL and consequent formation of concentrated thick, rubbery mucus.[400, 404, 405]

MUC5AC and MUC5B form homotypic polymers through bonding into a mesh or via noncovalent calcium-dependent cross-linking between neighbouring polymers.[389, 404] Furthermore, the glycan side chains are capable of attaching to large quantities of liquid, providing mucus its lubrication properties in addition to providing a liquid reservoir for the PCL.[406] The hydration of mucus greatly affects its viscosity and how effectively it can be cleared by the cilia. Mucin hypersecretion or dysregulation of the liquid volume results in highly viscous mucus, causing adhesion to the airway and difficult clearance.[405, 407]

Mucus has several antimicrobial functions. It is mildly acidic with a physiological pH of 5.5-6.5 with a small capacity as a chemical buffer.[357] Additionally, mucin glycans can sequester pathogens by providing a range of glycoproteins for interaction with microbes. The mucus layer acts a physical barrier to most pathogens, however, as the gel mesh has a relatively large pore size, and is readily penetrated by small viruses. Immunoglobulins A (IgA) and G (IgG) are found in high concentrations in mucus, contributing to the mucosal immunity.[408, 409] Secretory IgA, is the predominant immunoglobulin on the mucosal surface and acts as a physical barrier against antigens.[410] In response to increased vascular permeability, IgG is secreted to facilitate antimicrobial functions.[409]

The protective properties of mucociliary clearance, nasal mucus and the paracellular barrier integrity are vital in protecting the nasal mucosa from the constant bombardment of inhaled pathogens and irritants. The understanding of ciliary structure, motility and their role in MCC has evolved over recent decades. However, further studies are required to understand the role and interplay of mucus in chronic inflammatory conditions such as CRS.

NASAL MUCUS COLLECTION

Nasal mucus analysis is a crucial step in improving our understanding of various pathological conditions in rhinology. The collection method remains contentious with no standardisation or clinical guidelines currently available. Sample collection from differing subsites of the nasal cavity has the potential to influence results, for instance, mucus within the sinuses may have a different composition to the anterior or posterior nasal cavity. Furthermore, sampling techniques are heterogenous across the literature. Despite these differences, they are generally based on three underlying principles: spontaneous secretion collection, nasal irrigation and absorption devices.[411] Ultimately, there is a fine balance between procuring enough sample volume to analyse low abundant proteins and minimising discomfort and artefact.

The collection of spontaneously secreted mucus can be performed via nose blowing or suction devices. The main disadvantage to both these techniques is healthy individuals rarely have enough secretions for reliable collection and analysis.[411] The nose blowing technique is a quick simple method where patients blow their nose into a plastic or aluminium handkerchief which is then transferred to an Eppendorf tube for laboratory analysis.[412] The advantageous aspect of this method is it allows a fixed dilution with no irritation of the nasal mucosa. Alternatively, the use of suction devices allows for direct aspiration of mucus into a collection tube with minimal mucosal trauma.[413] When tested in our department, thick rubbery mucus would obstruct the suction device or remain adherent within the suction tubing. Phosphate buffered saline (PBS) irrigation of the tubing was performed to transfer the mucus into an Eppendorf tube for laboratory analysis.[57] The concern of using PBS would be varying dilutional factors between samples depending on mucus viscosity. Furthermore, over dilution may limit detection of low abundance proteins.[408]

Nasal irrigation is a commonly utilised technique within the literature, with the employment of various lavage solutions.[414, 415] Generally, isotonic or hypertonic saline is applied to the nasal cavity via a wash or spray and collected in a container for analysis.[411] This requires a compliant patient and is not always well tolerated. This method overcomes the previous issue of minimal sample volume, particular in healthy patients. A major drawback is unpredictable quantities of irrigation fluid is swallowed, absorbed or lost leading to an imprecise dilutional factor. Thus, results may have great variability with risk of over dilution and not being able to identify low abundance proteins. Studies have suggested the use of albumin as an endogenous marker of nasal mucus dilution. The relative concentration of analytes can be calculated as an index of albumin.[416]

The use absorption devices induce capillary suction to collect fluid, mainly from the PCL of nasal mucus. Various materials have been employed including: cotton, filter paper and sponges.[8, 411, 417] The absorptive material is inserted into the nasal cavity, commonly between the inferior turbinate and nasal septum, for 5-10 minutes. This is followed by rapid centrifugation to extract the absorbed mucus and prevent drying.[418] Advantages of this technique include: minimal patient cooperation, fixed sample dilution and clear differentiation between separate nasal subsites and nostrils. The minor shortcoming is it may cause mild irritation of the nasal mucosa with potential artefact production. Ultimately, the absorption method has been identified as the most superior in detection and reproducibility compared to other collection methods.[411]

Mucus collection techniques have gradually evolved with the common goal of obtaining valid and reproducible results with accurate assessments of a range of rhinological diseases. The idyllic method would involve the collection of sufficient sample volumes without significant

dilution with minimal trauma to the target mucosa. Thus, the absorption technique appears to be the most reproducible and well tolerated technique currently in the literature capable of detecting a range of immunoglobulins and cytokines.[8, 417]

MUCOSAL BARRIER FUNCTION ASSESSMENT

The assessment of the mucosal barrier incorporates a combination of structural and functional analyses. Functional assessments include transepithelial electrical resistance, macromolecule permeability and ciliary beat frequency. Structural analysis utilises microscopy in conjunction with immunofluorescence staining of tight junction proteins. In sinonasal barrier research, experiments are conducted in-vitro on primary human nasal epithelial cells (HNECs). These cells are collected from both healthy and CRS patients intraoperatively and grown to confluence on air-liquid-interface (ALI) cultures for experimentation.[180] Culturing cells on semipermeable supports, such as an Transwell plates (BD Biosciences, San Jose, California USA) used in ALI culture, allows nutrient supply from the basolateral compartment and exposure to air in the apical compartment.[419] This simulates in-vivo conditions of native HNECs.

TRANSEPITHELIAL ELECTRICAL RESISTANCE

Transepithelial electrical resistance (TER) provides an in-vitro measurement of intercellular junction integrity. Specifically, it provides real-time quantitative information about the ionic conductance of the paracellular pathway across the epithelial monolayer. Preparation of TER measurements require two components: a confluent cell monolayer cultured on a semipermeable membrane with apical and basolateral compartments and an Epithelial Voltohmmeter (EVOM) (Figure 2.11). One electrode is placed in the apical chamber and the other in the basolateral chamber. The EVOM generates an alternating current (AC) at 12.5 Hz across the STX2 (“chopstick”) electrode pair. The ohmic resistance is then calculated as a ratio

of the voltage and current, based on Ohm's law, in units of Ω.cm^2. [420] As the AC is applied across the cell monolayer, it traverses the transcellular and paracellular pathways.[421] The transcellular pathway is composed of the apical and basolateral membranes, whereas the paracellular pathway is composed of cell-cell contacts and cell substrates.[422] "Leaky" epithelia are defined as TER values below 1000 Ω.cm^2, indicating paracellular conductance greater than transcellular conductance.[421] Thus, the measurement of TER reflects changes in the paracellular units, consisting mainly of tight junction strands. Consequently, TER has been applied for the assessment of tight junction permeability following exposure to toxins and treatment solutions in CRS.[57, 423]

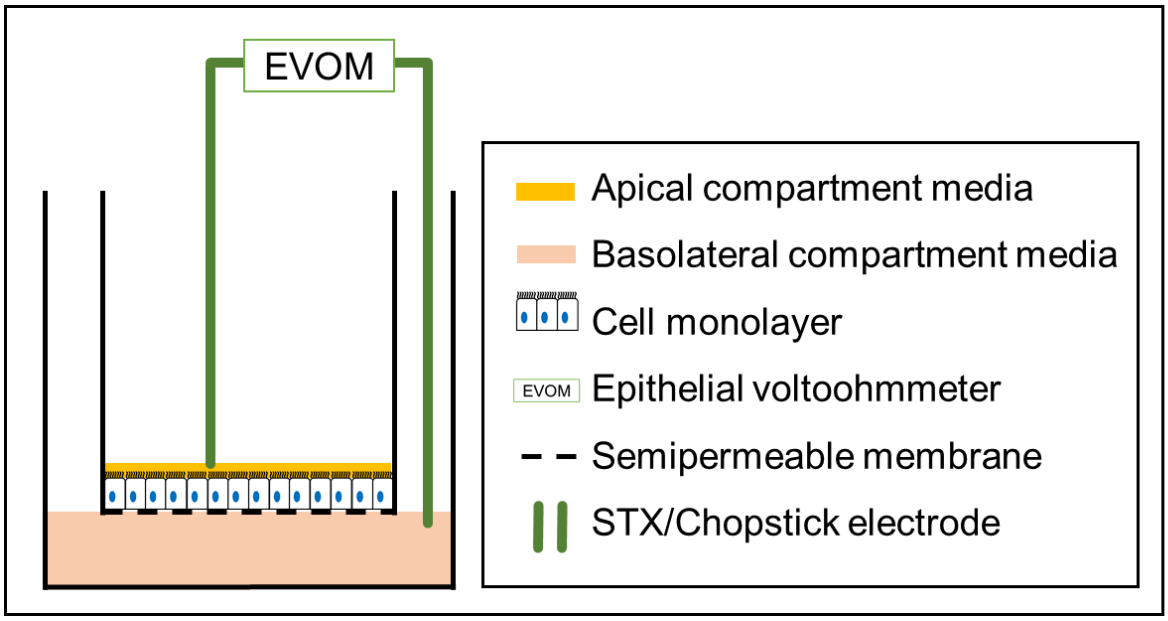

Figure 2.11. Transepithelial electrical resistance.

The configuration of the EVOM with chopstick electrodes within an air-liquid interface culture measuring the TER of the epithelial cell monolayer.

The TER measurements are greatly influenced by a range of equipment-, experimental- and operator-specific factors. Equipment factors include the specific device used, semipermeable membrane material and membrane pore size.[424] Experimental factors influencing results include the temperature, apical and basolateral compartment media and cell line utilised.

Studies have demonstrated ideal conditions for TER measurements to be at 37ºC.[420] Furthermore, culture period is another important factor to consider, as 21 days is thought to be optimal time for tight junction formation.[425, 426] Lastly, operator specific factors include correct electrode placement as TER readings are highly reliant on electrode positioning. Additionally, careful placement of electrodes without disruption of the cell monolayer is crucial. Thus, recording multiple measurements from a large number of ALI cultures may minimise this bias.

PARACELLULAR PERMEABILITY ASSAY

The paracellular permeability to macromolecules is determined by the leak pathway and provides information on the rate of flux across the cell monolayer of a pre-determined macromolecule. Previously employed marker molecules include inulin, mannitol, albumin, fluorescein isothiocyanate (FITC)-labelled dextran and horseradish peroxidase.[420, 427] These compounds are applied to the apical chamber of the ALI culture, and after a predetermined time, the supernatant is collected from the basolateral compartment for analysis. The quantity of fluorescent macromolecule passage is determined via a fluorescence microplate reader. Higher levels of marker macromolecules detected in the basolateral supernatant implies greater paracellular permeability. The permeability is quantified by the permeability coefficient (Papp, cm/second), based on the flux of the selected tracer across the monolayer.[420, 428] The following equation is utilised: $Papp = \left(\frac{dQ}{dt}\right) \times \frac{1}{A.C0}$, where $\frac{dQ}{dt}$ is the compound quantity over time, A is the area of the membrane *and* C_0 is the starting concentration of the compound.[429] Similarly to TER, the activity of these compounds is influenced by varying temperatures, pH and semipermeable membrane pore sizes.[420] Together with TER measurements, paracellular permeability assays can provide important information regarding the epithelial barrier status.[430]

IMMUNOFLUORESCENT MICROSCOPY

Immunofluorescent microscopy is a valuable method of identifying and localising integral and scaffolding proteins at the apical intercellular junction. A laser scanning confocal microscope is employed to visualise specific proteins in three planes.[431] Intercellular junctional proteins from TJs, AJs, GJs and desmosomes can be stained to display varying patterns of localisation and configuration. Following exposure to irritants or treatment solutions, specific intercellular junctional reorganisation or disruption is observed under confocal microscopy.[55, 432] This method of structural analysis coincides well with the functional assessments of barrier integrity and paracellular function described above.

CILIARY BEAT FREQUENCY

Ciliary beat frequency measurements provide vital information regarding real-time cilia function. This is performed with an inverted microscope and the specialised program Sisson-Ammons Video Analysis (SAVA) to visualise, record and calculate CBF. The HNEC cell monolayer grown to confluence differentiates and develops cilia over four to six weeks, which can be identified on microscopy.[433, 434] As cilia motility is affected by temperature, experimentation should be conducted at 37^{O}C, similar to TER.[357] Baseline and post-treatment CBF can be determined to ascertain the effects of exposure to irritants and treatment solutions.[423]

CHAPTER 3: PROTEOMICS

BACKGROUND

Proteomics is the systematic identification and quantification of proteins within a biological system at specific point in time. The goal of proteomics is to procure a comprehensive and integrated assessment of cellular biology through studying all the proteins present with their associated interactions. Specifically, this involves reviewing protein interactions, modifications, functions and localisation to formulate a comprehensive three-dimensional (3D) cellular map.[435] Proteins are under constant alteration via posttranslational modifications, translocations, synthesis or degradation from both internal and external cues. Thus, the cellular proteome is a dynamic entity, where analysis only reflects the immediate cellular environment during sample collection. The evolution of proteomic analysis has led to the integration of numerous scientific disciplines including molecular and cellular biology, bioinformatics and analytical chemistry with the utilisation of multifaceted instruments and software such as electrophoresis, chromatography and mass spectrometry.

Histologically, proteomics began with mapping proteins from *Escherichia coli* and guinea pigs.[436, 437] One-dimensional (1-DE) and two-dimensional (2-DE) protein gel electrophoresis became valuable techniques for separating proteins for visualisation, without protein identifying capabilities. Edman degradation was the breakthrough microsequencing technique that was capable of identifying the proteins from 2-DE.[438-440] The most important advancement in proteomic analysis has been the development of mass spectrometry (MS) technology.[441] Over recent decades, the sensitivity and accuracy of protein identification and quantification have increased dramatically.[441, 442] Furthermore, as MS is able to analyse protein mixtures with high throughput capabilities, it has largely replaced Edman sequencing as the primary protein identification tool.[435]

The evolution of proteomics is a direct result of advances in the large-sale nucleotide sequencing of genomic DNA. In 1995, *Haemophilus influenzae* was the first organism to have its complete genome sequenced.[443] The Human Genome Project began in 1988, with the full sequence completed in 2003.[444] These studies have assisted in formulating detailed databases vital in the protein identification process.[445, 446] Irrespective of technological advances in MS, without information from these DNA sequences, protein identification would be challenging.

PROTEOMIC PRINCIPLES

The study of proteins is the next vital step in understanding the intricacies of cellular biology and processes. Previously, mRNA expression analysis with serial analysis of gene expression (SAGE) and DNA microarray technology were performed to understand physiological and pathological cellular processes.[447, 448] However, mRNA does not reflect intracellular protein content and expression as it is only one component in the complex sequence of events in protein synthesis. Firstly, mRNA is influenced by posttranscriptional control via polyadenylation, alternative splicing and mRNA editing which can generate numerous protein isoforms.[449] Secondly, mRNA is translationally regulated. Thirdly, synthesised proteins are prone to posttranslational modifications, proteolysis and compartmentalisation.[450] Posttranslational modifications occur secondary to a variety of intra- and extracellular signals.[451] Protein phosphorylation is a common and vital signalling process with dysregulation leading to a range of pathologies.[452] Protein localisation is another important cellular regulatory mechanism.[453] Identifying the subcellular localisation of proteins, improves the 3D protein mapping within the cells to improve our understanding of protein regulation.[435] Lastly, studying protein-protein interactions are fundamental to understanding vital cellular processes including cell growth, cell cycle regulation and apoptosis.[454] Proteomics aims to incorporate knowledge from all these

properties exhibited by proteins to formulate a better understanding of cellular processes in healthy and diseased tissue.

The fundamental approach to studying the function of proteins within complex biological processes is through correlation of protein expression during states of biological change. The study of proteomics can be stratified into three areas: expression, structural and functional proteomics. Investigating the quantitative protein expression differences between samples is referred to as expression proteomics. In this process, entire proteomes can be compared, which is important in identifying distinct proteins in signal transduction pathways in disease-specific processes. Structural proteomics aims to identify protein structures within organelles, determining subcellular localisation and characterise protein-protein interactions.[455] This method is important in establishing cellular architecture and exploring the unique properties of cells from their specific protein expressions. Lastly, functional proteomics involves studying isolated protein complexes, which can provide important information regarding protein signalling, drug-protein interactions and disease-specific mechanisms.[435] Thus the approach and technique applied will depend on the research question and the proteomic area of interest.

As described above, the process of protein identification and analysis has evolved over recent decades. Advances in technology and equipment have allowed for improvements in sensitivity and resolution of proteins identified. Proteomic experiments can be stratified into three components: protein separation and isolation, protein structure acquisition and database utilisation with protein identification.[435]

PROTEIN SEPARATION AND ISOLATION

The analysis of complex protein mixtures obtained from tissues and secretions is commonly encountered. It is vital to resolve these protein mixtures into individual components to improve protein visualisation, identification and characterisation. This can be achieved with a range of gel-based or non-gel-based approaches.

GEL-BASED APPROACHES

Polyacrylamide gel electrophoresis is the most effective and commonly utilised method of protein separation and isolation of complex protein mixtures. Proteins are initially solubilised in sodium dodecyl sulphate (SDS) prior to separation. 1-DE is a commonly utilised technique to resolve protein mixtures, where proteins are separated based on molecular mass. It has been found to be a reproducible technique capable of identifying proteins between 10 to 300 kDa. Furthermore, protein samples with exceptionally high or low isoelectric points that cannot be separated by 2-DE can be pre-fractionated by 1-DE to increase protein identification.[456] Typically, 1-DE is employed in the characterisation of proteins following a protein purification process for complex analytes, due to its limited resolving power. Thus, the use of 2-DE is a more sensitive approach for analysing complex protein mixtures, such as cell lysates.

In 2-DE, proteins are separated by net charge in the first dimension and molecular mass in the second dimension. This technique produces protein "spots" with higher resolution than 1-DE protein "bands". Furthermore, 2-DE is also a powerful technique capable of resolving, characterising and cataloguing thousands of proteins.[446, 457, 458] The addition of dyes, such as Coomassie Blue or Sypro Ruby, aid imaging software in visualising and analysing gel samples. A significant advantage of 2-DE is the ability to distinguish proteins that have undergone posttranslational modifications. For example, phosphorylated proteins can be distinguished

from nonophosphorylated proteins by their differences in molecular mass and charge in 2-DE.[459] Additionally, different forms of proteins arising from mRNA splicing or proteolytic processing can also be separated and isolated. The primary application of 2-DE is in protein expression profiling where the protein expression from two samples are compared qualitatively and quantitatively. The presence or absence of spots indicates differences in protein expression with varying intensity of spots providing information on protein expression levels. This technique is useful in comparing normal tissues with diseased tissues or following drug treatments.[460, 461] The employment of immobilised pH gradients in 2-DE is a significant advancement in improving resolution and reproducibility.[462, 463] A high degree of accuracy is required in spot detection and annotation, as this has great implications in the downstream protein identification. A range of computer software and molecular scanners have been suggested to assist in this process of identifying and quantifying proteins between samples.[464, 465]

Difference gel electrophoresis (DIGE) employs fluorescent dyes to tag proteins from different samples.[466] These tagged protein samples are run on the same 2D gel and post-run fluorescence imaging superimposes the two samples to identify protein differences. The amine-reactive dyes bind to common proteins from both samples to ensure they have the same relative mobility, thus aiding in identifying differentially expressed proteins. Ultimately, this avoids the need for numerous 2-DE gels for comparison.[467]

Despite the versality of gel-based techniques, both 1-DE and 2-DE are slow and labour-intensive with little scope for automation. Similar to 1-DE, 2-DE is also limited by the number and type of proteins that can be resolved. Large or hydrophobic proteins and high acidity (pH<3) or basicity (pH>10) both negatively influence protein mobility through the gel.[463] These

issues can be addressed with altering the solubilisation conditions and pH gradients of the protein mixtures. Furthermore, low abundance protein detection is difficult in total cell lysates.[446, 468] In crude cell extracts, high abundance proteins dominate the gel, making the detection of low abundance proteins difficult. Due to these limitations, the optimal application of 2-DE is in the analysis of pre-purified samples, protein complexes or sub-proteomes instead of whole proteomes.[435]

NON-GEL-BASED APPROACHES

The challenges and limitations present in gel-based protein separation and isolation has led to the development of different approaches in an attempt to bypass or work in unison with gel electrophoresis. The digestion of proteins into peptides, with peptide purification, prior to MS analyses has been utilised. These peptide purification methods are centred on the use of various chromatography techniques, separating proteins based on charge, size and affinity to biological molecules.

Ion exchange chromatography (IEC) separates proteins based on charge and is stratified into two types: anion- and cation-exchange chromatography.[469] As the sample traverses the columns, the stationary phase (Ion exchanger) binds to molecules of its opposite charge. These bound molecules are then eluted with an eluant of gradually increasing concentration gradient or changes in pH. Size exclusion chromatography (SEC) separates proteins based on molecular size through a porous matrix.[469] In affinity chromatography, proteins are separated via reversible interactions between proteins and the affinity ligand of the chromatographic matrix.[469] Targeted molecules bind to the stationary phase, based on a unique property, and the mobile phase carries away the non-target molecules. An elution buffer is applied to the columns

to release the bound target molecules, resulting in a highly purified sample. These techniques are commonly employed to aid in sample separation and identification.

Multidimensional chromatography-based profiling of intact proteins has emerged as an effective alternative to gel electrophoresis separation prior to MS. These techniques include nonporous reversed-phase high pressure liquid chromatography (RP-HPLC) and 2D liquid chromatography (2DLC).[470] During the first dimension, proteins are separated according to their isoelectronic point. This is followed by RP-HPLC with nonporous silica where proteins are further separated based on their surface hydrophobicity. This system can be automated, and when combined with an electrospray ionisation time of flight-based mass spectrometer, permitting a faster separation process.[471] Additionally, the volatile mobile phase aids the MS to accurately detect intact-protein molecular-weight information and posttranslational modifications.[470]

Multidimensional protein identification technology (MudPIT) is a popular protein profiling technique capable of extracting peptide sequences directly from complex proteolytic digests. Initially, peptides are eluted through the cation-exchange column with a continuous gradient of salt concentration. With every increment of the gradient, peptides pass through a RP-HPLC column to undergo a second-dimension separation and further salt removal. Finally, the sample enters the mass spectrometer for tandem mass spectrometry analysis.[470]

PROTEIN ACQUISITION

Protein acquisition is the next vital step in protein identification. As previously discussed, Edman sequencing was first ground-breaking technique utilised in protein identification.

Advances in technology and the invention of mass spectrometers have led to significant improvements in protein acquisition.

EDMAN SEQUENCING

Initially developed by Edman in 1949, Edman sequencing is capable of identifying the amino-acid sequences in peptides and proteins. This method involves labelling and cleavage of the N-terminal amino-acid with phenyl isothiocyanate. Under alkaline conditions, this forms a phenylthiocarbamoyl derivative which is analysed in chromatography or electrophoresis to identify the amino-acid. This process is continued for the remaining amino acids, up to 30 in a sequence.[438] As time has progressed, advances in sequencing technology has improved sensitivity and ease of this technique. Edman sequencing is usually employed in identifying proteins transferred to membranes. Thus, establishment of membranes compatible with sequencing chemicals allow for effective Edman sequencing following SDS-polyacrylamide gel electrophoresis.[472, 473]

MASS SPECTROMETRY

Mass spectrometry is currently the most utilised method for identification of protein structure through amino acid sequences or peptide masses searched against protein and nucleotide databases. Additional benefits of MS include detecting protein modifications and quantitative protein expression. The process of MS protein identification can be summarised into 3 principles: (1) transforming molecules into a gaseous phase, (2) separating ions based on mass and charge within an electric or magnetic field and (3) the quantity of the product ion is measured based on their mass-to-charge ratio (*m/z)*.[469] This procedure is divided into four stages: (1) sample preparation, (2) sample ionisation, (3) mass analysis and (4) peptide fragmentation.[435] Mass spectrometers are composed of 4 components: the ionisation source,

one or more mass analysers, an ion mirror and a detector. Mass spectrometers are named based on their ionisation source and mass analyser.

SAMPLE PREPARATION

Sample preparation for proteomic MS analysis is commonly performed with polyacrylamide 1-DE or 2-DE.[474] Sample purification prior to gel electrophoresis is required for complex protein mixtures, such as cell lysates, to aid in improving resolution and reducing artefacts. Effective protein separation within the gel is vital for peptide extraction and improved sensitivity of MS analysis. Peptide extraction from the gel is generally conducted as an "in-gel" digestion with proteases, such as trypsin.[475] This transformation of proteins into peptides provides more detailed and reproducible data. The post-digestion sample undergoes further purification with RP-HPLC.[435] The removal of gel contaminants such as salts, buffers and detergents aim to reduce artefacts during MS analysis.[476]

SAMPLE IONISATION

Samples must be converted to desolvated ions as MS can only analyse dry and charged molecules. Common techniques utilised to ionise peptides include electrospray ionisation (ESI) and matrix-assisted laser desorption/ionisation (MALDI). Both techniques convert peptides into ions through the addition or removal of protons without loss of sample integrity. This is an important property as it permits accurate mass data collection of the protein in their native state.

In ESI, the sample traverses a microcapillary tube into the orifice of the mass spectrometer. A fine mist of charged droplets are generated from the potential difference between the microcapillary tube and mass spectrometer inlet.[476, 477] Gradual evaporation of these ultrafine droplets results in desolvated ions (Figure 3.1).[477] Advancements in ESI include the

introduction of nanospray ionisation where the microcapillary tube orifice diameter is 1 to 2 µm with low flow rates of 5 to 10 nl/min.[478] This reduced flow rate greatly reduces sample consumption with increased analysis time.[475] To improve accuracy and throughput, liquid chromatography (LC) systems are coupled with ESI sources to automate sample purification and delivery into the mass spectrometer.

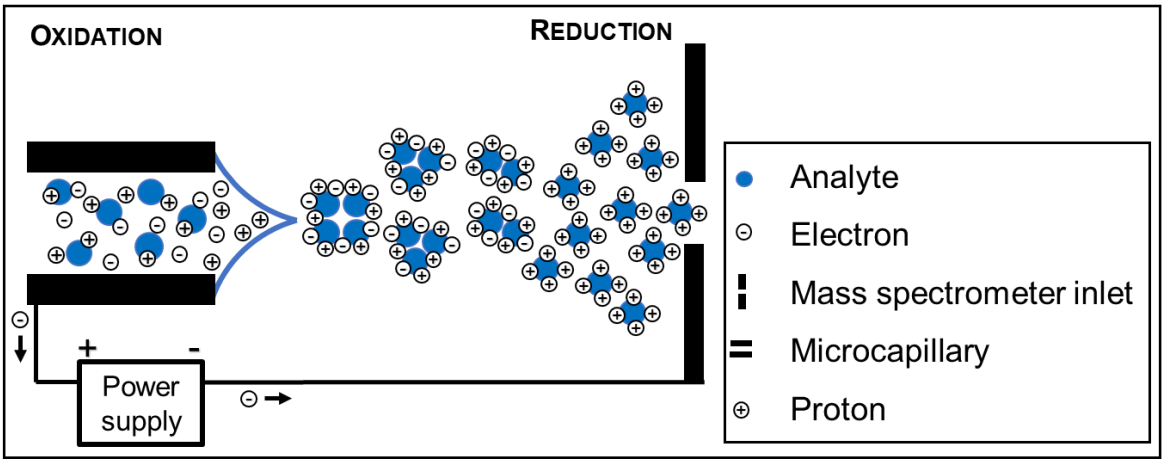

Figure 3.1. Electrospray ionisation.

The fine mist of charged droplets are generated from the microcapillary tube. Gradual evaporation of these ultrafine droplets results in desolvated ions entering the mass spectrometer inlet. Adapted from Konermann et al.[479]

In MALDI, the sample is spotted along an energy-absorbing matrix, typically composed of 2,5-dihydroxybenzoic acid or α-cyan-4-hydroxycinnamic acid, on a plate and allowed to dry to form crystals. Laser irradiation is directed onto the analyte-matrix, inducing a vibrational excitation of the matrix molecules. Clusters of the analyte-matrix complex are released as a gaseous phase from the sample plate. The analyte ions are ionised through proton transfer from the matrix molecules (Figure 3.2).[480] The matrix is vital in this process as it acts a buffer for the fragile protein analyte against the laser. The ionised sample is then sent to the mass analyser for analysis. The key advantage of MALDI is this whole process can be automated.

Furthermore, samples do not always need to be purified following in-gel digestion, unlike ESI.[481]

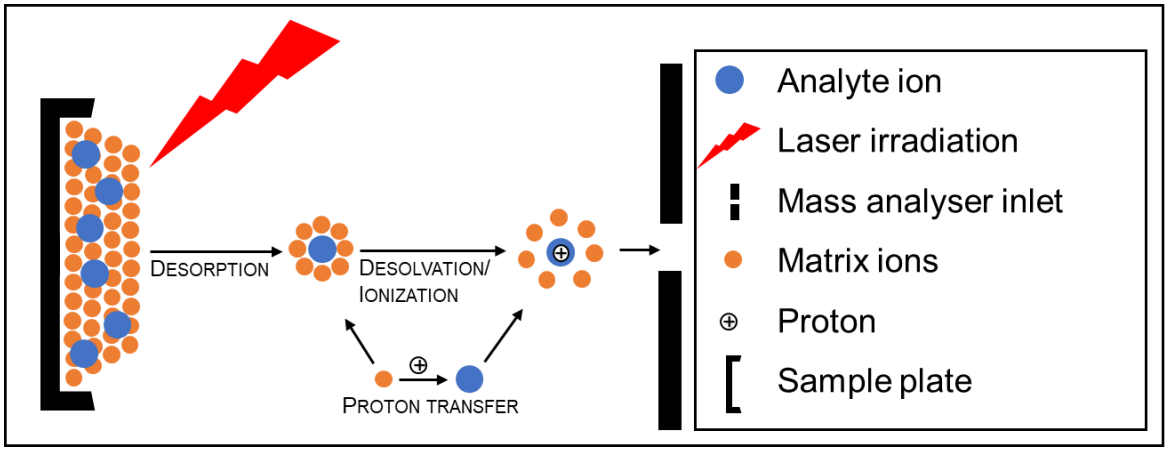

Figure 3.2. Matrix-assisted laser desorption/ionisation.

Laser irradiation of the analyte-matrix complex induces the formation of ionised molecular ions through desorption and ionisation. Adapted from Singhal et al.[482]

MASS ANALYSIS

Mass analysis is performed by mass analysers within the mass spectrometer where the ionised molecular ions are resolved based on their mass and charge state. The mass analyser generates a mass spectrum, which is a plot of relative ion abundance against *m/z*. This analysis of peptides and proteins require MS instruments having effective algorithms for peak picking, charge-state recognition and deisotoping. Furthermore, the generation of high-quality parent and fragment mass spectral ion peak lists are vital when used to search the numerous protein databases.[470] Various mass spectrometers are employed across the field of proteomics as there is no single analyser suitable for all applications.

Ion trap mass analysers are capable of trapping and "storing" ions in a 3D electric field and selectively ejecting them for analysis.[476] It is composed of a ring electrode situated between two opposite facing end cap electrode plates. Ions are trapped between the electrodes by the

oscillating radiofrequency (RF) field with a superimposed direct current (DC) potential. Ions with specific *m/z* are selectively ejected into the detector by changing the RF potential (Figure 3.3). The ability to trap and accumulate ions improves the sensitivity. However, despite improvements in technology, ion traps have low resolving power compared to newer types of mass analysers.

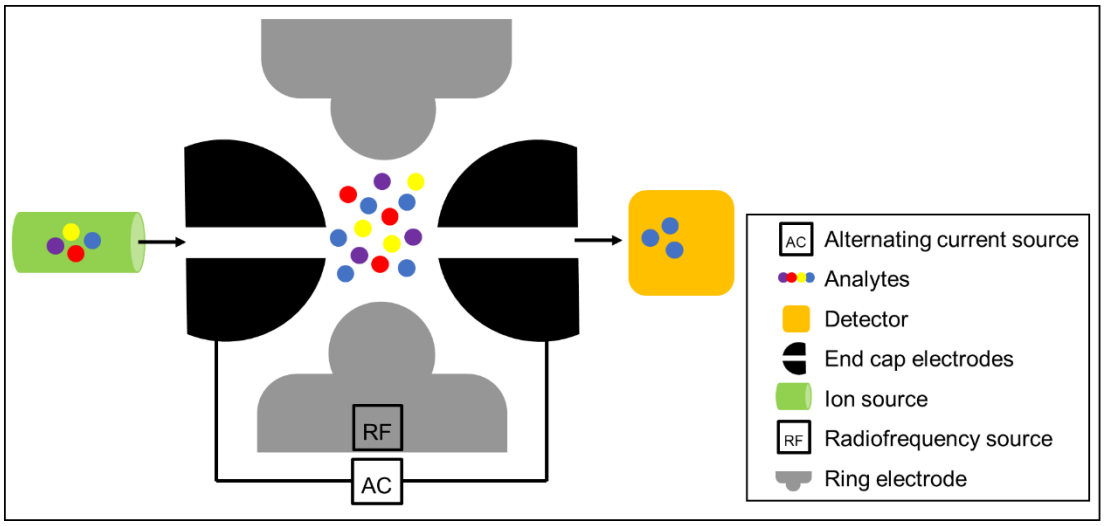

Figure 3.3. Ion trap mass analyser.

Ions are trapped between in an electric field generated by the ring electrode and end cap electrodes. Ions with specific *m/z are ejected into the detector for analysis. Adapted from Haag et al.*[483]

Quadrupole mass analysers are capable of transmitting and filtering ions of various *m/z*. It is composed of four electric field generating parallel metal rods, the quadrupole, which ions traverse from the ionisation source to the detector.[476] A RF potential with a superimposed DC potential is transmitted through these rods inducing oscillation of passing ions (Figure 3.4). By varying the DC and RF potentials, the trajectory of the ions with specific *m/z* will change. Consequently, ions with the stable trajectories are filtered through the quadrupole and ions with unstable trajectories will collide with the rods and be filtered out.[483] Additionally, quadrupoles can function in "RF-only" mode where the analyser functions to transmit ions between different

areas of the mass spectrometer or as a collision cell. Within the collision cell, collision-induced dissociation (CID) occurs when transmitted ions collide with an inert gas (commonly argon or nitrogen) present within the cell, leading to ion fragmentation. Alteration of the RF potential changes the amount of ion fragmentation. Quadrupole mass analysers are popular due to their low cost, durability and reliability. Additionally, they are commonly utilised in tandem with each other, in triple quadrupole mass spectrometers, or with other mass analysers, such as time-of-flight.

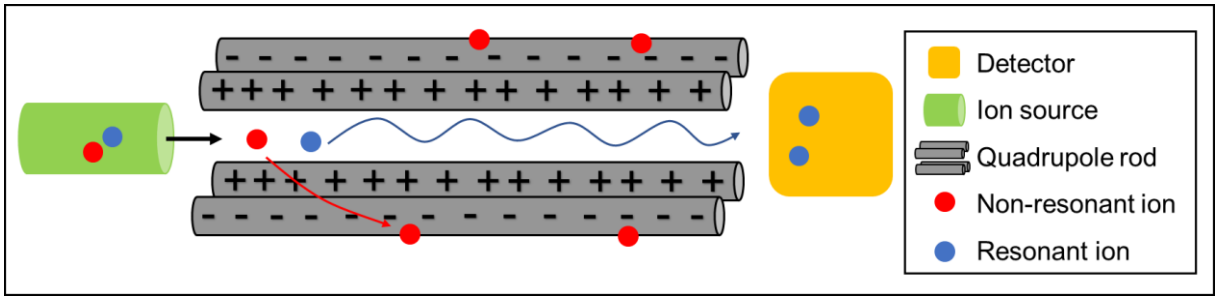

Figure 3.4. Quadrupole mass analyser.

Resonant ions with a specific m/z traverse the quadrupole with a stable trajectory to the detector for analysis. Ions with an unstable trajectory collide with the quadrupole rods and are consequently filtered out. Adapted from Haag et al.[483]

Time-of-flight (TOF) mass analysers are capable of calculating ion *m/z* through measuring the time required for ions to traverse the length of the flight tube. As ions with differing *m/z* are accelerated through the field with the same kinetic energy, arrival times at the detector will differ (Figure 3.5). The mass is a calculated as function of travel time as the initial kinetic energy and flight tube length are constant. Furthermore, ion mirrors are incorporated to increase the flight tube length to increase the mass resolution, through correcting minor differences in kinetic energies.[476] A key advantage of TOF mass analysers is the ability to detect the largest mass range of all analysers.

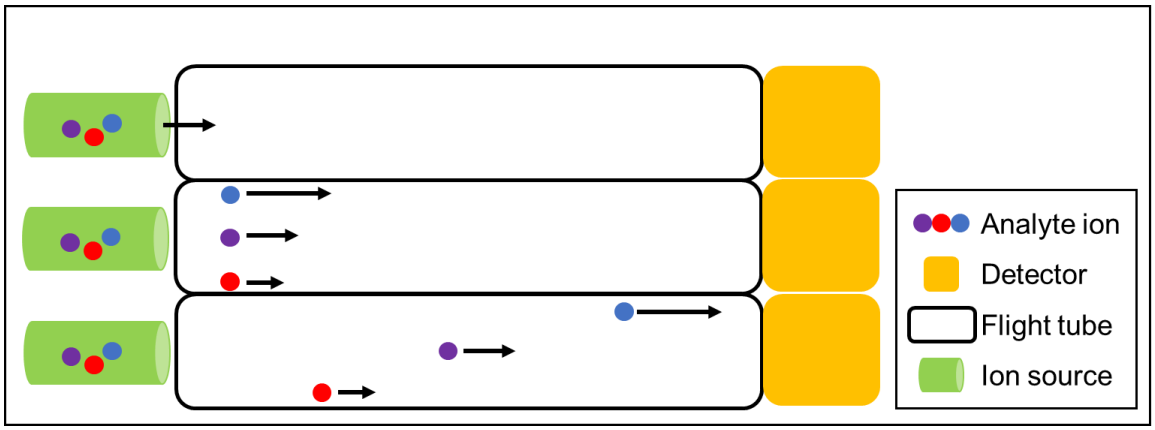

Figure 3.5. Time-of-flight mass analyser.

Ions are accelerated through the flight tube with the same initial kinetic energy. Differing arrival times are due to varying m/z of the individual ions. Adapted from Haag et al.[483]

The Fourier transform ion cyclotron resonance (FT-ICR) mass analyser is a high-resolution ion-trapping analyser useful in complex protein mixtures.[484] Packets of ions are introduced and trapped into a magnetic field, called a Penning trap. These ions assume a circular motion in a perpendicular plane to the magnetic field, where the angular frequency is known as the cyclotron frequency. Excitation by the RF field induces the ions to have higher cyclotron orbits leading to detection. Signal intensity detected by the receiver plates are digitised according to time and converted to a frequency spectrum via the Fourier transform.[483] The key advantage of the FT-ICR analyser is its vast resolving power. This requires large superconducting magnets which are both expensive and space occupying. Additionally, liquid helium is required to as coolant further adding to the cost. Due to these factors, FT-ICR mass analysers are uncommonly utilised.

The orbitrap is an ion trap mass analyser that induces oscillations of trapped ions whilst travelling in an orbital motion around the central spindle. In contrast to the magnetic field generated by the FT-ICR analyser, the orbitrap induces oscillations with an electric field. It is

composed of two outer hollow concave electrodes surrounding an inner spindle electrode covered by a thin dielectric material. (Figure 3.6) A linear electric field is created between the outer electrodes when a voltage is applied. Packets of ions are introduced through a hole in the outer electrodes and travel between the inner and outer electrodes in a spiral path. Harmonic axial oscillation of the ions occurs secondary to the conical shape of the electrodes, which is detected by the outer electrodes. Acting as receiver plates, these outer electrodes convert this signal from the time domain to a frequency domain, similar to the FT-ICR analyser. Orbitraps have high resolving power with high molecular weight compounds, such as proteins. Furthermore, when compared to the FT-ICR analyser, the orbitrap is a smaller machine without the need for cryogenic coolants.

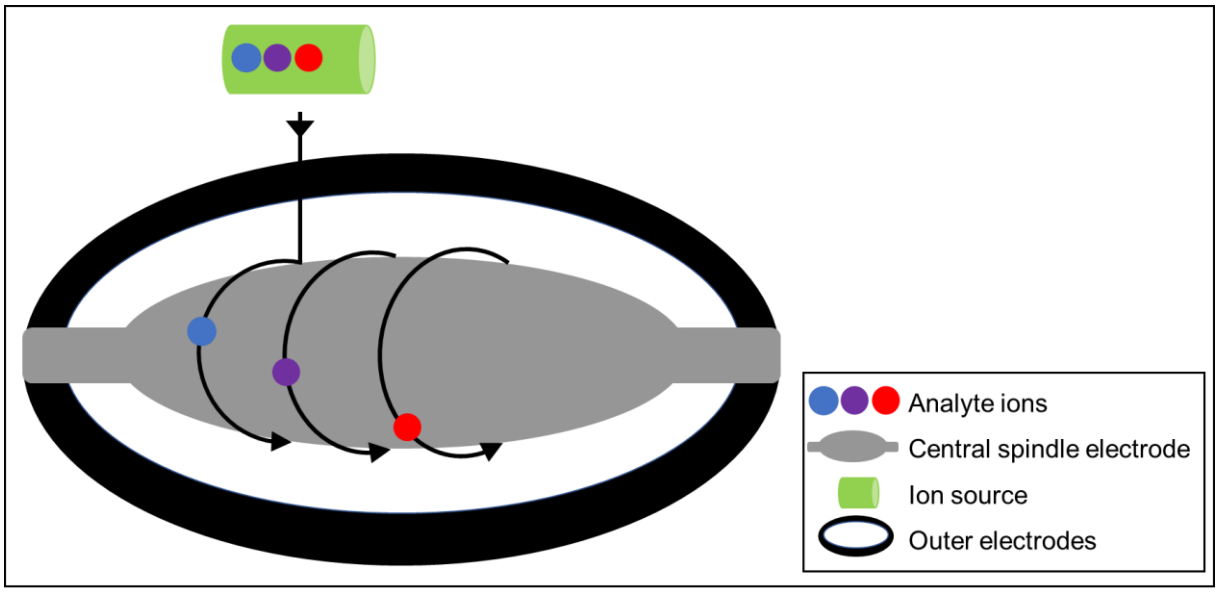

Figure 3.6. Orbitrap mass analyser.

Ions enter the electric field travelling in a spiral path around the inner spindle electrode. The outer electrodes detect oscillations from the spiralling ions, converting the signal to a frequency domain. Adapted from Haag et al.[483]

TANDEM MASS ANALYSERS

Mass spectrometers commonly utilise consecutively arranged mass analysers, called tandem mass spectrometers, to improve resolution and sensitivity. Generally, the first analyser selects ions with a particular *m/z* value, and induces CID, where the following product ions are analysed by the second mass analyser.[483] The conversion of kinetic energy from the collision to internal energy of the ions causes the breakage of bonds within the analyte. These product ions provide further information regarding the structure of the protein assessed.

Tandem mass spectrometry (MS/MS) is performed to acquire the amino acid sequence, where proteins and peptides are fragmented into smaller peptides.[485] Peptide ions undergo fragmentation upon entering the collision chamber and interacting with collision gases. Fragmentation primarily occurs along the peptide backbone, however, cleavage can also occur along amino acids chains.[476, 486] The introduction of fragmentation nomenclature is useful in describing the various cleavage types. If a charge is maintained following cleavage of a peptide bond at the N-terminal, this is deemed a *b-ion*. Alternatively, if the charge is maintained at the C-terminal, this is designated a *y-ion*.[487-489] The mass difference between neighbouring b- and y-ions correspond to distinct amino acids. Thus, peptide sequences can be extrapolated from amino acids identified. The exception to this rule is isoleucine and leucine, as both have identical masses. They can be differentiated with the cleavage of the amino acid side chains. These complex processes are performed by a range of mass analysers including: quadrupole, time-of-flight and ion trap analysers.

Triple quadrupole mass spectrometers are useful in amino acid sequence identification. Three quadrupole analysers are used in tandem and commonly referred to as Q1, Q2 and Q3.[483] The Q1 analyser is capable of scanning a range of *m/z* values or selectively filtering ions of a particular *m/z* value. As the ions pass into Q2, this quadrupole acts the collision cell causing

ion fragmentation. Ultimately, the product ions are sent into Q3 to acquire a mass spectrum.[489, 490]

Quadrupole-TOF mass spectrometers are hybrid instruments indicated in protein identification and protein modification characterisation. The characteristics of quadrupole and TOF analysers differ in that the former operates more effectively with a continuous stream of ions, whereas the later prefers pulses or packets of ions. Thus, for these analysers to work synchronously, the TOF analyser is arranged perpendicularly to the quadrupole analyser. This layout allows ions to traverse the quadrupole and pass into the perpendicularly located TOF analyser with a set of push and puller plates between the analysers.[483] The largest advantage of this technique is the higher resolution and accuracy with amplified scanning speeds compared to the triple quadrupole. Furthermore, its compatibility with LC allows for rapid MS/MS analysis.

MALDI-TOF is an effective automated first-pass device for protein identification utilising peptide mass fingerprinting (PMF). It is commonly the method of choice for large-scale proteomic analysis due to its ability to be automated.[491] The disadvantage of MALDI is the reduced sensitivity in protein identification compared ESI mass spectrometers.

The TOF-TOF mass spectrometer performs CID between the two TOF analysers. As ions travel through the first flight tube, they become separated based on the *m/z* value according to their velocity. The time-ion-selector gate filters ions with a particular *m/z* value based on their arrival time. Upon passing this gate, ions are decelerated prior to entering the collision cell for CID. Finally, the product ions are reaccelerated and traverse the second TOF analyser for analysis. This rapid analysing technique is useful in trypsin digested peptides, particularly in combination with MALDI.[483]

DATABASE UTILISATION

The final stage of protein and peptide identification involves searching and matching mass spectrometric data against an up-to-date protein database. Protein identification by mass spectrometers is performed through masses from peptide peaks or from the MS/MS fragmentation spectrum of peptides.[470] As with all research, the quality of the data generated is dependent on the quality of the data inputted into the mass spectrometer. Furthermore, the quality of the database utilised in conjunction with specific search parameters are vital to obtaining confident protein identification. The two common methods of database searches include the PMF and amino acid sequence databases.

In PMF, the peptide mass of the unknown protein is compared to a theoretical peptide mass in the database. Protein identification occurs when there is significant overlap of the mass spectrum between the real and theoretical samples.[492, 493] The primary advantage of this method is the capability for full automation. The main disadvantage of this technique is ambiguity in protein identification with complex protein mixtures. Furthermore, changes in peptide mass following posttranslational modifications in the unknown sample will not match with unmodified samples in the database.[494] Generally, PMF is useful in organisms with small, completed sequenced genomes.

Amino acid sequence database searching is the most specific method of protein identification.[495] Proteins or peptides of interest undergo dissociation into fragment ions within a mass spectrometer. The resulting precursor peptide mass and resulting fragment ion masses are searched against known peptides within the database.[496] This technique is far more specific than PMF with a significant advantage of use in peptide mixtures. Pattern recognition algorithms are capable of rapidly identifying proteins, however, manual review with sequence

identification is commonly required to prevent incorrect protein identification. Methods of increasing the confidence of protein identification includes analysis of individual gel spots or bands to reduce sample complexity. Secondly, the MASCOT search program employs a probability-based scoring algorithm assigning scores to proteins identified, reducing false positives.[470] Despite these improvements, this process remains time consuming requiring considerable computing power.

Bioinformatics is a rapidly evolving field with capabilities of managing complex high throughput data generated from proteomics experiments. A large issue with proteomics is the analysis of high quantities of data and establishing associations with genomics and metabolomics.[469] Thus, a range of programs and algorithms have been developed to establish protein and regulatory pathways from identified proteins present in the analyte. Gene set enrichment analysis (GSEA) a common method of interpreting gene expression from the vast number of proteins within a sample, and identifying associations with disease processes.[497] This technique utilises a powerful biostatistical software to identify biological processes from the differentially expressed proteins with the aid of genome databases. This is a vital step in understanding the cellular proteome, as proteins uncommonly act alone, they generally interact with other proteins to form complexes and intricate process leading to specific biological effects.[469] The integration of bioinformatic analysis enables further understanding of the intricate relationship between proteins and the subsequent changes in cellular pathways and biological processes.

NASAL MUCUS PROTEOMICS

The proteomic analysis of nasal mucus is a rapidly developing field exploring the physiological and pathological mechanisms involved in CRS. These advances are paramount in

understanding the various heterogenous inflammatory profiles present, thus allowing clinicians and researchers to effectively classify CRS endotypes. Understanding these complex and intricate upstream processes involved in the chronic inflammatory nature of CRS will provide insights into the downstream clinical manifestations. Various studies have investigated differences between the healthy and CRS proteome with samples collected from mucus and mucosa. A differential expression of proteins involved in inflammatory responses, oxidative stress and impaired mucosal immunity was found in CRS samples.[498, 499] *Tewfik et al* found reduced lysosome C precursor in CRSwNP patients, a protein with bacteriolytic activity.[500] Interestingly, the most recent study directly comparing the CRS and healthy proteome was published over 9 years ago.[499] Substantial advances in MS instrumentation with improvements in processing speed, sensitivity and resolution has occurred. Therefore, an up-to-date systematic review of the literature is required to determine the progress of CRS proteomics to direct future research. Ultimately, improvement in the understanding CRS endotypes through protein interactions and cellular processes will assist in guiding management plans for these patients.

CONCLUSION

Proteomic analysis is an exciting and rapidly evolving field secondary to the significant improvements in technology. Growing knowledge of sample processing and purification techniques have allowed improved analysis with MS. Ongoing improvements in automated platforms will decrease human error and speed up the processing and analysis of complex protein mixtures. These improvements in instrumentation and methodology greatly increase sensitivity and proteome coverage. Proteomics in CRS is an exciting frontier, with rapidly expanding knowledge and techniques improving our understanding of the complex interactions between proteins in CRS pathophysiology.

CHAPTER 4: THESIS

Chronic rhinosinusitis (CRS) is a clinical syndrome characterised by the persistent mucosal inflammation of the nasal cavity and paranasal sinuses. Globally, it has significant effects on the quality of life of many sufferers with a large burden on the healthcare system. There is yet to be a consensus on the pathophysiology of CRS, with numerous hypothesise proposed. The immune barrier hypothesis proposes the chronic inflammation leading to barrier dysfunction inducing the development of CRS. The overactivation of inflammatory cells, such as neutrophils, with subsequent secretion of neutrophil serine proteases (NSPs) may cause collateral damage to the host tissue. Studies have identified increased activation of proinflammatory cytokines following neutrophil chemotaxis during states of inflammation. Elevated levels of NSPs are associated with a range of chronic inflammatory lung diseases. Furthermore, neutrophilia is a common finding in histological sections of CRS mucosa. Thus, it is important to determine if NSPs are detrimental to mucosal barrier function in the nasal cavity and paranasal sinuses.

Since the shift away from the fungal hypothesis, the research focusing on nasal mucus has decreased. Mucus overproduction is a commonly reported symptom manifesting as rhinorrhoea or postnasal drip. By understanding the interaction between nasal mucus and mucosa is an important first step in understanding the mucosal barrier function in healthy and inflammatory states. Secondly, by investigating differences between healthy and CRS mucus composition will aid in understanding CRS pathophysiology and its endotypes. By identifying increased expression of certain inflammatory pathways present in CRS mucus may ultimately help direct further research into targeted treatments for these patients.

AIMS

1. Determine the effects of healthy and CRS mucus on the human nasal epithelial cells and barrier function
2. Identify how neutrophil serine proteases interact with the human nasal epithelial cell barrier
3. Systematically review the literature on healthy and CRS proteome to identify the current progress and deficiencies in the literature
4. Identify the different proteome composition between healthy and CRS mucus samples and investigate differences in cellular processes present from the proteins identified.

CHAPTER 5: BARRIER DISRUPTIVE EFFECTS OF MUCUS ISOLATED FROM CHRONIC RHINOSINUSITIS PATIENTS

STATEMENT OF AUTHORSHIP

Title of Paper	Barrier disruptive effects of mucus isolated from chronic rhinosinusitis patients
Publication Status	☑ Published ☐ Accepted for Publication ☐ Submitted for Publication ☐ Unpublished and Unsubmitted work written in manuscript style
Publication Details	Kao SS, Ramezanpour M, Bassiouni A, Finnie J, Wormald PJ, Vreugde S, et al. Barrier disruptive effects of mucus isolated from chronic rhinosinusitis patients. Allergy. 2020;75(1):200-3.

Principal Author

Name of Principal Author (Candidate)	Stephen Kao		
Contribution to the Paper	Experimental design, Collection of mucus and tissue samples, Conducted experiments, Data interpretation and analyses, Manuscript preparation.		
Overall percentage (%)	80%		
Certification:	This paper reports on original research I conducted during the period of my Higher Degree by Research candidature and is not subject to any obligations or contractual agreements with a third party that would constrain its inclusion in this thesis. I am the primary author of this paper.		
Signature		Date	24.03.2020

Co-Author Contributions

By signing the Statement of Authorship, each author certifies that:

i. the candidate's stated contribution to the publication is accurate (as detailed above);
ii. permission is granted for the candidate in include the publication in the thesis; and
iii. the sum of all co-author contributions is equal to 100% less the candidate's stated contribution.

Name of Co-Author	Mahnaz Ramezanpour		
Contribution to the Paper	Project supervision, Assistance in conducting experiments, Manuscript editing		
Signature		Date	20.03.2020

Name of Co-Author	Ahmed Bassiouni		
Contribution to the Paper	Statistical analysis, Manuscript editing		
Signature		Date	24.03.2020

Name of Co-Author	John Finnie		
Contribution to the Paper	Assistance with pathology review, Manuscript editing		
Signature		Date	6.03.2020

Name of Co-Author	Peter-John Wormald		
Contribution to the Paper	Project supervision, Manuscript editing		
Signature		Date	17.03.2020

Name of Co-Author	Sarah Vreugde		
Contribution to the Paper	Project supervision, Manuscript editing, Assistance with experimental design		
Signature		Date	20.03.2020

Name of Co-Author	Alkis James Psaltis		
Contribution to the Paper	Project supervision, Manuscript editing, Corresponding author		
Signature		Date	17.03.2020

CITATION

Kao SS, Ramezanpour M, Bassiouni A, Finnie J, Wormald PJ, Vreugde S, et al. Barrier disruptive effects of mucus isolated from chronic rhinosinusitis patients. Allergy. 2020;75(1):200-3.

LETTER TO THE EDITOR

To the Editor,

Chronic rhinosinusitis (CRS) is a heterogeneous disease involving a complex interplay of host, microbial and environmental factors. Phenotypically, CRS is divided into two subtypes: CRS with nasal polys (CRSwNP) or without nasal polyps (CRSsNP). Patients with these subtypes have different inflammatory profiles, suggesting a possible underlying difference in pathophysiology.[1] Common to both however, is the ultimate disruption of the normal mucosal barrier, considered the first line of defence against airborne pathogens.[204, 205] The immune barrier hypothesis proposes that chronic inflammation with barrier dysfunction triggers the development and ongoing symptoms of CRS.[1] This theory is supported from findings in cystic fibrosis patients who demonstrate a higher incidence of CRS and show mucociliary dysfunction, diminished tight junction protein expression and increased epithelial permeability.[220, 232, 233] The aim of this study was to investigate the effect of nasal mucus from healthy control and CRS patients on the barrier function and the immune response of primary human nasal epithelial cells.

Mucus samples were collected from 122 patients (35 Healthy controls, 48 CRSsNP and 39 CRSwNP) and applied to primary human nasal epithelial cells in air-liquid-interface (HNEC-ALI) cultures from 9 independent donors (3 non-CRS controls, 5 CRSwNP, 1 CRSsNP) (Supplementary Table 5.1). Mucus was collected using a previous validated technique that involved placing a polyurethane foam between the inferior turbinate and nasal septum for 10 minutes in patients prior to endoscopic sinus surgery.[501] Of the 122 patients recruited, 106 mucus samples were utilised in the transepithelial electrical resistance (TER) experiments, 73 with ciliary beat frequency (CBF) experiments, 106 with cytotoxicity assays, 92 with IL-8

enzyme-linked immunosorbent assays (ELISA) and 78 with IL-6 ELISA. Detailed methodology is included in the online supplementary.

At baseline, control HNEC-ALI cultures had significantly higher TER than CRS HNEC-ALI (1.55 vs 1.35) (P=0.012) (Supplementary Figure 5.1A). Healthy control mucus applied to HNEC-ALI cultures from all donors demonstrated a significantly higher TER compared to PBS-negative control, CRSsNP and CRSwNP (1.173 vs 0.952 vs 0.9157 vs 0.930, respectively) (P<0.05 for all groups) (Figure 5.1A). Subgroup analysis of nasal mucus applied to HNEC-ALI cultures from healthy controls (1.486) demonstrated a significantly higher TER compared to negative control (1.062) and CRSwNP mucus (0.9337) (Supplementary 5.1B) (P=0.008). The application of healthy control and CRSsNP mucus samples to control HNEC-ALI cultures demonstrated increased TER compared to CRSwNP mucus. Furthermore, the application of all mucus types to CRSwNP HNEC-ALI cultures demonstrated significantly reduced TER compared to the application on HNEC-ALI cultures from control patients (P<0.0001) (Figure 5.1B).

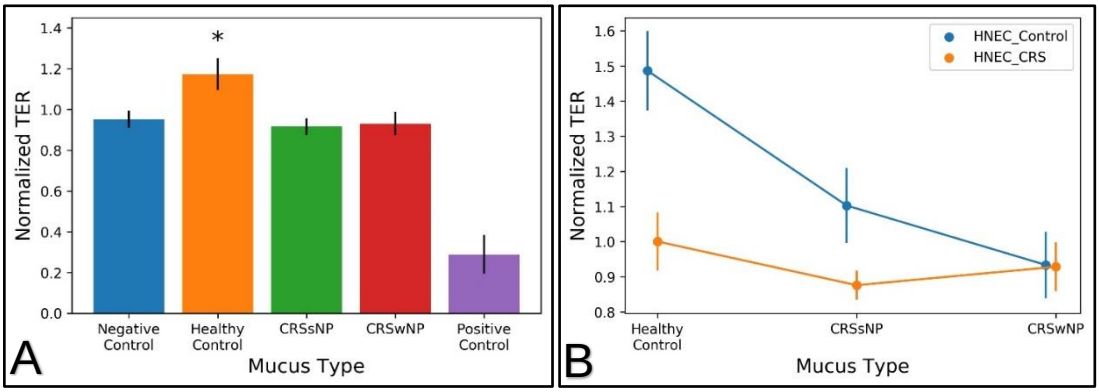

Figure 5.1. The effect of mucus type obtained from healthy controls or CRS patients on the TER *at six hours of exposure.*

*The TER values are normalized to baseline readings and shown as a mean ± SEM for n=106. A, Healthy control mucus caused significant increase in TER compared to negative control, CRSsNP and CRSwNP mucus when applied to HNEC-ALI from control, CRSsNP and CRSwNP patients. B, CRS HNEC-ALI demonstrated significantly reduced TER compared to control HNEC-ALI when healthy mucus and CRSsNP mucus was applied. *P<0.05.*

There was no significant difference in baseline CBF between HNEC-ALI from control or CRSwNP patients. Application of PBS to the HNECs for up to 6 hours did not affect CBF and maintained baseline readings (1.056). The application of healthy control mucus to the HNEC-ALI cultures demonstrated a significant increase in CBF compared to negative control and mucus harvested from CRSsNP and CRSwNP (1.862 vs 1.056 vs 1.465 vs 1.422, in healthy control vs negative control, CRSsNP and CRSwNP respectively) (P=0.0024). There was no significant difference in the effect of mucus from CRSsNP and CRSwNP on CBF (Figure 5.2A). Subgroup analysis demonstrated significantly higher CBF when healthy control mucus was applied to control HNEC-ALI compared to CRSsNP mucus (1.921 vs 1.344) (P=0.012) (Supplementary Figure 5.1C).

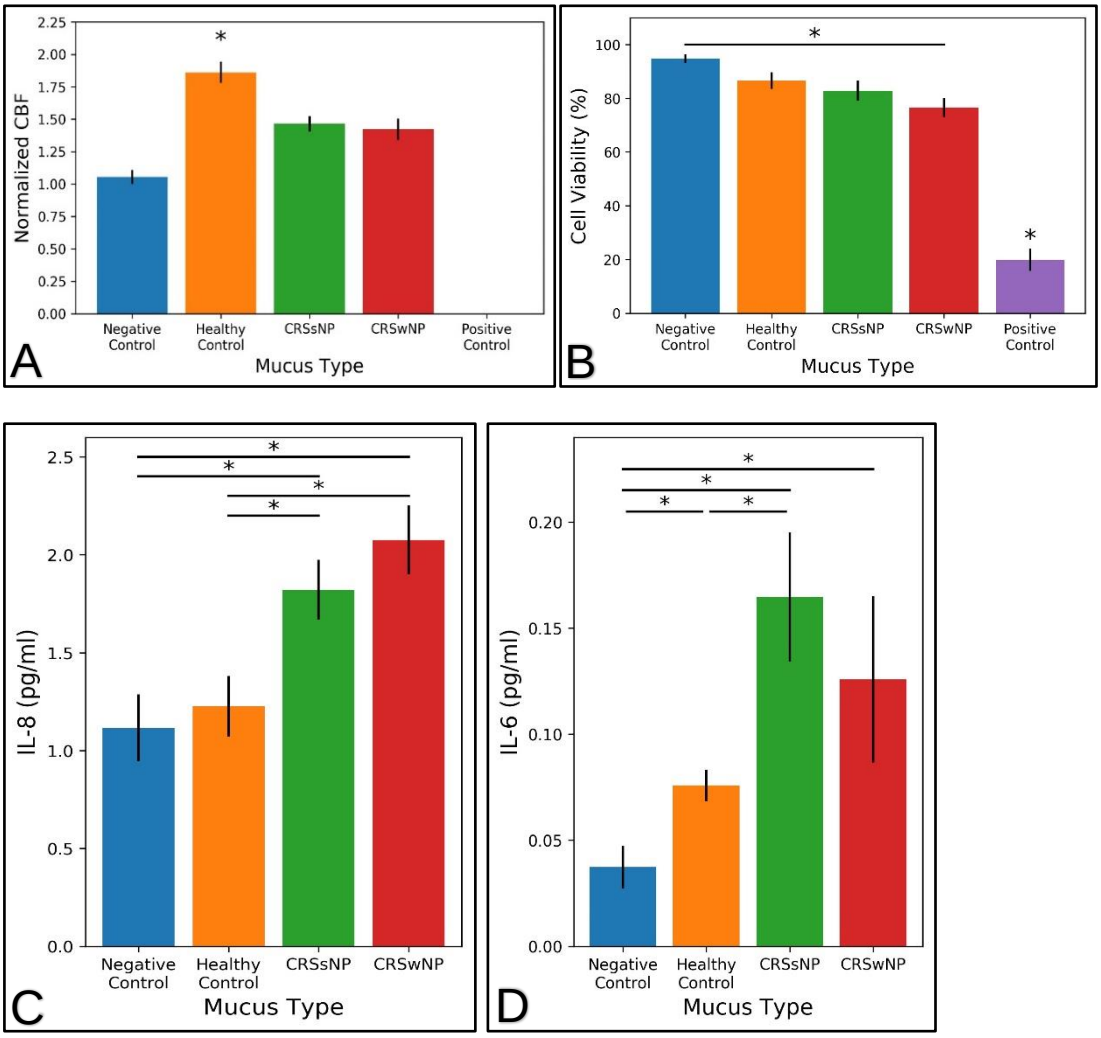

Figure 5.2. CBF, Cell viability, IL-8 and IL-6 release from HNEC-ALI cultures.

Values are shown as a mean ± SEM. **(A)** *Healthy control mucus demonstrated a significant increase in CBF compared to negative control, CRSsNP, CRSwNP mucus.* **(B)** *Reduced cell viability with CRSwNP mucus compared to negative control.* **(C)** *Significant increase in IL-8 release with CRS mucus compared to healthy control mucus and negative control.* **(D)** *Significant increase in IL-6 release with CRSsNP mucus compared to healthy control mucus. Significantly lower IL-6 release with negative control compared to healthy control and CRS mucus. Negative control = PBS. *P<0.05.*

Compared to PBS-negative control, application of mucus from CRSwNP patients significantly reduced cell viability of HNEC-ALI cultures (P=0.024). Mucus from healthy controls or CRSsNP did not affect cell viability compared to control (P>0.05) (Figure 5.2B).

The application of mucus from CRSwNP (2.002pg/ml) and CRSsNP (1.732pg/ml) on HNEC-ALI cultures induced a significant increase in IL-8 release compared to healthy control mucus (1.226pg/ml) and PBS-negative control (1.115pg/ml) (P=0.034). There was no significant difference in IL-8 release after application of PBS and healthy control mucus or between CRSsNP and CRSwNP mucus (Figure 5.2C). Similarly, mucus from CRSsNP patients induced an increased release of IL-6 by HNEC-ALI cells compared to mucus from healthy control patients (0.759 vs 0.174pg/ml, P=0.008) (Figure 5.2D). IL-6 release was higher after the application of healthy control (0.0759 pg/ml), CRSsNP (0.174 pg/ml) and CRSwNP (0.126 pg/ml) mucus compared to negative control (0.0373) (P=0.012). No statistically significant difference in IL-6 release was observed between healthy control and CRSwNP mucus or between CRSsNP and CRSwNP.

To our knowledge, this is the first study to investigate the effect of nasal mucus on the mucosal epithelial barrier and immune response of HNEC-ALI. The results from this study suggest that mucus from healthy controls may have a protective effect on mucosal barrier structure and function as evidenced by an increased TER and CBF compared to negative control. In contrast, mucus from CRS patients did not appear to confer this protective effect. In fact, CRSwNP mucus samples had cytotoxic effects on HNEC-ALI cultures and both CRSsNP and CRSwNP mucus induced increased IL-8 and IL-6 cytokine release by the cells compared to negative control. This in addition to the finding of a lower baseline TER measurement in CRSwNP HNEC compared with control HNEC, adds further support to the proposed mucosal barrier

dysfunction hypothesis of CRS.[202] Further research is required to ascertain the differing composition between CRS and healthy mucus samples to improve the understanding of CRS and its pathophysiology with the goal of improving treatment paradigm.

Stephen Shih-Teng Kao MBBS MClinSc[1]

Mahnaz Ramezanpour PhD[1]

Ahmed Bassiouni MBBCH PhD[1]

John Finnie BVSc PhD FRCVS[2]

Peter-John Wormald MD FRACS[1]

Sarah Vreugde MD PhD[1]

Alkis James Psaltis MBBS PhD FRACS[1]

ACKNOWLEDGEMENTS

This project was supported by Adelaide University Research Training Program Scholarship, Bertha Sudholz Scholarship and Garnett Passe Rodney Williams Memorial Foundation Scholarship to SSK.

SUPPLEMENTARY MATERIAL

MATERIALS AND METHODS

Research approval was granted by The Queen Elizabeth Hospital Human Research Ethics Committee, Adelaide, Australia (HREC/15/TQEH/132). Mucus was obtained from patients undergoing endoscopic sinus surgery for CRS at The Queen Elizabeth Hospital, Adelaide, Australia. Patients were defined as CRSwNP and CRSsNP according to EPOS guidelines.[1] Healthy control patients were patients undergoing endoscopic skull base procedures or septoplasty with no clinical or radiological evidence of sinus disease. Prior to study enrolment, written informed consent was obtained from patients in conjunction with comorbidities and disease severity scores (SNOT-22, Lund-Mackay, Lund-Kennedy). Nasal mucosa and polyp tissue collected intraoperatively was reviewed by a pathologist. Exclusion criteria included patients less than 18 years of age, pregnancy and systemic immunosuppression.

Mucus Collection

Polyurethane foam (5 x 25 mm) was placed between the inferior turbinate and nasal septum for 10 minutes in patients prior to surgery, and stored in microcentrifuge tubes with Spin-X inserts (Corning, New York, United States) at 4^{o}C for transfer.[501] Nasal mucus was extracted from the sponge by centrifugation at 13,000 rpm for 10 minutes and frozen at -80^{o}C until later analysis.

Harvesting Human Nasal Epithelial Cells and Air-Liquid Interface

Primary human nasal epithelial cells (HNECs) were harvested intraoperatively by gentle brushing of nasal polyps in CRSwNP patients, or nasal mucosa from the middle and inferior turbinates in CRSsNP and control patients as previously published from our department.[180] HNECs were expanded in PneumaCult^{TM} Ex Plus Basal Media (Stemcell Technologies, Australia) within collagen coated flasks (Thermo Scientific, Waltham, USA) until 80%

confluence then seeded onto collagen coated Transwell plates (BD Biosciences, San Jose, California USA) at a density of 7 x 10^4. Once the HNECs completely covered the surface of the Transwell membrane, all Ex Plus media was removed from both the apical and basal chambers. PneumaCult^{TM} ALI Basal Media with Supplement and Maintenance Supplement (Stemcell Technologies, Australia) was applied to the basal chamber. The cultures were maintained for a minimum of 21 days for development of tight junctions.

Transepithelial Electrical Resistance

Transepithelial electrical resistance (TER) was performed with the EVOM volt-ohm meter (World Precision Instruments, Sarasota, FL, USA) for 6 hours. Baseline TER measurements were conducted by applications of 50µL of phosphate buffered saline (PBS) to the apical chamber of HNEC-ALI wells maintained at 37ºC with utilisation of a heating platform. Only wells displaying baseline resistance readings greater than 1000Ω/cm^2 were included. PBS was replaced with 50µL of mucus, diluted 1:1 with PBS, ensuring complete coverage of the cell layer. Negative controls were 50µL of PBS and positive controls were of 50µL of 10% Triton X-100, each time applied in the apical chamber.

Ciliary Beat Frequency

Ciliary beat frequency (CBF) was measured using an inverted microscope (Olympus IX70, Tokyo, Japan) and recorded using the Model Basler acA645-100µm USB3 camera (Basler AG, Ahrensburg, German). Sisson-Ammons Video Analysis (SAVA) system was employed to analyse the video samples. Baseline CBF was obtained from cells with 50µL of PBS applied to the apical chamber. The PBS was replaced with 50µL of mucus was (Diluted 1:1 with PBS). Negative controls were 50µL of PBS and positive controls were 50µL of 10% Triton X-100 applied to the apical chamber.

Cytotoxicity Assay

Lactate dehydrogenase (LDH) assay was performed on the basal medium after cells were exposed to mucus for 24 hours. All measurements were performed in duplicate. CytoTox 96 reagent (Promega, Australia) was added to the basal media in a 96-well clear bottom plate and stored in a dark room at room temperature for 30 minutes. Stop solution was applied and the plate was read at absorbance of 490nm on the microplate reader (FLUOstar Optima, BMG Labtech, Ortenberg, Germany).

Expression of IL-6 and IL-8 in HNEC-ALI Supernatants

Supernatant was collected from the basal chamber after 24 hours of exposure and transferred to 96 well plates with all measurements duplicated (CorningCostar cell culture plates). Interleukin-6 and interleukin-8 protein levels were identified through IL-6 and IL-8 enzyme-linked immunosorbent assay (ELISA) kit (BD Biosciences, Franklin Lakes, NJ) as per manufacturer's instructions.

Paracellular Permeability

Paracellular permeability of the HNEC-ALI was measured at 24 hours of exposure to mucus. FITC-dextran (Sigma-Aldrich, St. Louis, Missouri,) was applied to the apical chamber for 2 hours. The quantity of FITC-dextran in the basal media was measured with a microplate reader (FLOUstar Optima, BMG Labtech, Ortenberg, Germany).[502]

Statistical Analysis

R statistical software was used for statistical analysis.[503] Data was presented as the mean +/- standard error of the mean (SEM). TER and CBF values were normalised against time zero. Kruskal-Wallis test was used to assess the effects of differing mucus samples for TER, CBF,

LDH Assay, Permeability assay, IL-6 and IL-8. Posthoc permutation t-tests were employed. Permutation ANOVA was used to assess the confounding effect of mucus on control, CRSsNP and CRSwNP HNEC. P-values < 0.05 were deemed statistically significant.

RESULTS

There was no significant difference in the FITC-dextran permeability assay following the application of healthy control, CRSsNP and CRSwNP mucus.

Supplementary Table 5.1. Patient demographics.

	Healthy Control (n = 35)	CRSsNP (n = 48)	CRSwNP (n = 39)	P-value
Age, mean (SD), y	47.92 (16.43)	47.38 (16.47)	49.26 (17.18)	0.867
Male/Female	20/15	28/20	19/20	0.358
Smoker	3	9	12	0.06
Asthma	1	8	15	0.001
GORD	4	14	5	0.350
T2DM	0	0	8	0.001
Hypersensitivity-any	4	19	16	0.002
Aspirin Sensitivity	0	2	5	0.107
SNOT-22 total score, mean (SD)	30.9 (20.8)	41.57 (25.19)	48.5 (22.3)	0.036
Lund-Mackay total score, mean (SD)	0.44 (0.73)	7.29 (4.08)	14.7 (5.11)	0.002
Lund-Kennedy total score, mean (SD)	1.89 (1.96)	5.98 (3.28)	11.23 (3.16)	0.001
Volume of mucus (µl), mean (SD)	168.3 (146.06)	117.9 (131.46)	169.5 (174.66)	0.038

Abbreviations: CRSsNP = Chronic rhinosinusitis without nasal polyposis, CRSwNP = Chronic rhinosinusitis with nasal polyposis. GORD = Gastroeosophageal reflux disease. T2DM = Type 2 diabetes mellitus. SNOT-22 = 22-Item SinoNasal Outcome Test. SD = Standard deviation.

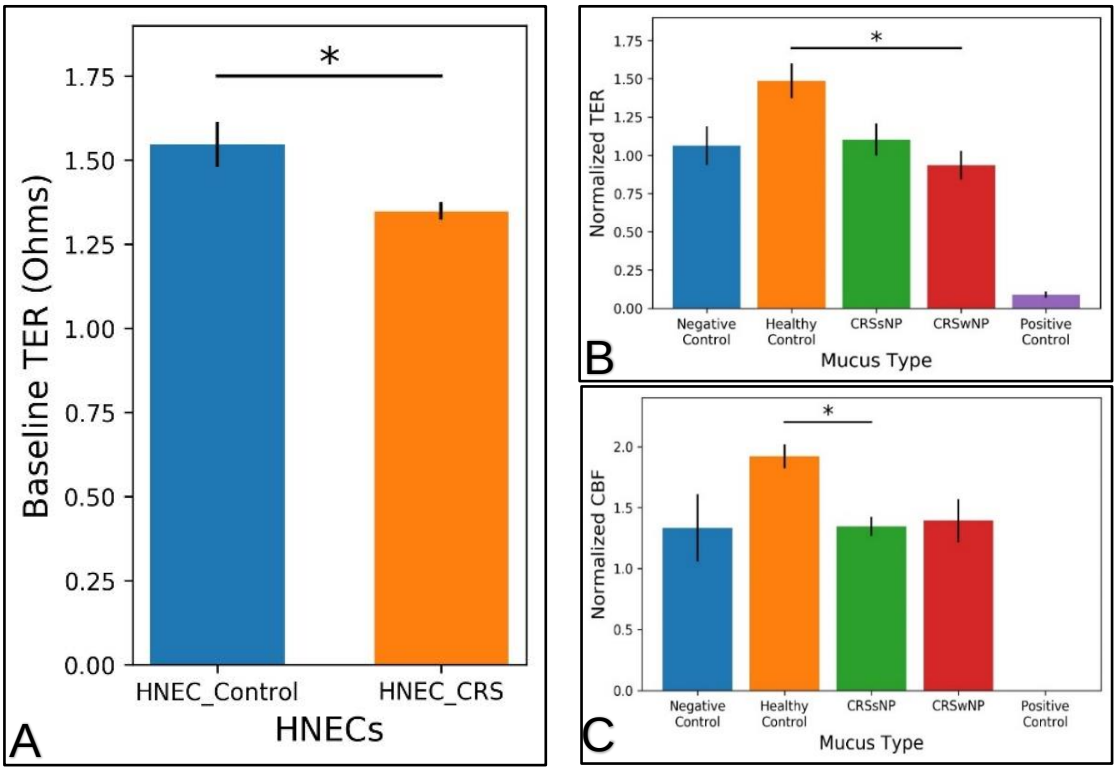

Supplementary Figure 5.1. Baseline TER of healthy and CRS HNEC-ALI and effect of mucus from healthy or CRS on the TER and CBF on HNEC from controls.

(A) *Raw baseline TER values as shown as a mean ± SEM. Control HNEC-ALI demonstrated significantly higher TER at baseline compared to CRS HNEC-ALI (1.55 ± 0.068 vs 1.35 ± 0.026).* ***(B)*** *TER and CBF values are normalized to baseline readings and shown as a mean ± SEM. Healthy mucus caused a significant increase in TER compared to CRSwNP and negative control.* **(C)** *Healthy mucus demonstrated significantly higher CBF compared to CRSsNP. *P<0.05.*

CHAPTER 6: THE EFFECT OF NEUTROPHIL SERINE PROTEASES ON HUMAN NASAL EPITHELIAL CELL BARRIER FUNCTION.

STATEMENT OF AUTHORSHIP

Title of Paper	The effect of neutrophil serine proteases on human nasal epithelial cell barrier function.
Publication Status	☑ Published ☐ Accepted for Publication ☐ Submitted for Publication ☐ Unpublished and Unsubmitted work written in manuscript style
Publication Details	How to Cite this Article: Kao, SS, Ramezanpour, M, Bassiouni, A, Wormald, PJ, Psaltis, AJ, Vreugde, S. The effect of neutrophil serine proteases on human nasal epithelial cell barrier function. Int Forum Allergy Rhinol. 2019; 9: 1220– 1226.

Principal Author

Name of Principal Author (Candidate)	Stephen Kao		
Contribution to the Paper	Experimental design, Collection of tissue samples, Conducted experiments, Data interpretation and analyses, Manuscript preparation.		
Overall percentage (%)	80%		
Certification:	This paper reports on original research I conducted during the period of my Higher Degree by Research candidature and is not subject to any obligations or contractual agreements with a third party that would constrain its inclusion in this thesis. I am the primary author of this paper.		
Signature		Date	24.03.2020

Co-Author Contributions

By signing the Statement of Authorship, each author certifies that:

i. the candidate's stated contribution to the publication is accurate (as detailed above);
ii. permission is granted for the candidate in include the publication in the thesis; and
iii. the sum of all co-author contributions is equal to 100% less the candidate's stated contribution.

Name of Co-Author	Mahnaz Ramezanpour		
Contribution to the Paper	Project supervision, Assistance in conducting experiments, Manuscript editing		
Signature		Date	20.03.2020

Name of Co-Author	Ahmed Bassiouni		
Contribution to the Paper	Statistical analysis, Manuscript editing		
Signature		Date	24.03.2020

Name of Co-Author	Peter-John Wormald		
Contribution to the Paper	Project supervision, Manuscript editing		
Signature		Date	17.03.2020

Name of Co-Author	Alkis James Psaltis		
Contribution to the Paper	Project supervision, Manuscript editing		
Signature		Date	17.03.2020

Name of Co-Author	Sarah Vreugde		
Contribution to the Paper	Project supervision, Manuscript editing, Assistance with experimental design, Corresponding author		
Signature		Date	20.03.2020

CITATION

How to Cite this Article: Kao, SS, Ramezanpour, M, Bassiouni, A, Wormald, PJ, Psaltis, AJ, Vreugde, S. The effect of neutrophil serine proteases on human nasal epithelial cell barrier function. Int Forum Allergy Rhinol. 2019; 9: 1220– 1226.

ABSTRACT

Introduction

The neutrophil serine proteases neutrophil elastase (NE), cathepsin G (CG) and proteinase 3 (PR3) are implicated in the regulation of inflammatory conditions. *P. aeruginosa* elastase (PE), also a serine protease, has been found to behave similarly to neutrophil elastase and has been proposed to assist the pathogen in evading the host immune response. The effect of serine proteases on human nasal epithelial barrier function requires further investigation to better understand the pathophysiology of inflammatory conditions.

Methods

Purified human neutrophil serine proteases and PE were applied to air-liquid interface cultures of primary human nasal epithelial cells (ALI-HNEC) from six patients. Barrier integrity and function was assessed via transepithelial electrical resistance (TER), permeability assays, immunofluorescence of Zona Occludens-1 (ZO-1) and cilia beat frequency (CBF) measurements. Cytotoxicity assays were employed to assess cell viability. IL-6 and IL-8 ELISA assessed cytokine release from ALI-HNEC.

Results

The application of serine proteases demonstrated detrimental effects on ALI-HNEC barrier integrity. Reduction in TER occurred with NE, CG and PE with increased paracellular permeability with NE, CG, PR3 and PE. Discontinuous tight junctions with reduction in ZO-1 expression were identified using immunofluorescence. Neutrophil serine proteases were not toxic cells to the HNEC and had no detrimental effects on the CBF.

Conclusions

Serine proteases derived from neutrophils and from *P. aeruginosa* demonstrated detrimental effects on the mucosal barrier integrity with increased permeability, allowing for potential bacterial invasion. This finding may further assist in understanding the pathophysiology present in chronic inflammatory airway diseases.

Keywords: Serine proteases, Pseudomonas elastase, Tight junctions, Zonula occudens-1 protein, Chronic rhinosinusitis

INTRODUCTION

The pseudostratified, ciliated epithelial cells present in the human nasal mucosa are the first line of defence against inhaled pathogens. Tight junctions located on the apical region of these cells consist of integral membrane proteins including occludins and claudins. Zona occludens-1 (ZO-1), a peripheral membrane protein, acts as a scaffold, anchoring tight junction proteins to the actin cytoskeleton.[504] Together, these proteins regulate the flow of water and solutes through the paracellular space. The integrity of these proteins is critical for forming an adequate mucosal barrier structure and function, preventing the invasion of pathogens and allergens into the submucosa leading to inflammation.[504] It has been hypothesised that the disruption of tight junctions with associated mucosal barrier dysfunction contributes to the pathogenesis of chronic rhinosinusitis.[1]

Neutrophils are an essential component of the innate immune system against the invasion of pathogens. They are the first cells to migrate to sites of inflammation and responsible for phagocytosis in bacterial infections.[94] Neutrophil serine proteases (NSP) including neutrophil elastase (NE), cathepsin G (CG) and proteinase 3 (PR3) are released from neutrophils in non-oxidative pathways for intracellular and extracellular pathogen destruction.[94] The activation and accumulation of neutrophils with associated release of serine proteases leads to inflammation and tissue destruction.[94] Interleukin-6 (IL-6) and interleukin-8 (IL-8) are important inflammatory mediators implicated in chronic inflammatory diseases including chronic rhinosinusitis, cystic fibrosis and acute respiratory distress syndrome.[154, 505] Mucociliary clearance is a vital aspect in the defence of the respiratory tract. Chronic inflammation and elevated neutrophil burden has been associated with impaired mucus clearance and cilia function.[506, 507] In such conditions, these cytokines play a vital role in the

regulation of the innate and acquired immunity in part by disruption of the airway epithelial barrier following exposure to different cytokines.[180]

Bacteria such as *Pseudomonas aeruginosa* can also produce proteases. *P. aeruginosa*, an opportunistic gram-negative pathogen, is commonly associated with cystic fibrosis and recalcitrant chronic rhinosinusitis. It has numerous virulence factors allowing it to evade the immune system leading to increased vascular permeability and degradation of extracellular matrix components. *P. aeruginosa* elastase (PE) has been found to behave similarly to neutrophil elastase and has been proposed to mimic endogenous anti-inflammatory mechanisms thus evading the host response.[56] PE causes tight junction disruption and cytoskeletal reorganisation with associated increased paracellular permeability in lung epithelial cells [55]. Further studies have correlated PE-induced mucosal membrane barrier degradation and dysfunction in CRS with objective disease severity scores.[55, 57]

The aim of this study was to determine the effects of NSP and PE on barrier and cilia function of human nasal epithelial cells grown in air-liquid interface *in vitro.* An improved understanding of the effects of these enzymes in the innate immune system in association with chronic inflammatory conditions will allow for advancements in the management of these diseases.

MATERIALS AND METHODS

Primary human nasal epithelial cell harvest

The Queen Elizabeth Hospital Human Research Ethics Committee, Adelaide, Australia granted ethics for cytological nasal brushings (Reference number: HREC15/TQEH/132).[180] Prior to endoscopic sinus surgery or skull base surgery, written informed consent was obtained from all patients. Patients were defined as chronic rhinosinusitis with nasal polyposis as per the European Position Paper on Rhinosinusitis and Nasal Polyps (EPOS) guidelines.[1] Control patients were defined as patients undergoing endoscopic skull base surgery or septoplasty without clinical or radiological evidence of sinus disease. Exclusion criteria included patients less than 18 years of age, active smokers, active or previous malignancy and immunosuppression. Intra-operative nasal brushings were taken from nasal polyps in CRSwNP patients or the middle and inferior turbinates from control patients.

Reagents

Human neutrophil elastase (ab91099) and Human cathepsin G (ab911122) were purchased from Abcam (MA, USA) and prepared according the manufacturer's specifications and stored at -80^{o}C. Both samples were diluted to 10µg/ml with 1x phosphate buffered saline (PBS).[107] Human proteinase 3 was purchased from Sigma-Aldrich (MO, USA) and diluted to 0.1µg/ml with 1xPBS. *Pseudomonas aeruginosa* elastase (324676) was obtained from Merck (Victoria, Australia) and diluted to 50µg/ml with 1xPBS.

Primary Human Nasal Epithelial Cell culture at Air-Liquid Interface

Primary human nasal epithelial cells (HNEC) were transported in RPMI Media 1640 (Gibco, Co Dublin, Ireland) on ice. The HNEC were expanded until 80% confluence in PneumaCult^{TM} Ex Plus Basal Media (Stemcell Technologies, Australia) within collagen coated flasks (Thermo

Scientific, Walthman, MA, USA) at routine cell culture conditions of 37°C humidified air with 5% CO_2. Cells were harvested when 80% confluent for seeding onto collagen-coated 6.5-mm permeable polyester Transwell membranes with 0.4-μm pores (Stemcell technologies, Australia) at a density of 70,000 cells per well. Cell cultures were maintained with PneumaCult™ Ex Plus Basal Media for 3 to 4 days at 37°C with 5% CO2. The apical and basal media was then removed, and the basal media replaced with PneumaCult™ ALI differentiation media (StemCell Technologies, Australia).

Transepithelial Electrical Resistance

Transepithelial electrical resistance (TER) was measured with the EVOM volt-ohmmeter (World Precision Instruments, Sarasota, FL, USA). 100μL of warmed PBS was applied to the apical chambers of all ALI wells to measure the baseline TER. A heating platform was utilised to maintain cells at 37°C during measurements. HNEC with baseline resistance of greater than 1000Ω.cm^2 were included in this study. Following baseline measurements, PBS was replaced with neutrophil serine proteases Neutrophil elastase (NE), cathepsin G (CG), proteinase 3 (PR3) or *Pseudomonas aeruginosa* elastase (PE) in the apical chamber. 100μL of PBS and 10% Triton X-100 was applied to the apical chamber of the negative and positive control, respectively. Serine proteases and *Pseudomonas Elastase* were heat-inactivated to 65°C for 30 minutes and used as an additional negative control. Time points included baseline and 6 hours. Based on our previous studies, measurements were performed at 6 hours as this demonstrated the most significant change across all groups with reduction of confounding external factors.[229, 423]

Paracellular permeability

Paracellular permeability of the HNEC-ALI was measured at 6 hours of exposure to reagents. FITC-dextran 3mg/mL (Sigma-Aldrich, St. Louis, Missouri, USA) in PBS was applied to the

apical chamber for 2 hours. Supernatant from the basal chamber was collected and the amount of FITC-dextran was measured with a microplate reader (FLOUstar Optima, BMG Labtech, Ortenberg, Germany).[507]

Ciliary Beat Frequency

Ciliary Beat Frequency **(**CBF) of HNEC-ALI cultures was assessed using a 20 X objective, and X1.5 magnification on an inverted microscope (Olympus IX70, Tokyo, Japan). Video was recorded using the Model Basler acA645-100µm USB3 camera (Basler AG, Ahrensburg, German) at 100 frames per second at a resolution of 640 x 480 pixels. Sisson-Ammons Video Analysis (SAVA) system was employed to analyse the video samples.

Baseline CBF was obtained from cells with 100µL of PBS applied to the apical chamber. The apical chambers were applied with 100µL of neutrophil serine proteases NE, CG, PR3 or PE. 100µL of heat-inactivated proteases were applied to the apical chamber for negative control. 100µL of 10% Triton X-100 was applied to the apical chamber of positive controls. All measurements were taken at room temperature from two separate regions of each culture. Sequential readings were taken every 2 hours. Between readings, the HNEC-ALI cultures were stored in the incubator at 37^{O}C. As per the TER experiment, the CBF was stable for the first 6 hours and decreased in all HNEC-ALI, including controls. Thus, CBF measurements were limited to 6 hours to limit confounding factors.

Cytotoxicity Assay

Cell viability was identified through a cytotoxicity assay where the amount of lactate dehydrogenase (LDH) was measured after 6 hours. 50µl supernatant from the basal chamber of the HNEC-ALI culture was transferred to a 96-well clear-bottom plate. 50 µl of CytoTox 96

(Promega, Australia) was added to the supernatant and stored in a dark room at room temperature for 30 minutes. The plate was read at absorbance of 490nm on the microplate reader (FLOUstar Optima, BMG Labtech, Ortenberg, Germany).

Immunofluorescence of ZO-1

Immunofluorescence was performed after 6 hours of exposure to reagents of HNEC-ALI. Cells were fixed in 2.5% formalin in PBS for 10 minutes, washed with PBS and air-dried. 0.1% Triton X-100 was applied to cells for 15 minutes to assist with permeabilising. The fixed cells were washed with PBS and blocked with Protein Block (Dako, Glostrup, Denmark) for 1 hour. Mouse monoclonal anti-human ZO-1 (Invitrogen, Calsbad, CA, USA) 5µL/mL was mixed with 1 x PBS and applied to the HNEC-ALI membranes and incubated overnight at 4^{o}C. Samples were washed with PBST 0.05% prior to application of secondary antibodies: Alexa Fluor 488 conjugated anti-mouse (1:200) (Jackson ImmunoResearch Labs, Wast Grove, PA, USA) was applied at room temperature for 1 hour. Samples were washed with PBST and 4',6-diamidino-2-phenylindole (DAPI; Sigma Aldrich) was applied for 10 minutes to stain nuclei. After final wash with PBST, membranes were transferred to a glass slide and a drop of anti-fade mounting medium (Dako, Glostrup, Denmark) was applied prior to cover slipping. Cells were visualised with the use of the Zeiss LSM 700 inverted confocal microscope (Carl Zeiss, Oberkochen, Germany). Image acquisition was performed with Zeiss ZenBlue (Germany).

Expression of IL-6 and IL-8 in HNEC-ALI Supernatants

Interleukin-6 (IL-6) and interleukin-8 (IL-8) cytokines were measured from the basal supernatant HNEC-ALI cultures after 6 hours of exposure to the treatments. Enzyme-linked immunosorbent assay (ELISA) kits (BD Biosciences, Franklin Lakes, NJ) for both IL-6 and IL-8 were used as per manufacturer's instructions. All measurements were performed in duplicate.

Results were expressed in pg/mL. Standard curve was utilised to calculated for protein concentration.

Statistical Analysis

R Core Team (2018). R: A language and environment for statistical computing. (R Foundation for Statistical Computing, Vienna, Austria) was used for statistical analysis. Data was presented as the mean +/- standard error of the mean (SEM). TER and CBF values were normalised against time zero (baseline reading). Kruskal-Wallis test was used to assess the effects of differing mucus samples for TER, Permeability assay, CBF, LDH Assay, IL-6 and IL-8. Posthoc permutation t-tests were employed. P values <0.05 were deemed statistically significant.

RESULTS

Neutrophil elastase (NE) 10µg/ml, cathepsin G (CG) 10µg/ml, proteinase 3 (PR3) 0.1µg/ml and Pseudomonas elastase (PE) 50µg/ml was applied to HNEC-ALI cultures from 6 patients (3 Control, 3 CRSwNP). Two patients were male, and four were female with an average age of 49.3 (Range: 29-67). Two patients had documented asthma and one patient had aspirin sensitivity. Demographics are specified in Table 1.

Table 6.1 Patient Demographics

	Control	**CRSwNP**
Age	55.3 (SD 14.2)	43.3 (SD 20.6)
Male/Female	1/2	1/2
GERD	1	1
Asthma	1	1
Aspirin hypersensitivity	0	1
SNOT-22	-	59 (SD 19)
Lund-Mackay CT Score	-	14 (SD 6.2)
Lund-Kennedy	-	10.7 (SD 4.2)

CRSwNP = Chronic rhinosinusitis with nasal polyposis; CT = Computed tomography; GERD = gastroesophageal reflux disease; SD = standard deviation; SNOT-22 = 22-item Sino-Nasal Outcome Test.

Neutrophil Elastase, Cathepsin G and Pseudomonas Elastase Reduce Transepithelial Electrical Resistance of Human Nasal Epithelial Cells

The TER (normalised to values at time=0) of the PBS-treated negative control and of heat-inactivated serine proteases and pseudomonas elastase remained at baseline 6 hours after application of test solutions (PBS = 0.938, denatured neutrophil elastase = 0.90, denatured

cathepsin G = 0.97, denatured proteinase 3 = 0.94, denatured pseudomonas elastase 1.05, all P>0.05) (Figure 1 and results not shown). There was a significant reduction in TER values for neutrophil elastase (0.66, P=0.022), cathepsin G (0.672, P=0.017) and pseudomonas elastase (0.593, P=0.010) at 6 hours of exposure compared to control. There were no significant differences in TER between the individual reagents (Figure 6.1).

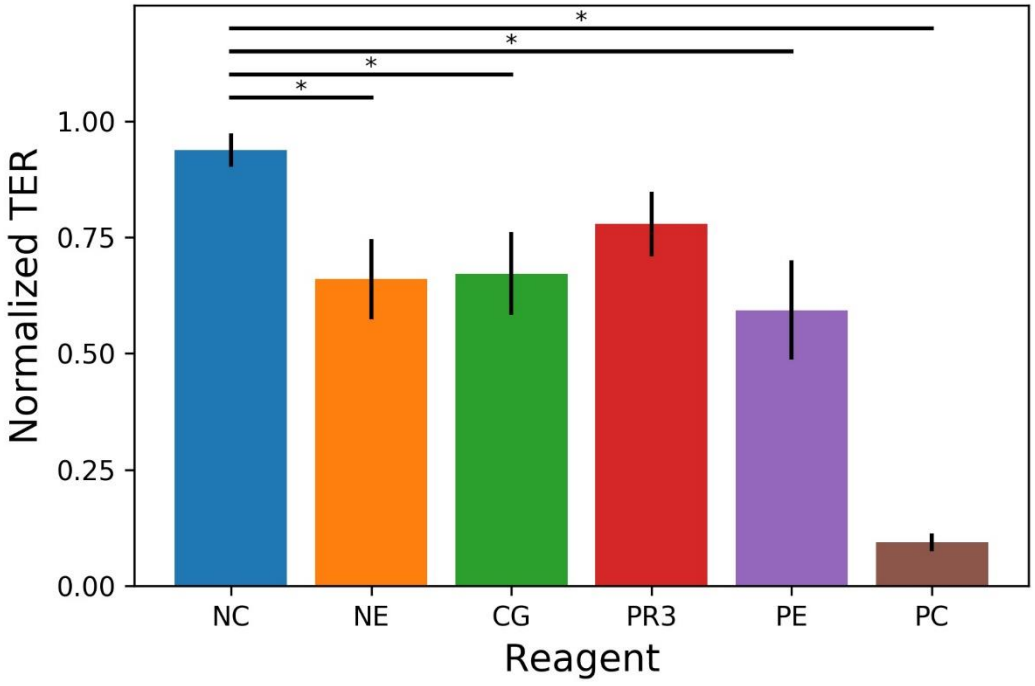

Figure 6.1. The effect of neutrophil serine proteases on the TER of HNEC *at 6 hours of exposure.*

*The values are normalized and shown as a mean ± SEM for n=6 patients. Neutrophil elastase (NE), cathepsin G (CG) and pseudomonas elastase (PE) but not proteinase 3 (PR3) demonstrated significantly reduced TER compared to negative control (NC) and normalised to TER at time=0. Negative control = PBS. Positive control (PC) = 10% Triton-X. *P<0.05, Kruskal-Wallis test with posthoc permutation t-test.*

Increased Paracellular Permeability Following Application of Neutrophil Serine Proteases and Pseudomonas Elastase to Human Nasal Epithelial Cells

Application of all the neutrophil serine proteases and pseudomonas elastase demonstrated significant increases in paracellular permeability of FITC-dextrans compared to negative control ($P<0.05$) (Figure 6.2). Cathepsin G demonstrated the greatest effect with 463% of FITC-dextran crossing the cell monolayer. This was followed by PE, PR3 and NE with 235%, 210% and 151%, respectively. There was no significant difference in permeability between individual reagents (Figure 6.2).

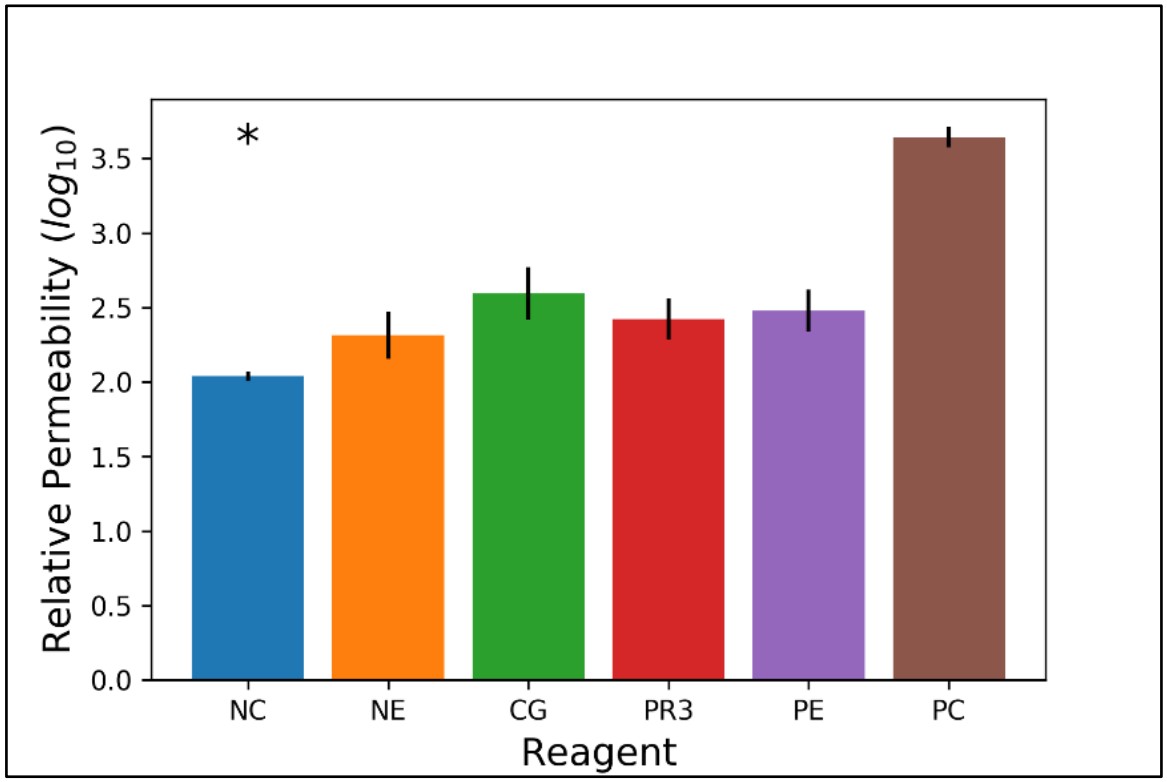

Figure 6.2. The effect of neutrophil serine proteases and pseudomonas elastase on the paracellular permeability of HNEC.

*The values are shown as a mean ± SEM for n=6 patients. All neutrophil serine proteases and pseudomonas elastase demonstrated increased paracellular permeability compared to negative control. Negative control = PBS. Positive control = 10% Triton-X. *P<0.05, Kruskal-Wallis test with posthoc permutation t-test. NC = Negative control, NE = Neutrophil elastase, CG = Cathepsin G, PR3 = Proteinase 3, PE = Pseudomonas elastase, PC = Positive control.*

Reduction in Tight Junction Protein ZO-1 Following Application of Neutrophil Serine Proteases and Pseudomonas elastase

Tight junction protein ZO-1 was assessed in the HNEC-ALI cultures after exposure to NSP and PE. Continuous tight junctions were observed with negative control cells with moderate disruption observed with exposure to PR3. The exposure to NE, CG and PE demonstrated loss of ZO-1 and discontinuous tight junctions (Figure 6.3).

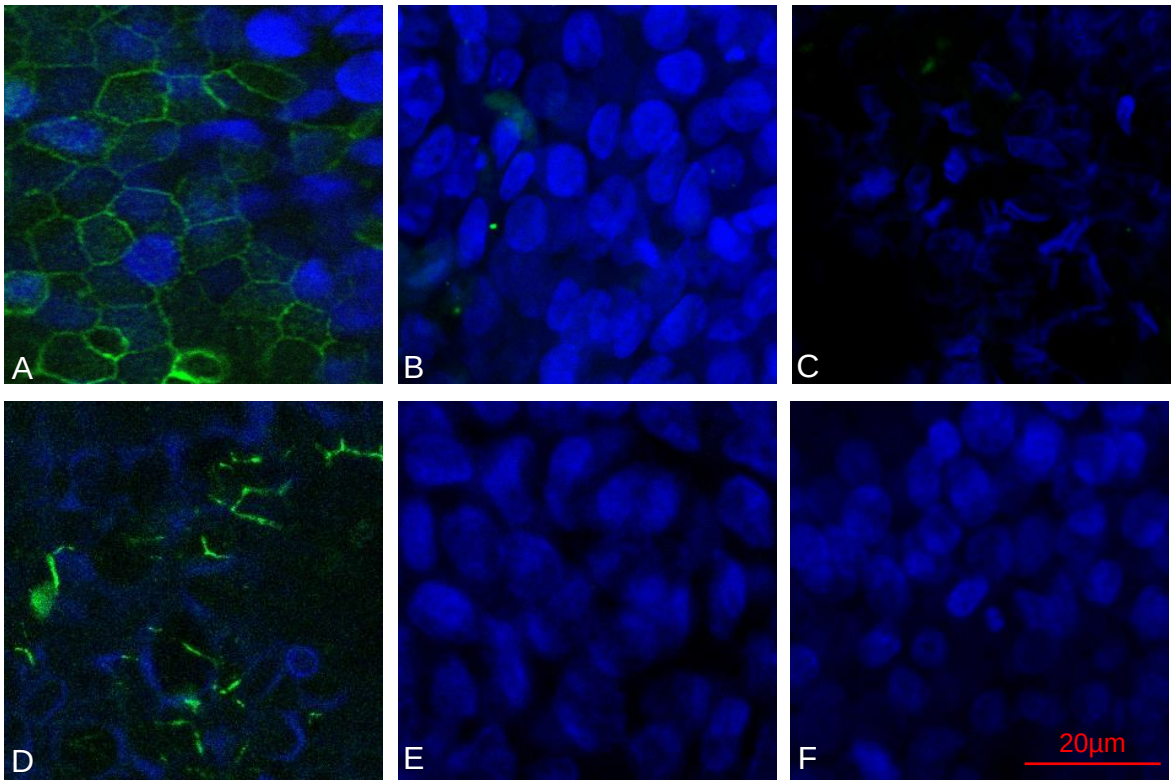

Figure 6.3. Discontinuous immunolocalisation of ZO-1 following exposure to neutrophil serine proteases and pseudomonas elastase.

(A) *PBS-exposed HNEC-ALI demonstrating normal immunolocalisation of ZO-1.* **(B)** *Exposure to neutrophil elastase,* **(C)** *exposure to cathepsin G,* **(D)** *exposure to proteinase 3,* **(E)** *exposure to pseudomonas elastase and* **(F)** *exposure to triton X-100 positive with demonstration of reduced/absent ZO-1 expression.*

Ciliary Beat Frequency was not significantly affected with application of NSP and pseudomonas elastase

Ciliary beat frequency was not signifcantly affected following the expsoure to NSP or PE at 6 hours compared to PBS-treated cells ($P>0.05$) (Figure 6.4).

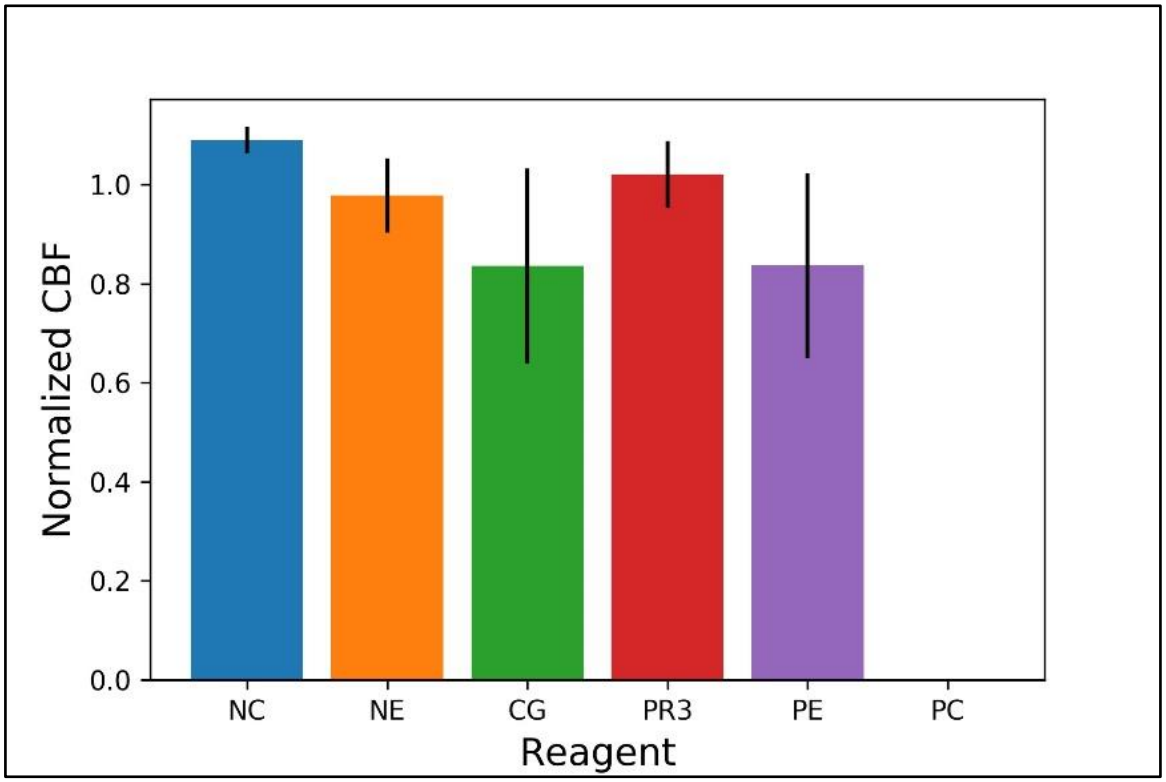

Figure 6.4. The effect of neutrophil serine proteases and pseudomonas elastase on the CBF of HNEC.

*The values are normalized and shown as a mean ± SEM for n=6 patients. All neutrophil serine proteases and pseudomonas elastase did not have a significant effect on CBF compared to negative control. Negative control = PBS. Positive control = 10% Triton-X. *P<0.05, Kruskal-Wallis test with posthoc permutation t-test. NC = Negative control, NE = Neutrophil elastase, CG = Cathepsin G, PR3 = Proteinase 3, PE = Pseudomonas elastase, PC = Positive control.*

No Significant Cytotoxic effects with application of NSP and pseudomonas elastase

The application of NSP and PE at 6 hours did not yield statistically significant differences in cell cytotoxicity compared to negative control cells treated with PBS (P>0.05) (Figure 6.5).

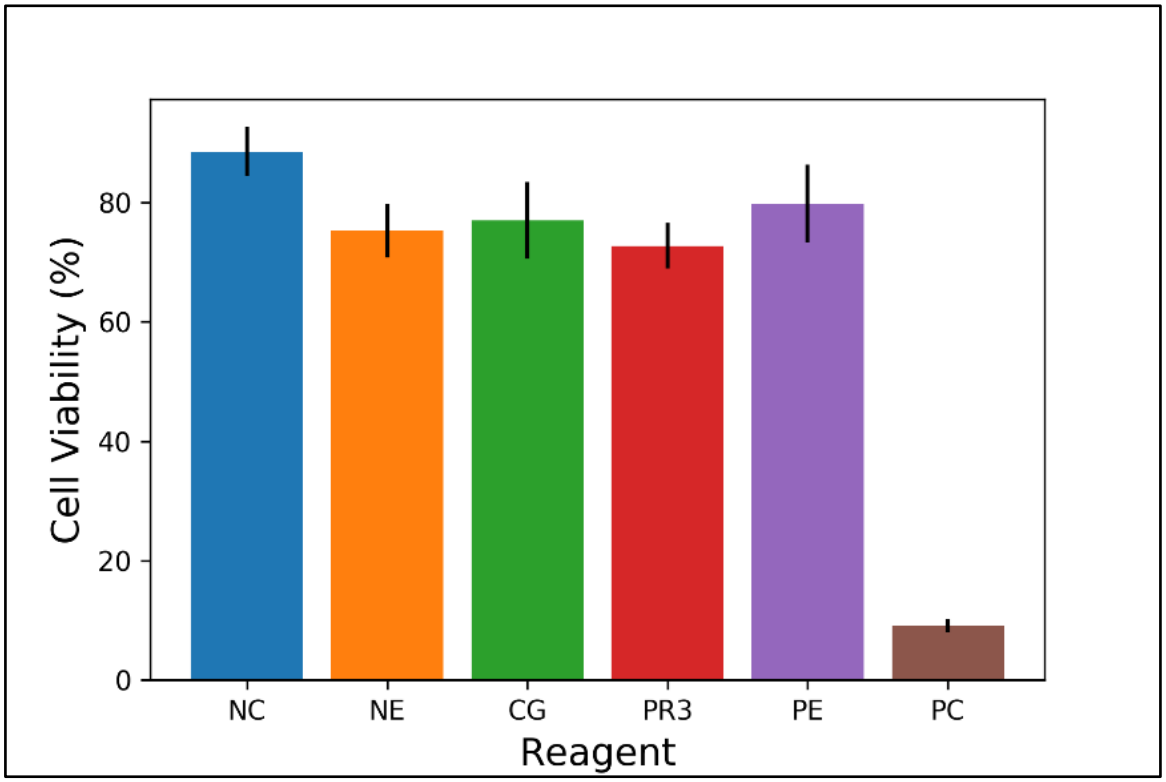

Figure 6.5. The effect of neutrophil serine proteases and pseudomonas elastase on the cell viability of HNEC.

The values are shown as a mean ± SEM for n=6 patients. All neutrophil serine proteases and pseudomonas elastase did not have a significant effect on cell viability compared to negative control. Negative control = PBS. Kruskal-Wallis test with posthoc permutation t-test. NC = Negative control, NE = Neutrophil elastase, CG = Cathepsin G, PR3 = Proteinase 3, PE = Pseudomonas elastase, PC = Positive control.

No Significant Effect on IL-6 and IL-8 Production Following Exposure to NSP by HNEC-ALI

Following 6 hours of exposure to NSP and PE, there were no statistically significant differences in release of IL-8 from the HNEC-ALI ($P>0.05$) (Figure 6.6). Levels of IL-6 release were below the detection limit.

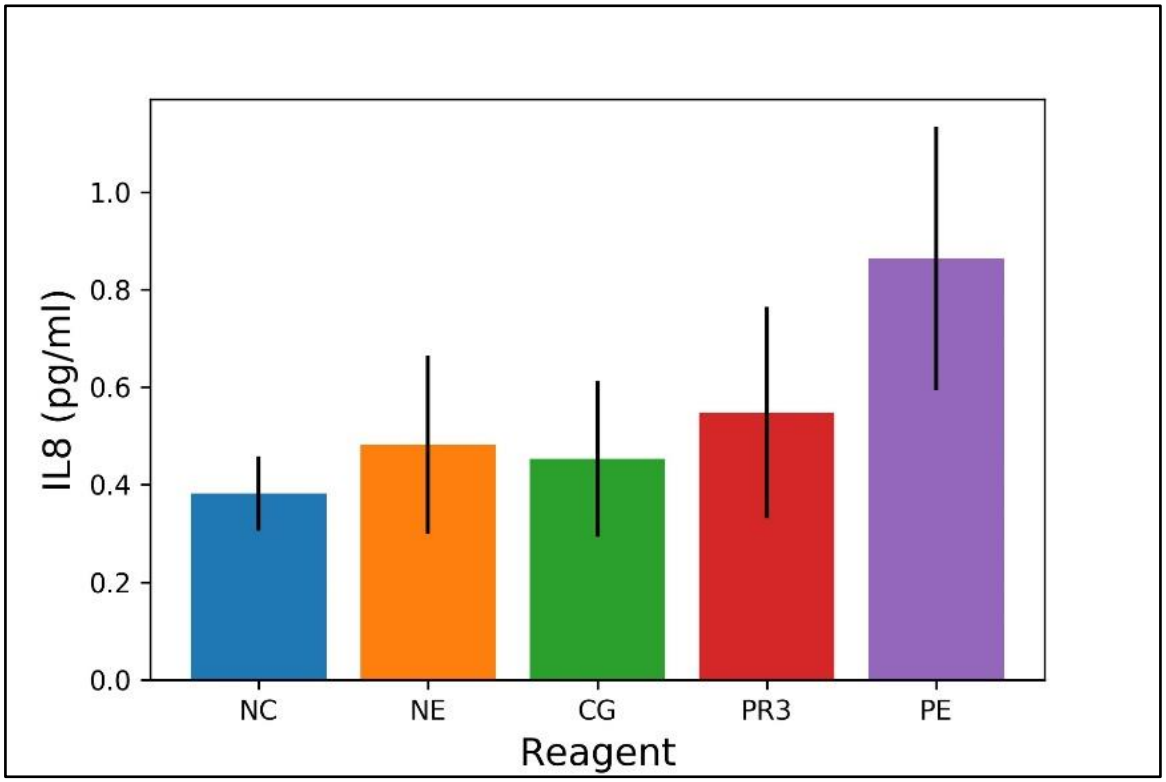

Figure 6.6. The effect of neutrophil serine proteases and pseudomonas elastase on IL-8 production from HNEC.

*The values are shown as a mean ± SEM for n=6 patients. All neutrophil serine proteases and pseudomonas elastase did not have a significant effect on IL-8 release from HNEC compared to negative control. Negative control = PBS. *P<0.05, Kruskal-Wallis test with posthoc permutation t-test. NC = Negative control, NE = Neutrophil elastase, CG = Cathepsin G, PR3 = Proteinase 3, PE = Pseudomonas elastase.*

DISCUSSION

This study investigated the effects of neutrophil serine proteases (NSP) on barrier function of primary human nasal epithelial cells grown at an air liquid interface. The application of NSP demonstrated epithelial tight junction disruption, evidenced by reduction in TER, increased paracellular permeability and disruption of ZO-1 immunolocalisation, without inducing cellular toxicity. These findings indicate the collateral damage on mucosal barrier structure and function from neutrophils during chronic inflammatory conditions of the upper airways, such as chronic rhinosinusitis.

Neutrophils play a vital role in acute inflammation and defence against microbial infections via a Th1 immune response. Neutrophilic infiltrations within the mucosa in the context of chronic inflammatory conditions such as chronic rhinosinusitis with nasal polyposis (CRSwNP) have also been described.[508] Elevated levels of IL-6, a stimulator of proinflammatory acute phase proteins, and IL-8, a neutrophil chemotactic cytokine, have both been found in nasal charge of CRS patients.[8, 509] Particularly, CRSwNP in East Asian populations have demonstrated neutrophilic infiltrations also in the context of Th17/Th2 inflammatory patterns.[175, 180, 510] This increased neutrophilia in CRSwNP patients has been associated with poorer treatment outcomes and likely plays a part in the pathogenesis of CRS.[511]

Mucosal barrier dysfunction has been proposed to have a critical role in the etiopathogenesis of CRS.[1] Recent studies have identified the release of the cytokine oncostatin M from neutrophils with associated disruption of the epithelial barrier in CRSwNP.[93, 510] This study adds to these findings demonstrating NSP also contributes the barrier dysfunction. NSP are multifunctional enzymes released by neutrophils in inflammatory regulation and pathogen destruction. Neutrophil elastase, cathepsin G and proteinase 3 are all capable of intracellular and

extracellular killing of pathogens.[94] These properties responsible for pathogen destruction might at the same time cause collateral damage to host tissue, which is observed in chronically inflamed mucosal tissue such as in CRS. Our study found the effects of these serine proteases were inactivated through heating, indicating that the effects were due to the action of the proteases on HNEC-ALI cultures rather than impurities that might be present in those extracts.

Neutrophil elastase has been demonstrated to impair epithelial defence against bacterial infection in a bronchial epithelial model.[107] Exposure of neutrophil elastase to bronchial epithelial cells demonstrated degradation of the airway epithelial host defence protein short palate, lung and nasal epithelial clone 1 (PLUNC1). Additionally, there was a dose dependent relationship between neutrophil elastase and PLUNC1 reduction and increased bacterial load.[107] Our findings of reduced TER and increased paracellular permeability in the nasal epithelial model support this finding of barrier dysfunction secondary to NSP exposure. This epithelial barrier dysfunction is likely secondary to reduced expression of tight junction proteins. Neutrophil elastase can cause cleavage of E-cadherin, an intercellular junction protein, thus disrupting cell-cell adhesion.[108] We demonstrated marked reduction in ZO-1 immunolocalisation in nasal epithelial cells after exposure to neutrophil elastase and cathepsin G. This disruption in the membrane barrier may allow for bacterial invasion into the submucosa of CRS patients, worsening disease severity.

P. aeruginosa elastase has been demonstrated to disrupt the mucosal barrier through the disorganisation of tight junction proteins.[55] Additionally, *P. aeruginosa* elastase has the ability to inhibit pro-inflammatory responses through cleaving thrombin and releasing C-terminal derived peptide. The release from this peptide binds to pathogen-associated lipopolysaccharide preventing cell activation and consequent proinflammatory responses.[56] These virulence

mechanisms may contribute to the recalcitrant nature of *P. aeruginosa* infections in CRS. This study demonstrates the detrimental effects of *P. aeruginosa* elastase on the mucosal barrier, and further research is required to ascertain differences in neutrophil elastase and *P. aeruginosa* elastase to allow for more targeted therapies.

Cilia function is a paramount aspect of the upper airways defence system, where dysfunction is observed in chronic conditions such as cystic fibrosis.[512] Protease-activated receptor 2 (PAR-2) located basolaterally, has been demonstrated to be involved in the regulation of airway secretions and ciliary beat frequency.[513] Thus the apical application of neutrophil serine does not affect CBF. Neutrophil elastase and cathepsin G have been demonstrated to be potent secretagogues for airway glandular serous cells.[514] The degradation of secretory products like chondroitin sulfate proteoglycans may contribute to abnormal secretions observed in inflammatory airways disease. The composition and amount of mucus secretions released induced by NSP was outside the scope of this study, however, there was no significant effect on the cilia function on control or CRSwNP human nasal epithelial cells.

One limitation of this study is that the concentration of NSP and NE varied from 0.1 µg/ml (PR3) to 10µg/ml for CG and NE and 50µg/ml for PE. Concentrations of active NSP *in vivo* vary depending on the degree of inflammation ranging from negligible in healthy airway secretions to exceeding 100µg/ml in cystic fibrosis patients.[514, 515] 10µg/ml of NE and CG was used as it was deemed the physiological dose commonly employed in the literature.[107, 108, 515] Interestingly, PE behaves similarly to NE, potentially allowing pathogen invasion leading to further inflammation and tissue damage.[56] Concentrations of PE in sputum of cystic fibrosis patients vary from 0.01 to 110µg/ml [516] with concentration of 50µg/ml shown to disrupt the barrier *in vitro*.[57] Whilst the use of these varying dosages limits the possibility to compare the

potency of the different proteases, similar trends on mucosal barrier dysfunction and toxicity were observed for the different proteases. As IL-6 and IL-8 are transcriptionally regulated, longer times may have been required for the HNEC-ALI cultures to release these cytokines into the media for testing. This may explain the non-statistically significant results at six hours. Immunofluorescence conducted visually demonstrated reduced ZO-1 tight junction protein expression following serine proteases exposure, however, this disorganisation was not quantifiable via Western Blot analysis or mRNA change. Further studies are required to define the molecular mechanism of action of the proteases and to define the exact proteins affected.

This study has demonstrated the important effects of neutrophil serine proteases on human nasal epithelial cell barrier dysfunction. The impaired barrier function through disorganisation of tight junction proteins observed may account for barrier invasion by pathogens seen in chronic inflammatory airways diseases. Therapeutic intervention targeting neutrophil and pseudomonas serine proteases may offer benefits to the management of CRS and other inflammatory diseases.

ACKNOWLEDGEMENTS

This project was supported by Adelaide University Research Training Program Scholarship, Bertha Sudholz Scholarship and Garnett Passe Rodney Williams Memorial Foundation Scholarship to SSK.

CHAPTER 7: SCOPING REVIEW OF CHRONIC RHINOSINUSITIS PROTEOMICS.

STATEMENT OF AUTHORSHIP

Title of Paper	Scoping review of chronic rhinosinusitis proteomics
Publication Status	☑ Published ☐ Accepted for Publication ☐ Submitted for Publication ☐ Unpublished and Unsubmitted work written in manuscript style
Publication Details	Kao SS, Bassiouni A, Ramezanpour M, Chegeni N, Colella AD, Chataway TK, et al. Scoping review of chronic rhinosinusitis proteomics. Rhinology. 2020.

Principal Author

Name of Principal Author (Candidate)	Stephen Kao		
Contribution to the Paper	Experimental design, Study selection, Data collection, Data analysis, Manuscript preparation.		
Overall percentage (%)	80%		
Certification:	This paper reports on original research I conducted during the period of my Higher Degree by Research candidature and is not subject to any obligations or contractual agreements with a third party that would constrain its inclusion in this thesis. I am the primary author of this paper.		
Signature		Date	24.03.2020

Co-Author Contributions

By signing the Statement of Authorship, each author certifies that:

i. the candidate's stated contribution to the publication is accurate (as detailed above);
ii. permission is granted for the candidate in include the publication in the thesis; and
iii. the sum of all co-author contributions is equal to 100% less the candidate's stated contribution.

Name of Co-Author	Ahmed Bassiouni		
Contribution to the Paper	Study selection, Data collection, Data analysis		
Signature		Date	24.03.2020

Name of Co-Author	Mahnaz Ramezanpour		
Contribution to the Paper	Study selection, Data analysis, Manuscript editing		
Signature		Date	20.03.2020

Name of Co-Author	Nusha Chegeni		
Contribution to the Paper	Assisted with experiments, Manuscript editing		
Signature		Date	20.03.2020

Name of Co-Author	Alex Colella		
Contribution to the Paper	Assisted with experiments, Manuscript editing		
Signature		Date	20.03.2020

Name of Co-Author	Timothy Chataway		
Contribution to the Paper	Project supervision, Manuscript editing, Data analysis		
Signature		Date	20.03.2020

Name of Co-Author	Peter-John Wormald		
Contribution to the Paper	Project supervision, Manuscript editing		
Signature		Date	17.03.2020

Name of Co-Author	Sarah Vreugde		
Contribution to the Paper	Project supervision, Manuscript editing		
Signature		Date	20.03.2020

Name of Co-Author	Alkis James Psaltis		
Contribution to the Paper	Project supervision, Manuscript editing, Assistance with study design, Corresponding author		
Signature		Date	17.03.2020

CITATION

Kao SS, Bassiouni A, Ramezanpour M, Chegeni N, Colella AD, Chataway TK, et al. Scoping review of chronic rhinosinusitis proteomics. Rhinology. 2020.

ABSTRACT

Introduction

Progressive advances in proteomic technology has improved our understanding of the chronic rhinosinusitis (CRS) pathogenesis and endotypes. This scoping review aims to present a comprehensive and descriptive analysis of nasal mucosa and mucus proteome of CRS patients.

Methods

Studies investigating the proteome of nasal mucosa and mucus from healthy and CRS patients via mass spectrometry were included. Critical appraisal of methodological quality was conducted with extraction of protein lists. Gene set enrichment analysis (GSEA) was performed on studies including CRS patients.

Results

2962 proteins were identified in the 21 studies included in this review. Eleven studies investigated the nasal mucus proteome and ten studies investigated the nasal mucosa proteome. Studies demonstrated heterogeneity in patients, sampling and mass spectrometry methodology. Samples from CRS patients suggested a trend in enrichment of immune system and programmed cell death pathways. Increased expression of proteins involved in cellular components including the cytoskeleton and adherens junctions was also present in CRS.

Conclusions

Alterations in the healthy sinonasal proteome may lead to the increased immunological, metabolic and tissue remodelling processes observed in CRS. However, it is difficult to draw significant conclusions from the GSEA due to the heterogeneity present in the limited literature

available. These findings allow us to direct further research to better understand CRS pathogenesis and its endotypes.

Keywords: Chronic rhinosinusitis, Mucus, Proteomics, Scoping review, Mass Spectrometry

INTRODUCTION

Chronic rhinosinusitis (CRS) is characterised by persisting inflammation of the mucosa in the nasal cavity and paranasal sinuses. The current phenotypic classification of CRS is divided into CRS without nasal polyps (CRSsNP) or CRS with nasal polyps (CRSwNP). These phenotypes, however, do not cover the diverse cellular pathways involved in the complex pathogenesis of CRS. Advances in laboratory techniques has led to investigating CRS endotypes, enabling a better understanding of upstream pathogenic factors that lead to CRS disease manifestation and recalcitrance. Ultimately, CRS endotypes may allow clinicians to predict disease prognosis and develop personalised treatment regimes.

The mucosal barrier, in concert with an effective mucociliary transport system and a protective mucus layer interact together with the innate and humoral immune system to maintain homeostasis in health. Tight junctions located on the apical aspects of cell membranes inhibit the flow of solutes and water into the paracellular space in addition to forming cell polarity.[504, 517, 518] Studies have demonstrated down regulation of tight junction transmembrane and associated proteins with reduced transmembrane electrical resistance in patients with CRS.[204, 519, 520] Furthermore various inflammatory cytokines including IL-17, IL-33, TLSP have been implicated in the pathogenesis of CRS and nasal polyp formation.[180, 521-523] The heterogeneity of immune responses in CRS endotypes certainly plays a significant role in the manifestation of the disease.

Nasal mucus, a vital component of the mucociliary clearance system, is produced by seromucinous glands, goblet cells and the transudation of plasma. It is composed of glycoproteins and polysaccharide chains organised into two layers; the lower periciliary layer and the superficial viscous layer.[357, 359] The antimicrobial effects of nasal mucus have been well

studied.[357, 359] The overproduction of viscous nasal mucus is commonly reported amongst CRS patients manifested as rhinorrhoea and postnasal drip. This tenacious mucus adversely affects ciliary function, leading to stasis that may result in a nidus for bacterial growth.[524-526]

The proteomic analysis of nasal mucus and mucosa is a rapidly evolving field exploring the physiological and pathological mechanisms involved in CRS. In this form of analysis, mucus and tissue samples collected from patients undergo gel electrophoresis or liquid chromatography to separate the proteins.[500] Proteins are subjected to mass spectrometry (MS) for identification of peptide sequences, which are compared against known protein databases. Previous studies have provided insight into the proteins involved in various immune responses from mucus and mucosa collected from CRS patients.[461, 499, 500] The aim of this scoping review was to perform a comprehensive review of the current literature on the CRS proteome and to ascertain differences between CRS and healthy patients. Ultimately, improving the knowledge of CRS endotypes through cellular pathways present will guide prognostication and treatment regimens for CRS patients.

MATERIALS AND METHODS

The search strategy aimed to capture all English language studies published in Pubmed, CINAHL, Embase and Cochrane CENTRAL databases since their creation. A preliminary initial search of the Pubmed database using the keywords “Chronic rhinosinusitis”, “Mucus”, and “Proteomics” was initially performed to identify further relevant key words to be included in the final search strategy of all databases (Supplementary Figure 7.1). A second search using all identified keywords and medical subject headings were applied across all databases. This review adhered to the PRISMA guidelines for reporting systematic reviews. The reference lists of all selected studies were searched for additional studies.

Studies conducting proteomic analysis on patients 18 years or older via mass spectrometry on mucus samples or nasal mucosa collected from healthy or CRS patients were included. Studies conducting bottom up proteomics were included, with studies investigating select proteins were excluded. Patients diagnosed with acute sinusitis or allergic rhinitis or exposure to chemicals or fumes were excluded. Studies utilising tissue collected from the olfactory bulb, olfactory epithelium, nerve tissue, or tissue grown in vitro were excluded. Proteins mentioned in systemic reviews, meta-analyses, literature reviews and conferences abstracts were excluded to prevent duplication of data.

Papers retrieved that met all inclusion criteria were assessed by two independent reviewers (SSK, AB) for methodological validity prior to inclusion in the review. Differences in assessments between reviewers were resolved through discussion with a third reviewer (TC).

Data extraction focused on proteins identified through mass spectrometry in healthy and CRS patients. Key data extracted included disease status (Healthy or CRS), tissue collection method,

tissue specimen examined (Mucus or Mucosa), analytical platform and protein composition. Proteins identified were stratified by mucus or mucosa origin and disease status.

Statistical Analysis

Statistical analysis was conducted with R statistical software (R Core team, Vienna, Austria).[503] All proteins identified from studies were matched manually with their Uniprot accession numbers, protein name and gene. Proteins not in the Uniprot database or not from Homo Sapiens genus were excluded from the analysis. Proteins were stratified into their presence in either CRS, healthy groups or both for mucus and mucosa samples. Mucus and mucosa protein lists were processed separately, due to their differing constituents. Gene set enrichment analysis (GSEA) was conducted, clustering the available differentially expressed genes for analysis. This was performed by uploading protein lists to Enrichr™ (Ma'ayan Laboratory, USA), a web-based software.[527, 528] Reactome 2016 pathway database identified cellular pathways, and the Gene Ontology database identified biological processes, cellular components and molecular functions. Only significant results (Adjusted P-value <0.05 calculated by Enrichr™) were included for further analysis. Mucus and mucosa GSEA results were combined for analysis. No further analysis was possible due to the lack of available numeric quantifiable data from the studies included in the review.

The cellular pathways generated from CRS mucus and mucosa were then combined. This was also performed for the biological processes, cellular components and molecular functions. The same was performed for proteins unique to the healthy group, and proteins present in both healthy and CRS groups.

RESULTS

The search identified a total of 591 studies in English, with 526 remaining after duplicates were removed. Titles and abstracts were reviewed against the inclusion criteria yielding a total of 52 studies for full text analysis. 21 studies met the inclusion criteria (Supplementary Figure 7.2).

Studies included were published between 2004 to 2018 originating from Austria[413, 529], Canada[500], China[498], Finland[530], France[531], Germany[461, 532], Italy[533], Portugal[534, 535], South Korea[536, 537], Sweden[538-542] and USA[499, 543, 544].

From the 21 studies, a total of 345 patients were included, consisting of 302 healthy control patients and 43 CRS patients (CRSwNP 34 and CRSsNP 9). Eleven studies involved mucus samples; seven collected by nasal lavage fluid washes and four by suction. Ten studies involved sampling of the nasal mucosa, five by mucosal brushing and five by intraoperative biopsies.

A total of 2962 proteins were identified after removal of duplicates in the 21 studies. 549 proteins were identified in mucus samples, consisting of 45 unique to CRS samples, 398 unique to healthy and 106 common in both groups. 2829 proteins were identified in mucosa samples, including six unique to CRS samples, 2771 unique to healthy and 52 common in both groups (Supplementary Table 7.1).

Critical Analysis of Included Studies

All 21 studies included in this review focused on the identification and analysis of the nasal mucus and mucosa proteome and all included analysis of control donors and/or CRS patients. Only data from healthy and CRS patients was extracted and included in this review. The focus of the included studies was to identify and ascertain differences in the nasal mucus or tissue

proteome between CRS patients and controls, however, there was considerable variability in patient demographics and clinical status. Four studies obtained samples from healthy and allergic rhinitis patients before and after pollen seasons to compare changes in proteome.[529, 530, 538, 541] The allergic rhinitis protein content was excluded from this review, and only the healthy proteome was included in the overall protein list. One study did not document the number of patients included,[532] and two studies did not include patient age.[538, 540] These three studies consisted of only healthy patients, and the proteins identified were included in the catalogue of proteins in this review (Supplementary Figure 7.2). CRS was diagnosed via nasoendoscopic examination in all cases, with the addition of CT imaging in three studies.[498, 499, 536] Minimal details were given across the included studies regarding polyp grades and CT scores with one study grading polyp severity in CRS patients.[461] Studies defined healthy patients who demonstrated no clinical or CT evidence of allergic rhinitis or CRS. One study included two smokers[536] and two studies utilised oral steroids.[461, 499] These details are summarised in Supplementary Table 7.2.

There was heterogeneity between studies regarding sample collection and preparation prior to analysis with the mass spectrometer. Nasal mucus was collected via nasal lavage fluid (NLF) in seven studies and suction in four studies (Table 7.1). Nasal tissue samples were collected as nasal brushings in five studies and biopsy of nasal mucosa (inferior turbinate, polyp, ethmoid or sphenoid sinuses) in five studies (Table 7.2). Heterogeneity in sample collection method and site of tissue extraction is a potential for confounding bias. Seven studies performed additional immunochemistry on cells to identify cellular changes in healthy and CRS patients.[498, 499, 533, 534, 536, 537, 539] These studies identified a range of nasal mucosal and inflammatory cells, however, there is limited reporting of which specific cell types were tested during the proteomic experiments.

Nasal tissue sample preparation prior to mass spectrometry analysis was variable, however, followed the same principles across all the studies. Nasal mucus samples were run through 2D Gel electrophoresis in seven studies.[413, 529, 531, 532, 538, 539, 542] Protein spots of interest were cut and underwent trypsin digestion prior to mass spectrometry analysis. Nasal tissue samples all underwent tissue lysis through combinations of lysis buffers and mechanical disruption via sonification. Protein was collected from these lysed cells and run through 2D gel electrophoresis in eight of the studies.[461, 498, 499, 530, 533, 534, 536, 537]

Various techniques of mass spectrometry were employed across the 21 included studies, where some studies used two different techniques. Ion trap LC-MS/MS was used in ten studies, matrix assisted laser desorption/ ionisation mass spectrometry (MALDI-TOF) was used in ten studies, electrospray-ionisation quadrupole time-of-flight mass spectrometry (ESI-Q-TOF) was used in three studies and liquid chromatography/ quadrupole time-of-flight mass spectrometry (LC-Q-TOF) was used in one study (Table 7.1 and Table 7.2). Notably, the most recent of these studies was published 8 years ago, and since then, there have been considerable advances in MS equipment speed, resolution and sensitivity. Furthermore, various protein identification criteria were employed, including 2-4 peptides present, 10-20% sequence coverage and false discovery rates of less than 5%.

Table 7.1 Studies Investigating Proteomics of Nasal Mucus

Author	Disease Status	Patients	Collection Method	MS Method	MS Equipment	Proteins Identified
Benson et al.[543]	CRSsNP	6	NLF	Nano-LC-MS/MS	LC (Michrom BioResources Inc; CA, USA), LTQ Linear ion trap MS (ThermoFinnigan; CA, USA)	129
Casado et al.[544]	Healthy	10	NLF	Micro-Capillary LC ESI-Q-TOF MS	CapLC (Waters; Milford, USA), ESI-Q-TOF MS (Micromass; Manchester, UK)	111
Debat et al.[531]	Healthy	16	Suction	MALDI-TOF MS	Voyager DE STR+ TOF-MS (Applied Biosystems; CA, USA)	75
Ghafouri et al.[538]	Healthy	5	NLF	MALDI-TOF-MS Nanoelectrospray MS/MS	Voyager DE PRO MS (Applied Biosystems; CA, USA), API Q-STAR Pulzer i (Applied biosystems; CA, USA) with nanoelectrospray ion source (MDS-Protana; Odense, Denmark)	20
Lindahl et al.[539]	Healthy	7	NLF	MALDI-TOF MS	Voyager DE STR MS (PE-Biosystems; CA, USA) or Bruker Reflex (Bruker Daltonics; Bremen, Germany)	12
Mortstedt et al.[540]	Healthy	8	NLF	Micro-LC-MS/MS Nano-LC-Q-TOF MS	LC (UFLCXR, Shimadzu Corporation; Kyoto, Japan), QTRAP 5500 hybrid triple quadrupole/ linear ion trap MS (Applied Biosystems/ MDS Sciex; MA, USA) LC (Agilent 1100 series; CA, USA), QSTAR pulsar hybrid quadrupole TOF MS (Applied Biosystems/MDS Sciex; MA, USA)	331
Schoenebeck et al.[532]	Healthy	N/A	NLF	Nano-LC-MS/MS Micro-LC-MS/MS	LC (Ultimate HPLC system, Dionex; Idstein, Germany), HCT ultra PTM analysis system (Bruker Daltonic; Bremen, Germany), LC (HP Ultimate 300 system, Dionex; Idstein, Germany), LTQ OrbiTrap Velos MS (Thermofisher Scientific; MA, USA)	34
Tewfik et al.[500]	Healthy CRSwNP	4 4	Suction	Micro-LC-MS/MS	LC (Agilent Technologies; Ontario, Canada), QTRAP 4000 (Sciex-Applied Biosystems; Ontario, Canada)	35
Tomazic et al.[413]	Healthy	29	Suction	Nano-LC-MS/MS	Nano-HPLC (Agilent 1200 series; Vienna, Austria), LTQ-FT MS (Thermo Scientific; Vienna, Austria)	247
Tomazic et al.[529]	Healthy	12	Suction	Nano-LC-MS/MS	Nano-HPLC (Agilent 1200 series; Vienna, Austria), LTQ-FT MS (Thermo Scientific; Vienna, Austria)	366
Wahlen et al.[542]	Healthy	13	NLF	MALDI-TOF MS	Voyager DE PRO (Applied Biosystems; CA, USA)	48

HPLC: High performance liquid chromatography; LC: Liquid Chromatography; NLF: Nasal lavage fluid; MS: Mass spectrometry; LC-MS/MS: Liquid chromatography-tandem mass spectrometry; ESI-Q-TOF: Electrospray-ionisation quadrupole time-of-flight mass spectrometry; LC-Q-TOF: Liquid chromatography/ quadrupole time-of-flight mass spectrometry; MALDI-TOF MS: Matrix Assisted Laser Desorption/ Ionisation mass spectrometry.

Table 7.2. Studies Investigating Proteomics of Nasal Mucosa

Author	Disease Status	Patients	Collection Method	MS Method	MS Equipment	Proteins Identified
Farajzadeh Deroede et al.[461]	CRSwNP	3	Biopsy (Polyp tissue)	MALDI-TOF-MS	Proteome-Analyser 4700 (Applied Biosystems; CA, USA)	11
Gelardi et al.[533]	Healthy	4	Nasal brushing	MALDI-TOF-MS	Voyager DE PRO MS (Applied Biosystems; CA, USA)	18
Kim et al.[536]	CRSwNP	13	Biopsy (Polyp tissue)	Nano-LC-MS/MS	Agilent 1100 Series LC/MSD Trap XCT MS (Agilent Technologies; Ontario, Canada)	15
Lee et al.[537]	Healthy	10	Biopsy (Inferior turbinate)	MALDI-TOF MS	Voyager DE STR MS (Applied biosystems; CA, USA)	78
Min-Man et al.[498]	Healthy CRSsNP CRSwNP	7 7 7	Biopsy (Polyp tissue, Inferior turbinate)	MALDI-TOF MS ESI-Q-TOF MS	N/A	30
Ndika J et al.[541]	Healthy	10	Nasal Brushing	Nano-LC-MS/MS	LC (EASY nano LC 1000 (Proxeon, Thermo Fischer Scientific; CA, USA), Electrospray ionization quadrapole-orbitrap MS (Q Exactive, Thermo Fisher Scientific; CA, USA)	Spring 2090 Autumn 2107
Roxo-Rosa et al.[534]	Healthy	8	Nasal Brushing	MALDI-TOF MS	Biflex III (Bruker Daltonik; Bremen, Germany), Voyager DE STR MS (Applied Biosystems; Ontario, Canada)	65
Simoes et al.[535]	Healthy	129	Nasal Brushing	Micro-LC-MS/MS	Thermo LTQ linear ion trap spectrometer (Thermo Scientific, Waltham, MA)	1482
Suojalehto et al.[530]	Healthy	27	Nasal Brushing	ESI-Q-TOF MS	LC (EASY nano LC 1000 (Proxeon, Thermo Fischer Scientific; CA, USA), Electrospray ionisation quadrapole-orbitrap MS (Q Exactive, Thermo Fisher Scientific; CA, USA)	77
Upton DC et al.[499]	Healthy CRSwNP	3 3	Biopsy (Ethmoid, Sphenoid sinuses)	MALDI-TOF MS	Voyager DE Pro mass spectrometer (Protein Core Facility)	15

HPLC: High performance liquid chromatography; LC: Liquid Chromatography; MS: Mass spectrometry; LC-MS/MS: Liquid chromatography-tandem mass spectrometry; ESI-Q-TOF MS: Electrospray-ionisation quadrupole time-of-flight mass spectrometry; LC-Q-TOF MS: Liquid chromatography/ quadrupole time-of-flight mass spectrometry; MALDI-TOF MS: Matrix Assisted Laser Desorption/ Ionisation mass spectrometry;. Spring: Number of proteins identified in spring; Autumn: Number of proteins identified in autumn.

Nasal Mucus and Mucosa Proteome Gene Set Enrichment Analysis

There was substantial skew of studies investigating healthy mucus and mucosa samples compared to CRS samples. Thus, GSEA was only performed on the proteins identified in the six studies that sampled CRS patients. Two of these studies investigated nasal mucus[500, 543] and four studies examined the nasal mucosa.[461, 498, 499, 536] Three of these six studies directly compared the proteomes of CRS and healthy patients.[498-500] This was to reduce methodological bias in the analysis.

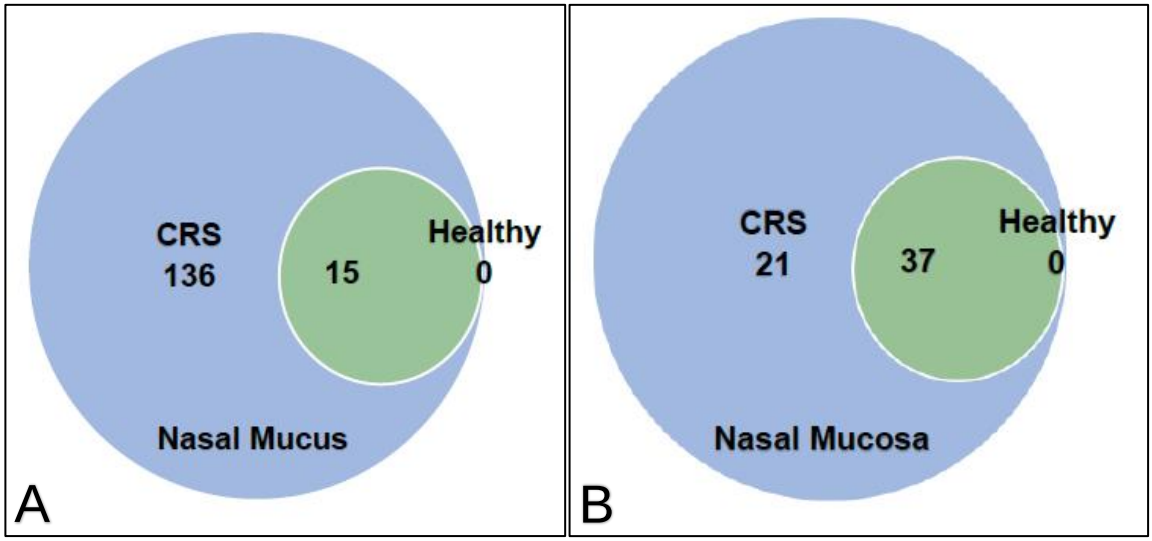

Figure 7.1. Venn diagram demonstrating total proteins identified in CRS and healthy patients in nasal mucus (A) and nasal mucosa (B).

151 proteins were identified in the two studies investigating the nasal mucus proteome (Supplementary Table 7.3 and Figure 7.1).[500, 543] 136 proteins were uniquely expressed in CRS mucus and 15 were found in both CRS and healthy mucus samples whilst no proteins were found to be unique to the healthy mucus proteome. 58 proteins were identified across four studies investigating the proteomics of nasal mucosa.[461, 498, 499, 536] 21 proteins were uniquely expressed in CRS mucosa, 37 proteins were present in both healthy and CRS mucosa and no proteins were unique to the healthy mucosa proteome (Figure 7.1).

CRS Proteome

Twenty-six cellular pathways were identified in the 136 uniquely expressed CRS mucus proteins and classified into six common groups (Supplementary Table 7.3). The pathways included immune system (42%), programmed cell death (19%), metabolism (16%), vesicle mediated transport (15%), homeostasis (4%) and signal transduction (4%) (Figure 7.2). No significant cellular pathways were identified in CRS mucosa samples.

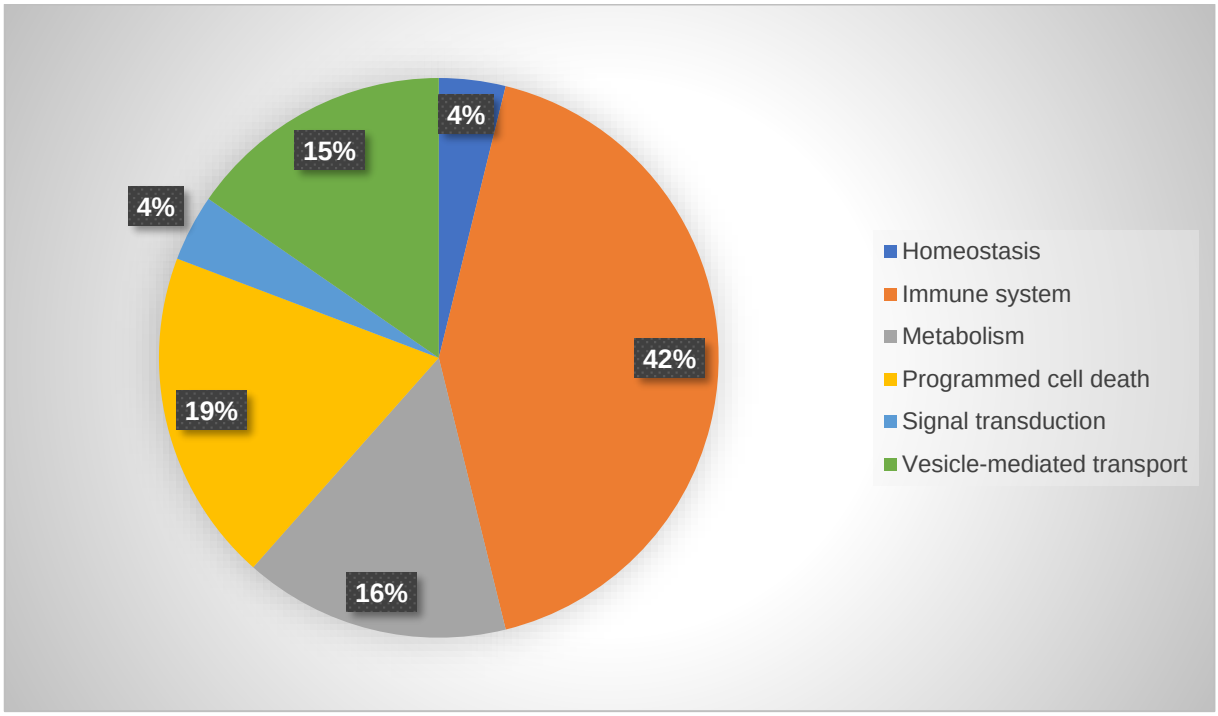

Figure 7.2. CRS cellular pathways.

Twenty-six cellular pathways identified, classified into six common groups. (%) Percentage of all identified cellular pathways in CRS samples.

Eighteen cellular components were uniquely identified in CRS mucus and mucosa samples, classified into six common groups consisting of secretory granules (44%), cytoskeleton (28%), adherens junction (11%), vacuoles (6%), mitochondrion (6%) and cytoplasmic vesicles (5%) (Supplementary Table 7.3 and Figure 7.3).

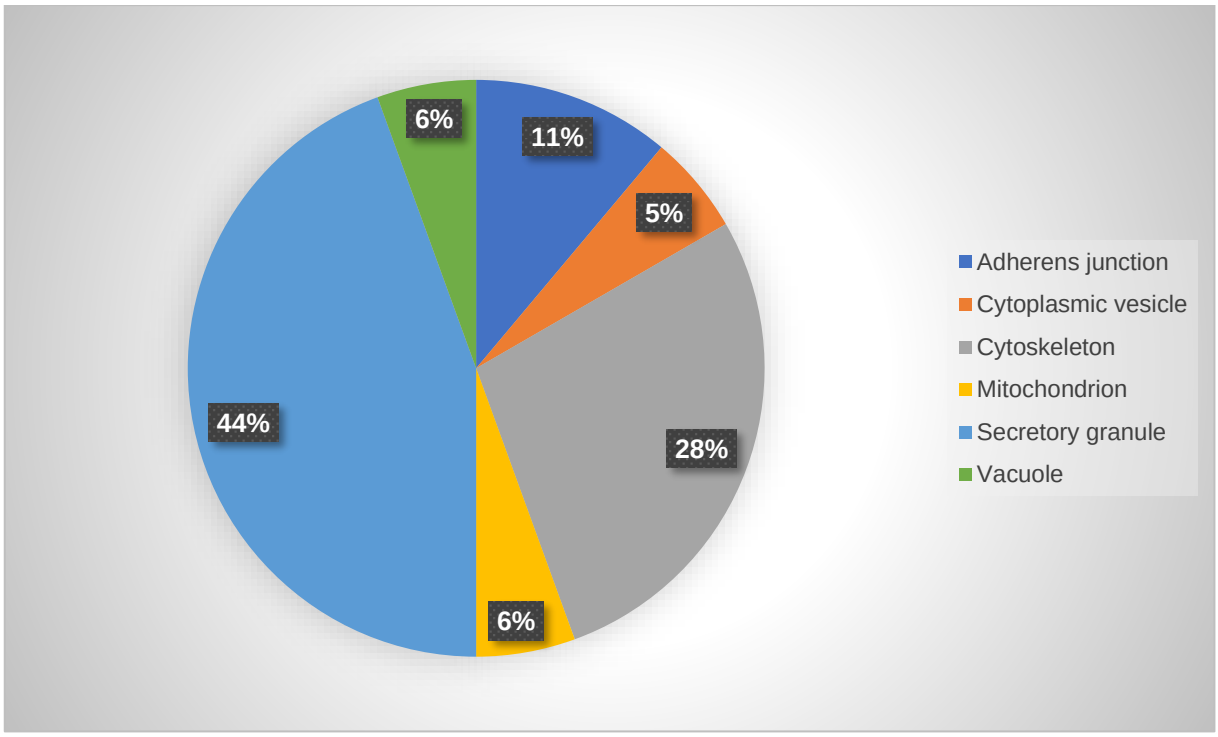

Figure 7.3. CRS cellular components.

Eighteen cellular components classified in six common groups. (%) Percentage of all identified cellular components in CRS samples.

Sixty-one biological processes were identified in CRS mucus and mucosa samples, stratified into 14 common groups (Supplementary Table 7.3). These processes included mainly immune system process (24%), cellular metabolic process (15%), metabolic process (13%), regulation of molecular function (6%) as well as anatomical structure development, biological regulation, cell activation, cellular component organisation, localisation, function, response to stimulus, sensory perception, system development and tissue homeostasis (all ≤5%) (Figure 7.4).

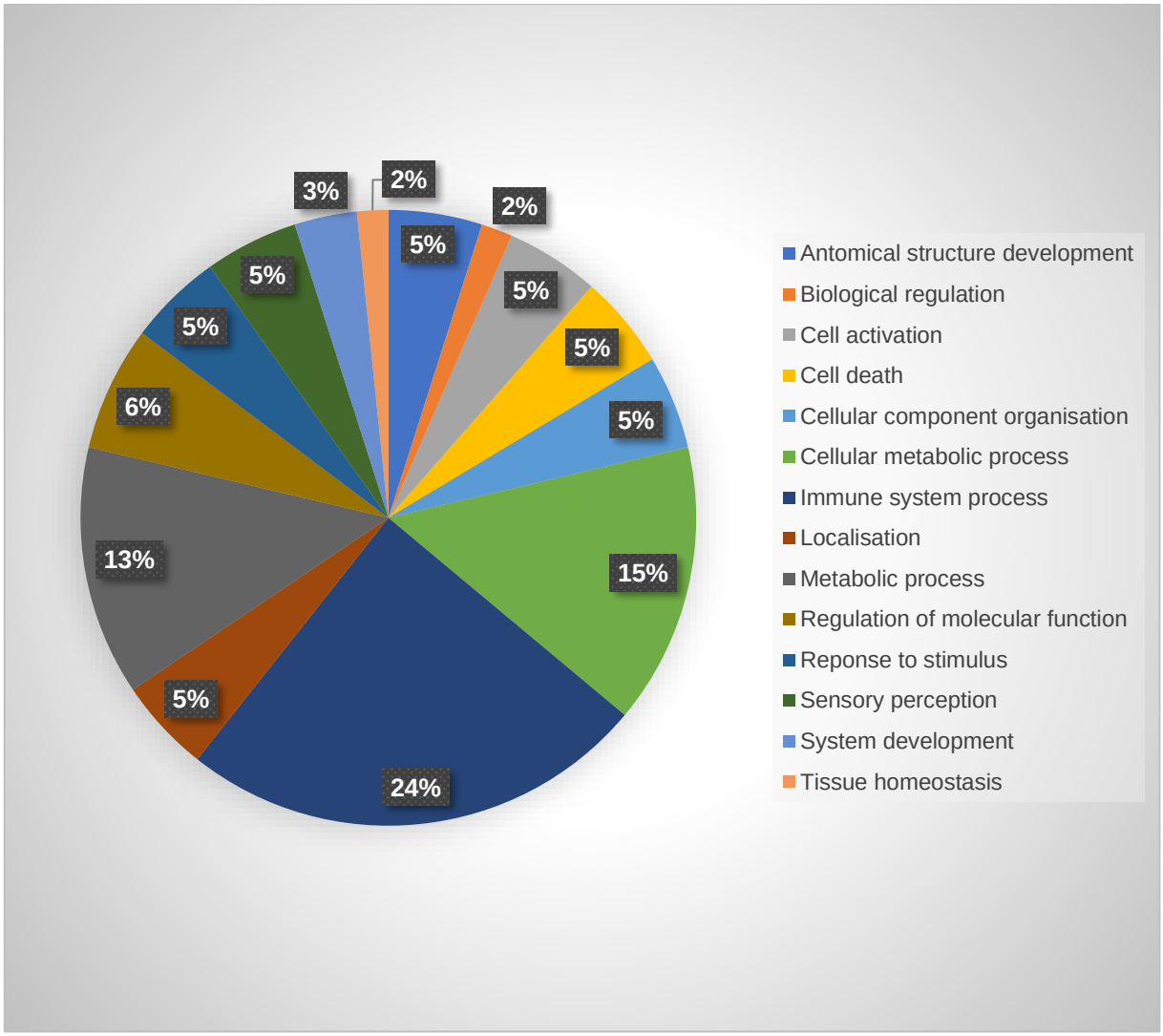

Figure 7.4. CRS biological processes.

Sixty-one biological processes classified into 14 common groups. (%) Percentage of all identified biological processes in CRS samples.

Eleven molecular functions were significantly present in CRS mucus, classified into three common functions consisting of binding (55%), molecular function regulation (27%) and catalytic activity (18%) (Supplementary Table 7.3 and Figure 7.5). No molecular functions were identified in CRS mucosa samples.

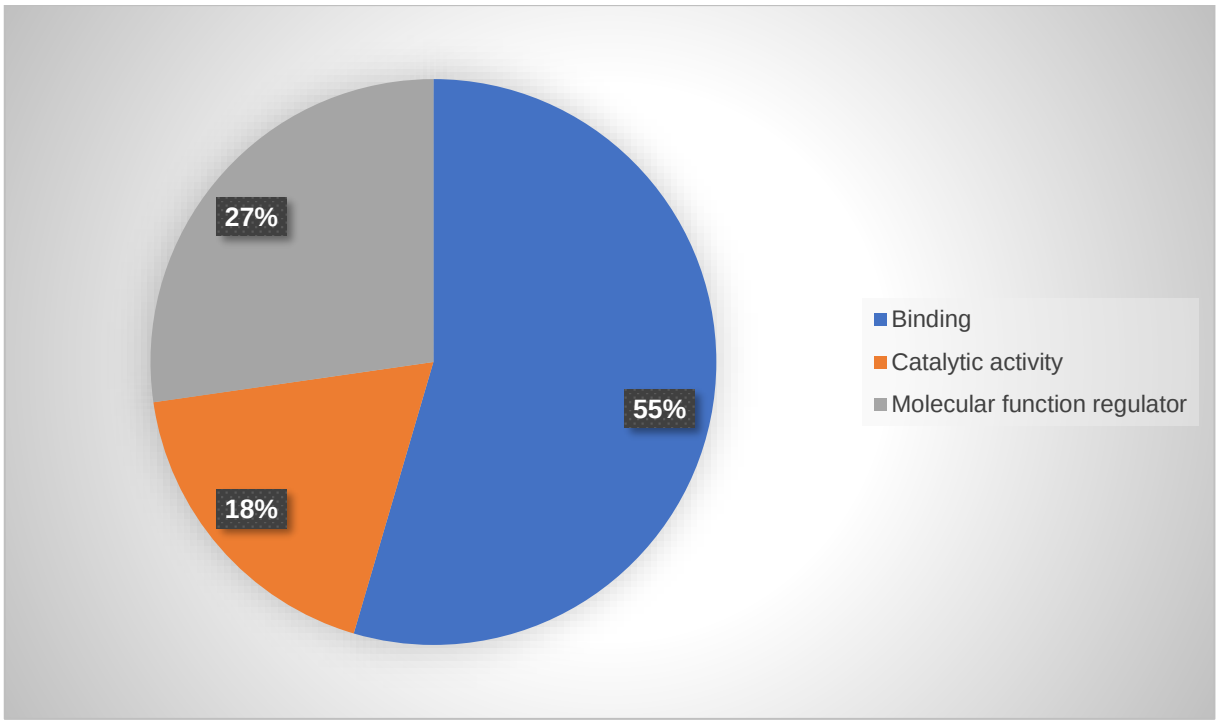

Figure 7.5. CRS molecular functions.

Eleven molecular functions classified into three common groups. (%) Percentage of all identified molecular functions in CRS samples.

Common Proteome in CRS and Healthy

All proteins identified in healthy mucus (15) and mucosa (37) samples were also present in CRS mucus and mucosa samples, respectively.

Thirteen cellular pathways were identified in both healthy and CRS mucus and mucosa samples were classifed into six common pathways: homeostasis (29%), metabolism (22%), vesicle-mediated transport (14%), signal transduction (14%), disease (14%) and cellular responses to external stimuli (7%) (Supplementary Table 7.3 and Figure 7.6).

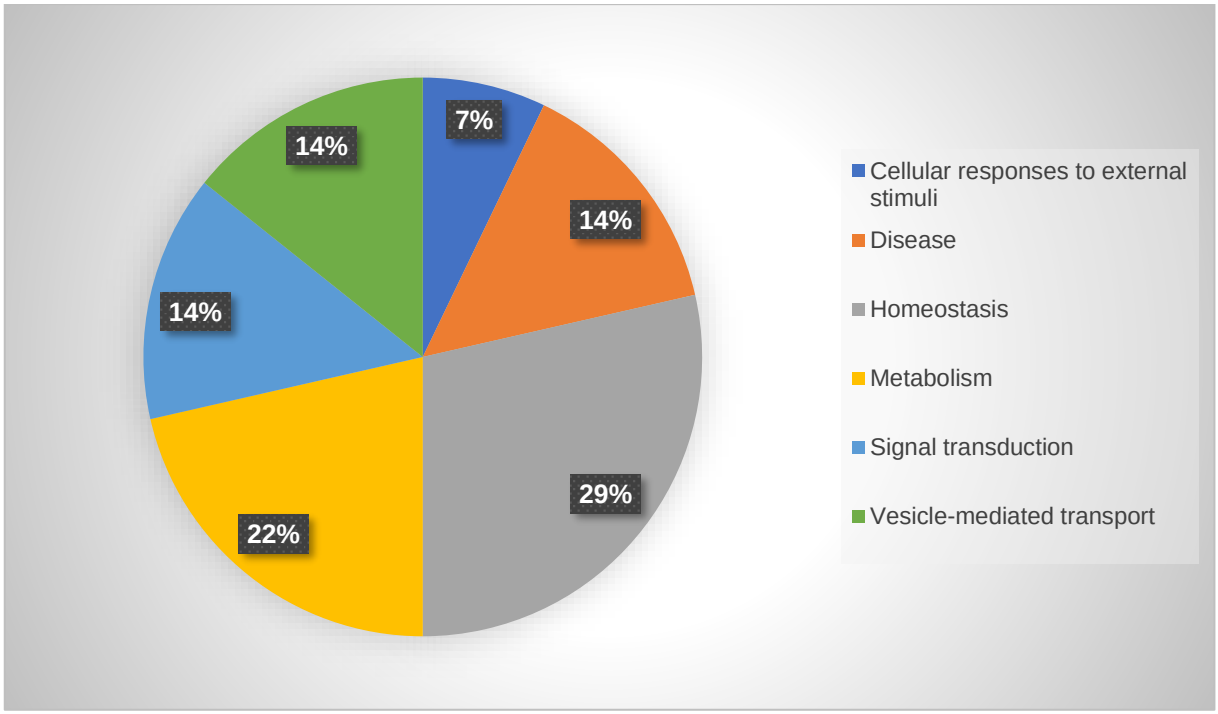

Figure 7.6. Healthy and CRS cellular pathways.

Thirteen cellular pathways identified and stratified into six common pathways. (%) Percentage of all identified cellular pathways in both healthy and CRS samples.

Fifteen cellular components were found to be present in both healthy and CRS mucus and mucosa samples. These were grouped into five common groups consisting of secretory granules (40%), cytoplasmic vesicles (27%), cytoskeleton (20%), mitochondrion (7%) and adherens junctions (6%) (Supplementary Table 7.3 and Figure 7.7).

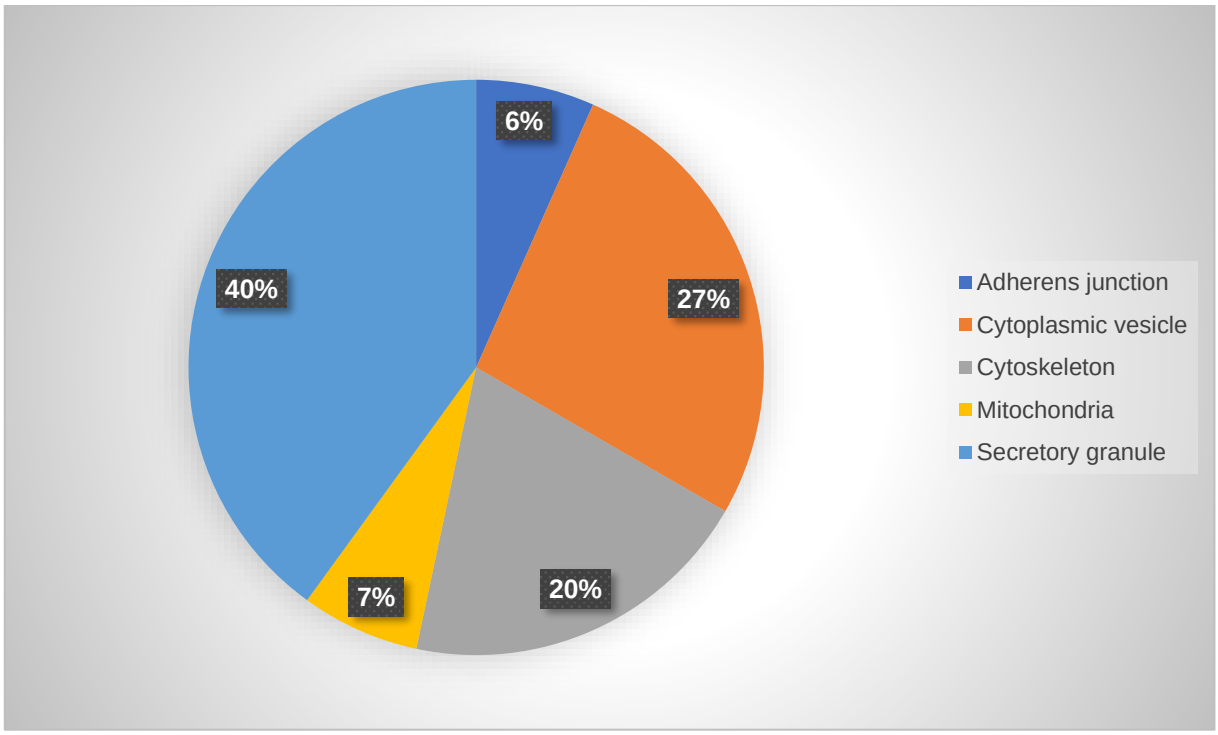

Figure 7.7. Healthy and CRS cellular components.

Fifteen cellular components identified and classified in five common groups. *(%) Percentage of all identified cellular components in both healthy and CRS samples.*

Thirty-one biological processes were present in both healthy and CRS mucus and mucosa samples (Supplementary Table 7.3). These were grouped into twelve common biological processes consisting mainly of immune processes (16%), response to stimulus (13%), metabolic process (10%), cellular metabolic process (10%), cellular response to chemical stimulus (10%), cell death (10%), cellular metabolic process (10%), export from cell (7%), as well as localisation, system processes, tissue homeostasis and tissue homeostasis, cell-cell adhesion and circulatory system (all ≤6%) (Figure 7.8).

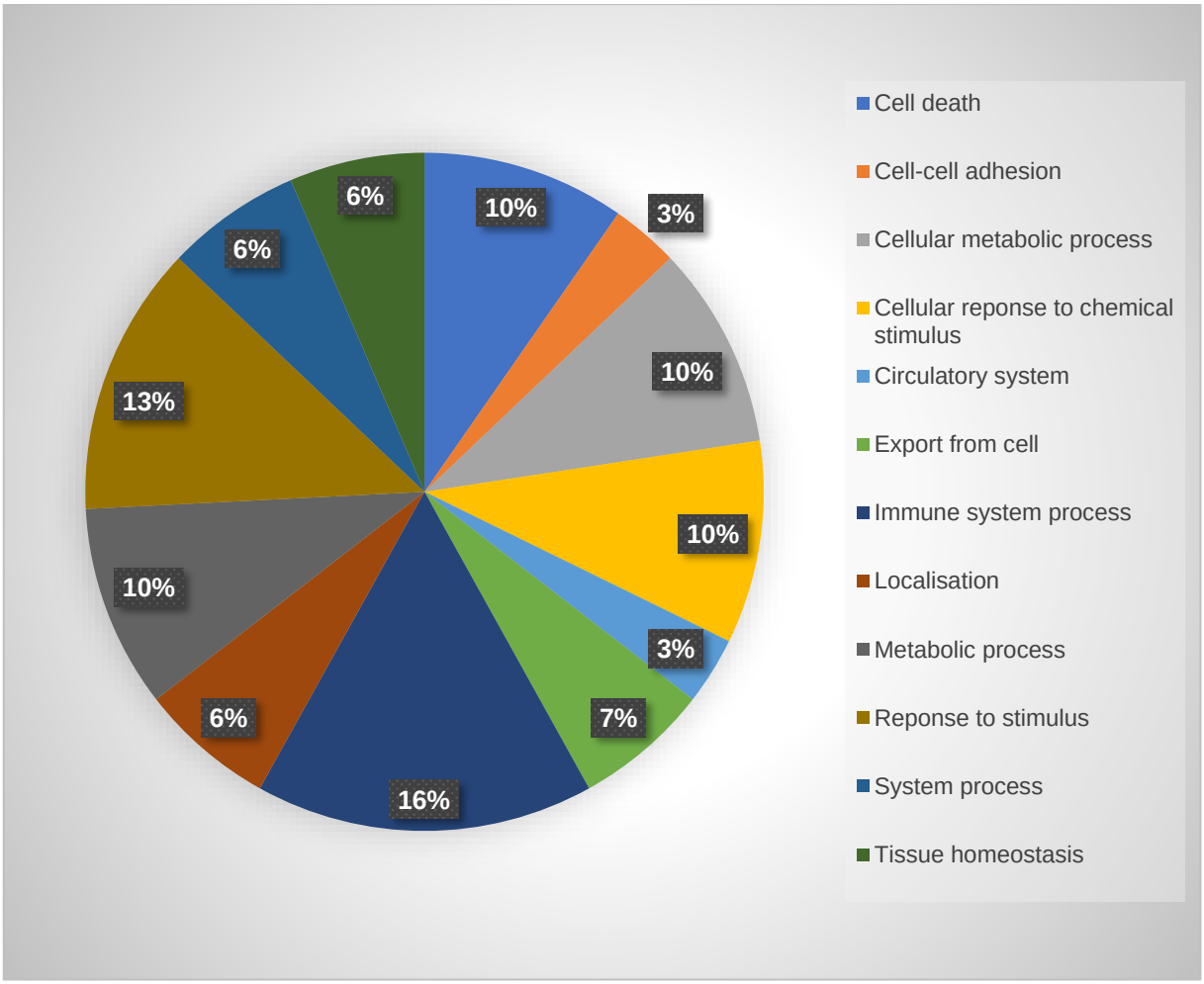

Figure 7.8. Healthy and CRS biological processes.

Thirty-one biological processes classified in twelve common biological processes. (%) Percentage of all identified biological processes.

Signal recognition particle binding (GO:0005047) was the only significant molecular function present in both CRS and healthy mucus samples (Supplementary Table 7.3). No other molecular functions were identified in either the healthy or CRS mucosa samples.

DISCUSSION

Chronic rhinosinusitis is a multifactorial disease believed to be secondary to a complex interplay between pathogens, the immune system and environmental factors. [1] This results in chronic mucosal inflammation and recurrent infections. The currently used phenotypic classification which is based on the presence or absence of polyps has been shown to be inadequate in defining the numerous inflammatory subtypes within CRS. To better define the heterogeneous disease process in CRS, there have been numerous studies investigating the pathophysiology and classification of CRS endotypes.[1, 521] This scoping review has identified 21 studies investigating the nasal mucus and mucosa proteome of healthy and CRS patients that may give insights into the protein composition and down-stream alterations that occur in sinus disease. The various methodologies of all included studies were summarised and critically appraised. There was significant heterogeneity in methodology and patients across the current available literature. Gene set enrichment analysis (GSEA) was conducted on six proteomic studies that had data comparing the proteome of CRS and healthy cohorts.[461, 498-500, 536, 543] These results suggest an increased proportion of both innate and adaptive immunologic pathways including complement, phagocytosis and B cell functions, with increases to tissue remodelling pathways, apoptosis and metabolic processes in CRS patients compared to the common proteome group. These differences as well as their associated imbalances in cellular pathways may account for the disease manifestation observed in CRS, however, further studies are required to confirm these findings.

Dysregulation of the innate and adaptive immune system response has been proposed as a contributing factor to the underlying chronic inflammatory state observed in CRS.[545, 546] Using GSEA this review demonstrated an increased presence of complement activation processes (GO:0006958) and phagocyte activity (GO:0006909) in the CRS group. Both these factors are

part of the innate immune system which is vital against inhaled pathogens in the airway. Studies have identified upregulation of complement components and deposition along the basement membrane in CRS nasal polyp tissue.[91, 92] This deposition is associated with epithelial-to-mesenchymal transition, a form of tissue remodelling observed in CRS mucosa.[221, 222] Additionally, C5a has been found to induce production of Oncostatin M, a potent cytokine, known to disrupt epithelial barrier integrity in CRSwNP.[93] Macrophages and neutrophils are prominent phagocytic cells in CRS, with their dysregulation potentially accounting for the epithelial injury and increased paracellular permeability observed in CRS.[545, 547, 548] The increased expression of these innate immune system pathways in CRS patients may account for the barrier dysfunction associated with the sinonasal inflammatory response. In turn, differences in pathway expression can used to endotype CRS and aid in prognostication and treatment.

Secretory granules are important constituents in phagocyte function in the innate immune response, with similar compositions found between the CRS and common proteome groups following GSEA. Elevated levels of neutrophils observed in CRS patients may lead to over production of neutrophil granules and serine proteases, which may lead to barrier disruption as collateral damage.[548] This review identified differences in endopeptidase (GO:0052548) and peptidase (GO:0052547) activity in CRS mucus which was not present in the common group. Neutrophil elastase, an endopeptidase, is vital in the fight against pathogens has been associated with epithelial barrier disruption.[548] The imbalance between proteases and protease inhibitors at the epithelial barrier is hypothesised to be an initiating and perpetuating factor in inflammatory airway disease.[549, 550] Further targeted studies are required to determine if differences in protein expression of these inflammatory mediators reflect the increased infiltration of inflammatory cells with consequent barrier disruption.

The adaptive immune response is also implicated in the pathogenesis of CRS. Our GSEA confirms this with increased proportion of B cell activation (GO:0050871) and function (GO:0050853) pathways in CRS mucus samples. These findings correlate with previous studies identifying elevated levels of B cells and plasma infiltrates in CRS.[551-553] B cells are fundamental in the adaptive immune response, by evolving into plasma cells or memory B cells upon activation. From research by our department, we have also recently demonstrated immune cell infiltrates clustering into germinal centres called tertiary lymphoid organs (TLO). We proposed that the presence of TLO in nasal polyp samples in recalcitrant CRS patients may be secondary to chronic antigen presentation.[554] Studies have speculated the role of TLO in the activation of autoreactive B and T cell clones in chronic inflammation and autoimmunity.[187, 191, 192] Further research is required to understand the contribution of the innate and adaptive immune response in CRS endotypes, and its role of tissue remodelling and the development of polyps.

GSEA also demonstrated an impairment in immune response against pathogen invasion including the defence response biological processes against bacterium (GO:0042742) and fungus (GO:0050832), that were only found to be present in the CRS group. These pathways need to be explored to determine if the proteins involved are downregulated or upregulated in CRS patients. Furthermore, three sensory perception processes identified in CRS mucus were involved with bitter taste. The bitter taste receptor gene family, particularly T2R38, has been associated with activation of the local innate immune response through increased mucociliary clearance and bactericidal activity.[159, 160] It has been proposed that polymorphisms in bitter taste receptors play a role in sinonasal immunity in CRS.[167] The impairment in immunological

pathways present may account for the impaired innate and adaptive immune response with secondary bacterial dysbiosis observed in CRS. [90, 555]

Tissue remodelling with associated barrier dysfunction secondary to inflammation is a hallmark feature of CRS.[556] Epithelial-to-mesenchymal transition (EMT) is a remodelling process where epithelial cells lose their normal morphology, polarity and junctional attachments to neighbouring cells becoming spindle shaped mesenchymal cells in response to chronic inflammation.[218] These cellular changes with loss of tight and adherens junctions from CRS mucosa are well documented.[219, 220] This review identified increased proportion of cytoskeletal and adherens junction components in the CRS group compared to the common proteome group. Furthermore, proteins involved in cell-cell binding played the largest role in molecular functions of the CRS group. These differences may reflect the cellular morphological changes observed in CRS described in the barrier disruption hypothesis of CRS pathogenesis. Lastly, the increased proportion of actin-filaments (GO:0005884) and intermediate filament cytoskeleton (GO:0045111) present in the CRS group may account for increased activity during tissue remodelling. Further research is required to identify differences in expression of barrier and cytoskeletal structure proteins that reflect the changes observed in CRS.

Interestingly, our review also showed an increased expression of programmed cell death pathways and biological processes to be present in CRS patients. Apoptosis has a fundamental role in regulating tissue homeostasis via the elimination of unwanted cells. The apoptotic cleavage pathway of cell adhesion proteins leads to rearrangements of tight junctions, adherens junctions and desmosomes. Immune-mediated apoptosis of intestinal epithelial cells demonstrated increased permeability with associated restructuring of epithelial cells.[557] Caspases released during apoptosis causes cleavage of desmosomal proteins leading to

disruption of cell-cell contacts. This is followed by remodelling of the intermediate filament cytoskeleton, as a homeostatic mechanism observed in colonic epithelial cells to maintain barrier function.[558] These findings correlate with cytokine-mediated changes in tight junctions with increased paracellular permeability present in inflammatory bowel disease.[559-561] This pathway may account for the increased paracellular permeability without epithelial cell cytotoxicity observed in human nasal epithelial cells exposed to CRS mucus.[520] Further research is required to determine differences in the upstream regulation of apoptotic pathways present in CRS, followed by clarifying if apoptosis-induced morphological changes in nasal epithelial is associated with barrier dysfunction and paracellular permeability.

The dysregulation of the coagulation cascade has been hypothesised to play a role in the pathogenesis of many inflammatory conditions including asthma, rheumatoid arthritis and Crohn's disease.[225] This review identified the platelet degranulation pathways with similar distributions in both groups. Elevated expression of platelet-derived growth factor (PDGF) has been identified in nasal polyps suggesting involvement in epithelial proliferation observed in CRS.[227] PDGF is chemotactic and mitogenic for fibroblasts, and involved in the pathogenesis of fibrosis.[228] Additionally, factor XIII-A in the coagulation cascade, present in platelets and macrophages, is also elevated in nasal polyp tissues of CRSwNP patients.[226] It was hypothesised that overproduction of factor XIII-A may lead to an accelerated coagulation cascade with subsequent excessive fibrin deposition, leading to tissue remodelling and oedema of the submucosa within nasal polyp tissue.[225] Further research is required to ascertain the differences in protein regulation upstream in platelet pathways which may be responsible for the increased fibrin deposition in tissue remodelling.

The maintenance of cellular metabolism is vital in healthy tissue homeostasis. This review identified increased expression of metabolic processes, particularly with carbohydrate metabolism, was present in the CRS-only group. Persistent exposure of nasal epithelial cells to external pathogens and irritants leads to injury with chronic healing and remodelling. Reactive oxygen species released in response to pathogens further add to the oxidative stress in chronic disease.[562] This process is counterbalanced by a range of antioxidant pathways identified in both healthy and CRS mucus. Previous studies have demonstrated reduced levels of antioxidant enzymes in CRS patients compared to healthy individuals.[563, 564] Consequently, the increased energy demand from their epithelial cells require a constant glucose reservoir for the maintenance of cell function and tissue integrity.[535] Elevated breath glucose has been identified in patients with cystic fibrosis without diabetes with inflammatory lung changes. It was hypothesised the elevated glucose in airway fluid was due to increased paracellular permeability and glucose leakage into respiratory fluid or impaired glucose removal.[565] Further studies are required to investigate imbalances between oxidant and antioxidant processes likely contributing to the inflammation of the epithelium observed in CRS patients.[566] Additionally, further research is required to determine if elevated levels of glucose are present in the nasal secretions of CRS patients, and its association with disease severity and barrier dysfunction.

Limitations

The proteomic analysis of nasal mucosa and mucus samples is a powerful technique in understanding CRS pathogenesis and its endotypes. Heterogeneity in methods of sample collection and location of tissue collected are potential areas of bias. Studies are required to determine if the proteome collected from nasal brushings are as representative as mucosal biopsy specimens. Furthermore, future research is required to determine differences between the nasal mucosa and mucus proteome samples from the same patients. Cellular lysates obtained

from nasal mucosa are more challenging to process due to the magnitude of proteins present compared to mucus. Additionally, the protein composition between healthy and CRS cells are likely similar as all cells require similar organelle to survive. The lack of cellular pathways identified from the GSEA of CRS mucosa is likely due to the decreased number of unique proteins (21 vs 136) identified and inputted into the analysis. Therefore secretions, such as mucus, may be more representative of the disease process.

Researchers should aim for a standardised mucus and mucosal collection method to reduce sample variability. Targeted methods of sample collection from specific subsites of the nasal cavity, such as with an absorbable sponge or suctioning, will provide more detailed information. Further studies should determine if samples collected from different subsites contain similar quantities of inflammatory cytokines and cells. Furthermore, differing sample processing methods, in conjunction with differing mass spectrometry methods adds confounding bias. Advances in mass spectrometry resolution and sensitivity will allow for the detection of lower abundance proteins present in mucus and mucosa samples to improve our understanding of CRS. GSEA was unable to be performed on all 21 studies due the skew of studies containing only healthy patients. This factor in conjunction with the heterogeneity in sample preparation and analysis across the studies was a potential for cumulative methodological bias. Therefore, this is a potential explanation for the lack of unique healthy proteins identified. The included studies reporting protein qualification was limited and thus this review was only able to comment on the presence of certain proteins and not the quantity. Due to this lack of standardised reporting of up-regulated and/or down-regulated proteins across the studies, we could not collate the data and express it in a meaningful and semi-quantitative way. This is a potential avenue for future research. Thus, GSEA conducted was only capable of presenting pathways present, and not which pathways were up- or down-regulated. Ultimately, more

studies with direct comparisons between healthy and CRS proteomes are required. This includes quantitative studies to determine differences in protein and cellular pathway expressions. Lastly, future studies require standardised reporting and methodology to allow improved comparisons in future reviews. Despite these limitations this review has been able to collate a comprehensive list of the nasal proteome, with a descriptive analysis of different cellular processes between healthy and CRS patients.

Conclusion

Proteomic analysis of nasal mucus and mucosa is a vital step in better understanding the pathophysiology of CRS and its endotypes. This descriptive scoping review has identified 2962 proteins from healthy and CRS patients in the current literature. Preliminary GSEA from the current limited and heterogenous literature suggests a trend of increased presence of immunological, metabolic, tissue remodelling and apoptotic pathways in CRS. Furthermore, the lack of standardisation in methodology across the current literature has been identified. We hope this review provides a reference resource of the current literature to improve standardisation of methodology and direct further research to improve the knowledge of CRS pathogenesis and endotypes.

ACKNOWLEDGEMENTS

This project was supported by Adelaide University Research Training Program Scholarship, Bertha Sudholz Scholarship and Garnett Passe Rodney Williams Memorial Foundation Scholarship to SSK.

SUPPLEMENTARY MATERIAL

SUPPLEMENTARY FIGURE 7.1 DATABASE SEARCH

Pubmed 26/03/2019

Sinusitis[mh] OR Sinus*[tw] OR Sinusitides[tw] OR Chronic rhinosinusitis[tw] OR CRS[tw] OR CRSwNP[tw] OR CRSsNP[tw] OR Nasal polyps[mh] OR Papillom*[tw] Polyps[mh] OR Polyp*[tw] OR Nose[mh] OR Nose[tw] OR Nasal*[tw]

AND

Mucus [mh] OR Mucus [tw] OR Bodily secretions [mh] OR Secret* [tw] OR Fluids and Secretions [mh] OR Fluid* [tw] OR Mucus membrane [mh] OR Mucus membrane [tw] OR Respiratory mucosa [mh] OR Respiratory mucosa [tw] OR Nasal mucosa [mh] OR Nasal mucosa [tw] OR Mucosa* [tw] OR Epitheli*[tw] OR Tissue* [tw]

AND

Proteomics [mh] OR Proteom* [tw] OR Proteogenomic [mh] OR Proteogenomic [tw] OR Secretome[tw]

Embase 26/03/2019

Sinusitis/syn OR Sinusitis/exp OR Sinus*:ti,ab OR "Chronic rhinosinusitis":ti,ab OR CRS:ti,ab OR CRSsNP:ti,ab OR "Nose polyp"/syn OR "Nose polyp"/exp OR "Nose polyp*":ti,ab OR "Nasal polyp*":ti,ab OR Papillom*:ti,ab Polyp/syn OR Polyp/exp OR Polyp*:ti,ab OR Nose/syn OR Nose/exp OR Nos*:ti,ab

AND

Mucus/syn OR Mucus/exp OR Mucus:ti,ab OR Mucosa*:ti,ab OR "Nose mucus"/syn OR "Nose mucus"/exp OR "Nose fluid":ti,ab OR "Nasal fluid":ti,ab OR Bodily secretions/syn OR Bodily secretions/exp OR Bodily secretion*:ti,ab OR Secret*:ti,ab OR Bodily fluid/syn OR Bodily fluid/exp OR Fluid*:ti,ab OR Mucosa/syn OR Mucosa/exp OR Nose mucosa/syn OR Nose mucosa/exp OR Paranasal sinus mucosa/syn OR Paranasal sinus mucosa/exp OR Nasal tissue/syn OR Nasal tissue/exp OR Tissue*:ti,ab OR Nose epithelium/syn OR Nose epithelium/exp OR Epitheli*:ti,ab

AND

Proteomics/syn OR Proteomics/exp OR Proteom*:ti,ab OR Proteogenomics/syn OR Proteogenomics/exp OR Proteogenomic*:ti,ab OR Secretome:ti,ab

CINAHL 26/03/2019

MH Sinusitis OR TI Sinus* OR AB Sinus* OR TA Chronic rhinosinusitis OR AB Chronic rhinosinusitis OR TI CRS OR AB CRS OR TI CRSsNP OR AB CRSsNP OR MH Nasal polyps OR TI Nasal polyp* OR AB Nasal polyp* OR TI Nose polyp* OR AB Nose polyp* OR TI Papillom* OR AB Papillom* OR MH Polyps OR TI Polyp* OR AB Polyp*

AND

MH Mucus OR TI Muc* OR AB Muc* OR TI Nasal muc* OR AB Nasal muc* OR TI Nasal fluid* OR AB Nasal fluid* OR MH Secretions OR MH Fluids and secretions OR TI Secret* OR AB Secret* OR TI Fluid* OR AB Fluid OR MH Mucus membrane OR MH Nasal mucosa OR MH Paranasal sinuses OR MH Tissue OR TI Tissue* OR AB Tissue* OR MH Epithelium OR TI Epitheli* OR AB Epitheli*

AND

MH Proteomics OR TI Proteomic* OR AB Proteomic* OR TI Proteogenomic* OR AB Proteogenomic* OR TI Secretome OR AB Secretome

Cochrane 26/03/2019

Sinus* OR Chronic rhinosinusitis OR CRS OR CRSsNP OR Nose polyp* OR Nasal polyp* OR Papillom* OR Polyp*

AND

Mucus* OR Muc* OR Secret* OR Fluid* OR Epitheli* OR Tissue*

AND

Proteom* OR Proteogenomic OR Secretome

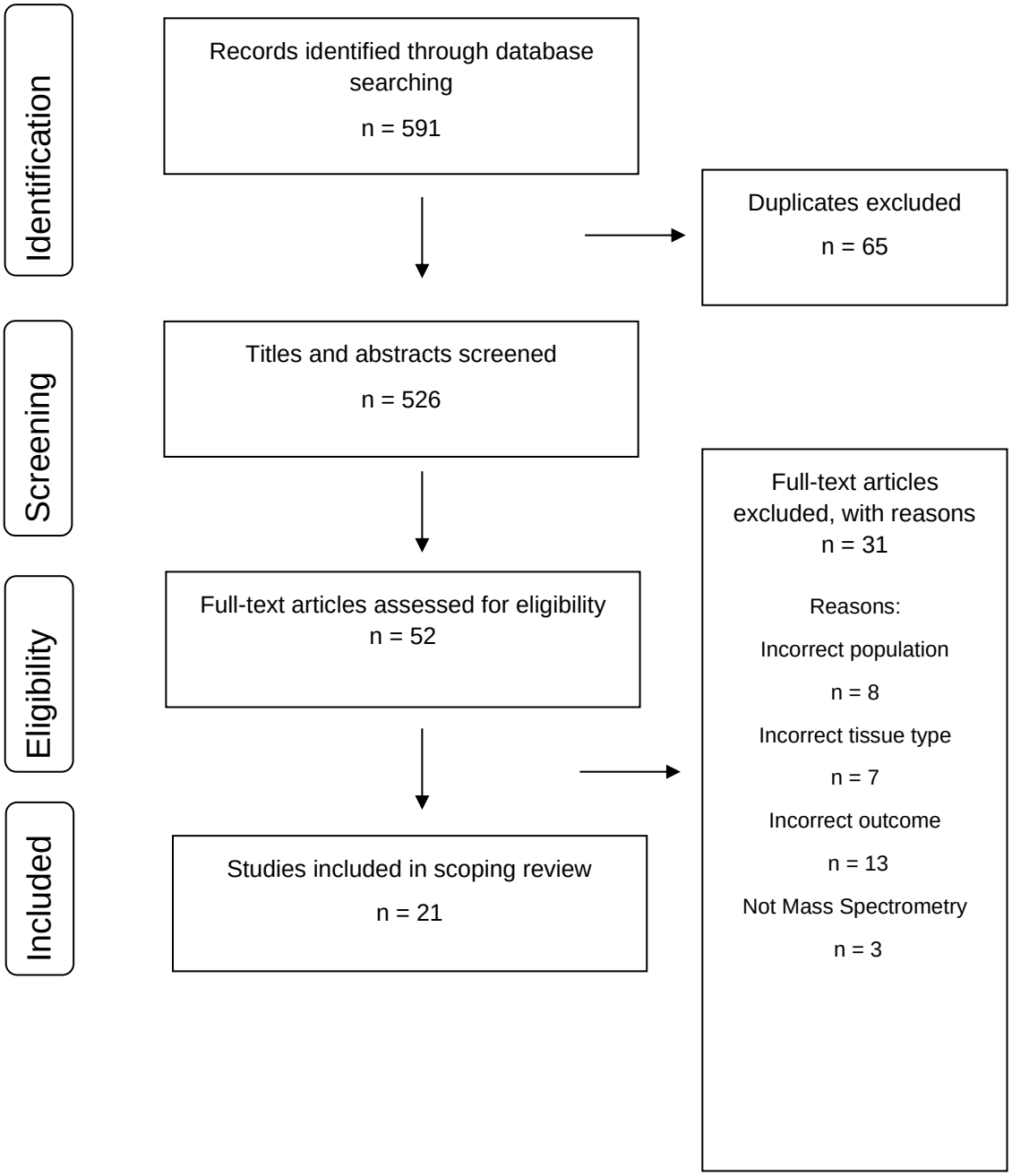

SUPPLEMENTARY FIGURE 7.2. PRISMA FLOW DIAGRAM.

Illustration of the systematic review process of study inclusion and exclusion.

SUPPLEMENTARY TABLE 7.1. COMPREHENSIVE PROTEIN LIST

Gene	UniProt	Studies
A1BG	M0R009	l,s,r
A2M	P01023	i,b,s,r,l,p,o
AAAS	Q9NRG9	o
AAMDC	E9PJP1	l
AARS	P49588	s,l
ABCA13	Q86UQ4	o
ABCA7	Q8IZY2	o
ABCB10	Q9NRK6	o
ABCB6	Q9NP58	o
ABCB7	O75027	o
ABCB8	Q9NUT2	o
ABCC1	P33527	o
ABCC3	O15438	o
ABCC4	O15439	o
ABCD1	P33897	o
ABCD3	P28288	l,o
ABCE1	P61221	l
ABHD10	Q9NUJ1	l
ABHD11	Q8NFV4	l
ABHD12	Q8N2K0	o
ABHD12B	Q7Z5M8	s
ABHD14B	Q96IU4	l
ABHD16A	O95870	o
ABHD6	Q9BV23	o
ABI1	Q8IZP0	l
ABRACL	Q9P1F3	l
ACAA1	P09110	l
ACAD8	Q9UKU7	l
ACAD9	Q9H845	o
ACADM	P11310	m,o,l
ACADS	P16219	o,l
ACADSB	P45954	l
ACADVL	P49748	o,l
ACAT1	P24752	o,l
ACAT2	Q9BWD1	l
ACBD3	Q9H3P7	o,l
ACBD7	Q8N6N7	l
ACIN1	Q9UKV3	o,l
ACLY	P53396	l
ACO1	P21399	o,l
ACO2	Q99798	o,l
ACOT13	Q9NPJ3	l
ACOT2	P49753	l
ACOT7	O00154	l
ACOT9	Q9Y305	l
ACOX3	O15254	l
ACP1	P24666	l
ACP2	P11117	o,l
ACP6	Q9NPH0	l
ACSF2	Q96CM8	l
ACSL1	P33121	o
ACSL3	O95573	o,l
ACSL5	Q9ULC5	o
ACSS1	Q9NUB1	l

ACTA2	P62736	o,l
ACTB	P60709	n,s,k,c,b,o,t,p,m,a,t,g
ACTBL2	Q562R1	s
ACTC1	P68032	s
ACTG1	P63261	n,r,c,t,l,t
ACTN1	P12814	s,o,l
ACTN4	O43707	s,r,o,l,p
ACTR1A	P61163	l
ACTR1B	P42025	l
ACTR2	P61160	r,o,l
ACTR3	P61158	s,r,o,l,d
ACY1	F8WC59	l
ACYP1	P07311	l
ADAM10	O14672	o
ADAR	P55265	o,l
ADCYAP1	P18509	j,j
ADD1	P35611	l
ADH1A	P07327	o
ADH1B	P00325	l
ADH1C	P00326	s,r,l,o
ADH5	P11766	l
ADH7	P40394	r,s,l
ADI1	Q9BV57	l
ADIRF	Q15847	l,o
ADK	P55263	l
ADPRHL2	Q9NX46	l
ADRM1	Q16186	l
ADSL	P30566	l
ADSS	P30520	l
ADSSL1	Q8N142	l
AFDN	P55196	l
AFG3L2	Q9Y4W6	o
AFM	P43652	l
AGK	Q53H12	l,o
AGL	P35573	l
AGPAT3	Q9NRZ7	o
AGPAT5	Q9NUQ2	o
AGPS	O00116	l
AGR2	O95994	s,r,o,l
AGR3	Q8TD06	l,o
AGT	P01019	s,l
AHCY	P23526	l,o
AHNAK	Q09666	o,l
AHSA1	O95433	s,l
AHSG	P02765	s,r,u,l,a
AIF1	P55008	l
AIFM1	O95831	l,o
AIFM2	Q9BRQ8	b
AIMP1	Q12904	l
AIMP2	Q13155	l
AIP	O00170	l
AK1	P00568	s,o,l
AK2	P54819	o,l
AK3	Q9UIJ7	o,l
AK7	Q96M32	l
AK8	Q96MA6	l
AKAP4	Q5JQC9	s,o
AKR1A1	P14550	s,r,c,m,p,l,o

AKR1B10	O60218	o,l
AKR1C1	Q04828	r,s,o,l
AKR1C2	P52895	s,l,o,m
AKR1C3	P42330	l
AKR7A2	O43488	l,o
AKT1S1	Q96B36	l
ALAD	P13716	l
ALB	H0YA55	u,s,r,k,b,c,i,f,u,q,p,m,o,e,q,a
ALCAM	Q13740	o,l
ALDH16A1	Q8IZ83	l
ALDH18A1	P54886	l,o
ALDH1A1	P00352	c,s,r,o,m,t,e,l,p,t,d
ALDH1A3	P47895	l
ALDH1B1	P30837	l
ALDH1L1	O75891	l
ALDH2	P05091	b,o,l,e
ALDH3A1	P30838	r,s,c,p,e,o,l
ALDH3A2	P51648	o,l
ALDH3B1	P43353	o,l
ALDH4A1	P30038	g
ALDH5A1	P51649	o,l
ALDH7A1	P49419	o,l
ALDH8A1	Q9H2A2	m
ALDH9A1	P49189	l,o
ALDOA	P04075	s,r,o,p,l,a
ALDOC	P09972	s,o,l
ALG1	Q9BT22	o,l
ALG14	Q96F25	o
ALG2	Q9H553	o
ALG5	Q9Y673	o
ALG9	Q9H6U8	o
ALOX15	P16050	s,r,o,l
ALOX5AP	P20292	o
ALPL	P05186	o
ALYREF	Q86V81	l
AMBN	Q9NP70	s
AMBP	P02760	l
AMDHD2	Q9Y303	l
AMY1A	P04745	k,l
AMY1B	P04745	k,l
AMY1C	P04745	k,l
AMY2B	P19961	a
ANG	P03950	l
ANK1	P16157	o
ANK3	Q12955	o,l
ANKEF1	Q9NU02	s
ANKS1A	Q92625	l
ANP32A	P39687	l
ANP32B	Q92688	l
ANP32E	Q9BTT0	l
ANPEP	P15144	o,l
ANXA1	P04083	n,s,r,k,c,l,p,m,t,o,a,t
ANXA11	P50995	o,l
ANXA2	P07355	n,s,r,b,c,p,m,l,o,a
ANXA3	P12429	n,s,r,c,p,l,o
ANXA4	P09525	l,o
ANXA5	P08758	s,r,p,m,l,o
ANXA6	P08133	l,o

ANXA7	P20073	c,o,l
ANXA8	P13928	l
AP1B1	H7C034	l
AP1G1	B4DGE1	l,o
AP1M1	Q9BXS5	l
AP1M2	Q9Y6Q5	l
AP2A1	O95782	l,o
AP2B1	P63010	l
AP2M1	Q96CW1	l
AP2S1	P53680	l
AP3B1	O00203	l,o
AP3D1	O14617	l
APCS	P02743	p,l
APEH	P13798	l
APEX1	P27695	o,l
API5	Q9BZZ5	l
APMAP	Q9HDC9	o,l
APOA1	P02647	r,f,s,k,u,b,c,o,t,l,t
APOA2	P02652	r,s,l
APOA4	P06727	c,l
APOB	P04114	l
APOC3	P02656	h
APOD	P05090	b
APOH	P02749	r,l
APOL2	Q9BQE5	o
APOOL	Q6UXV4	o
APPL2	Q8NEU8	l
APRT	P07741	p,o,l
AQP5	P55064	o

ARCN1	P48444	o,l
ARF1	P84077	r,o
ARF3	P61204	s,l
ARF4	P18085	l
ARF6	P62330	l
ARFGAP3	Q9NP61	l
ARFGEF1	Q9Y6D6	l
ARFGEF3	Q5TH69	o
ARFIP1	P53367	l
ARFIP2	P53365	l
ARHGAP1	Q07960	l,o
ARHGAP18	Q8N392	l
ARHGDIA	P52565	r,s,o,j,l,m,j
ARHGDIB	P52566	n,r,s,o,t,l,j,t,j
ARHGEF16	Q5VV41	l
ARID3B	Q8IVW6	s
ARL1	P40616	l
ARL3	P36405	l
ARL6IP5	O75915	o,l
ARMCX3	Q9UH62	o
ARMT1	Q9H993	l
ARPC1A	Q92747	l
ARPC1B	O15143	l
ARPC2	O15144	o,l
ARPC3	O15145	o,l
ARPC4	P59998	r,o,l
ARPC5	O15511	s,l
ARPC5L	Q9BPX5	l
ARPP19	P56211	l

ARRB1	P49407	l
ARSD	P51689	o
ASAH1	Q13510	s,o,l
ASL	P04424	l
ASMT	P46597	l,l
ASNA1	O43681	l
ASPH	Q12797	o
ASPRV1	Q53RT3	a
ASRGL1	Q7L266	l
ASS1	P00966	l,p,o
ATAD3A	Q9NVI7	l,o
ATG3	Q9NT62	l
ATG7	O95352	l
ATIC	P31939	o,l
ATL3	F5H6I7	l
ATOX1	O00244	l
ATP12A	P54707	o
ATP13A1	Q9HD20	o
ATP1A1	P05023	o,l
ATP1B1	P05026	o,l
ATP1B3	P54709	o,l
ATP2A1	O14983	o
ATP2A2	P16615	o,l
ATP2A3	Q93084	o,l
ATP2B1	P20020	o
ATP2B4	P23634	o,l
ATP2C1	P98194	o
ATP5F1A	P25705	s,l,o
ATP5F1B	P06576	r,c,s,m,l,o
ATP5F1C	P36542	l,o
ATP5MD	Q96IX5	l
ATP5ME	P56385	l,o
ATP5MF	P56134	l,o
ATP5MG	O75964	l,o
ATP5PB	P24539	l,o
ATP5PD	O75947	m,o,l,j
ATP5PF	P18859	l
ATP5PO	P48047	l,o
ATP6AP1	Q15904	o
ATP6V0A1	Q93050	o
ATP6V0A2	Q9Y487	o
ATP6V0A4	Q9HBG4	o
ATP6V0C	P27449	o
ATP6V0D1	P61421	h
ATP6V1A	P38606	o,l,h
ATP6V1B2	P21281	l
ATP6V1C1	P21283	l
ATP6V1D	Q9Y5K8	l
ATP6V1E1	P36543	o
ATP6V1F	Q16864	l
ATP6V1H	Q9UI12	l
ATP7B	P35670	o
ATP8B1	O43520	o
ATP9A	O75110	o
AZGP1	P25311	b,u,r,k,s,l,p,a
AZU1	P20160	s
B2M	P61769	f,b,s,r,k,l,a
B3GAT3	O94766	o

B3GNT3	Q9Y2A9	o
B4GALT4	O60513	o
BAG1	Q99933	l
BAG3	O95817	l
BAG5	G3V274	l
BAG6	P46379	l
BAIAP2	Q9UQB8	l
BANF1	O75531	l
BAP18	Q8IXM2	l
BASP1	P80723	r,k,o,l
BBS1	Q8NFJ9	l
BCAM	P50895	o
BCAP29	Q9UHQ4	o
BCAP31	P51572	l,o
BCAS1	O75363	l,o
BCAT2	O15382	l
BCCIP	Q9P287	l
BDH1	Q02338	o,l
BDH2	Q9BUT1	l
BFSP1	Q12934	h
BHMT	E5RJH0	g
BID	P55957	l
BLMH	Q13867	l
BLVRA	P53004	l
BLVRB	P30043	o,l
BOLA2	Q9H3K6	l
BOLA2B	Q9H3K6	l
BPGM	P07738	s
BPHL	Q86WA6	l

BPI	P17213	b,r,s,o
BPIFA1	Q9NP55	s,r,b,f,l,p,m,e,o,j,a,j
BPIFB1	Q8TDL5	s,k,r,b,l,o
BPIFB2	Q8N4F0	s,r,k,q,l,q
BPIFB3	P59826	s
BPIFB4	P59827	s,r,k,l,o
BPNT1	O95861	l,m
BRCC3	P46736	l
BRI3BP	Q8WY22	o
BROX	Q5VW32	l
BSG	P35613	o
BTF3	P20290	l
BUB3	O43684	l
BUD31	P41223	l
BZW2	Q9Y6E2	l
C11orf54	Q9H0W9	l
C12orf10	Q9HB07	l
C1QB	P02746	l
C1QBP	Q07021	l,o
C1QC	P02747	l,p
C1R	P00736	l
C1orf87	Q8N0U7	l
C21orf59-TCP10L	H7BZW1	l
C2CD2L	O14523	o
C3	P01024	s,r,k,b,p,l,o
C4A	P0C0L4	b,l,o
C4B	P0C0L5	s,r,l
C4BPA	P04003	l,o

C4BPB	P20851	h
C4B_2	P0C0L5	s,r,l
C5	P01031	s,l
C6	P13671	l
C7	P10643	l
C8B	P07358	l
C8G	P07360	l
C9	P02748	l
C9orf64	Q5T6V5	l
CA1	P00915	c,t,l,o,t
CA13	Q8N1Q1	l
CA2	P00918	b,l,o
CAB39	Q9Y376	l
CACYBP	Q9HB71	l
CAD	P27708	l,o
CALM1	P0DP23	s,r,l,a
CALM2	P0DP24	o
CALML3	P27482	o,l
CALML5	Q9NZT1	r,k,l,a
CALR	P27797	c,m,o,l
CALU	O43852	o,l
CAMK2D	Q13557	l
CAMP	P49913	s,o
CAND1	Q86VP6	l,o
CANX	P27824	o,l
CAP1	Q01518	r,s,o,l
CAPG	P40121	s,o,l
CAPN1	P07384	o,l
CAPN13	Q6MZZ7	l
CAPN2	P17655	o,l
CAPN5	O15484	o
CAPNS1	P04632	s,l,o
CAPRIN1	Q14444	l
CAPS	Q13938	s,r,c,l,p,o,m
CAPZA1	P52907	s,o,l
CAPZA2	P47755	l
CAPZB	P47756	s,o,l
CARHSP1	Q9Y2V2	l
CARMIL1	Q5VZK9	l
CARS	P49589	l
CASK	O14936	l
CASP1	P29466	l
CASP12	Q6UXS9	s
CASP14	P31944	r,k,a
CASP3	P42574	l
CASP7	P55210	l
CAST	P20810	o,l
CAT	P04040	s,r,p,o,l,t,t
CBR1	P16152	s,r,o,l
CBR3	O75828	l
CBS	P35520	h
CBX3	Q13185	o,l
CBX5	P45973	l
CC2D1A	Q6P1N0	l
CCAR2	Q8N163	o,l
CCDC102B	Q68D86	s
CCDC124	Q96CT7	l
CCDC151	A5D8V7	l

CCDC17	Q96LX7	l
CCDC170	Q8IYT3	o
CCDC171	Q6TFL3	s
CCDC22	O60826	l
CCDC39	Q9UFE4	l,l
CCDC47	Q96A33	o
CCDC6	Q16204	l
CCDC78	A2IDD5	l
CCDC81	Q6ZN84	m
CCND1	P24385	h
CCS	O14618	l
CCT2	P78371	c,o,l
CCT3	P49368	o,l
CCT4	P50991	o,l
CCT5	P48643	c,l,o
CCT6A	P40227	l
CCT7	Q99832	l
CCT8	P50990	o,l,d
CD14	P08571	o,l
CD2AP	Q9Y5K6	l
CD38	P28907	o
CD44	P16070	o,l
CD47	Q08722	o
CD59	P13987	o,l
CD5L	O43866	l
CD63	P08962	o
CD74	P04233	o,l
CD81	P60033	o
CD82	P27701	o

CD9	P21926	o,l
CD97	P48960	o
CDA	P32320	s,r
CDC37	Q16543	o,l
CDC42	P60953	l
CDC5L	Q99459	l
CDCP1	Q9H5V8	o
CDH1	P12830	o,l
CDIPT	O14735	o
CDK5	Q00535	l
CDK5RAP3	Q96JB5	l
CDKL1	Q00532	s
CDS1	Q92903	o,l
CDS2	O95674	o
CDV3	Q9UKY7	l
CEACAM5	P06731	o,l
CENPF	P49454	m
CEP128	Q6ZU80	o
CEP131	Q9UPN4	o
CEP135	Q66GS9	l,o
CERS2	Q96G23	o
CES1	P23141	s,o,l
CES2	O00748	o,l
CETN2	P41208	l
CFAP20	Q9Y6A4	l
CFAP52	Q8N1V2	l
CFAP57	Q96MR6	l
CFAP70	Q5T0N1	l
CFB	P00751	r,u,s,p,l

CFH	P08603	l
CFI	P05156	l
CFL1	P23528	s,r,o,l,p
CGN	Q9P2M7	l
CGNL1	Q0VF96	s
CHCHD10	Q8WYQ3	l
CHCHD3	Q9NX63	o
CHD4	Q14839	o
CHDH	Q8NE62	o
CHI3L2	Q15782	s
CHL1	O00533	l
CHMP4B	Q9H444	l
CHMP5	Q9NZZ3	l
CHORDC1	Q9UHD1	l
CHP1	Q99653	o
CHTOP	Q9Y3Y2	o
CIAO1	O76071	l
CIB1	Q99828	l,h
CIRBP	Q14011	l
CISD1	Q9NZ45	o,l
CKAP4	Q07065	o,l
CKAP5	Q14008	s
CKB	P12277	s,r,c,l,p,o
CKMT1A	P12532	l,o
CKMT1B	P12532	l,o
CLC	Q05315	l,t,p,t
CLDN1	O95832	o,l
CLDN3	O15551	o,l
CLDN4	O14493	l
CLDN6	P56747	l
CLDN7	O95471	l
CLDN9	O95484	l
CLEC3B	P05452	l
CLEC4F	Q8N1N0	k
CLIC1	O00299	c,r,s,o,p,l
CLIC6	Q96NY7	o,l
CLINT1	H0YCL3	l,o
CLIP1	P30622	l
CLMN	Q96JQ2	l
CLTA	P09496	l,o
CLTC	Q00610	r,s,l,o
CLU	P10909	b,s,r,k,o,l
CLUH	O75153	l
CMAS	Q8NFW8	l
CMBL	Q96DG6	l
CMPK1	P30085	j,o,l,m,j
CMPK2	Q5EBM0	l
CNBP	P62633	l
CNDP2	Q96KP4	s,r,l,o
CNN1	P51911	o
CNN2	Q99439	s,l
CNP	P09543	o
CNTN2	Q02246	s
COASY	Q13057	l,o
COG5	Q9UP83	o
COG7	P83436	l
COG8	Q96MW5	l
COL1A1	P02452	a

COL1A2	P08123	o,a
COL28A1	Q2UY09	s
COL4A3BP	Q9Y5P4	l
COL5A3	P25940	s
COL7A1	Q02388	o
COMMD3	Q9UBI1	l
COMMD9	Q9P000	l
COMT	P21964	l
COPA	P53621	o,l
COPB1	P53618	o,l
COPB2	P35606	o
COPE	O14579	l
COPG1	H0Y8X7	l
COPG2	Q9UBF2	l
COPS2	P61201	l
COPS4	Q9BT78	h,l
COPS5	Q92905	l
COPS6	Q7L5N1	l
COPS7A	Q9UBW8	l
COPS8	Q99627	l
COPZ1	F8VXR1	l
COQ6	Q9Y2Z9	s
CORO1A	P31146	s,r,o,l
CORO1B	Q9BR76	l
CORO1C	Q9ULV4	l
CORO7	P57737	l
COTL1	Q14019	l
COX4I1	P13073	l,o
COX5A	P20674	l,o
COX5B	P10606	l,o
COX6A1	P12074	l
COX6B1	P14854	l
COX6C	P09669	o
COX7A2	P14406	l,o
COX7B	P24311	o
COX7C	P15954	o
CP	P00450	s,r,i,o,l
CPB2	Q96IY4	l
CPD	O75976	o
CPNE1	Q99829	l
CPNE3	O75131	l
CPPED1	Q9BRF8	l
CPS1	P31327	g
CPSF3	Q9UKF6	l
CPSF6	Q16630	l
CPSF7	Q8N684	l
CPT1A	P50416	o
CPT2	P23786	l,o
CRABP2	P29373	l
CRIP1	P50238	l
CRIP2	P52943	l
CRISP3	P54108	r,s,l
CRK	P46108	l
CRKL	P46109	l
CRNN	Q9UBG3	l
CROCC	Q5TZA2	o,l
CROCCP3	Q8IVE0	l
CROT	Q9UKG9	l

CRYL1	Q9Y2S2	l
CRYM	Q14894	o,l
CRYZ	Q08257	o,l
CRYZL1	O95825	l
CS	O75390	o,l
CSDE1	O75534	l
CSE1L	P55060	s,l
CSF1	P09603	h
CSK	P41240	l
CSNK1A1	P48729	l
CSNK2A1	P68400	l
CSRP1	P21291	l
CSRP2	Q16527	l
CST1	P01037	f,c,s,k,l
CST3	P01034	f,s,r,k,l
CST4	P01036	s,r,k,l,a
CSTA	P01040	f,l,a
CSTB	P04080	s,r,k,o,l,a
CTBP1	Q13363	l
CTBP2	P56545	l
CTNNA1	E5RJP7	l,o
CTNNA2	P26232	l
CTNNB1	P35222	o,l
CTNNBL1	Q8WYA6	l
CTNND1	C9JZR2	l,o
CTPS1	P17812	l
CTPS2	Q9NRF8	l
CTSB	P07858	r,o,m,h,l
CTSC	P53634	l
CTSD	P07339	s,r,o,m,l
CTSG	P08311	s,r,o,l
CTSH	P09668	l
CTSS	P25774	l
CTSZ	Q9UBR2	l
CTTN	Q14247	o,l
CUL1	Q13616	s,l
CUL2	Q13617	l
CUL3	Q13618	l
CUL5	Q93034	l
CUTA	O60888	l
CXCL1	P09341	l
CXCL17	Q6UXB2	r
CYB561	P49447	o
CYB5A	P00167	l
CYB5B	J3QR91	l,o
CYB5R1	Q9UHQ9	l
CYB5R2	Q6BCY4	l
CYB5R3	P00387	o,l
CYBA	P13498	o
CYBB	P04839	o
CYBC1	Q9BQA9	o
CYC1	P08574	o,l
CYCS	P99999	l,o
CYFIP1	Q7L576	o,l
CYP1B1	Q16678	o
CYP2A6	P11509	o
CYP2J2	P51589	o
CYP2S1	Q96SQ9	o,l

CYP3A43	Q9HB55	a
CYP4B1	P13584	o
CYP4F11	Q9HBI6	o
CYP4F12	Q9HCS2	o
CYP4F2	P78329	o
CZIB	Q9NWV4	l
DAD1	P61803	o
DAG1	Q14118	l
DARS	P14868	l,o
DAW1	Q8N136	l
DAZAP1	Q96EP5	l
DBI	P07108	r,s,l
DBNL	Q9UJU6	l,o
DCD	P81605	s,r,o,a
DCPS	Q96C86	l
DCTD	P32321	l
DCTN1	Q14203	l
DCTN2	Q13561	l
DCTN4	Q9UJW0	l
DCUN1D1	Q96GG9	l
DCXR	Q7Z4W1	l
DDAH1	O94760	l
DDAH2	O95865	l
DDB1	Q16531	l,o
DDI2	Q5TDH0	l
DDOST	P39656	l,o
DDRGK1	Q96HY6	o,l
DDTL	A6NHG4	l
DDX1	Q92499	l
DDX17	Q92841	o,l
DDX18	Q9NVP1	o
DDX19B	Q9UMR2	l
DDX21	Q9NR30	o
DDX39A	O00148	o
DDX39B	Q13838	l
DDX3X	O00571	l,o
DDX42	Q86XP3	l
DDX46	Q7L014	l
DDX5	P17844	o,l
DDX51	Q8N8A6	o
DDX58	O95786	l
DDX6	P26196	o,l
DECR1	Q16698	o,l
DEFA1	P59665	s,o,a
DEFA1B	P59665	s,o,a
DEFA3	P59666	r,k
DERL1	Q9BUN8	o
DES	P17661	m,o
DFFA	O00273	l
DGAT1	O75907	o
DGKA	P23743	l
DGLUCY	Q7Z3D6	l
DHCR7	Q9UBM7	o
DHODH	Q02127	o
DHRS1	Q96LJ7	l
DHRS3	O75911	o
DHRS7	Q9Y394	o,l
DHRS7B	Q6IAN0	l

DHRS9	Q9BPW9	l,o
DHX15	O43143	o,l
DHX30	Q7L2E3	o
DHX9	Q08211	o,l
DIABLO	Q9NR28	l,l
DIAPH1	O60610	l
DIDO1	Q9BTC0	o
DIS3	Q9Y2L1	l
DLAT	P10515	o,l
DLD	P09622	l,o
DLST	P36957	o,l
DMBT1	Q9UGM3	r,s,k,l,o
DMTF1	Q9Y222	h
DNAH5	Q8TE73	l,o
DNAH8	Q96JB1	o
DNAH9	Q9NYC9	l,o
DNAI1	Q9UI46	l
DNAI2	Q9GZS0	l
DNAJA1	P31689	l
DNAJA2	O60884	l
DNAJA3	Q96EY1	o
DNAJA4	Q8WW22	l
DNAJB1	P25685	l
DNAJB12	Q9NXW2	o
DNAJB13	P59910	l
DNAJB6	O75190	l
DNAJC11	Q9NVH1	l,o
DNAJC13	O75165	o
DNAJC2	Q99543	l
DNAJC8	O75937	l
DNAL1	Q4LDG9	l
DNALI1	O14645	l
DNM1L	O00429	l
DNM2	P50570	l
DNPEP	Q9ULA0	l
DNPH1	O43598	l
DOHH	Q9BU89	l
DPCD	Q9BVM2	l
DPP3	Q9NY33	l
DPP7	Q9UHL4	l
DPY30	Q9C005	l
DPYS	Q14117	l
DPYSL2	Q16555	l
DRG1	Q9Y295	l
DRG2	P55039	l
DSG1	Q02413	a
DSG2	Q14126	o,l
DSG3	P32926	o,l
DSP	P15924	l,o,a
DSTN	P60981	s,l
DTX3L	Q8TDB6	l
DUOX1	Q9NRD9	o
DUOX2	Q9NRD8	o
DUSP23	Q9BVJ7	l
DYNC1H1	Q14204	l,o
DYNC1I2	Q13409	l,o
DYNC1LI1	Q9Y6G9	l
DYNC1LI2	O43237	l

DYNC2H1	Q8NCM8	l
DYNLL1	P63167	l
DYNLRB1	Q9NP97	l
DYNLRB2	Q8TF09	l
DYNLT1	P63172	l
DYSF	O75923	o
EBP	Q15125	l
ECE1	P42892	o
ECH1	Q13011	l,o
ECHDC1	Q9NTX5	l
ECHS1	P30084	o,j,m,l,j
ECI1	P42126	o,l
ECPAS	Q5VYK3	l
EDC4	Q6P2E9	l
EDF1	O60869	l
EEA1	Q15075	l
EEF1A1	P68104	s,o,a
EEF1A1P5	Q5VTE0	r,l
EEF1B2	P24534	l,o
EEF1D	P29692	l,o
EEF1E1	O43324	l
EEF1G	P26641	l
EEF2	P13639	s,r,l,o
EFCAB1	Q9HAE3	l
EFHC1	Q5JVL4	l
EFHC2	Q5JST6	l
EFHD2	Q96C19	l
EFTUD2	Q15029	l
EGFR	P00533	o

EHD2	Q9NZN4	h
EHD3	Q9NZN3	l
EHD4	Q9H223	o,l
EHHADH	Q08426	o
EIF1	P41567	l
EIF1AY	O14602	l
EIF2A	Q9BY44	l
EIF2AK2	P19525	l
EIF2B1	Q14232	l
EIF2B2	P49770	l
EIF2B3	Q9NR50	l
EIF2S1	P05198	l,d
EIF2S2	P20042	l
EIF2S3	P41091	l
EIF3A	Q14152	l,o
EIF3B	P55884	l
EIF3C	Q99613	o,l
EIF3D	O15371	l
EIF3E	P60228	l
EIF3F	O00303	l
EIF3G	O75821	l
EIF3H	O15372	l
EIF3I	Q13347	l,h
EIF3K	Q9UBQ5	l
EIF3L	Q9Y262	l
EIF3M	Q7L2H7	l
EIF4A1	P60842	s,o,l
EIF4A2	Q14240	l
EIF4A3	P38919	o,l

EIF4B	P23588	o,l
EIF4E	P06730	l
EIF4G1	Q04637	l,o
EIF4G2	P78344	o
EIF4H	Q15056	l
EIF5	P55010	l
EIF5A	P63241	r,l
EIF5B	O60841	l
EIF6	P56537	l
ELANE	P08246	s,r,k,o,l
ELAVL1	Q15717	l,o
ELMOD2	Q8IZ81	o
ELOB	Q15370	l
EMC1	Q8N766	o
EMC3	Q9P0I2	o
EMC6	Q9BV81	o
EMC7	Q9NPA0	o
EMD	P50402	o,l

EML1	O00423	l
EML2	O95834	l
EML4	Q9HC35	l
EMP2	P54851	c
ENDOG	Q14249	l
ENO1	P06733	c,s,r,n,m,l,o,a
ENO2	P09104	h,l
ENOPH1	Q9UHY7	l
ENSA	O43768	l
ENTPD3	O75355	o
EPB41L1	Q9H4G0	o,l
EPB42	P16452	o
EPCAM	P16422	l,o
EPHA2	P29317	o
EPHX1	P07099	o,l
EPHX2	P34913	l
EPM2AIP1	Q7L775	l
EPPK1	P58107	s,l,o
EPRS	P07814	l,o
EPS8	Q12929	l
EPS8L2	Q9H6S3	l
EPX	P11678	o
ERAP1	Q9NZ08	o,l
ERBB2	P04626	o
ERGIC1	Q969X5	l,o
ERH	P84090	o
ERICH3	Q5RHP9	l
ERICH5	Q6P6B1	o
ERLIN1	O75477	o
ERLIN2	O94905	l,o
ERMP1	Q7Z2K6	o
ERN2	Q76MJ5	o
ERO1A	Q96HE7	o,l
ERP29	P30040	m,o,l
ERP44	Q9BS26	o,l
ESD	P10768	l,p
ESYT1	Q9BSJ8	l,o
ESYT2	A0FGR8	o
ETF1	P62495	l
ETFA	P13804	l,o
ETFB	P38117	l
ETFDH	Q16134	o,l
ETHE1	O95571	o,l
EVPL	Q92817	o,l
EWSR1	Q01844	o,l
EXD2	Q9NVH0	o
EXOC1	Q9NV70	l
EXOC2	Q96KP1	l
EZR	P15311	s,r,o,l
F11R	Q9Y624	o
F12	P00748	l
F13B	P05160	l
F2	P00734	r,l
F3	P13726	o,l
FABP1	P07148	g
FABP4	P15090	c
FABP5	Q01469	r,s,n,u,k,o,l,p,a
FAF2	Q96CS3	o

FAH	P16930	l
FAHD1	Q6P587	l
FAM107B	Q9H098	l
FAM114A1	Q8IWE2	l
FAM120A	Q9NZB2	o,l
FAM162A	Q96A26	o
FAM169A	Q9Y6X4	s
FAM174A	Q8TBP5	o
FAM3C	Q92520	o
FAM3D	Q96BQ1	l,o
FAM49B	Q9NUQ9	l
FAM81B	Q96LP2	l,o
FAM98C	Q17RN3	l
FANCD2	Q9BXW9	l
FARSA	Q9Y285	l
FARSB	Q9NSD9	l
FASN	P49327	o,l
FAT3	Q8TDW7	l
FAU	P62861	l
FBL	P22087	o,l
FBLN1	P23142	l
FBP1	P09467	s,o,l
FBXL4	Q9UKA2	l
FBXO2	Q9UK22	l
FBXO22	Q8NEZ5	l
FBXW9	Q5XUX1	l
FCGBP	Q9Y6R7	s,r,k,o,l
FCGR3B	O75015	l
FCSK	Q8N0W3	l

FDFT1	P37268	o
FDPS	P14324	l
FDXR	P22570	o,l
FECH	P22830	o
FEN1	P39748	l
FER1L6	Q2WGJ9	l
FERMT3	Q86UX7	l
FGA	P02671	s,r,l,o
FGB	P02675	b,s,r,k,l,o
FGG	P02679	s,r,l,j,o,j
FH	P07954	o,l
FHAD1	B1AJZ9	l
FHIT	P49789	l
FIS1	Q9Y3D6	l
FKBP11	Q9NYL4	o
FKBP1A	P62942	s,l
FKBP2	P26885	l
FKBP3	Q00688	l
FKBP4	Q02790	l
FKBP5	Q13451	l
FKBP8	Q14318	o
FLAD1	Q8NFF5	l
FLG	P20930	r,a
FLII	Q13045	l
FLNA	P21333	o,l
FLNB	O75369	o,l
FLOT1	O75955	l,o
FLOT2	Q14254	o
FMC1	Q96HJ9	l

FMO3	P31513	l,o
FN1	P02751	o,l
FNTA	P49354	l
FOXO3	O43524	l
FSCN1	Q16658	l
FTH1	P02794	l
FTL	P02792	l
FTO	Q9C0B1	l
FUBP1	Q96AE4	o,l
FUCA1	P04066	l
FUS	P35637	o,l
FUT2	Q10981	o
FUT3	P21217	o,l
FUT6	P51993	o,l
FUT8	Q9BYC5	o
G3BP1	Q13283	l,o
G6PD	P11413	r,l
GAA	P10253	o,l
GALE	Q14376	l
GALK1	P51570	l
GALM	Q96C23	l
GALNT1	Q10472	o
GALNT12	Q8IXK2	o
GALNT4	Q8N4A0	o
GALNT5	Q7Z7M9	o
GALNT6	Q8NCL4	l
GALNT7	Q86SF2	o
GANAB	Q14697	o,l
GAPDH	P04406	s,r,c,o,l,p,t,a,t
GAPVD1	Q14C86	l
GAR1	Q9NY12	o
GARS	P41250	l,o
GART	P22102	l
GATD3A	P0DPI2	o,l
GBE1	Q04446	l
GBP1	P32455	l
GBP2	P32456	l
GBP4	Q96PP9	l
GBP5	Q96PP8	l
GBP6	Q6ZN66	l
GC	P02774	r,s,u,k,c,l
GCA	P28676	l
GCHFR	P30047	l
GCLC	P48506	o,l
GCLM	P48507	l
GCN1	Q92616	o,l
GDAP1	Q8TB36	o
GDI1	P31150	l
GDI2	P50395	r,s,o,l,p
GDPD3	Q7L5L3	o
GDPGP1	Q6ZNW5	l
GFAP	P14136	b
GFPT1	Q06210	o,l
GGCT	O75223	l
GGPS1	O95749	l
GH1	P01241	s
GHITM	Q9H3K2	o
GIPC1	O14908	l

GK3P	Q14409	l
GLA	P06280	l,h
GLB1	P16278	o,l
GLCE	O94923	o
GLG1	Q92896	o,l
GLIPR2	Q9H4G4	o
GLO1	Q04760	l,j
GLOD4	Q9HC38	l
GLRX	P35754	l
GLRX3	O76003	l
GLTP	Q9NZD2	l
GLUD1	P00367	c,o,l
GLUD2	P49448	m
GLUL	P15104	o,l
GM2A	P17900	l
GMDS	O60547	l
GMFB	P60983	l
GMFG	O60234	l
GMPPA	Q96IJ6	l
GMPPB	Q9Y5P6	l
GMPR	P36959	l
GMPR2	Q9P2T1	l
GMPS	P49915	l
GNA11	P29992	o,l
GNAI1	P63096	o
GNAI2	P04899	o,l
GNAI3	P08754	o
GNAS	Q5JWF2	o
GNB1	P62873	o,l
GNB2	P62879	l
GNE	Q9Y223	l
GNG12	Q9UBI6	o
GNG13	Q9P2W3	h
GNG5	P63218	o
GNL1	P36915	l
GNPDA1	P46926	l
GNPDA2	Q8TDQ7	l
GNPNAT1	Q96EK6	l
GNS	P15586	l
GOLGB1	Q14789	o,l
GOLM1	Q8NBJ4	o,l
GOLPH3L	Q9H4A5	l
GOLT1B	Q9Y3E0	o
GORASP2	Q9H8Y8	l
GOSR1	O95249	o
GOT1	P17174	l
GOT2	P00505	l,o
GPAA1	O43292	o
GPD1L	Q8N335	l
GPD2	P43304	o,l
GPI	P06744	s,r,l,p,o
GPNMB	Q14956	l
GPR107	Q5VW38	o
GPR89A	B7ZAQ6	o
GPS1	Q13098	l
GPX1	P07203	o,l
GPX2	P18283	l
GPX4	P36969	l

GRB2	P62993	l
GRHPR	Q9UBQ7	l
GRN	P28799	s,r,l
GSDMB	Q8TAX9	l
GSDMD	P57764	l
GSN	P06396	s,r,o,l
GSPT1	P15170	l
GSR	P00390	o,l
GSS	P48637	l,p
GSTA1	P08263	s,c,l,o
GSTA2	P09210	r,l,e
GSTA3	Q16772	l
GSTA5	Q7RTV2	l
GSTK1	Q9Y2Q3	o,l
GSTM1	P09488	l
GSTM2	P28161	l
GSTM3	P21266	l,h
GSTM4	Q03013	l
GSTO1	P78417	o,l
GSTP1	P09211	c,s,r,e,m,o,l,p,a,j
GSTT1	P30711	l
GSTZ1	O43708	l
GTF2I	P78347	l
GTPBP1	O00178	l
GUSB	P08236	l
GYG1	P46976	l
GYS1	P13807	l
H1F0	P07305	o,l
H1FX	Q92522	l

H2AFV	Q71UI9	l
H2AFY	O75367	l,o
H2AFY2	Q9P0M6	l
H2AFZ	P0C0S5	s
H3F3A	P84243	s
H3F3B	P84243	s
H6PD	O95479	l
HACD3	Q9P035	l
HADH	Q16836	l,o
HADHA	P40939	o,l
HADHB	P55084	o,l
HAGH	Q16775	l
HAL	P42357	p
HARS	P12081	l,p
HBA1	P69905	s,r,b,c,k,o,l,a
HBA2	P69905	s,r,b,c,k,o,l,a
HBB	P68871	s,r,b,c,q,p,m,o,e,l,q,a
HBD	P02042	s,o,l
HBG1	P69891	o
HCLS1	P14317	l
HDAC1	Q13547	l
HDDC2	Q7Z4H3	l
HDDC3	Q8N4P3	l
HDGF	P51858	o,l
HDGFL3	Q9Y3E1	l
HDHD2	Q9H0R4	l
HDHD3	Q9BSH5	l
HDLBP	Q00341	o,l
HEATR1	Q9H583	l

HEBP1	Q9NRV9	l
HEBP2	Q9Y5Z4	o,l
HERC4	Q5GLZ8	l
HEXA	P06865	l
HEXB	P07686	l,o
HIBADH	P31937	o,l
HIBCH	Q6NVY1	l
HID1	Q8IV36	o
HINT1	P49773	l
HINT2	Q9BX68	o,l
HIST1H1A	Q02539	o,l
HIST1H1B	P16401	o,l
HIST1H1C	P16403	o
HIST1H1D	P16402	r
HIST1H1E	P10412	s,l
HIST1H2AA	Q96QV6	o
HIST1H2AB	P04908	o
HIST1H2AC	Q93077	k
HIST1H2AD	P20671	r,o
HIST1H2AE	P04908	o
HIST1H2AH	Q96KK5	s
HIST1H2BA	Q96A08	b,o
HIST1H2BB	P33778	o
HIST1H2BC	P62807	o
HIST1H2BE	P62807	o
HIST1H2BF	P62807	o
HIST1H2BG	P62807	o
HIST1H2BI	P62807	o
HIST1H2BJ	P06899	s
HIST1H2BK	O60814	s
HIST1H2BL	Q99880	l
HIST1H2BM	Q99879	r
HIST1H3A	P68431	s,o
HIST1H3B	P68431	s,o
HIST1H3C	P68431	s,o
HIST1H3D	P68431	s,o
HIST1H3E	P68431	s,o
HIST1H3F	P68431	s,o
HIST1H3G	P68431	s,o
HIST1H3H	P68431	s,o
HIST1H3I	P68431	s,o
HIST1H3J	P68431	s,o
HIST1H4A	P62805	b,s,r,l,o,a
HIST1H4B	P62805	b,s,r,l,o,a
HIST1H4C	P62805	b,s,r,l,o,a
HIST1H4D	P62805	b,s,r,l,o,a
HIST1H4E	P62805	b,s,r,l,o,a
HIST1H4F	P62805	b,s,r,l,o,a
HIST1H4H	P62805	b,s,r,l,o,a
HIST1H4I	P62805	b,s,r,l,o,a
HIST1H4J	P62805	b,s,r,l,o,a
HIST1H4K	P62805	b,s,r,l,o,a
HIST1H4L	P62805	b,s,r,l,o,a
HIST2H2AA3	Q6FI13	l
HIST2H2AA4	Q6FI13	l
HIST2H2AB	Q8IUE6	k
HIST2H2AC	Q16777	s
HIST2H3A	Q71DI3	s,r

HIST2H3C	Q71DI3	s,r
HIST2H3D	Q71DI3	s,r
HIST2H4A	P62805	b,s,r,l,o,a
HIST2H4B	P62805	b,s,r,l,o,a
HIST3H2BB	Q8N257	l
HIST3H3	Q16695	o
HIST4H4	P62805	b,s,r,l,o,a
HK1	P19367	o,l
HK3	P52790	l
HLA-A	P01892	l,l,h,l
HLA-B	P01889	o,l,o,h
HLA-C	P30510	l
HLA-DPA1	P20036	l
HLA-DQB1	P01920	o
HLA-DRA	P01903	l,o
HLA-DRB1	P13760	l
HM13	Q8TCT9	o
HMGA1	P17096	l
HMGB1	P09429	s,l
HMGB2	P26583	s,l
HMGB3	O15347	l
HMGCL	P35914	o,l
HMGCS2	P54868	o,l
HMGN1	P05114	o
HMGN2	P05204	o
HMGN5	P82970	l
HMOX2	P30519	o
HNMT	P50135	l
HNRNPA0	Q13151	l
HNRNPA1	P09651	l,o
HNRNPA1L2	Q32P51	s
HNRNPA2B1	P22626	r,s,o,l
HNRNPA3	P51991	s,o,l
HNRNPAB	Q99729	l
HNRNPC	P07910	r,s,o,l
HNRNPCL1	O60812	o
HNRNPD	Q14103	r,s,o,l
HNRNPDL	O14979	l
HNRNPF	P52597	l,o
HNRNPH1	P31943	o,l
HNRNPH2	P55795	l
HNRNPH3	P31942	o,l
HNRNPK	P61978	c,r,s,o,l
HNRNPL	P14866	l
HNRNPM	P52272	r,o,l
HNRNPR	O43390	o,l
HNRNPU	Q00839	o,l
HNRNPUL1	Q9BUJ2	l
HNRNPUL2	Q1KMD3	o,l
HOXA4	Q00056	o
HOXB4	P17483	o
HP	P00738	b,s,r,f,k,o,p,l,a
HP1BP3	Q5SSJ5	l
HPR	P00739	a
HPRT1	P00492	l
HPX	P02790	u,s,r,k,c,l
HRG	P04196	r,l
HRNR	Q86YZ3	a

HSBP1	O75506	l
HSD11B2	P80365	o
HSD17B10	Q99714	l,o
HSD17B11	Q8NBQ5	o
HSD17B12	Q53GQ0	o,l
HSD17B13	Q7Z5P4	l,o
HSD17B4	P51659	o,l
HSD17B8	Q92506	o
HSDL2	Q6YN16	l
HSP90AA1	P07900	s,r,o,l
HSP90AB1	P08238	s,o,l
HSP90AB2P	Q58FF8	l
HSP90B1	P14625	t,o,d,t,l
HSPA14	Q0VDF9	l,l
HSPA1A	P0DMV8	s,r,c,l,o,m
HSPA1L	P34931	o
HSPA2	P54652	o,l
HSPA4	P34932	o
HSPA4L	O95757	l
HSPA5	P11021	c,l,o,m,d
HSPA8	P11142	s,c,o,l,p,m
HSPA9	P38646	c,m,o,l,g
HSPB1	P04792	s,r,k,c,o,l,p,m,a
HSPB11	Q9Y547	l
HSPBP1	Q9NZL4	l
HSPD1	P10809	c,l,o,m,g
HSPE1	P61604	l,o
HSPG2	P98160	s
HSPH1	Q92598	l

HTATIP2	Q9BUP3	o
HTRA1	Q92743	l
HTRA2	O43464	l
HTT	P42858	o
HUWE1	Q7Z6Z7	l
HYOU1	Q9Y4L1	l,o
IAH1	Q2TAA2	l
IARS	P41252	l
IARS2	Q9NSE4	l
ICAM3	P32942	o
IDE	P14735	l
IDH1	O75874	r,s,c,p,o,l
IDH2	P48735	o,l
IDH3A	P50213	o,l
IDH3G	P51553	l
IDI1	Q13907	l
IDO1	P14902	l
IFI16	Q16666	l,o
IFI35	P80217	l
IFIT1	P09914	l
IFIT3	O14879	l
IFIT5	Q13325	l
IFITM1	P13164	o
IFT122	Q9HBG6	l
IFT140	Q96RY7	l
IFT172	Q9UG01	l
IFT20	Q8IY31	l
IFT27	H0Y6C7	l
IFT46	Q9NQC8	l

IFT57	Q9NWB7	l
IFT74	Q96LB3	l,h
IFT80	Q9P2H3	l
IGF1R	P08069	o
IGFALS	P35858	l
IGHA1	P01876	q,s,k,u,r,b,l,p,q,a
IGHA2	P01877	i,s,k,b,l,o,a
IGHD	P01880	l
IGHG1	P01857	b,u,s,k,r,l,o,a
IGHG2	P01859	s,k,b,l,a
IGHG3	P01860	s,b,l,a
IGHG4	P01861	s,l,a
IGHM	A0A1B0GUU9	b,r,s,k,b,l,p,o,a
IGHV1-2	P23083	l
IGHV1-46	P01743	k
IGHV3-13	P01766	r,s,l
IGHV3-23	P01764	r,k,s,l,a
IGHV3-30	P01768	s,h
IGHV3-33	P01772	k,h
IGHV3-48	P01763	l
IGHV3-53	P01767	s,l
IGHV3-7	P01780	r,s,l
IGHV4-34	P06331	s,l
IGKC	P01834	u,s,k,r,l,o,a,d
IGKV1-16	P04430	l
IGKV1-17	P01599	l
IGKV1-39	P01597	s
IGKV1-5	P01602	q,s,l,q
IGKV1D-12	P01611	s
IGKV1D-33	P01593	s,r,b,l
IGKV2D-28	P01615	s,l
IGKV3-11	P04433	s,l
IGKV3-20	P01619	s,k,r,b,l
IGKV4-1	P06312	s,b,l
IGLC1	P0CG04	k,a
IGLC2	P0DOY2	b,s,r,l,o
IGLC3	P0DOY3	s,h
IGLC7	A0M8Q6	s
IGLL1	P15814	l
IGLL5	B9A064	s,l
IGLV1-47	P01700	s,k
IGLV1-51	P01701	l
IGLV2-11	P01706	b
IGLV3-19	P01714	s,r,l
IGLV3-21	P80748	s,k,r,l
IGLV3-25	P01717	s,l
IL1RN	P18510	l
ILF2	Q12905	o,l
ILF3	Q12906	o,l
ILVBL	A1L0T0	l
IMMT	Q16891	o
IMPA1	P29218	l
IMPDH2	P12268	l
INPP1	P49441	l
INPP4B	O15327	l
IPO4	Q8TEX9	l
IPO5	O00410	l
IPO7	O95373	l

IQGAP1	P46940	o,l,d
IQGAP2	Q13576	l
IRF2BP2	Q7Z5L9	l
IRF6	O14896	l
IRGQ	Q8WZA9	l
IRX4	P78413	s
ISG15	P05161	l
ISG20	Q96AZ6	l
ISOC1	Q96CN7	l
ISOC2	Q96AB3	l
IST1	P53990	l
ISYNA1	Q9NPH2	l
ITGA2	P17301	o,l
ITGA3	P26006	o
ITGA6	P23229	o
ITGAM	P11215	o
ITGAV	P06756	o
ITGB1	P05556	o,l
ITGB2	P05107	o
ITGB4	P16144	o
ITIH1	P19827	l
ITIH2	P19823	l
ITIH4	Q14624	l
ITLN1	Q8WWA0	l
ITPA	Q9BY32	l
ITPR1	Q14643	o
ITPR2	Q14571	s
ITPR3	Q14573	o
IVD	P26440	l
IVL	P07476	o,a
JCHAIN	P01591	n,f,r,b,c,s,k,q,l,a,q
JMJD7	P0C870	l
JPT1	Q9UK76	l
JPT2	Q9H910	l
JUP	P14923	o,l,a
KARS	Q15046	l
KCNIP3	Q9Y2W7	h
KCNJ5	P48544	h
KCTD12	Q96CX2	l
KDM5A	P29375	s
KHDRBS1	Q07666	l
KHSRP	Q92945	l,o
KIAA1217	Q5T5P2	o
KIAA1328	Q86T90	s
KIF13B	Q9NQT8	l
KIF21A	Q7Z4S6	l
KIF2A	O00139	l
KIF5B	P33176	o,l
KLC4	Q9NSK0	l
KLHL34	Q8N239	s
KLK11	Q9UBX7	l
KLK7	P49862	p
KLRF1	Q9NZS2	s
KMT2B	Q9UMN6	o
KNG1	P01042	r,l
KPNA3	O00505	l
KPNA4	O00629	l
KPNB1	Q14974	l,o

KPRP	Q5T749	a
KRT1	P04264	b,s,r,o
KRT10	P13645	b,s,r,o,a
KRT12	Q99456	b
KRT13	P13646	s,o
KRT14	P02533	b,s,o,a
KRT15	P19012	o
KRT16	P08779	b,s,o,a
KRT17	Q04695	o,a
KRT18	P05783	s,r,c,o,l
KRT19	P08727	b,s,c,o,m,l
KRT2	P35908	s,b,o,a
KRT20	P35900	a
KRT23	Q9C075	o
KRT28	Q7Z3Y7	b
KRT3	P12035	b,o,a
KRT31	Q15323	a
KRT32	Q14532	a
KRT33A	O76009	a
KRT33B	Q14525	a
KRT34	O76011	a
KRT35	Q92764	a
KRT36	O76013	r,a
KRT37	O76014	a
KRT38	O76015	a
KRT4	P19013	b,s,o,a
KRT5	P13647	b,s,o,m,a
KRT6A	P02538	b,s,c,o,a
KRT6B	P04259	b,s,a
KRT6C	P48668	b,k
KRT7	P08729	s,b,c,o,a
KRT76	Q01546	a
KRT77	Q7Z794	a
KRT79	Q5XKE5	b,a
KRT8	P05787	b,s,c,j,o,t,m,j,t
KRT81	Q14533	a
KRT82	Q9NSB4	a
KRT83	P78385	a
KRT84	Q9NSB2	a
KRT85	P78386	a
KRT86	O43790	a
KRT9	P35527	b,s,r,o,a
KRTAP10-3	P60369	a
KRTAP13-2	Q52LG2	a
KRTAP2-4	Q9BYR9	a
KRTAP4-9	Q9BYQ8	a
KRTAP9-8	Q9BYQ0	a
KTN1	Q86UP2	o,l
KYAT3	Q6YP21	l
KYNU	Q16719	l
LACRT	Q9GZZ8	k,s,r,l,a
LACTB2	Q53H82	l
LAMB4	A4D0S4	l
LAMP1	P11279	o,l
LAMTOR1	Q6IAA8	o
LANCL1	O43813	l
LANCL2	Q9NS86	l
LAP3	P28838	c,r,l,o

LARS	Q9P2J5	l
LAS1L	Q9Y4W2	o
LASP1	Q14847	l,o
LBR	Q14739	o
LCMT1	Q9UIC8	h
LCN1	P31025	n,b,u,s,r,k,f,l,a
LCN15	Q6UWW0	s,r,k,n,l
LCN2	P80188	u,r,s,b,k,o,l
LCP1	P13796	s,r,o,l
LCP2	Q13094	l
LDHA	P00338	s,l,o,a
LDHB	P07195	s,r,l,o
LEG1	Q6P5S2	q,s,r,k,l,q
LEMD3	Q9Y2U8	o
LETM1	O95202	o
LGALS1	P09382	l
LGALS3	P17931	s,o,l
LGALS3BP	Q08380	r,s,k,l,o
LGALS7	P47929	l,a
LGALS7B	P47929	l,a
LGMN	Q99538	l
LHPP	Q9H008	l
LIMA1	Q9UHB6	o,l
LIMK2	P53671	l
LLGL2	Q6P1M3	o,l
LMAN1	P49257	o,l
LMAN2	Q12907	o,l
LMNA	P02545	r,o,l,a
LMNB1	P20700	l,o
LMNB2	Q03252	l,o
LMO7	Q8WWI1	o,l
LNPK	Q9C0E8	o
LONP1	P36776	l
LPCAT2	Q7L5N7	o
LPCAT3	Q6P1A2	o
LPCAT4	Q643R3	o
LPGAT1	Q92604	o
LPO	P22079	s,r,l
LPP	Q93052	l
LRBA	P50851	o,l
LRG1	P02750	k,l
LRIG1	Q96JA1	o
LRP1B	Q9NZR2	s
LRPPRC	P42704	o,l
LRRC46	Q96FV0	l
LRRC47	Q8N1G4	l,o
LRRC59	Q96AG4	o,l
LRRC71	Q8N4P6	l
LRRFIP1	Q32MZ4	o,l
LSM2	Q9Y333	l
LSM3	P62310	l
LSM5	Q9Y4Y9	l
LSP1	P33241	s,l
LSR	Q86X29	o
LSS	P48449	o
LTA4H	P09960	r,l,o
LTF	P02788	f,b,c,u,s,r,k,q,o,p,l,a,q
LUM	P51884	l

LXN	Q9BS40	l
LY6D	Q14210	o
LYN	P07948	o,l
LYPLA1	O75608	l
LYPLAL1	Q5VWZ2	l
LYST	Q99698	o
LYZ	P61626	f,c,b,u,s,r,k,q,o,l,a,q
LZIC	Q8WZA0	l
LZTFL1	Q9NQ48	l
M6PR	P20645	o
MAGED2	Q9UNF1	l
MAGI1	Q96QZ7	l
MAGOHB	Q96A72	l
MAN2A1	Q16706	o
MANF	P55145	l
MAOA	P21397	l,o
MAOB	P27338	l,o
MAP1A	P78559	l
MAP4	P27816	o,l
MAPK1	P28482	l
MAPK11	Q15759	h
MAPK14	Q16539	l
MAPK3	P27361	l
MAPRE1	Q15691	l
MAPRE3	Q9UPY8	l
Mar-05	Q9NX47	o
MARCKS	P29966	o,l
MARCKSL1	P49006	o
MARS	P56192	l,o

MAT2A	P31153	l
MAT2B	Q9NZL9	l
MATK	P42679	s
MATR3	P43243	l,l,o,o
MAX	Q6V3B1	m
MB	P02144	l,a
MBOAT2	Q6ZWT7	o
MCCC1	Q96RQ3	l,o
MCCC2	Q9HCC0	l
MCEMP1	Q8IX19	o
MCM2	P49736	l
MCTS1	Q9ULC4	l
MCU	Q8NE86	l
MDH1	P40925	r,s,o,l
MDH2	P40926	r,s,o
ME1	P48163	l
ME2	P23368	o,l
METAP1	P53582	l
METAP2	P50579	l
METTL7A	Q9H8H3	o,l
MFN2	O95140	o
MGA	Q8IWI9	s
MGAT1	P26572	o
MGAT2	Q10469	o
MGMT	P16455	l
MGST1	P10620	o,l
MGST2	Q99735	o
MGST3	O14880	o,l
MICU2	Q8IYU8	o

MIEN1	Q9BRT3	l
MIER1	Q8N108	h
MIF	P14174	s,l
MLEC	Q14165	l,o
MLF1	P58340	l
MMP10	P09238	l
MMP8	P22894	s,r,l
MMP9	P14780	s,r,o,l
MMS19	Q96T76	l
MMUT	P22033	l
MNAT1	P51948	h
MNDA	P41218	s,r,o,l
MOB1B	Q7L9L4	l
MOGS	Q13724	o,l
MOS	P00540	s
MPC2	O95563	o
MPI	P34949	l
MPO	P05164	s,r,k,o,l
MPST	P25325	l
MRI1	Q9BV20	l
MRPL12	P52815	l
MRPL15	Q9P015	o
MRPS31	Q92665	l
MSH2	P43246	l
MSI2	Q96DH6	l
MSLN	Q13421	s,k,l
MSMB	P08118	s,r,k,l
MSN	P26038	s,o,l
MSRA	Q9UJ68	l

MST1R	Q04912	o
MT-CO2	P00403	o,l
MT-ND1	P03886	o
MT-ND4	P03905	o
MT-ND5	P03915	o,l
MTAP	Q13126	l
MTCH1	Q9NZJ7	o,l
MTCH2	Q9Y6C9	o,l
MTDH	Q86UE4	o
MTFP1	Q9UDX5	o
MTHFD1	P11586	l
MTPN	P58546	l
MTREX	P42285	l
MTX1	Q13505	o
MUC1	P15941	o,l
MUC13	Q9H3R2	o
MUC16	Q8WXI7	l
MUC2	Q02817	o,l
MUC4	Q99102	o,l
MUC5AC	P98088	b,s,k,l
MUC5B	Q9HC84	b,q,s,r,k,l,q
MUC7	Q8TAX7	s,r,k
MVK	Q03426	l
MVP	Q14764	o,l
MX1	P20591	l,o
MXRA7	P84157	o
MYADM	Q96S97	o
MYBBP1A	Q9BQG0	o
MYCBP	Q99417	l

MYDGF	Q969H8	o,l
MYF5	P13349	h
MYH10	P35580	o
MYH11	P35749	o
MYH13	Q9UKX3	a
MYH14	Q7Z406	o,l
MYH9	P35579	s,r,o,l,a
MYL12A	P19105	l
MYL4	P12829	j,j
MYL6	P60660	s,o,l
MYO1B	O43795	o,l
MYO1C	O00159	o
MYO1D	O94832	l,o
MYO1E	Q12965	l
MYO1G	B0I1T2	m
MYO5B	Q9ULV0	l,o
MYO5C	Q9NQX4	o
MYO6	Q9UM54	o,l
MYOF	Q9NZM1	o,l
MYOZ2	Q9NPC6	s
NAA15	Q9BXJ9	l
NAA38	Q9BRA0	l
NAA50	Q9GZZ1	l
NACA	Q13765	o,l
NAE1	Q13564	l
NAGK	Q9UJ70	l,o
NAGLU	P54802	l
NAMPT	P43490	r,l,o
NANS	Q9NR45	o,l

NAP1L1	P55209	l
NAP1L4	Q99733	o,l
NAPA	P54920	l
NAPG	Q99747	l
NAPRT	Q6XQN6	l
NARS	O43776	l
NASP	P49321	o,l
NAT1	P18440	l
NAT10	Q9H0A0	o
NAXD	Q8IW45	l
NAXE	Q8NCW5	l
NCBP1	Q09161	l
NCEH1	Q6PIU2	o
NCF1C	A8MVU1	l
NCF4	Q15080	h
NCKAP1	Q9Y2A7	o,l
NCL	P19338	o,l
NCLN	Q969V3	o
NCS1	P62166	h
NCSTN	Q92542	o
NDC1	Q9BTX1	o
NDE1	Q9NXR1	h
NDRG2	Q9UN36	l
NDUFA10	O95299	l
NDUFA11	Q86Y39	l
NDUFA12	Q9UI09	o
NDUFA13	Q9P0J0	o,l
NDUFA4	O00483	o
NDUFA4L2	Q9NRX3	l

NDUFA5	Q16718	l
NDUFA9	Q16795	l,o
NDUFB10	O96000	o
NDUFB4	O95168	o,l
NDUFB6	O95139	o
NDUFB7	P17568	o
NDUFB8	O95169	o
NDUFC2	O95298	o
NDUFS1	P28331	o,l
NDUFS2	O75306	l,o
NDUFS3	O75489	l,m,o
NDUFS5	O43920	l
NDUFS7	O75251	o
NDUFS8	O00217	o,j,j
NDUFV1	P49821	l
NDUFV2	P19404	l
NEB	P20929	o
NECAP2	Q9NVZ3	l
NEDD8	Q15843	l
NEFL	P07196	h
NEO1	Q92859	s
NFKB1	P19838	l
NHLRC2	Q8NBF2	l
NIBAN1	Q9BZQ8	o,l
NIBAN2	Q96TA1	o,l
NIF3L1	Q9GZT8	l
NIPSNAP1	Q9BPW8	o
NIPSNAP2	O75323	o,l
NIPSNAP3A	Q9UFN0	l

NIT1	Q86X76	l
NIT2	Q9NQR4	l
NLN	Q9BYT8	o
NME1	P15531	p
NME2	P22392	r,p
NME2P1	O60361	l
NME3	Q13232	o
NME4	O00746	j,j
NME5	P56597	l
NMES1	Q9C002	l
NMI	Q13287	l
NMRAL1	Q9HBL8	l
NMT1	P30419	l
NNT	Q13423	l,o
NOL3	O60936	l
NOLC1	Q14978	l,o
NONO	Q15233	o,l
NOP56	O00567	o
NOP58	Q9Y2X3	l,o
NOS2	P35228	o
NPC1	O15118	o
NPC2	P61916	s,r,l
NPEPL1	Q8NDH3	l
NPEPPS	P55786	o,l
NPLOC4	Q8TAT6	l
NPM1	P06748	l,o
NPR3	P17342	h
NPTN	Q9Y639	l,o
NQO1	P15559	s,r,l,o

NQO2	P16083	l
NRBP1	Q9UHY1	l
NRDC	O43847	l
NSDHL	Q15738	o
NSF	P46459	o,l
NSFL1C	Q9UNZ2	l
NSUN2	Q08J23	l
NT5C	Q8TCD5	l
NT5C2	P49902	l
NT5C3A	Q9H0P0	l
NT5DC1	Q5TFE4	l
NUCB1	Q02818	o,l
NUCB2	P80303	s,r,k,o,l
NUCKS1	Q9H1E3	l
NUDC	Q9Y266	o,l
NUDCD2	Q8WVJ2	l
NUDT12	Q9BQG2	l
NUDT14	O95848	l
NUDT15	Q9NV35	l
NUDT16	Q96DE0	l
NUDT16L1	Q9BRJ7	l
NUDT2	P50583	l
NUDT21	O43809	l
NUDT5	Q9UKK9	l
NUDT9	Q9BW91	l
NUMA1	Q14980	o,l
NUP155	O75694	o
NUP160	Q12769	o
NUP205	Q92621	l,o
NUP210	Q8TEM1	o
NUP62	P37198	l
NUP93	Q8N1F7	l,o
NUTF2	P61970	l
NXN	Q6DKJ4	l
OAS2	P29728	l,o
OAS3	Q9Y6K5	l,o
OAT	P04181	o,l
OBP2A	Q9NY56	c
OBSCN	Q5VST9	o
OCIAD2	Q56VL3	l
ODF3B	A8MYP8	l
OGDH	Q02218	o,l
OGFR	Q9NZT2	l
OLA1	Q9NTK5	o,l
OPA1	O60313	o,l
OPLAH	O14841	l
OPRPN	Q99935	s,r,k,l
OR1L6	Q8NGR2	s
ORM1	P02763	s,r,u,q,l,a,q
ORM2	P19652	s,l
OSBP	P22059	l
OSBPL5	Q9H0X9	o
OSBPL8	Q9BZF1	o
OSCP1	Q8WVF1	l
OSTF1	Q92882	l
OTOR	Q9NRC9	h
OTUB1	Q96FW1	o,l
OXA1L	Q15070	l,o

OXCT1	P55809	o,l
OXR1	Q8N573	l
OXSR1	O95747	l
P3H1	Q32P28	h
P4HB	P07237	r,m,o,l,p,d
PA2G4	Q9UQ80	l
PABPC1	P11940	o,l
PABPC4	Q13310	l
PABPN1	Q86U42	l
PACRG	Q96M98	l
PACSIN2	Q9UNF0	l
PAFAH1B1	P43034	o,l
PAFAH1B2	P68402	l
PAFAH1B3	Q15102	l
PAICS	P22234	l
PAIP1	Q9H074	l
PAK1	Q13153	l
PAK2	Q13177	l
PALLD	Q8WX93	l
PAPSS1	O43252	l
PAPSS2	O95340	l
PARK7	Q99497	s,r,j,m,o,l,j,d
PARP1	P09874	l
PARP10	Q53GL7	l
PARP4	Q9UKK3	s,l
PARP9	Q8IXQ6	l
PATJ	Q8NI35	s
PBDC1	Q9BVG4	l
PBLD	P30039	l

PCBD1	P61457	l
PCBD2	Q9H0N5	l
PCBP1	Q15365	o,l
PCBP2	Q15366	o,l
PCK2	Q16822	l
PCM1	Q15154	o,l
PCMT1	P22061	l
PCNA	P12004	l
PCNT	O95613	l,o
PCYOX1	Q9UHG3	o
PCYT1B	Q9Y5K3	l
PDAP1	Q13442	l
PDCD10	Q9BUL8	l
PDCD11	Q14690	o
PDCD4	Q53EL6	l
PDCD5	O14737	l
PDCD6	O75340	l
PDCD6IP	Q8WUM4	l
PDCL	Q13371	h
PDE12	F6T1Q0	l
PDE1A	P54750	h
PDE9A	O76083	h
PDHA1	P08559	l,o
PDHB	P11177	j,l,j
PDIA3	P30101	r,c,m,o,l
PDIA4	P13667	o,l
PDIA6	Q15084	o,l
PDLIM1	O00151	o,l
PDLIM4	P50479	l

PDLIM5	Q96HC4	l
PDS5A	Q29RF7	r
PDXDC1	Q6P996	l
PDXK	O00764	o,l
PEA15	Q15121	l
PEBP1	P30086	r,s,p,t,l,o,t
PEBP4	Q96S96	l
PELP1	Q8IZL8	o
PEPD	P12955	l
PEX11B	O96011	o
PFAS	O15067	l
PFDN2	Q9UHV9	l
PFDN4	Q9NQP4	l
PFDN5	Q99471	l
PFDN6	O15212	l
PFKL	P17858	l,o
PFKM	P08237	l
PFKP	Q01813	l,o
PFN1	P07737	s,r,k,o,l
PFN2	P35080	l
PGAM1	P18669	c,s,r,o,l
PGD	P52209	s,r,p,h,l,o
PGK1	P00558	s,r,o,l
PGLS	O95336	o,l
PGLYRP1	O75594	s,l
PGLYRP2	Q96PD5	l
PGM1	P36871	o,l
PGM2	Q96G03	l
PGM2L1	Q6PCE3	l
PGM3	O95394	l
PGP	A6NDG6	l
PGRMC1	O00264	l,o
PGRMC2	O15173	o
PHB	P35232	c,o,l,m
PHB2	Q99623	o,l
PHF6	Q8IWS0	s
PHGDH	O43175	l
PHPT1	Q9NRX4	l,h
PHYHD1	Q5SRE7	l
PI3	P19957	r,k,l
PIGG	Q5H8A4	o
PIGO	Q8TEQ8	o
PIGR	P01833	r,s,u,k,b,c,o,p,l,a
PIN1	Q13526	l
PIP	P12273	n,f,b,s,r,k,u,l,p,a
PIP4K2C	Q8TBX8	l
PIR	O00625	l
PITHD1	Q9GZP4	l
PITPNA	Q00169	l
PITPNB	P48739	l
PITRM1	Q5JRX3	l
PKM	P14618	s,r,c,o,l,p,a
PKP1	Q13835	o,a
PKP2	Q99959	l,o
PKP3	Q9Y446	o
PLA2G2A	P14555	s,r,k
PLAA	Q9Y263	l
PLBD1	Q6P4A8	l

PLCL2	Q9UPR0	b
PLD2	O14939	o
PLEC	Q15149	l,o
PLEK	P08567	l
PLEKHJ1	Q9NW61	l
PLG	P00747	b,l
PLGRKT	Q9HBL7	o
PLIN3	O60664	l
PLLP	Q9Y342	o
PLPBP	O94903	l
PLPP3	O14495	o
PLS1	Q14651	o,l
PLS3	P13797	l
PLTP	P55058	r,l
PML	P29590	o,l
PMM2	O15305	l
PMPCA	Q10713	l
PMPCB	O75439	l
PMVK	Q15126	l
PNN	Q9H307	o
PNP	P00491	l
PNPO	Q9NVS9	l
POC5	Q8NA72	o
PODXL	O00592	o
POF1B	Q8WVV4	o,l
POLE2	P56282	s
POLR1C	O15160	l
POLR2B	P30876	l
POLR2H	P52434	l

PON1	P27169	r,l
POR	P16435	o,l
POTEE	Q6S8J3	o
POTEJ	P0CG39	l
PPA1	Q15181	j,l,j
PPA2	Q9H2U2	o,l
PPCS	Q9HAB8	l
PPIA	P62937	s,r,o,p,l
PPIB	P23284	o,l
PPIC	P45877	l
PPID	Q08752	l
PPIL1	Q9Y3C6	l
PPIL3	Q9H2H8	l
PPL	O60437	o,l
PPM1B	O75688	l
PPM1F	P49593	l
PPM1G	O15355	l
PPME1	Q9Y570	l
PPOX	P50336	o,l
PPP1CA	P62136	o,l
PPP1CB	P62140	l
PPP1CC	P36873	l
PPP1R1A	Q13522	l
PPP1R7	Q15435	l
PPP1R8	Q12972	l
PPP2CA	P67775	h,l
PPP2CB	P62714	l
PPP2R1A	P30153	o,l
PPP2R2A	P63151	l

PPP3CA	Q08209	l
PPP4C	P60510	l
PPP4R3B	Q5MIZ7	l
PPP5C	P53041	l
PPP6C	O00743	l
PPT1	P50897	l
PRAF2	O60831	o
PRAM1	Q96QH2	s
PRB1	P04280	k
PRB2	P02812	c,s,r,k,a
PRB3	Q04118	o,a
PRB4	P10163	k,c
PRDM1	O75626	l
PRDX1	Q06830	c,s,r,o,m,l,p
PRDX2	P32119	c,s,b,j,o,m,l,p,a,j
PRDX3	P30048	o,l
PRDX4	Q13162	o,l
PRDX5	P30044	c,s,r,e,o,p,l
PRDX6	P30041	c,s,r,o,m,l
PREB	Q9HCU5	o
PREP	P48147	l
PRG4	Q92954	o
PRH1	P02810	s,a
PRH2	P02810	s,a
PRKAA1	Q13131	l
PRKACA	P17612	l
PRKAG1	P54619	l
PRKAR1A	P10644	l
PRKAR2A	P13861	l,o,h

PRKCD	Q05655	l
PRKCSH	P14314	l,o
PRKDC	P78527	o,l
PRKRA	O75569	l
PRMT1	Q99873	l
PRMT5	O14744	l
PRODH	O43272	o,h
PROM1	O43490	o,l
PROS1	P07225	l
PRPF19	Q9UMS4	o,l
PRPF6	O94906	o,l
PRPF8	Q6P2Q9	o,l
PRPS1	P60891	l
PRPS2	P11908	l
PRPSAP1	Q14558	l
PRPSAP2	O60256	l
PRR15	Q8IV56	l
PRR4	Q16378	b,s,r,k,l
PRRC1	Q96M27	l
PRRC2A	P48634	o
PRSS8	Q16651	o
PRTN3	P24158	s,r,l,o
PRUNE2	Q8WUY3	l
PRXL2A	Q9BRX8	o,l
PSAP	P07602	s,r,l,o
PSEN1	P49768	o
PSIP1	O75475	l
PSMA1	P25786	l,o
PSMA2	P25787	l

PSMA3	P25788	l,o
PSMA4	P25789	l
PSMA5	P28066	s,l,p
PSMA6	P60900	l
PSMA7	O14818	l
PSMB1	P20618	r,l
PSMB10	P40306	l
PSMB2	P49721	l,o
PSMB3	P49720	l
PSMB4	P28070	l
PSMB6	P28072	l
PSMB7	Q99436	l
PSMB8	P28062	l
PSMB9	P28065	l
PSMC1	P62191	l
PSMC2	P35998	l,o
PSMC3	P17980	l,o
PSMC4	P43686	l
PSMC5	P62195	l
PSMC6	P62333	l
PSMD1	Q99460	l
PSMD10	O75832	l
PSMD11	O00231	p,l
PSMD12	O00232	l
PSMD13	Q9UNM6	l
PSMD14	O00487	l,h
PSMD2	Q13200	l,o
PSMD3	O43242	l
PSMD4	P55036	l
PSMD5	Q16401	l
PSMD6	Q15008	l
PSMD7	P51665	l
PSMD8	P48556	l
PSMD9	O00233	l
PSME1	Q06323	r,o,j,l,h,j
PSME2	Q9UL46	r,o,l
PSME3	P61289	l
PSME4	Q14997	l
PSMF1	Q92530	l
PSMG2	Q969U7	l
PSPC1	Q8WXF1	l
PTBP1	P26599	s,o,l
PTBP3	O95758	l
PTDSS2	Q9BVG9	o
PTER	Q96BW5	l
PTGES	O14684	o
PTGES3	Q15185	l
PTGFRN	Q9P2B2	o
PTGR1	Q14914	l
PTGR2	Q8N8N7	l
PTMA	P06454	o
PTMS	P20962	o
PTPA	Q15257	l
PTPN1	P18031	o
PTPN11	Q06124	l
PTPN13	Q12923	c
PTPN6	P29350	l
PTPRC	P08575	o,l

PTPRJ	Q12913	o
PTRHD1	Q6GMV3	l
PUDP	Q08623	l
PUF60	Q9UHX1	l
PURA	Q00577	l
PURB	Q96QR8	l
PYCARD	Q9ULZ3	l
PYCR3	Q53H96	l
PYGB	P11216	r,l,o
PYGL	P06737	l
PYM1	Q9BRP8	l
QARS	P47897	l,o
QDPR	P09417	l
QSOX1	O00391	s,r,o,l
RAB10	P61026	l,o
RAB11A	P62491	o
RAB11B	Q15907	l
RAB13	P51153	o,l
RAB14	P61106	l,o
RAB18	Q9NP72	l
RAB1A	P62820	o
RAB1B	Q9H0U4	l,o
RAB21	Q9UL25	l,o
RAB22A	Q9UL26	o
RAB2A	P61019	o,l
RAB35	Q15286	o
RAB37	Q96AX2	o
RAB3C	Q96E17	h
RAB3D	O95716	l,o

RAB5A	P20339	o
RAB5B	P61020	l,o
RAB5C	P51148	o,l
RAB6A	P20340	o,l
RAB7A	P51149	l,o
RAB8A	P61006	l
RABGGTA	Q92696	l,h
RABL2A	Q9UBK7	l
RABL6	Q3YEC7	o,l
RAC1	P63000	o,l
RAC2	P15153	s,l
RACK1	P63244	l,o
RAD23B	P54727	o,l
RAD50	Q92878	l
RAI1	Q7Z5J4	o
RALA	P11233	o
RALGAPA1	Q6GYQ0	l
RALY	Q9UKM9	l
RAN	P62826	l
RANBP1	P43487	l
RANBP2	P49792	o
RANBP3	Q9H6Z4	h,l
RANGAP1	P46060	l
RAP1A	P62834	o
RAP1B	P61224	l
RARRES1	P49788	l
RARS	P54136	l,o
RBBP4	Q09028	l,o
RBBP7	Q16576	l

RBBP8	Q99708	b
RBBP9	O75884	l
RBKS	Q9H477	l
RBM12	Q9NTZ6	l
RBM14	Q96PK6	o
RBM25	P49756	l
RBM3	P98179	s,l
RBM39	Q14498	l
RBM47	A0AV96	l
RBMX	P38159	o,l
RBP1	P09455	l
RBP4	P02753	j,l,j
RCC1	P18754	l
RCC2	Q9P258	l
RCN1	Q15293	l,o
RCN2	Q14257	l
RDH10	Q8IZV5	l
RDH11	Q8TC12	o
RDH14	Q9HBH5	o
RDX	P35241	l
RECQL	F5H2L2	l
REEP5	Q00765	o
RELA	Q04206	l
RELCH	Q9P260	l
RER1	O15258	o
RETN	Q9HD89	r,l
RETREG3	Q86VR2	o
RETSAT	Q6NUM9	o
RHBDD2	Q6NTF9	l
RHOA	P61586	l
RHOC	P08134	l
RHOG	P84095	o
RHOT2	Q8IXI1	o,l
RIDA	P52758	l,g
RMDN3	Q96TC7	o,l
RMND1	Q9NWS8	o
RNASE1	P07998	s,r,k,l
RNASE2	P10153	l
RNASE3	P12724	s,r,l,o
RNASE4	P34096	l
RNASET2	O00584	l
RNF170	Q96K19	o
RNF213	Q63HN8	o,l
RNF40	O75150	l
RNH1	P13489	o,l
RNMT	O43148	l
RNPEP	Q9H4A4	l
RO60	P10155	l
ROCK2	O75116	l
ROPN1L	Q96C74	l
RPA1	P27694	l
RPA3	P35244	l
RPE	Q96AT9	l
RPIA	P49247	l
RPL10	P27635	o
RPL10A	P62906	l,o
RPL10L	Q96L21	o
RPL11	P62913	l,o

RPL12	P30050	l,o
RPL13	P26373	l,o
RPL13A	P40429	l
RPL14	P50914	l,o
RPL15	P61313	l
RPL17	P18621	l,o
RPL18	Q07020	l,o
RPL18A	Q02543	l,o
RPL19	P84098	l,o
RPL21	P46778	o
RPL22	P35268	l
RPL23	P62829	l,o
RPL23A	P62750	l,o
RPL24	P83731	l,o
RPL26	P61254	l
RPL26L1	Q9UNX3	o
RPL27	P61353	l
RPL27A	P46776	l,o
RPL28	P46779	o
RPL29	P47914	o
RPL3	P39023	l,o
RPL30	P62888	l
RPL31	P62899	l
RPL32	P62910	o
RPL34	P49207	o
RPL35	P42766	o
RPL35A	P18077	o
RPL37A	G5E9R3	l
RPL38	P63173	l

RPL4	P36578	l,o
RPL5	P46777	l,o
RPL6	Q02878	l,o
RPL7	P18124	l,o
RPL7A	P62424	l,o
RPL8	P62917	o
RPL9	P32969	l
RPL9P7	P32969	l
RPL9P8	P32969	l
RPL9P9	P32969	l
RPLP0	P05388	o
RPLP0P6	Q8NHW5	l
RPLP1	P05386	s,l
RPLP2	P05387	s,r,l,o
RPN1	P04843	l,o
RPN2	P04844	l,o
RPRD1B	Q9NQG5	l
RPS10P5	Q9NQ39	l
RPS11	P62280	l
RPS12	P25398	l
RPS13	P62277	l,o
RPS14	P62263	l,o
RPS15A	P62244	l,o
RPS16	P62249	l,o
RPS17	P08708	l,o
RPS18	P62269	l,o
RPS19	P39019	l,o
RPS2	P15880	l,o
RPS20	P60866	l,o

RPS21	P63220	l,o
RPS23	P62266	o
RPS24	P62847	l,o
RPS25	P62851	l,o
RPS26P11	Q5JNZ5	l
RPS27	P42677	l,o
RPS27L	Q71UM5	o
RPS28	P62857	l,o
RPS3	P23396	l,o
RPS3A	P61247	l,o
RPS4X	P62701	l,o
RPS5	P46782	l
RPS6	P62753	l,o
RPS6KA1	Q15418	l
RPS6KA3	P51812	l
RPS7	P62081	l,o
RPS8	P62241	l,o
RPS9	P46781	l,o
RPSA	P08865	l,o
RRAD	P55042	l
RRAS2	P62070	o,h
RRBP1	Q9P2E9	o,l
RSF1	Q96T23	k
RSL1D1	O76021	o
RSPH1	Q8WYR4	l
RSPH3	Q86UC2	l
RSPH4A	Q5TD94	l
RSPH9	Q9H1X1	l
RSU1	Q15404	l

RTCA	O00442	l
RTCB	Q9Y3I0	l
RTN3	O95197	o,l
RTN4	Q9NQC3	o,l
RTRAF	Q9Y224	l
RUNX2	Q13950	s
RUVBL1	Q9Y265	s,r,o,l
RUVBL2	Q9Y230	o,l
S100A10	P60903	o,l
S100A11	P31949	s,r,o,e,l,a
S100A12	P80511	s,r,l
S100A13	Q99584	l
S100A14	Q9HCY8	l,o
S100A16	Q96FQ6	o
S100A2	P29034	l
S100A4	P26447	r,l,o
S100A6	P06703	s,r,o,l
S100A7	P31151	s,r,l,a
S100A8	P05109	c,f,u,s,r,n,p,t,l,o,a,t
S100A9	P06702	c,i,f,q,s,u,r,n,l,p,o,q,a
S100P	P25815	s,r,l,o
SAA1	P0DJI8	l
SAE1	Q9UBE0	l
SAFB	Q15424	o
SAFB2	Q14151	l
SAG	P10523	h
SAMD9	Q5K651	l
SAMHD1	Q9Y3Z3	r,s,l,o
SAMM50	Q9Y512	o,l

SAR1A	Q9NR31	l
SAR1B	Q9Y6B6	l
SARG	Q9BW04	l
SARS	P49591	l
SART3	Q15020	l
SAXO2	Q658L1	l
SBDS	Q9Y3A5	l
SCAMP1	O15126	o
SCAMP2	O15127	o,l
SCAMP3	O14828	o
SCARB2	Q14108	l,o
SCCPDH	Q8NBX0	o,l
SCEL	O95171	o
SCFD1	Q8WVM8	l
SCGB1A1	P11684	q,s,r,k,q
SCGB1D1	O95968	k,s,r
SCGB1D2	O95969	k,s,r,l
SCGB2A1	O75556	f,s,r,k,l
SCGB2A2	Q13296	k,b
SCGN	O76038	h
SCIN	Q9Y6U3	l
SCLY	Q96I15	l
SCP2	P22307	l,o
SCPEP1	Q9HB40	l
SCRIB	Q14160	o
SCRN1	Q12765	l
SCRN2	Q96FV2	l
SDC1	P18827	o,l
SDC4	P31431	o,l

SDF4	G3V1E2	l
SDHA	P31040	o,l
SDHB	P21912	l
SDR39U1	Q9NRG7	l
SEC11A	P67812	o
SEC11C	Q9BY50	o
SEC13	P55735	l
SEC14L2	O76054	l
SEC14L3	Q9UDX4	l
SEC16A	O15027	l,o
SEC22B	O75396	o,l
SEC23A	Q15436	l
SEC23B	Q15437	l
SEC23IP	Q9Y6Y8	o,l
SEC24A	O95486	l
SEC24C	P53992	o,l
SEC24D	O94855	l
SEC31A	O94979	l
SEC61A1	P61619	o
SEC62	Q99442	o
SEC63	Q9UGP8	o
SEL1L3	Q68CR1	s
SELENBP1	Q13228	c,r,s,o,l,p,e
SELENOS	Q9BQE4	o
SEMG1	P04279	a
SEMG2	Q02383	a
SEPHS1	P49903	l
SEPHS2	Q99611	l
SEPTIN10	Q9P0V9	l

SEPTIN11	Q9NVA2	l
SEPTIN2	Q15019	o,h,l
SEPTIN6	Q14141	l
SEPTIN7	Q16181	l
SEPTIN8	Q92599	l
SEPTIN9	Q9UHD8	o,l
SERBP1	Q8NC51	l
SERINC1	Q9NRX5	o
SERPINA1	P01009	f,b,c,s,r,k,n,j,p,l,o,a,j
SERPINA3	P01011	s,r,k,l,a
SERPINA4	P29622	l
SERPINA6	P08185	l
SERPINB1	P30740	s,r,n,p,l,o
SERPINB10	P48595	l
SERPINB12	Q96P63	a
SERPINB13	Q9UIV8	l
SERPINB2	P05120	p,l,h
SERPINB3	P29508	s,r,b,c,m,p,l,e,o,a
SERPINB4	P48594	s,l,o,a,d
SERPINB5	P36952	o,l
SERPINB6	P35237	l
SERPINB9	P50453	l
SERPINC1	P01008	r,l
SERPIND1	P05546	l
SERPINF1	P36955	l
SERPINF2	P08697	l
SERPING1	P05155	l
SET	Q01105	s,l,o
SF3A1	Q15459	l
SF3A3	Q12874	l,o
SF3B1	O75533	o,l
SF3B2	Q13435	l
SF3B3	Q15393	l,o
SFN	P31947	s,n,l,o,p,a
SFPQ	P23246	o,l
SFXN1	Q9H9B4	o
SFXN2	Q96NB2	o
SFXN3	Q9BWM7	l,o
SFXN4	Q6P4A7	o
SGPL1	O95470	o
SGTA	O43765	l
SH2D4A	Q9H788	l
SH3BGRL	O75368	l,o
SH3BGRL2	Q9UJC5	l
SH3BGRL3	Q9H299	s,l
SH3GLB1	Q9Y371	l
SH3GLB2	Q9NR46	l
SHMT1	P34896	l
SHMT2	P34897	o
SHPK	Q9UHJ6	l
SHTN1	A0MZ66	l
SIGIRR	Q6IA17	o
SKIV2L	Q15477	l
SKP1	P63208	l
SLC12A2	P55011	l,o
SLC12A6	H0YMQ9	h,o
SLC12A7	Q9Y666	o
SLC16A1	P53985	o

SLC16A3	O15427	o
SLC16A6	O15403	s
SLC1A4	P43007	o
SLC1A5	Q15758	o
SLC22A18	Q96BI1	o
SLC22A4	Q9H015	o
SLC25A1	P53007	o,l
SLC25A10	Q9UBX3	o
SLC25A11	Q02978	l,o
SLC25A12	O75746	o,l
SLC25A13	Q9UJS0	l,o
SLC25A17	O43808	o
SLC25A20	O43772	o
SLC25A22	Q9H936	o
SLC25A24	Q6NUK1	l
SLC25A3	Q00325	l,o
SLC25A4	P12235	l,o
SLC25A5	P05141	l,o
SLC25A6	P12236	l,l,o,o
SLC27A1	Q6PCB7	o
SLC27A2	O14975	o,l
SLC27A3	Q5K4L6	o
SLC27A4	Q6P1M0	o
SLC2A1	P11166	o
SLC2A14	Q8TDB8	o
SLC33A1	O00400	o
SLC35A1	P78382	o
SLC35A3	Q9Y2D2	o
SLC35B2	Q8TB61	o
SLC35F6	Q8N357	o
SLC37A4	O43826	o
SLC3A2	P08195	o
SLC44A1	Q8WWI5	o
SLC44A2	Q8IWA5	o
SLC44A4	Q53GD3	o
SLC4A1	P02730	l,o
SLC4A4	Q9Y6R1	o
SLC5A1	P13866	o
SLC6A14	Q9UN76	o
SLC9A1	P19634	o
SLC9A3R1	O14745	l,o
SLK	Q9H2G2	l
SLPI	P03973	s,r,k,q,c,l,q
SMAD9	O15198	l
SMAP2	Q8WU79	l
SMARCA2	P51531	o
SMARCA5	O60264	o
SMARCC1	Q92922	s
SMC1A	Q14683	o,l
SMC3	Q9UQE7	o,l
SMPD2	O60906	o,l
SMPD3	Q9NY59	o
SMPD4	Q9NXE4	o
SMR3B	P02814	k
SMS	P52788	l
SMU1	Q2TAY7	l
SMYD5	Q6GMV2	l
SNAP23	O00161	o

SNAP91	O60641	l
SNCA	P37840	l
SNCG	O76070	l
SND1	Q7KZF4	o,l
SNRNP200	O75643	o,l
SNRNP40	Q96DI7	l
SNRNP70	P08621	o,l
SNRPA	P09012	l
SNRPA1	P09661	l
SNRPB	P14678	l
SNRPD1	P62314	s,l
SNRPD2	P62316	l
SNRPD3	P62318	l,o
SNRPE	P62304	l
SNRPF	P62306	l,o
SNU13	P55769	l
SNX11	Q9Y5W9	h
SNX16	P57768	h
SNX2	O60749	l
SNX3	O60493	l
SNX5	Q9Y5X3	l
SNX6	Q9UNH7	l
SOAT1	P35610	o
SOD1	P00441	c,s,r,o,j,p,l,j
SOD2	P04179	m,m,o,o,l,l
SOD3	P08294	h,l
SORD	Q00796	r,o,l
SORL1	Q92673	o
SP100	P23497	l

SPA17	Q15506	l
SPACA9	Q96E40	l
SPAG6	O75602	o,l
SPAG9	O60271	l
SPATA18	Q8TC71	o,l
SPATA6	Q9NWH7	l
SPCS1	Q9Y6A9	o
SPCS2	Q15005	o
SPCS3	P61009	o
SPEN	Q96T58	o
SPNS1	Q9H2V7	b
SPR	P35270	l
SPRR1A	P35321	r,l,a
SPRR1B	P22528	s,r,l,a
SPRR2B	P35325	r,a
SPRR3	Q9UBC9	r,l
SPTAN1	Q13813	l,o
SPTBN1	Q01082	o,l
SPTBN2	O15020	l,o
SQOR	Q9Y6N5	o,l
SRI	P30626	l,m
SRP14	P37108	l
SRP68	Q9UHB9	o,l
SRP72	O76094	l
SRPRA	P08240	o
SRPRB	Q9Y5M8	o
SRRM1	Q8IYB3	l
SRRM2	Q9UQ35	o
SRRT	Q9BXP5	l

SRSF1	Q07955	l,o
SRSF10	O75494	l
SRSF11	Q05519	l
SRSF2	Q01130	l,o
SRSF3	P84103	o,l
SRSF5	Q13243	l
SRSF7	Q16629	l,o
SSB	P05455	o,l
SSBP1	Q04837	l
SSH3	Q8TE77	l
SSR1	P43307	o,l
SSR3	Q9UNL2	o
SSR4	P51571	o,l
SSRP1	Q08945	l
ST13	P50502	o,l
ST14	Q9Y5Y6	o
ST3GAL4	Q11206	o
STARD10	Q9Y365	l
STAT1	P42224	l
STAT2	P52630	l
STAT3	P40763	o,l
STAT6	P42226	l
STATH	P02808	s,r,f,i,l
STAU1	O95793	l
STIM1	Q13586	o
STIM2	Q9P246	o
STIP1	P31948	c,o,l
STK24	Q9Y6E0	l
STK33	Q9BYT3	l
STK38	Q15208	l
STK39	Q9UEW8	l
STK4	Q13043	h
STMN1	P16949	l
STOM	P27105	o
STOML2	Q9UJZ1	o,l
STOML3	Q8TAV4	o
STRAP	Q9Y3F4	l
STS	P08842	o
STT3A	P46977	l,o
STT3B	Q8TCJ2	o
STX11	O75558	h
STX12	Q86Y82	o
STX18	Q9P2W9	o
STX4	Q12846	o
STX5	Q13190	o
STX7	O15400	o
STX8	Q9UNK0	o
STXBP3	O00186	o
SUB1	P53999	l
SUCLA2	Q9P2R7	o,l
SUCLG1	P53597	o,l
SUCLG2	Q96I99	o,l
SUGT1	Q9Y2Z0	l
SULT1A2	P50226	l
SULT1A3	P0DMM9	l
SULT2A1	Q06520	h
SUMF2	Q8NBJ7	l
SUN1	O94901	o

SUN2	Q9UH99	o
SURF1	Q15526	o
SURF4	O15260	l,o
SVIL	O95425	s
SWAP70	Q9UH65	l
SYNCRIP	O60506	l,o
SYNE1	Q8NF91	b,l,o
SYNE2	Q8WXH0	o,l
SYNGR1	O43759	o
SYNGR2	O43760	o
SYNJ2BP	P57105	o
SYPL1	Q16563	l
SYTL1	Q8IYJ3	l
SYVN1	Q86TM6	o
TACC2	O95359	l
TACSTD2	P09758	o,l
TAF15	Q92804	l
TAGLN2	P37802	s,r,o,l
TALDO1	P37837	s,r,l,o
TAOK1	Q7L7X3	g
TAP1	Q03518	o
TAP2	Q03519	l,o
TAPBP	O15533	o,l
TAPBPL	Q9BX59	o
TARDBP	Q13148	l
TARS	P26639	l
TAX1BP3	O14907	l
TBC1D1	Q86TI0	l,o
TBC1D15	Q8TC07	l

TBCA	O75347	l
TBCB	Q99426	l
TBCD	Q9BTW9	l
TBL2	Q9Y4P3	o
TCERG1	O14776	l
TCF3	P15923	i,f
TCIRG1	Q13488	o
TCN1	P20061	b,s,r,k,l
TCOF1	Q13428	o
TCP1	P17987	o,l
TECR	Q9NZ01	o,l
TEKT1	Q969V4	l
TEKT2	Q9UIF3	l
TERT	O14746	h
TES	Q9UGI8	l
TEX10	Q9NXF1	o
TF	P02787	s,r,k,q,i,b,c,p,l,o,a,q
TFAM	Q00059	l
TFF3	Q07654	s,r,l
TFG	Q92734	l
TFRC	P02786	o
TGM2	P21980	l,o
TGM3	Q08188	p,a
TGOLN2	O43493	o
THOP1	P52888	l
THRAP3	Q9Y2W1	o,l
THUMPD1	Q9NXG2	l
THYN1	Q9P016	l
TIGAR	Q9NQ88	l

TIMM17B	O60830	o
TIMM50	Q3ZCQ8	l,o
TIMMDC1	Q9NPL8	o
TIMP1	P01033	s,r,k,l
TIPRL	O75663	l
TJP2	Q9UDY2	o,l
TJP3	O95049	o,l
TKFC	Q3LXA3	l
TKT	P29401	s,r,k,o,l,g
TLN1	Q9Y490	l,o
TLR3	O15455	o
TM7SF2	O76062	o
TM9SF1	O15321	o
TM9SF2	Q99805	o,l
TM9SF3	Q9HD45	o,l
TM9SF4	Q92544	o
TMBIM6	P55061	o
TMCO1	Q9UM00	o
TMED1	Q13445	o
TMED10	P49755	l,o
TMED2	Q15363	o
TMED4	Q7Z7H5	o
TMED7	Q9Y3B3	l,o
TMED9	Q9BVK6	o,l
TMEM109	Q9BVC6	o
TMEM126A	Q9H061	o
TMEM128	Q5BJH2	o
TMEM14C	Q9P0S9	o
TMEM165	Q9HC07	o
TMEM173	Q86WV6	l,o
TMEM200C	A6NKL6	s
TMEM205	Q6UW68	l
TMEM231	Q9H6L2	l
TMEM245	Q9H330	o
TMEM259	Q4ZIN3	o
TMEM30A	Q9NV96	o
TMEM30B	Q3MIR4	o
TMEM33	P57088	o
TMEM63A	O94886	o
TMEM63B	Q5T3F8	o
TMEM65	Q6PI78	o
TMEM67	Q5HYA8	o
TMOD3	Q9NYL9	l
TMPO	P42166	o,l
TMPRSS11D	O60235	o
TMPRSS4	Q9NRS4	o
TMSB4X	P62328	s,r,l,o
TMTC3	Q6ZXV5	o
TMUB1	Q9BVT8	o
TMX1	Q9H3N1	o,l
TMX3	Q96JJ7	o
TMX4	Q9H1E5	o
TNC	P24821	l
TNFAIP8	O95379	l
TNIK	Q9UKE5	l
TNPO1	Q92973	l
TNXB	P22105	s
TOM1	O60784	l

TOMM22	Q9NS69	o
TOMM34	Q15785	l
TOMM40	O96008	o
TOMM70	O94826	l,o
TOP2B	Q02880	o
TOR1AIP1	Q5JTV8	o,l
TP53I3	Q53FA7	l
TP53RK	Q96S44	l
TPBG	Q13641	o
TPD52	P55327	l
TPD52L2	O43399	l
TPI1	P60174	n,c,s,r,l,o,a
TPM1	P09493	o,j,p,j
TPM3	P06753	c,r,s,o,m,l
TPM4	P67936	o,p,l
TPMT	P51580	l
TPP1	O14773	o,l
TPP2	P29144	l
TPPP	O94811	l
TPPP3	Q9BW30	r,s,o,l
TPR	P12270	l
TPRKB	Q9Y3C4	l
TPT1	P13693	j,p,l,o,j
TRA2A	Q13595	l
TRA2B	P62995	l
TRADD	Q15628	l
TRAM1	Q15629	o
TRANK1	O15050	l
TRAPPC3	O43617	l

TRBC1	P01850	h
TRBV16	A0A087WV62	h
TRIM2	Q9C040	l
TRIM25	Q14258	l
TRIM28	Q13263	l,o
TRIM29	Q14134	o,l
TRIM56	Q9BRZ2	o
TRIP11	Q15643	o
TRIP12	Q14669	o
TRIP6	Q15654	l
TRMT112	Q9UI30	l
TRMT12	Q53H54	m
TRMT61A	Q96FX7	l
TRPM4	Q8TD43	o
TSC22D1	Q15714	l
TSG101	Q99816	l
TSGA10	Q9BZW7	l
TSN	Q15631	l
TSNAX	Q99598	l
TSPAN1	O60635	s,l
TSPAN3	O60637	o
TST	Q16762	o,l
TSTA3	Q13630	l,p
TSTD1	Q8NFU3	l
TTBK1	Q5TCY1	b
TTC21A	Q8NDW8	l
TTC25	Q96NG3	l
TTC26	A0AVF1	l
TTLL12	Q14166	l

TTN	Q8WZ42	s,r,o,l
TTR	P02766	r,s,i,l,j,j
TUBA1A	Q71U36	s,l,o,a
TUBA1B	P68363	s,r,c,m,l
TUBA1C	Q9BQE3	c,m
TUBA4A	P68366	c,l
TUBA8	Q9NY65	c
TUBB	P07437	s,c,m,l,o
TUBB1	Q9H4B7	o
TUBB2B	Q9BVA1	l
TUBB3	Q13509	l
TUBB4A	P04350	s,l
TUBB4B	P68371	r,s,o
TUBB6	Q9BUF5	l
TUBB8	Q3ZCM7	l
TUFM	P49411	c,m,l,o
TUSC3	Q13454	o
TWF1	Q12792	l
TWF2	Q6IBS0	l
TXN	P10599	s,r,o,l,p,e
TXN2	Q99757	l
TXNDC12	O95881	l
TXNDC17	Q9BRA2	l
TXNDC5	Q8NBS9	j,l,j
TXNL1	O43396	l
TXNRD1	Q16881	r,s,l
TXNRD2	Q9NNW7	l
TYMP	P19971	s,r,o,l
U2AF1	Q01081	o
U2AF1L4	Q8WU68	l
U2AF2	P26368	l
UAP1	Q16222	l
UBA1	P22314	s,r,o,l
UBA2	Q9UBT2	l
UBA3	Q8TBC4	l
UBA5	Q9GZZ9	l
UBA52	P62987	l
UBA6	A0AVT1	l
UBC	P0CG48	s,o,a
UBE2A	P49459	l
UBE2D3	P61077	l
UBE2I	P63279	l
UBE2K	P61086	l
UBE2L3	P68036	l
UBE2L6	O14933	l
UBE2M	P61081	l
UBE2N	P61088	o,l
UBE2O	Q9C0C9	l
UBE2V1	Q13404	l
UBLCP1	Q8WVY7	l
UBQLN1	Q9UMX0	l
UBR4	Q5T4S7	l
UBXN1	Q04323	l
UBXN11	Q5T124	l
UBXN4	Q92575	o
UBXN6	Q9BZV1	l
UCHL3	P15374	l
UCHL5	Q9Y5K5	l

UFC1	Q9Y3C8	l
UFD1	Q92890	l
UFL1	O94874	l,o
UFM1	P61960	l
UGDH	O60701	s,o,l
UGGT1	Q9NYU2	o,l
UGP2	Q16851	l
UGT1A6	P19224	o
UGT2A1	Q9Y4X1	o,l
UMPS	P11172	l
UNC93B1	Q9H1C4	o
UPF1	Q92900	l
UQCR10	Q9UDW1	l
UQCRB	P14927	l,o
UQCRC1	P31930	c,l,o,j,j
UQCRC2	P22695	l,o
UQCRFS1	P47985	o
UQCRFS1P1	P0C7P4	l
UQCRH	P07919	l
UQCRQ	O14949	o
URB2	Q14146	b
UROD	P06132	l
USO1	O60763	l
USP14	P54578	l
USP5	P45974	l,t,o,t
USP7	Q93009	l
USP9X	Q93008	l,o
UTRN	P46939	o,l
VAMP2	P63027	o
VAMP8	Q9BV40	o,l
VANGL1	Q8TAA9	o
VAPA	Q9P0L0	o,l
VAPB	O95292	l
VARS	P26640	l,o
VASP	P50552	o,l
VAT1	Q99536	l,o
VBP1	P61758	l
VCL	P18206	o,l
VCP	P55072	r,c,s,l,o
VDAC1	P21796	o,l
VDAC2	P45880	o,l
VDAC3	Q9Y277	o,l
VILL	O15195	l
VIM	P08670	s,r,o,l,a
VMO1	Q7Z5L0	l
VPS13C	Q709C8	l,o
VPS26A	O75436	l
VPS29	Q9UBQ0	l
VPS35	Q96QK1	l
VPS36	Q86VN1	l
VPS4A	Q9UN37	l
VPS4B	O75351	l
VPS9D1	Q9Y2B5	o
VTA1	Q9NP79	l
VTI1B	Q9UEU0	o
VTN	P04004	l
VWA5A	O00534	l
WARS	P23381	r,l,p,o

WASF2	Q9Y6W5	l
WASHC2A	Q641Q2	l
WASHC4	Q2M389	l
WDR1	O75083	o,l
WDR13	Q9H1Z4	l
WDR54	Q9H977	l
WDR61	Q9GZS3	l
WDR77	Q9BQA1	l
WDR92	Q96MX6	l
WFDC2	Q14508	s,r,k,l
WFS1	O76024	o
WHAMM	Q8TF30	l
WRB	O00258	o
XDH	P47989	l
XPNPEP1	Q9NQW7	l
XPO1	O14980	l
XPO7	Q9UIA9	l
XRCC5	P13010	o,l
XRCC6	P12956	o,l
XRN2	Q9H0D6	l
YARS	P54577	l
YARS2	Q9Y2Z4	o
YBX1	P67809	o
YBX3	P16989	o,l
YIF1A	O95070	o
YIPF3	Q9GZM5	o
YIPF6	Q96EC8	o
YME1L1	Q96TA2	o
YWHAB	P31946	s,o
YWHAE	P62258	s,o,l,p
YWHAG	P61981	s,o,l
YWHAH	Q04917	o,l
YWHAQ	P27348	s,l,o
YWHAZ	P63104	s,r,o,l,p,a
ZC3H15	Q8WU90	l
ZDHHC13	Q8IUH4	o
ZFAND1	Q8TCF1	l
ZFP2	Q6ZN57	m
ZG16B	Q96DA0	k,b,s,r,l
ZMPSTE24	O75844	l,o
ZMYND10	O75800	l
ZNF106	Q9H2Y7	s
ZNF165	P49910	s
ZNF185	O15231	o,l
ZNF207	O43670	l
ZNF263	O14978	s
ZNF609	O15014	g
ZSCAN31	Q96LW9	h
ZW10	O43264	l

Studies

	Author	Title
a	Benson et al.	Extensive fractionation and identification of Proteins within nasal lavage fluids from allergic rhinitis and asthmatic chronic rhinosinusitis patients
b	Casado et al.	Identification of human nasal mucous proteins using proteomics
c	Debat et al.	Identification of human olfactory cleft mucus proteins using proteomic analysis
d	Farajzadeh Deroee et al.	Regression of polypoid nasal mucosa after systemic corticosteroid therapy: a proteomics study
e	Gelardi et al.	Proteomic analysis of human nasal mucosa: different expression profile in rhino-pathologic states
f	Ghafouri et al.	Comparative proteomics of nasal fluid in seasonal allergic rhinitis
g	Kim et al.	Fatty acid binding protein 1 is related with development of aspirin-exacerbated respiratory disease
h	Lee et al.	Proteomic analysis of normal human nasal mucosa: Establishment of a two-dimensional electrophoresis reference map
i	Lindahl et al.	Nasal lavage fluid and proteomics as means to identify the effects of the irritating epoxy chemical dimethylbenzylamine
j	Min-Man et al.	Differential proteomic analysis of nasal polyps, chronic sinusitis, and normal nasal mucosa tissues
k	Mortstedt et al.	Screening method using selected reaction monitoring for targeted proteomics studies of nasal lavage fluid
l	Ndika J et al.	Epithelial proteome profiling suggests the essential role of interferon-inducible proteins in patients with allergic rhinitis
m	Roxo-Rosa et al.	Proteomic analysis of nasal cells from cystic fibrosis patients and non-cystic fibrosis control individuals: search for novel biomarkers of cystic fibrosis lung disease
n	Schoenebeck et al.	Improved preparation of nasal lavage fluid (NLF) as a non-invasive sample for proteomic biomarker discovery
o	Simoes et al.	Molecular profiling of the human nasal epithelium: A proteomics approach
p	Suojalehto et al.	Nasal protein profiles in work-related asthma caused by different exposures
q	Tewfik et al.	Proteomics of nasal mucus in chronic rhinosinusitis
r	Tomazic et al.	Nasal mucus proteomic changes reflect altered immune responses and epithelial permeability in patients with allergic rhinitis
s	Tomazic et al.	Seasonal proteome changes of nasal mucus reflect perennial inflammatory response and reduced defence mechanisms and plasticity in allergic rhinitis
t	Upton DC et al.	Chronic rhinosinusitis with nasal polyps: a proteomic analysis
u	Wahlen et al.	Protein profiles of nasal lavage fluid from individuals with work-related upper airway symptoms associated with mouldy and damp buildings

SUPPLEMENTARY TABLE 7.2. STUDY DEMOGRAPHICS

Author	Patient Selection	Diagnostic Criteria	Comorbidities	Smoking	Oral Steroid
Benson et al.	NR	NR	Asthma	0	0
Casado et al.	Outpatient Clinic	Clinical symptoms (Facial pain, tenderness, mucopurulent discharge)	0	NR	0
Debat et al.	Hospital Clinic	Nasoendoscopy	0	0	0
Ghafouri et al.	NR	Nasal symptoms scores Nasoendoscopy	0	0	0
Lindahl et al.	NR	Nasoendoscopy	DMBA exposure	0	NR
Mortstedt et al.	NR	NR	NR	NR	NR
Schoenebeck et al.	NR	NR	0	NR	NR
Tewfik et al.	Outpatient Clinic	Nasoendoscopy CT Sinuses (Sinus Health Allergy Partnership criteria)	0	0	0
Tomazic et al.	NR	Nasoendoscopy (EPOS Criteria)	0	NR	0
Tomazic et al.	NR	Nasoendoscopy (EPOS Criteria)	0	0	0
Wahlen et al.	NR	NR	0	0	NR
Farajzadeh Deroee et al.	Hospital Clinic	Nasoendoscopy	0	0	3
Gelardi et al.	Hospital Clinic	Clinical symptoms Nasoendoscopy	0	NR	NR
Kim et al.	NR	Clinical symptoms Nasoendoscopy CT Sinuses	Asthma ATA 8 AERD 5	ATA 2	0
Lee et al.	NR	Clinical symptoms Nasoendoscopy	0	NR	0
Min-Man et al.	Hospital Clinic	Nasoendoscopy CT Sinuses	0	NR	0
Ndika J et al.	Hospital Clinic	Seasonal allergy symptoms questionnaire	0	0	NR
Roxo-Rosa et al.	NR	Clinical symptoms	0	0	0
Simoes et al.	NR	NR	NR	NR	NR
Suojalehto et al.	Hospital Clinic	NR	0	0	NR
Upton DC et al.	Outpatient Clinic	Nasoendoscopy CT Sinuses (AAO-HNS CRS TF criteria)	NR	0	3

AAO-HNS: American Academy of Otolaryngology-Head and Neck Surgery Chronic Rhinosinusitis Task Force; ATA: Aspirin-tolerant asthma; AERD: Aspirin-exacerbated respiratory disease; DMBA: Dimethylbenzylamine; EPOS: European Position Paper on Chronic Rhinosinusitis and Nasal Polyps; NR: Not reported.

SUPPLEMENTARY TABLE 7.3. CELLULAR PATHWAYS, CELLULAR COMPONENTS/ BIOLOGICAL PROCESSES/ MOLECULAR FUNCTIONS

Cellular Pathways

Pathway	Classification	Source	Genes	Adjusted P-value
Antigen activates B Cell Receptor (BCR) leading to generation of second messengers_Homo sapiens_R-HSA-983695	Immune system	Mucus CRS	IGHM;IGKC;IGHV3-23;IGLC1;CALM1	0.00148
Apoptosis_Homo sapiens_R-HSA-109581	Programmed cell death	Mucus CRS	DSP;UBC;LMNA;PKP1;DSG1;SFN;VIM;YWHAZ	0.00152
Apoptotic cleavage of cell adhesion proteins_Homo sapiens_R-HSA-351906	Programmed cell death	Mucus CRS	DSP;DSG1;PKP1	0.00373
Apoptotic cleavage of cellular proteins_Homo sapiens_R-HSA-111465	Programmed cell death	Mucus CRS	DSP;LMNA;DSG1;PKP1;VIM	0.00054
Apoptotic execution phase_Homo sapiens_R-HSA-75153	Programmed cell death	Mucus CRS	DSP;LMNA;DSG1;PKP1;VIM	0.00199
Binding and Uptake of Ligands by Scavenger Receptors_Homo sapiens_R-HSA-2173782	Vesicle-mediated transport	Mucus CRS	COL1A1;COL1A2;IGKC;IGHV3-23;HP;IGLC1;HBA1;HPR;IGHA2	0
Binding and Uptake of Ligands by Scavenger Receptors_Homo sapiens_R-HSA-2173782	Vesicle-mediated transport	Mucus Healthy Mucus CRS	IGKV1-5;ALB;HBB;IGHA1	0.00017
CD22 mediated BCR regulation_Homo sapiens_R-HSA-5690714	Immune system	Mucus CRS	IGHM;IGKC;IGHV3-23;IGLC1	0.00059
Classical antibody-mediated complement activation_Homo sapiens_R-HSA-173623	Immune system	Mucus CRS	IGHG3;IGHG4;IGHG1;IGHG2;IGKC;IGHV3-23;IGLC1	0.00001

Complement cascade_Homo sapiens_R-HSA-166658	Immune system	Mucus CRS	IGHG3;IGHG4;IGHG1;IGHG2;IGKC;IGHV3-23;IGLC1	0.00017
Creation of C4 and C2 activators_Homo sapiens_R-HSA-166786	Immune system	Mucus CRS	IGHG3;IGHG4;IGHG1;IGHG2;IGKC;IGHV3-23;IGLC1	0.00001
Detoxification of Reactive Oxygen Species_Homo sapiens_R-HSA-3299685	Cellular responses to external stimuli	Mucosa Healthy Mucosa CRS	PRDX2;CAT;SOD1	0.02341
Diseases associated with visual transduction_Homo sapiens_R-HSA-2474795	Disease	Mucosa Healthy Mucosa CRS	RBP4;TTR	0.02021
FCERI mediated Ca+2 mobilization_Homo sapiens_R-HSA-2871809	Immune system	Mucus CRS	IGKC;IGHV3-23;IGLC1;CALM1	0.04948
Fcgamma receptor (FCGR) dependent phagocytosis_Homo sapiens_R-HSA-2029480	Immune system	Mucus CRS	IGHG3;IGHG4;IGHG1;IGHG2;IGKC;IGHV3-23;MYH9;IGLC1;ACTB	0.00003
FCGR activation_Homo sapiens_R-HSA-2029481	Immune system	Mucus CRS	IGHG3;IGHG4;IGHG1;IGHG2;IGKC;IGHV3-23;IGLC1	0.00001
Gluconeogenesis_Homo sapiens_R-HSA-70263	Metabolism	Mucus CRS	TPI1;ENO1;ALDOA;GAPDH	0.00462
Glucose metabolism_Homo sapiens_R-HSA-70326	Metabolism	Mucus CRS	TPI1;PKM;UBC;ENO1;ALDOA;CALM1;GAPDH	0.00017
Glycolysis_Homo sapiens_R-HSA-70171	Metabolism	Mucus CRS	TPI1;PKM;ENO1;ALDOA;GAPDH	0.00028
Initial triggering of complement_Homo sapiens_R-HSA-166663	Immune system	Mucus CRS	IGHG3;IGHG4;IGHG1;IGHG2;IGKC;IGHV3-23;IGLC1	0.00003
Metabolism of carbohydrates_Homo sapiens_R-HSA-71387	Metabolism	Mucus CRS	TPI1;PKM;AMY2B;UBC;ENO1;CALM1;ALDOA;GAPDH	0.04885
Metabolism of fat-soluble vitamins_Homo sapiens_R-HSA-6806667	Metabolism	Mucosa Healthy Mucosa CRS	RBP4;TTR;APOA1	0.02495

Metabolism_Homo sapiens_R-HSA-1430728	Metabolism	Mucosa Healthy Mucosa CRS	ECHS1;APOA1;NME4;PDHB;CA1;RBP4;TTR;NDUFS8;ALDH1A1;CAT;CMPK1;UQCRC1;PSME1;GAPDH	0.00556
Platelet degranulation_Homo sapiens_R-HSA-114608	Homeostasis	Mucosa Healthy Mucosa CRS	SERPINA1;FGG;APOA1;SOD1	0.02114
Platelet degranulation_Homo sapiens_R-HSA-114608	Homeostasis	Mucus CRS	SERPINA3;SERPINA1;AHSG;CALM1;ALDOA	0.04631
Platelet degranulation_Homo sapiens_R-HSA-114608	Homeostasis	Mucus Healthy Mucus CRS	ORM1;TF;ALB	0.03116
Programmed Cell Death_Homo sapiens_R-HSA-5357801	Programmed cell death	Mucus CRS	DSP;UBC;LMNA;PKP1;DSG1;SFN;VIM;YWHAZ	0.00155
Regulation of actin dynamics for phagocytic cup formation_Homo sapiens_R-HSA-2029482	Immune system	Mucus CRS	IGHG3;IGHG4;IGHG1;IGHG2;IGKC;IGHV3-23;MYH9;IGLC1;ACTB	0.00001
Response to elevated platelet cytosolic Ca2+_Homo sapiens_R-HSA-76005	Homeostasis	Mucosa Healthy Mucosa CRS	SERPINA1;FGG;APOA1;SOD1	0.01902
Response to elevated platelet cytosolic Ca2+_Homo sapiens_R-HSA-76005	Homeostasis	Mucus Healthy Mucus CRS	ORM1;TF;ALB	0.02685
Retinoid cycle disease events_Homo sapiens_R-HSA-2453864	Disease	Mucosa Healthy Mucosa CRS	RBP4;TTR	0.02274
Retinoid metabolism and transport_Homo sapiens_R-HSA-975634	Metabolism, Signal transduction	Mucosa Healthy Mucosa CRS	RBP4;TTR;APOA1	0.01948
RHO GTPases activate PKNs_Homo sapiens_R-HSA-5625740	Signal transduction	Mucus CRS	HIST1H4A;MYH9;SFN;YWHAZ	0.04735
Role of phospholipids in phagocytosis_Homo sapiens_R-HSA-2029485	Immune system	Mucus CRS	IGHG3;IGHG4;IGHG1;IGHG2;IGKC;IGHV3-23;IGLC1	0.00003

Scavenging of heme from plasma_Homo sapiens_R-HSA-2168880	Vesicle-mediated transport	Mucus CRS	IGKC;IGHV3-23;HP;IGLC1;HPR;HBA1;IGHA2	0.00001
Scavenging of heme from plasma_Homo sapiens_R-HSA-2168880	Vesicle-mediated transport	Mucus Healthy Mucus CRS	IGKV1-5;ALB;HBB;IGHA1	0.00005
Signal Transduction_Homo sapiens_R-HSA-162582	Signal transduction	Mucosa Healthy Mucosa CRS	ANXA1;FGG;PEBP1;APOA1;PDHB;ACTB;ACTG1;ADCYAP1;RBP4;TTR;ARHGDIA;ARHGDIB;ALDH1A1;PSME1	0.01752
Translocation of GLUT4 to the plasma membrane_Homo sapiens_R-HSA-1445148	Vesicle-mediated transport	Mucus CRS	MYH13;SFN;CALM1;YWHAZ	0.0494
Vesicle-mediated transport_Homo sapiens_R-HSA-5653656	Vesicle-mediated transport	Mucus CRS	SERPINA1;IGHV3-23;HP;HPR;HBA1;YWHAZ;COL1A1;COL1A2;IGKC;UBC;MYH13;SFN;IGLC1;CALM1;IGHA2	0.00017

CRS: Chronic rhinosinusitis.

Cellular Components

Cellular Component	Classification	Source	Genes	Adjusted P-value
actin filament (GO:0005884)	Cytoskeleton	Mucosa Healthy Mucosa CRS	ANXA1;TPM1;ACTG1	0.01684
azurophil granule (GO:0042582)	Secretory granule	Mucus CRS	SERPINB3;SERPINA3;PIGR;ANXA2;FABP5;DEFA1;S100A7;HRNR	0.00049
azurophil granule lumen (GO:0035578)	Secretory granule	Mucus CRS	SERPINB3;SERPINA3;ANXA2;FABP5;DEFA1;S100A7;HRNR	0.00014
cytoplasmic vesicle lumen (GO:0060205)	Cytoplasmic vesicle	Mucus CRS	EEF1A1;SERPINA3;CSTB;PKM;AHSG;GSTP1;HBA1;ALDOA;S100A8;S100A11	0
cytoplasmic vesicle lumen (GO:0060205)	Cytoplasmic vesicle	Mucus Healthy Mucus CRS	TF;HBB;S100A9	0.00735
cytoplasmic vesicle lumen (GO:0060205)	Cytoplasmic vesicle	Mucosa Healthy Mucosa CRS	CAT;APOA1;S100A8;HSP90B1	0.01417
cytoskeleton (GO:0005856)	Cytoskeleton	Mucus CRS	KRT4;JUP;HSPB1;KRT77;ACTB;TUBA1A;KRT17;KRT16;MYH9;VIM;ALDOA;GAPDH;S100A8	0.00232
cytoskeleton (GO:0005856)	Cytoskeleton	Mucosa Healthy Mucosa CRS	ARHGDIA;ARHGDIB;TPM1;KRT8;GAPDH;ACTB;S100A8;ACTG1	0.00089
endocytic vesicle lumen (GO:0071682)	Cytoplasmic vesicle	Mucus Healthy Mucus CRS	HBB;LTF	0.00593
endocytic vesicle lumen (GO:0071682)	Cytoplasmic vesicle	Mucosa Healthy Mucosa CRS	APOA1;HSP90B1	0.03186
ficolin-1-rich granule (GO:0101002)	Secretory granule	Mucus CRS	EEF1A1;DSP;CSTB;SERPINB12;SERPINA1;PKM;CALML5;JUP;GSTP1;PKP1;DSG1;ALDOA	0
ficolin-1-rich granule lumen (GO:1904813)	Secretory granule	Mucus CRS	EEF1A1;CSTB;SERPINA1;PKM;CALML5;JUP;GSTP1;ALDOA	0.00012
ficolin-1-rich granule membrane (GO:0101003)	Secretory granule	Mucus CRS	DSP;SERPINB12;DSG1;PKP1	0.025

focal adhesion (GO:0005925)	Adheren junction	Mucus CRS	ANXA1;JUP;HSPB1;MYH9;VIM;B2M;YWHAZ;ACTB;S100A7	0.0243
focal adhesion (GO:0005925)	Adheren junction	Mucosa CRS	HSPA9;ACTR3;HSPA5;IQGAP1;P4HB	0.00632
focal adhesion (GO:0005925)	Adheren junction	Mucosa Healthy Mucosa CRS	ANXA1;CAT;ACTB;HSP90B1;ACTG1	0.0357
intermediate filament (GO:0005882)	Cytoskeleton	Mucus CRS	KRT82;FLG;DSP;KRT4;KRT3;KRT2;KRT7;KRT5;KRT10;KRT76;KRT20;KRT84;KRT16;KRT14;PKP1;VIM;KRT6A	0
intermediate filament cytoskeleton (GO:0045111)	Cytoskeleton	Mucus CRS	DSP;FLG;KRT4;KRT3;KRT2;KRT7;KRT5;KRT76;KRT10;KRT20;KRT17;KRT16;KRT14;PKP1;VIM;S100A8;KRT6A	0
keratin filament (GO:0045095)	Cytoskeleton	Mucus CRS	KRT82;KRT4;KRT3;KRT14;KRT5;KRT84	0
mitochondrial matrix (GO:0005759)	Mitochondria	Mucosa CRS	HSPA9;ALDH4A1;RIDA;CPS1;HSPD1	0.00631
mitochondrion (GO:0005739)	Mitochondria	Mucosa Healthy Mucosa CRS	ECHS1;NDUFS8;CAT;UQCRC1;NME4;PDHB;PARK7;SOD1	0.04277
platelet alpha granule lumen (GO:0031093)	Secretory granule	Mucus CRS	SERPINA3;SERPINA1;AHSG;ALDOA	0.03316
polymeric cytoskeletal fiber (GO:0099513)	Cytoskeleton	Mucus CRS	FLG;DSP;ANXA1;KRT4;KRT3;KRT2;KRT7;KRT5;KRT76;KRT10;KRT20;TUBA1A;KRT16;KRT14;PKP1;VIM;KRT6A	0
polymeric cytoskeletal fiber (GO:0099513)	Cytoskeleton	Mucosa Healthy Mucosa CRS	ANXA1;TPM1;KRT8;ACTG1	0.04082
secretory granule lumen (GO:0034774)	Secretory granule	Mucus CRS	SERPINB3;SERPINA3;CSTB;SERPINA1;JUP;ANXA2;AHSG;GSTP1;DEFA1;HRNR;EEF1A1;PKM;FABP5;ALDOA;B2M;S100A8;S100A11;S100A7	0
secretory granule lumen (GO:0034774)	Secretory granule	Mucus Healthy Mucus CRS	ORM1;TF;SLPI;ALB;LYZ;S100A9;LTF	0
secretory granule lumen (GO:0034774)	Secretory granule	Mucosa Healthy Mucosa CRS	SERPINA1;TTR;FGG;CAT;APOA1;S100A8;TXNDC5	0.00073
specific granule (GO:0042581)	Secretory granule	Mucus Healthy Mucus CRS	ORM1;SLPI;LYZ;LTF	0.00057

specific granule lumen (GO:0035580)	Secretory granule	Mucus Healthy Mucus CRS	ORM1;SLPI;LYZ;LTF	0.00002
tertiary granule (GO:0070820)	Secretory granule	Mucus CRS	DSP;CSTB;SERPINB12;PKP1;DSG1;ALDOA;B2M	0.0047
tertiary granule (GO:0070820)	Secretory granule	Mucus Healthy Mucus CRS	ORM1;HBB;LYZ;LTF	0.00051
tertiary granule lumen (GO:1904724)	Secretory granule	Mucus Healthy Mucus CRS	ORM1;HBB;LYZ;LTF	0.00002
vacuolar lumen (GO:0005775)	Vacuole	Mucus CRS	SERPINB3;SERPINA3;ANXA2;FABP5;DEFA1;S100A7;HRNR	0.00454

CRS: Chronic rhinosinusitis.

Biological Processes

Biological Process	Classification	Source	Genes	Adjusted P-value
4-hydroxyproline metabolic process (GO:0019471)	Cellular metabolic process	Mucosa CRS	ALDH4A1;P4HB	0.02989
antibacterial humoral response (GO:0019731)	Immune system process	Mucus CRS	IGHM;BPIFA1;SEMG2;SEMG1;DEFA1;IGHA2	0.00004
antibacterial humoral response (GO:0019731)	Immune system process	Mucus Healthy Mucus CRS	SLPI;IGHA1;JCHAIN;LTF	0.00003
antigen receptor-mediated signaling pathway (GO:0050851)	Immune system process	Mucus CRS	IGHG3;IGHG4;IGHM;IGHG1;IGHG2;IGKC;IGHV3-23;UBC;IGLC1;IGHA2	0.00144
antimicrobial humoral immune response mediated by antimicrobial peptide (GO:0061844)	Immune system process	Mucus CRS	BPIFA1;SEMG1;DEFA1;GAPDH;KRT6A;S100A7	0.0002
ATP generation from ADP (GO:0006757)	Cellular metabolic process	Mucus CRS	LDHA;TPI1;PKM;ALDOA	0.00269
B cell receptor signaling pathway (GO:0050853)	Immune system process	Mucus CRS	IGHG3;IGHG4;IGHM;IGHG1;IGHG2;IGKC;IGHV3-23;IGLC1;IGHA2	0.00001
canonical glycolysis (GO:0061621)	Metabolic process	Mucus CRS	TPI1;PKM;ENO1;ALDOA;GAPDH	0.00016
carbohydrate catabolic process (GO:0016052)	Metabolic process	Mucus CRS	LDHA;TPI1;PKM;ALDOA	0.01105
cellular protein metabolic process (GO:0044267)	Cellular metabolic process	Mucus Healthy Mucus CRS	TF;BPIFB2;ALB;LYZ;LTF	0.01029
cellular response to oxidative stress (GO:0034599)	Cellular response to chemical stimulus	Mucosa Healthy Mucosa CRS	PRDX2;TPM1;CAT;PARK7;SOD1	0.00231

cellular response to superoxide (GO:0071451)	Cellular reponse to chemical stimulus	Mucosa Healthy Mucosa CRS	PRDX2;SOD1	0.04045
complement activation, classical pathway (GO:0006958)	Immune system process	Mucus CRS	IGHG3;IGHG4;IGHM;IGHG1;IGHG2;IGKC;IGHV3-23;IGLC1;IGHA2	0.00004
defense response to bacterium (GO:0042742)	Reponse to stimulus	Mucus CRS	IGHM;IGHV3-23;DEFA1;IGHG3;IGHG4;IGHG1;BPIFA1;IGHG2;IGKC;SEMG2;PRB3;SEMG1;IGLC1;IGHA2;LACRT;S100A8;KRT6A;S100A7	0
defense response to bacterium (GO:0042742)	Reponse to stimulus	Mucus Healthy Mucus CRS	SLPI;LYZ;IGHA1;S100A9;JCHAIN;LTF	0.00002
defense response to fungus (GO:0050832)	Reponse to stimulus	Mucus Healthy Mucus CRS	S100A9;LTF	0.02586
detection of chemical stimulus involved in sensory perception of bitter taste (GO:0001580)	Sensory perception	Mucus CRS	PIGR;AZGP1;PIP;CST4	0.01812
detection of chemical stimulus involved in sensory perception of taste (GO:0050912)	Sensory perception	Mucus CRS	PIGR;AZGP1;PIP;CST4	0.02456
endocytosis (GO:0006897)	Localisation	Mucus CRS	ANXA1;IGKC;AHSG;IGHV3-23;IGLC1;HPR;HBA1;IGHA2	0.04151
endocytosis (GO:0006897)	Localisation	Mucus Healthy Mucus CRS	IGKV1-5;ALB;HBB;IGHA1;JCHAIN	0.00066
epidermal cell differentiation (GO:0009913)	Antomical structure development	Mucus CRS	DSP;FLG;CSTA;ANXA1;KRT16;KRT10;SPRR2B;SPRR1A;TGM3;IVL;SPRR1B;S100A7	0
epidermis development (GO:0008544)	Antomical structure development	Mucus CRS	DSP;FLG;CALML5;KRT2;KRT34;KRT5;KRT32;KRT31;KRT85;KRT9;KRT83;HRNR;CASP14;KRT17;FABP5;KRT16;KRT14;SPRR2B;SPRR1A;SPRR1B;S100A7	0
establishment of skin barrier (GO:0061436)	Antomical structure development	Mucus CRS	FLG;KRT16;SFN;HRNR	0.00059

Fc receptor mediated stimulatory signaling pathway (GO:0002431)	Immune system process	Mucus CRS	IGHG3;IGHG4;IGHG1;IGHG2;IGKC;IGHV3-23;IGLC1;ACTB	0.00063
Fc-gamma receptor signaling pathway (GO:0038094)	Immune system process	Mucus CRS	IGHG3;IGHG4;IGHG1;IGHG2;IGKC;IGHV3-23;IGLC1;ACTB	0.00062
Fc-gamma receptor signaling pathway involved in phagocytosis (GO:0038096)	Immune system process	Mucus CRS	IGHG3;IGHG4;IGHG1;IGHG2;IGKC;IGHV3-23;IGLC1;ACTB	0.0006
glomerular filtration (GO:0003094)	System process	Mucus Healthy Mucus CRS	IGHA1;JCHAIN	0.01092
gluconeogenesis (GO:0006094)	Metabolic process	Mucus CRS	TPI1;ENO1;ALDOA;GAPDH	0.01912
glucose catabolic process to pyruvate (GO:0061718)	Metabolic process	Mucus CRS	TPI1;PKM;ENO1;ALDOA;GAPDH	0.00015
glycolytic process (GO:0006096)	Cellular metabolic process	Mucus CRS	LDHA;TPI1;PKM;ALDOA	0.00199
glycolytic process through glucose-6-phosphate (GO:0061620)	Cellular metabolic process	Mucus CRS	TPI1;PKM;ENO1;ALDOA;GAPDH	0.00016
heart contraction (GO:0060047)	Circulatory system	Mucosa Healthy Mucosa CRS	MYL4;TPM1;SOD1	0.04
hexose biosynthetic process (GO:0019319)	Metabolic process	Mucus CRS	TPI1;ENO1;ALDOA;GAPDH	0.02409
homotypic cell-cell adhesion (GO:0034109)	Cell-cell adhesion	Mucosa Healthy Mucosa CRS	FGG;ACTB;ACTG1	0.03709
humoral immune response mediated by circulating immunoglobulin (GO:0002455)	Immune system process	Mucus CRS	IGHG3;IGHG4;IGHM;IGHG1;IGHG2;IGKC;IGHV3-23;IGLC1;IGHA2	0.00004

hydrogen peroxide metabolic process (GO:0042743)	Cellular metabolic process	Mucosa Healthy Mucosa CRS	PRDX2;CAT;PARK7;SOD1	0.00024
intermediate filament organization (GO:0045109)	Cellular component organisation	Mucus CRS	DSP;KRT14;PKP1;KRT20;KRT9	0.00001
keratinocyte differentiation (GO:0030216)	System development	Mucus CRS	DSP;FLG;CSTA;ANXA1;KRT16;KRT10;SPRR2B;SPRR1A;TGM3;IVL;SPRR1B;S100A7	0
negative regulation of apoptotic process (GO:0043066)	Cell death	Mucosa CRS	HSPA9;FABP1;HSPA5;GSTP1;GLO1;HSPD1	0.02026
negative regulation of apoptotic process (GO:0043066)	Cell death	Mucosa Healthy Mucosa CRS	PRDX2;ANXA1;ARHGDIA;CAT;PARK7;TPT1;HSP90B1;TXNDC5;SOD1	0.00048
negative regulation of cellular protein metabolic process (GO:0032269)	Cellular metabolic process	Mucus CRS	SERPINB3;CSTB;CSTA;GAPDH;CST4	0.03466
negative regulation of endopeptidase activity (GO:0010951)	Regulation of molecular function	Mucus CRS	SERPINB3;SERPINA3;SERPINB4;SERPINB12;SERPINA1;AHSG;GAPDH;CST4	0.00003
negative regulation of peptidase activity (GO:0010466)	Regulation of molecular function	Mucus CRS	SERPINB3;SERPINA3;SERPINB4;CSTB;SERPINB12;CSTA;SERPINA1;AHSG;GAPDH	0
negative regulation of programmed cell death (GO:0043069)	Cell death	Mucosa CRS	HSPA9;FABP1;HSPA5;GSTP1;GLO1;HSPD1	0.01505
negative regulation of programmed cell death (GO:0043069)	Cell death	Mucosa Healthy Mucosa CRS	PRDX2;ANXA1;ARHGDIA;CAT;PARK7;TPT1;HSP90B1;TXNDC5	0.00112
negative regulation of proteolysis (GO:0045861)	Cellular metabolic process	Mucus CRS	SERPINB3;CSTB;SERPINB4;CSTA;CST4	0.00133
neutrophil activation involved in immune response (GO:0002283)	Immune system process	Mucus CRS	DSP;SERPINB3;SERPINA3;PIGR;CSTB;SERPINB12;SERPINA1;CALML5;JUP;ANXA2;AHSG;GSTP1;DEFA1;HRNR;EEF1A1;PKM;FABP5;PKP1;DSG1;ALDOA;B2M;S100A8;S100A11;S100A7	0
neutrophil activation involved in immune	Immune system process	Mucus Healthy Mucus CRS	ORM1;SLPI;HBB;LYZ;S100A9;LTF	0.00069

response (GO:0002283)				
neutrophil degranulation (GO:0043312)	Immune system process	Mucus CRS	DSP;SERPINB3;SERPINA3;PIGR;CSTB;SERPINB12;SERPINA1;CALML5;JUP;ANXA2;AHSG;GSTP1;DEFA1;HRNR;EEF1A1;PKM;FABP5;PKP1;DSG1;ALDOA;B2M;S100A8;S100A11;S100A7	0
neutrophil degranulation (GO:0043312)	Immune system process	Mucosa Healthy Mucosa CRS	ORM1;SLPI;HBB;LYZ;S100A9;LTF	0.00079
neutrophil mediated immunity (GO:0002446)	Immune system process	Mucus CRS	DSP;SERPINB3;SERPINA3;PIGR;CSTB;SERPINB12;SERPINA1;CALML5;JUP;ANXA2;AHSG;GSTP1;DEFA1;HRNR;EEF1A1;PKM;FABP5;PKP1;DSG1;ALDOA;B2M;S100A8;S100A11;S100A7	0
neutrophil mediated immunity (GO:0002446)	Immune system process	Mucus Healthy Mucus CRS	ORM1;SLPI;HBB;LYZ;S100A9;LTF	0.00062
nicotinamide nucleotide metabolic process (GO:0046496)	Cellular metabolic process	Mucus CRS	LDHA;TPI1;PKM;ALDOA	0.02575
pattern recognition receptor signaling pathway (GO:0002221)	Immune system process	Mucosa Healthy Mucosa CRS	FGG;S100A8;HSP90B1	0.03975
peptide cross-linking (GO:0018149)	Cellular metabolic process	Mucus CRS	FLG;DSP;CSTA;ANXA1;KRT2;KRT10;SPRR2B;SPRR1A;TGM3;SPRR1B;IVL	0
peptidyl-cysteine modification (GO:0018198)	Cellular metabolic process	Mucosa Healthy Mucosa CRS	PARK7;S100A8	0.03937
phagocytosis (GO:0006909)	Localisation	Mucus CRS	IGHG3;IGHG4;IGHM;IGHG1;IGHG2;ANXA1;IGKC;IGHV3-23;MYH9;IGLC1;IGHA2	0
phagocytosis, engulfment (GO:0006911)	Localisation	Mucus CRS	IGHG3;IGHG4;IGHM;IGHG1;IGHG2;IGKC;IGHV3-23;MYH9;IGLC1;IGHA2	0
plasma membrane invagination (GO:0099024)	Cellular component organisation	Mucus CRS	IGHG3;IGHG4;IGHM;IGHG1;IGHG2;IGKC;IGHV3-23;MYH9;IGLC1;IGHA2	0
platelet aggregation (GO:0070527)	Reponse to stimulus	Mucosa Healthy Mucosa CRS	FGG;ACTB;ACTG1	0.02851

platelet degranulation (GO:0002576)	Export from cell	Mucus Healthy Mucus CRS	ORM1;TF;ALB	0.03274
platelet degranulation (GO:0002576)	Export from cell	Mucosa Healthy Mucosa CRS	SERPINA1;FGG;APOA1;SOD1	0.03797
positive regulation of B cell activation (GO:0050871)	Cell activation	Mucus CRS	IGHG3;IGHG4;IGHM;IGHG1;IGHG2;IGKC;IGHV3-23;IGLC1;IGHA2	0.00003
positive regulation of lymphocyte activation (GO:0051251)	Cell activation	Mucus CRS	IGHG3;IGHG4;IGHM;IGHG1;IGHG2;IGKC;IGHV3-23;IGLC1;IGHA2	0.00001
positive regulation of metabolic process (GO:0009893)	Metabolic process	Mucus Healthy Mucus CRS	IGHA1;JCHAIN	0.02714
positive regulation of respiratory burst (GO:0060267)	Metabolic process	Mucus Healthy Mucus CRS	IGHA1;JCHAIN	0.00831
protein heterooligomerization (GO:0051291)	Cellular component organisation or biogenesis	Mucus CRS	HIST1H4A;ANXA2;SEMG2;SEMG1;HBA1	0.00266
pyruvate metabolic process (GO:0006090)	Cellular metabolic process	Mucus CRS	LDHA;TPI1;PKM;ALDOA	0.02748
receptor-mediated endocytosis (GO:0006898)	Localisation	Mucus Healthy Mucus CRS	IGKV1-5;ALB;HBB;IGHA1;JCHAIN	0.00025
regulation of acute inflammatory response (GO:0002673)	Reponse to stimulus	Mucus CRS	IGHG3;IGHG4;IGHG1;IGHG2;IGKC;GSTP1;IGHV3-23;IGLC1	0.00033
regulation of apoptotic process (GO:0042981)	Cell death	Mucosa CRS	HSPA9;FABP1;HSPA5;GSTP1;GLO1;TAOK1;HSPD1	0.01647
regulation of apoptotic process (GO:0042981)	Cell death	Mucosa Healthy Mucosa CRS	PRDX2;ANXA1;ARHGDIA;CAT;NME4;PARK7;TPT1;HSP90B1;TXNDC5;SOD1	0.00197
regulation of B cell activation (GO:0050864)	Cell activation	Mucus CRS	IGHG3;IGHM;IGHG4;IGHG1;IGHG2;IGKC;IGHV3-23;IGLC1;IGHA2	0.00001

regulation of complement activation (GO:0030449)	Immune system process	Mucus CRS	IGHG3;IGHG4;IGHG1;IGHG2;IGKC;IGHV3-23;IGLC1	0.00137
regulation of endopeptidase activity (GO:0052548)	Regulation of molecular function	Mucus CRS	SERPINB3;SERPINA3;SERPINB4;SERPINB12;SERPINA1;AHSG;GAPDH	0.00009
regulation of humoral immune response (GO:0002920)	Immune system process	Mucus CRS	IGHG3;IGHG4;IGHG1;IGHG2;IGKC;IGHV3-23;IGLC1	0.00165
regulation of immune effector process (GO:0002697)	Immune system process	Mucus CRS	IGHG3;IGHG4;IGHG1;IGHG2;IGKC;IGHV3-23;IGLC1	0.0017
regulation of peptidase activity (GO:0052547)	Regulation of molecular function	Mucus CRS	SERPINB3;SERPINB4;CSTB;CSTA	0.00085
regulation of protein activation cascade (GO:2000257)	Metabolic process	Mucus CRS	IGHG3;IGHG4;IGHG1;IGHG2;IGKC;IGHV3-23;IGLC1	0.00133
regulation of protein processing (GO:0070613)	Metabolic process	Mucus CRS	IGHG3;IGHG4;IGHG1;IGHG2;IGKC;IGHV3-23;IGLC1	0.00327
regulation of proteolysis (GO:0030162)	Metabolic process	Mucus CRS	SERPINB3;SERPINB4;CSTB;CSTA;CST4	0.00828
regulation of respiratory burst (GO:0060263)	Metabolic process	Mucus Healthy Mucus CRS	IGHA1;JCHAIN	0.01001
regulation of water loss via skin (GO:0033561)	Biological regulation	Mucus CRS	FLG;KRT16;SFN;HRNR	0.00058
removal of superoxide radicals (GO:0019430)	Cellular reponse to chemical stimulus	Mucosa Healthy Mucosa CRS	PRDX2;SOD1	0.04334
renal filtration (GO:0097205)	System process	Mucus Healthy Mucus CRS	IGHA1;JCHAIN	0.01129
response to hydrogen peroxide (GO:0042542)	Reponse to stimulus	Mucosa Healthy Mucosa CRS	CAT;PARK7;SOD1	0.04154
response to unfolded protein (GO:0006986)	Reponse to stimulus	Mucosa CRS	HSPA9;HSPA5;HSPD1	0.02186

retina homeostasis (GO:0001895)	Tissue homeostasis	Mucus CRS	IGHG3;PIGR;AZGP1;IGKC;PIP;HSPB1;LCN1;B2M;IGHA2;ACTB;CST4	0
retina homeostasis (GO:0001895)	Tissue homeostasis	Mucus Healthy Mucus CRS	TF;ALB;LYZ;IGHA1;JCHAIN;LTF	0
retina homeostasis (GO:0001895)	Tissue homeostasis	Mucosa Healthy Mucosa CRS	ACTB;ACTG1;SOD1	0.03245
sensory perception of bitter taste (GO:0050913)	Sensory perception	Mucus CRS	PIGR;AZGP1;PIP;CST4	0.01951
skin development (GO:0043588)	System development	Mucus CRS	DSP;FLG;CSTA;ANXA1;KRT10;ASPRV1;KRT9;HRNR;COL1A1;COL1A2;KRT16;SFN;SPRR2B;SPRR1A;TGM3;IVL;SPRR1B;S100A7	0

CRS: Chronic rhinosinusitis.

Molecular Functions

Molecular Function	Classification	Group	Genes	Adjusted P-value
cadherin binding (GO:0045296)	Binding	Mucus CRS	LDHA;ANXA1;PKM;JUP;ANXA2;MYH9;SFN;ENO1;ALDOA;YWHAZ;S100A11	0.00294
cadherin binding involved in cell-cell adhesion (GO:0098641)	Binding	Mucus CRS	ANXA1;ANXA2;S100A11	0.03519
cysteine-type endopeptidase inhibitor activity (GO:0004869)	Molecular function regulator	Mucus CRS	SERPINB3;CSTB;CSTA;LCN1;CST4	0.00625
endopeptidase activity (GO:0004175)	Catalytic activity	Mucus CRS	IGHG3;IGHG4;CASP14;IGHG1;IGHG2;IGKC;PIP;IGHV3-23;IGLC1;ASPRV1	0.02312
endopeptidase inhibitor activity (GO:0004866)	Molecular function regulator	Mucus CRS	SERPINB3;SERPINA3;SERPINB4;CSTB;SERPINB12;CSTA;SERPINA1;AHSG;LCN1;GAPDH;CST4	0
immunoglobulin receptor binding (GO:0034987)	Binding	Mucus CRS	IGHG3;IGHM;IGHG4;IGHG1;IGHG2;IGKC;IGHV3-23;IGLC1;IGHA2	0
intermediate filament binding (GO:0019215)	Binding	Mucus CRS	KRT14;PKP1;VIM	0.00802
protease binding (GO:0002020)	Binding	Mucus CRS	COL1A1;SERPINB3;SERPINB4;CSTB;CSTA;COL1A2;SERPINA1;ANXA2;SEMG2;UBC;CST4	0
protein binding involved in cell-cell adhesion (GO:0098632)	Binding	Mucus CRS	ANXA1;ANXA2;S100A11	0.04508
serine-type endopeptidase activity (GO:0004252)	Catalytic activity	Mucus CRS	IGHG3;IGHG4;IGHG1;IGHG2;IGKC;IGHV3-23;IGLC1	0.04657
serine-type endopeptidase inhibitor activity (GO:0004867)	Molecular function regulator	Mucus CRS	SERPINB3;SERPINA3;SERPINB4;SERPINB12;SERPINA1	0.00817
signal recognition particle binding (GO:0005047)	Binding	Mucus Healthy Mucus CRS	TF;LTF	0.01688

CRS: Chronic rhinosinusitis.

CHAPTER 8: PROTEOMIC ANALYSIS OF NASAL MUCUS SAMPLES OF HEALTHY PATIENTS AND PATIENTS WITH CHRONIC RHINOSINUSITIS

STATEMENT OF AUTHORSHIP

Title of Paper	Proteomic analysis of nasal mucus samples of healthy patients and patients with chronic rhinosinusitis
Publication Status	☑ Published ☐ Accepted for Publication ☐ Submitted for Publication ☐ Unpublished and Unsubmitted work written in manuscript style
Publication Details	Kao SS, Bassiouni A, Ramezanpour M, Finnie J, Chegeni N, Colella AD, et al. Proteomic analysis of nasal mucus samples of healthy patients and patients with chronic rhinosinusitis. J Allergy Clin Immunol. 2020.

Principal Author

Name of Principal Author (Candidate)	Stephen Kao		
Contribution to the Paper	Study inception, Collection of mucus and tissue samples, Conducted experiments, Data interpretation and analyses, Manuscript preparation.		
Overall percentage (%)	80%		
Certification:	This paper reports on original research I conducted during the period of my Higher Degree by Research candidature and is not subject to any obligations or contractual agreements with a third party that would constrain its inclusion in this thesis. I am the primary author of this paper.		
Signature		Date	24.03.2020

Co-Author Contributions

By signing the Statement of Authorship, each author certifies that:

i. the candidate's stated contribution to the publication is accurate (as detailed above);
ii. permission is granted for the candidate in include the publication in the thesis; and
iii. the sum of all co-author contributions is equal to 100% less the candidate's stated contribution.

Name of Co-Author	Ahmed Bassiouni		
Contribution to the Paper	Statistical analysis, Manuscript editing		
Signature		Date	24.03.2020

Name of Co-Author	Mahnaz Ramezanpour		
Contribution to the Paper	Project supervision, Manuscript editing		
Signature		Date	20.03.2020

Name of Co-Author	John Finnie		
Contribution to the Paper	Assistance with pathology review, Manuscript editing		
Signature		Date	6.03.2020

Name of Co-Author	Nusha Chegeni		
Contribution to the Paper	Assisted with experiments, Manuscript editing		
Signature		Date	20.03.2020

Name of Co-Author	Alex Colella		
Contribution to the Paper	Assisted with experiments, Manuscript editing		
Signature		Date	20.03.2020

Name of Co-Author	Timothy Chataway		
Contribution to the Paper	Project supervision, Manuscript editing, Data analysis		
Signature		Date	20.03.2020

Name of Co-Author	Peter-John Wormald		
Contribution to the Paper	Project supervision, Manuscript editing		
Signature		Date	17.03.2020

Name of Co-Author	Sarah Vreugde		
Contribution to the Paper	Project supervision, Manuscript editing		
Signature		Date	20.03.2020

Name of Co-Author	Alkis James Psaltis		
Contribution to the Paper	Project supervision, Manuscript editing, Assistance with study design, Corresponding author		
Signature		Date	17.03.2020

CITATION

Kao SS, Bassiouni A, Ramezanpour M, Finnie J, Chegeni N, Colella AD, et al. Proteomic analysis of nasal mucus samples of healthy patients and patients with chronic rhinosinusitis. J Allergy Clin Immunol. 2020.

ABSTRACT

Introduction

Chronic rhinosinusitis (CRS) has a complex and multifactorial pathogenesis with a heterogeneous inflammatory profile. Proteomic analysis of nasal mucus may enable further understanding of protein abundances and biological processes present in CRS and its endotypes compared to healthy patients.

Objective

Determine differences in the nasal mucus proteome of healthy and CRS patients

Methods

Nasal mucus was obtained from healthy, CRS without nasal polyp (CRSsNP) and CRS with nasal polyp (CRSwNP) patients prior to surgery. Gel electrophoresis was performed to fractionate the complex protein extracts prior to mass spectrometry analysis. Gene set enrichment analysis was performed on differentially expressed proteins.

Results

Thirty-three patients were included in this study (12 healthy, 10 CRSsNP and 11 CRSwNP). 1142 proteins were identified in healthy mucus samples, 761 in CRSsNP and 998 in CRSwNP mucus samples. Dysfunction in immunological pathways, reduced cellular signalling and increased cellular metabolism with associated tissue remodelling pathways were present in CRS compared to healthy patients.

Conclusions

Significant downregulation of mucosal immunity and antioxidant pathways with increased tissue modelling processes may account for the clinical manifestations of CRS. Ultimately, the differing proteome and biological processes provides further insights into CRS pathogenesis and its endotypes.

Clinical Implications:

Identification of differences in immunological pathways between healthy and CRS patients will aim to guide future research in the development of targeted immunotherapies.

Capsule Summary

Advances in proteomic technology and analysis of nasal mucus has demonstrated significant differences in biological pathways that may guide further research in improving the understanding of CRS pathophysiology.

Keywords: Nasal mucus, Proteomics, Chronic rhinosinusitis, Nasal polyps, Endotypes, Proteins

INTRODUCTION

Chronic rhinosinusitis (CRS) endotypes and pathophysiology has evolved over time with hypotheses suggesting the involvement of pathogen dysbiosis, immune dysregulation and environmental factors.[1] Dysfunction of the epithelial barrier in CRS patients has also been suggested as a key event in the disease process, although the precise mechanism by which this occurs remains unknown. Recent work in our department has demonstrated that locally produced mucus may have an important effect on the nasal epithelial barrier with mucus from healthy patients shown to be associated with improved barrier integrity and mucociliary clearance, whereas mucus from CRS patients was found to be associated with increased mucosal inflammation.[520] Elevated cytokines in CRS mucus have been identified and suggested as a novel endotyping tool. [8, 520] Furthermore, accumulation and aberrant activation of neutrophils with associated release of neutrophil serine proteases, such as elastase, cathepsin G and proteinase 3, may contribute to the increased mucosal permeability.[510, 548] The different composition of healthy and CRS mucus and the regulation of inflammatory pathways may therefore contribute to the opposing effects on mucosal barrier function observed.

Proteomic analysis of nasal mucus is capable of providing further insights into the physiological and pathophysiological pathways present in CRS. A systematic review of the literature conducted in our department identified 21 studies investigating the proteome of nasal mucus and mucosa from healthy and CRS patients.[567] Gene set enrichment analysis of the differentially expressed proteins identified increased immunological, metabolic and tissue remodelling pathways and processes present in CRS patients compared with healthy patients. Notably, the most recent of these studies comparing the CRS and healthy proteome was published eight years ago,[536] and since then there have been considerable advances in mass spectrometry equipment speed, resolution and sensitivity. The primary aim of this study was to provide an

updated list of proteins and abundances in CRS and healthy patients. Secondly, we sought to perform gene set enrichment analysis to determine differences in biological processes that may account for disease processes in CRS and its endotypes

MATERIALS AND METHODS

The Queen Elizabeth Hospital Human Research Ethics Committee, Adelaide, Australia (Reference number: HREC/15/TQEH/132) approved the collection of nasal mucus. Chronic rhinosinusitis mucus samples were collected from patients having endoscopic sinus surgery at the Department of Otorhinolaryngology Head and Neck surgery, The Queen Elizabeth Hospital, Adelaide, Australia. Patient consent and mucus samples were obtained prior to surgery. Healthy mucus was collected from patients undergoing endoscopic skull base surgery or septoplasty with no clinical or radiological evidence of sinus disease. Patient comorbidities and disease severity were documented preoperatively. Nasal mucosa tissue was obtained intraoperatively and reviewed by a pathologist. Patients less than 18 years of age, pregnant and systemic immunosuppression were excluded.

Histology

Mucosal specimens were collected and fixed in 10% neutral buffered formalin, paraffin embedded and 6 µm sections cut and stained with hematoxylin and eosin. The inflammatory infiltrate was assessed at the site of maximal infiltration and the relative proportion, and number per high power field (x40 objective), of each inflammatory cell type calculated.

Mucus Collection and Analysis

Mucus collection and extraction was performed as per a previously published technique with polyurethane foam without application of local anaesthesia.[520] Nasal mucus sample preparation and liquid chromatography-tandem mass spectrometry (LC-MS/MS) analysis are described in detail in the supplementary methods section. In summary, protein digests were separated by nano-LC and analysed with a quadrupole time-of-flight mass spectrometer. Identified proteins were matched with the Uniprot database with MASCOT v2.6 (Matrix Science, London, UK).

Statistical Analysis

Statistical analysis was conducted with R Core Team statistical software.[503] Proteins identified were stratified into their presence in either CRS, healthy or both for mucus groups. Protein abundance between groups was automatically calculated from as exponentially modified abundance index (emPAI) by the MASCOT software. [568] The review by *Dowle* found emPAI values to be a reliable method of protein quantification.[569] These MASCOT-derived emPAI values were converted to molar percentages by normalising against the sum of all emPAI values.[569, 570] Fold difference was calculated from the sum of molar percentages in all replicates with student's t-test, with 1.3 fold difference considered significant based on *Dowle's* review.[569, 570] Gene set enrichment analysis (GSEA) was conducted on Enrichr™ (Ma'ayan Laboratory, NY, USA) on differentially expressed proteins across the three groups.[527, 528] Common gene sets from the differentially expressed proteins are grouped together to generate biological process and pathways based on the Gene Ontology database. Only significant results (Adjusted P-value <0.05 calculated by Enrichr™) were included for further analysis.

RESULTS

Thirty-three patients were included in this study (12 healthy, 10 CRSsNP and 11 CRSwNP) with a mean age of 46.2 (SD 16.6). Patient demographics were summarised in table 8.1. The nasal mucosal lamina propria of CRSwNP and CRSsNP patients showed increased eosinophil or lymphoplasmacytic infiltration, respectively. The eosinophil infiltration was diffusely distributed with occasional extension into the respiratory epithelium, whereas the infiltration of lymphocytes and plasma cells was either diffuse or perivascular (Figure 8.1). This was associated with tissue remodelling evidenced by respiratory epithelial hyperplasia, goblet cell hyperplasia, basement membrane thickening and occasional squamous metaplasia. Furthermore, the lamina propria demonstrated congestion, oedema with seromucous gland hyperplasia with abundant mucus production (Figure 8.2).

Table 8.1. Patient Demographics

	Healthy n (%)	CRSsNP n (%)	CRSwNP n (%)	P-value
Gender (M/F)	6/6	2/8	8/3	0.054
Age	46.2 (SD 19.1)	45.7 (SD 16.4)	46.6 (SD 15.4)	0.963
Revision Surgery	0 (0)	2 (20)	7 (64)	0.002
Reformed Smoker	1 (8)	1 (10)	1 (9)	0.574
Active Smoker	0 (0)	0 (0)	2 (18)	0.062
Asthma	1 (8)	2 (20)	4 (36)	0.258
GERD	1 (8)	2 (20)	1 (9)	0.991
Diabetes Mellitus	0 (0)	0 (0)	1 (9)	0.357
Aspirin Hypersensitivity	0 (0)	1 (10)	3 (27)	0.131
Aeroallergen Hypersensitivity	0 (0)	1 (10)	2 (18)	0.315
Antibiotic Hypersensitivity	0 (0)	1 (10)	0 (0)	0.305
Mucus Volume (µL)	235.8 (SD 180.5)	213 (SD 204.7)	290 (SD 177.6)	0.317
SNOT-22 score	-	58.6 (SD 31.0)	55 (SD 23.2)	0.416
Lund-Mackay Score	-	7.8 (SD 2.6)	14.5 (SD 5.2)	0.0008
Lund-Kennedy Score	-	5.6 (SD 2.5)	9.8 (SD 2.9)	0.004
Inflammatory Cell Predominance	-	Eosinophilic 2 (20) Lymphocytic 1 (10) Lymphoplasmacytic 4 (40) Unknown 3 (30)	Eosinophilic 5 (45) Lymphocytic 2 (18) Lymphoplasmacytic 1 (9) Unknown 3 (27)	0.589

CRSsNP: Chronic rhinosinusitis without nasal polyps, CRSwNP: Chronic rhinosinusitis with nasal polyps, GORD: Gastroesophageal reflux. SNOT-22: Sino-Nasal Outcome Test.

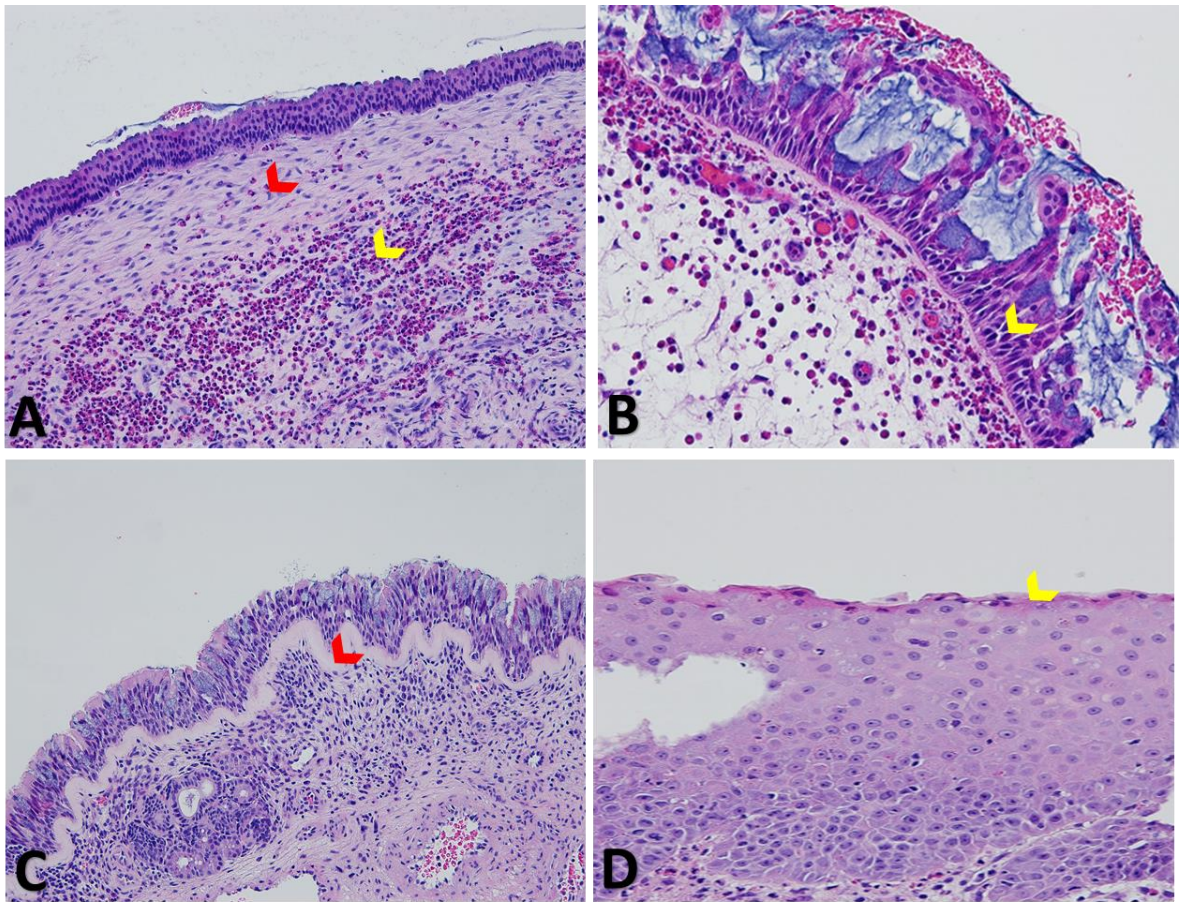

Figure 8.1. Histopathology of CRS mucosa demonstrating tissue remodelling.

(A) *Marked subepithelial fibrosis (red arrow) with diffuse lamina propria eosinophil infiltration (yellow arrow) in CRSwNP.* ***(B)*** *Respiratory epithelial and goblet cell hyperplasia (yellow arrow).* ***(C)*** *Respiratory epithelial hyperplasia with marked basement membrane thickening (Red arrow).* ***(D)*** *Squamous metaplasia (yellow arrow) of hyperplastic respiratory epithelium in CRSwNP.*

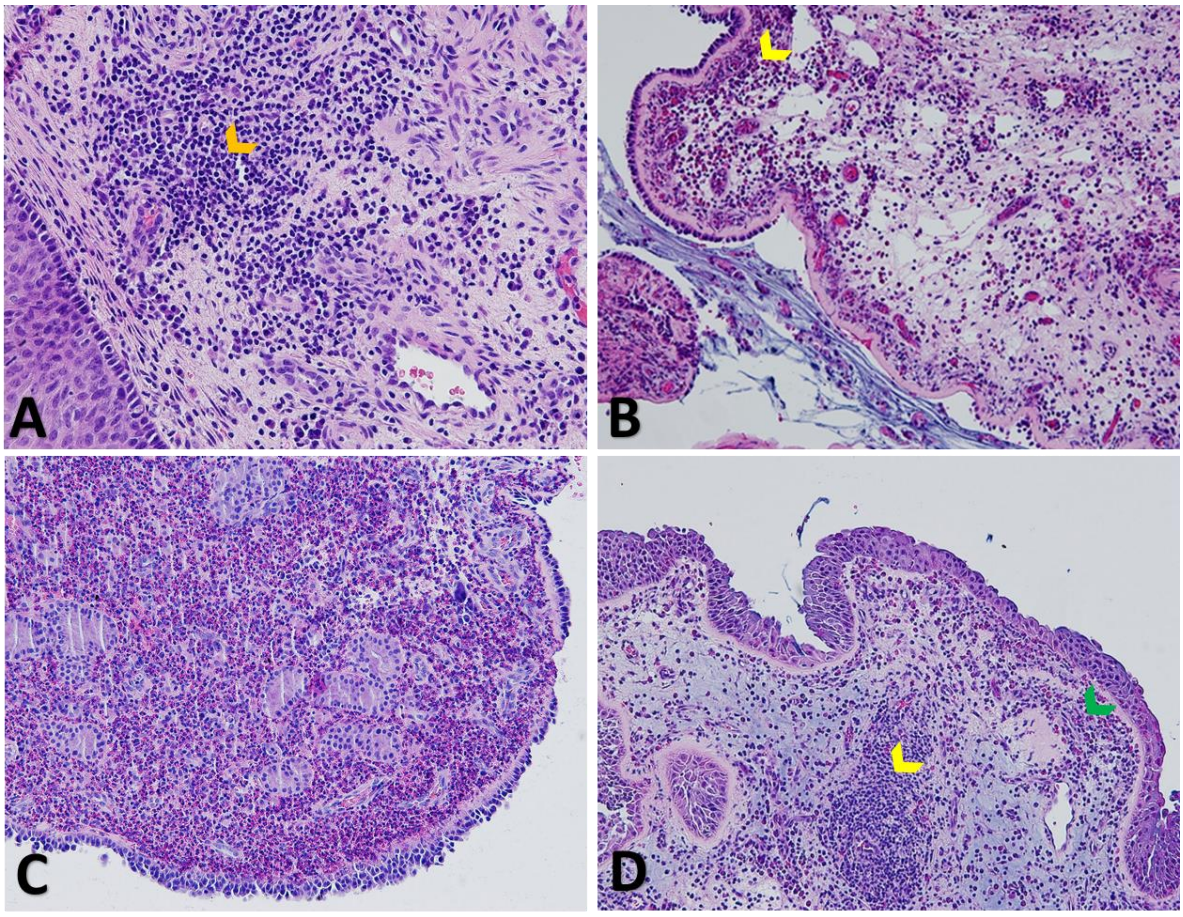

Figure 8.2. Histopathology of CRS mucosa demonstrating inflammatory cell infiltration. ***(A)*** *Marked lymphoplasmacytic infiltration (orange arrow) of the lamina propria in CRSsNP.* ***(B)*** *Diffuse eosinophil infiltration (yellow arrow) of oedematous lamina propria overlaid with extruded mucus and necrotic debris in CRSwNP.* ***(C)*** *Mucosal polyp with marked eosinophil infiltration.* ***(D)*** *Mucosal polypoid change with perivascular lymphocytic cuffing (yellow arrow), eosinophil infiltration (green arrow) and abundant mucus deposition in CRSwNP.*

1142 proteins were identified with at least two unique peptides across 12 healthy mucus samples. 761 and 998 proteins were identified with at least two unique peptides across 10 and 11 CRSsNP and CRSwNP mucus samples, respectively (Supplementary Table 8.1).

The healthy mucus proteome included 258 uniquely expressed proteins, not present in diseased mucus (Supplementary Table 2). Pairwise analysis between healthy and CRSwNP mucus

samples identified 11 differentially expressed proteins (Table 8.2). Pairwise analysis between healthy and CRSsNP mucus identified 30 differentially expressed proteins (Table 8.2)

Table 8.2. Significantly different proteins between groups

Healthy vs CRSwNP						
AMBP	APOD	DMBT1	KNG1	KRT35	KRT6C	LDHA
PI3	PIGR	POTEE	RBP4	SERPINA4		

Healthy vs CRSsNP						
ACTB	ADH1C	ADH7	ALDOA	CAPG	CFL1	CSTB
GC	GOT1	HNRNPA1	IDH1	KPRP	KRT14	KRT16
MDH1	MUC5AC	POTEE	PSMA1	PSMB2	RNH1	RPSA
S100A7	S100P	SERPINB3	TPM3	TUBA1C	TXN	UGP2
YWHAE	YWHAQ					

CRSsNP vs CRSwNP						
AMBP	APOA4	ARPC2	CAPG	CAPZA2	CSTB	GC
HPX	HRG	IGLV1-51	IGLV3-19	KRT72	KRT9	LRG1
MDH1	MUC5AC	MYO5A	SCGB1D2	SERPINB3	TPM3	

CRSsNP: Chronic rhinosinusitis without nasal polyposis, CRSwNP: Chronic rhinosinusitis with nasal polyposis

The CRS mucus proteome consisted of 268 uniquely expressed proteins, of which 97 were unique to CRSsNP mucus and 132 unique to CRSwNP mucus and 39 common to both (Supplementary Table 8.2). Pairwise analysis of CRSwNP and CRSsNP mucus samples identified 20 differentially expressed proteins (Table 8.2).

Gene Set Enrichment Analysis

Gene set enrichment analysis (GSEA) was conducted on the differentially expressed proteins across healthy, CRSsNP and CRSwNP mucus samples (Table 2). Biological processes were identified based on upregulation or downregulation of proteins and grouped according to the Gene ontology tree.

Downregulated biological processes in CRSsNP vs healthy mucus

One hundred and eighty-six significantly enriched biological processes were stratified into 11 groups based on the Gene ontology tree (Figure 8.3). These were identified from 27 differentially expressed proteins between CRSsNP and healthy mucus samples. Cellular (42%), metabolic (19%) and localisation (14%) processes were 75% of all downregulated biological processes in CRSsNP mucus compared to healthy mucus. Downregulated cellular processes included actin cytoskeletal organisation (GO:0030042, GO:0007015, GO:0008154), cell-cell signalling (GO:0060828, GO:0060071), immune response surface receptor signalling (GO:0038093, GO:0038095), cell cycle transition (GO:0010389, GO:1901990), cell differentiation processes (GO:2000736), apoptosis (GO:1901030, GO:1900739), cellular metabolic processes (GO:0006096, GO:0030091, GO:0070646, GO:0046394) and response to stimulus (Immune cell chemotaxis (GO:0090025, GO:0010819), hydrogen peroxide induced cell death (GO:1903205) and response to cytokines (GO:0033209, GO:0070498)]. Metabolic processes downregulated include ATP biosynthesis (GO:0006757), organic substance metabolic processes (Carbohydrate, protein and DNA) and fat-soluble vitamin metabolism (GO:0006775). Localisation processes down regulated in CRSsNP were associated with intracellular transport of proteins (GO:0046825, GO:0033158, GO:0030705), transmembrane transport (GO:1901379), calcium transport (GO:1901019) and immune cell chemotaxis (mononuclear cell GO:0071677, granulocyte GO:0071624 and T cell GO:2000406).

Downregulated biological processes in CRSwNP vs healthy mucus

Twenty-six significantly enriched biological processes were stratified into 8 groups (Figure 8.3). These were identified from 4 differentially expressed proteins between CRSwNP and healthy mucus samples. Cellular process (36%), response to stimulus (20%), developmental process (12%) and multicellular organismal process (12%) made up 80% of all downregulated CRSwNP biological processes. Downregulated cellular processes were composed of cell surface receptor signalling (GO:0002768, GO:0038093, GO:0007173) and cellular metabolic processes involved in ATP generation (GO:0006757) and carboxylic acid metabolism (GO:0032787, GO:0006090). Response to stimulus processes downregulated included detection (GO:0016045) and response to gram positive (GO:0050830) and negative bacterium (GO:0050829). Downregulated developmental processes included epithelial cell and tissue development (GO:0030855, GO:0060429). Lastly, multicellular organismal processes were system processes involved in bitter taste perception (GO:0050913, GO:0001580).

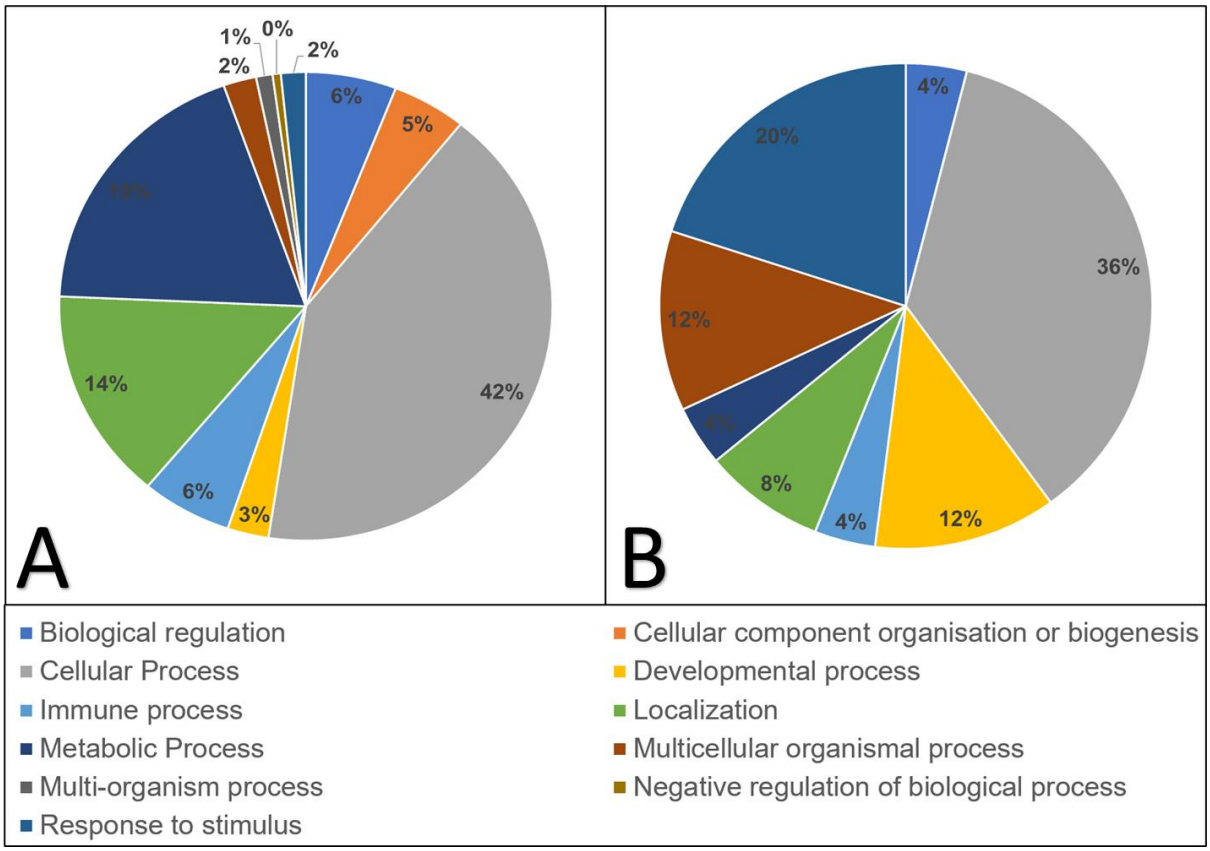

Figure 8.3. Downregulated biological processes in CRS vs healthy mucus.

(A) *CRSsNP vs healthy,* ***(B)*** *CRSwNP vs healthy. (%) of all biological processes.*

Upregulated biological processes in CRSsNP vs healthy mucus

Twenty-four significantly enriched biological processes were stratified into 9 groups (Figure 8.4). These were identified from 3 differentially expressed proteins between CRSsNP and healthy mucus samples. Developmental processes (29%), cellular component organisation or biogenesis (21%) and localisation processes (13%) were 63% of all upregulated biological processes in CRSsNP. All upregulated developmental processes were associated with anatomical structure development including epithelial barrier development (GO:0061436, GO:0008544, GO:0060429) and differentiation (GO:0009913, GO:0030216). Furthermore, cellular component organisation or biogenesis processes were all associated with cell junction (GO:0007044, GO:0031581) and cytoskeletal organisation (GO:0007010, GO:0045110,

GO:0045109). Localisation processes included negative regulation of cell motility (GO:2000146) and migration (GO:0030334, GO:0030336).

Upregulated biological processes in CRSwNP vs healthy mucus

Fifty-six significantly enriched biological processes were stratified into 12 groups (Figure 8.4). These were identified from differentially expressed proteins between CRSwNP and healthy mucus samples. Cellular processes (20%), response to stimulus (12%) and localisation (12%) and metabolic processes (11%) comprised 55% of all upregulated CRSwNP biological processes. Upregulated cellular processes included cell communication and signal transduction (GO:0010642, GO:0032873, GO:0046329, GO:0046328), protein metabolic processes (GO:0006464, GO:0032269, GO:0018149, GO:0045861), exocytosis (GO:0045055) and platelet degranulation (GO:0002576). Response to stimulus processes downregulated included negative regulation of inflammatory response (GO:0050728), response to reactive oxygen species (GO:0000302), response to axon injury (GO:0048678), regulation of blood coagulation (GO:0030193), negative regulation of blood coagulation (GO:0030195). Localisation processes included intracellular protein transport (GO:1900181, GO:0090317, GO:0042308, GO:0046823, GO:0042306) and regulation of lymphocyte (GO:2000402) and T cell migration (GO:2000404). Metabolic processes include carbohydrate (GO:0019318, GO:0006006), lipid (GO:0045833), protein (GO:0030162) and heme (GO:0006787, GO:0042167) metabolic processes.

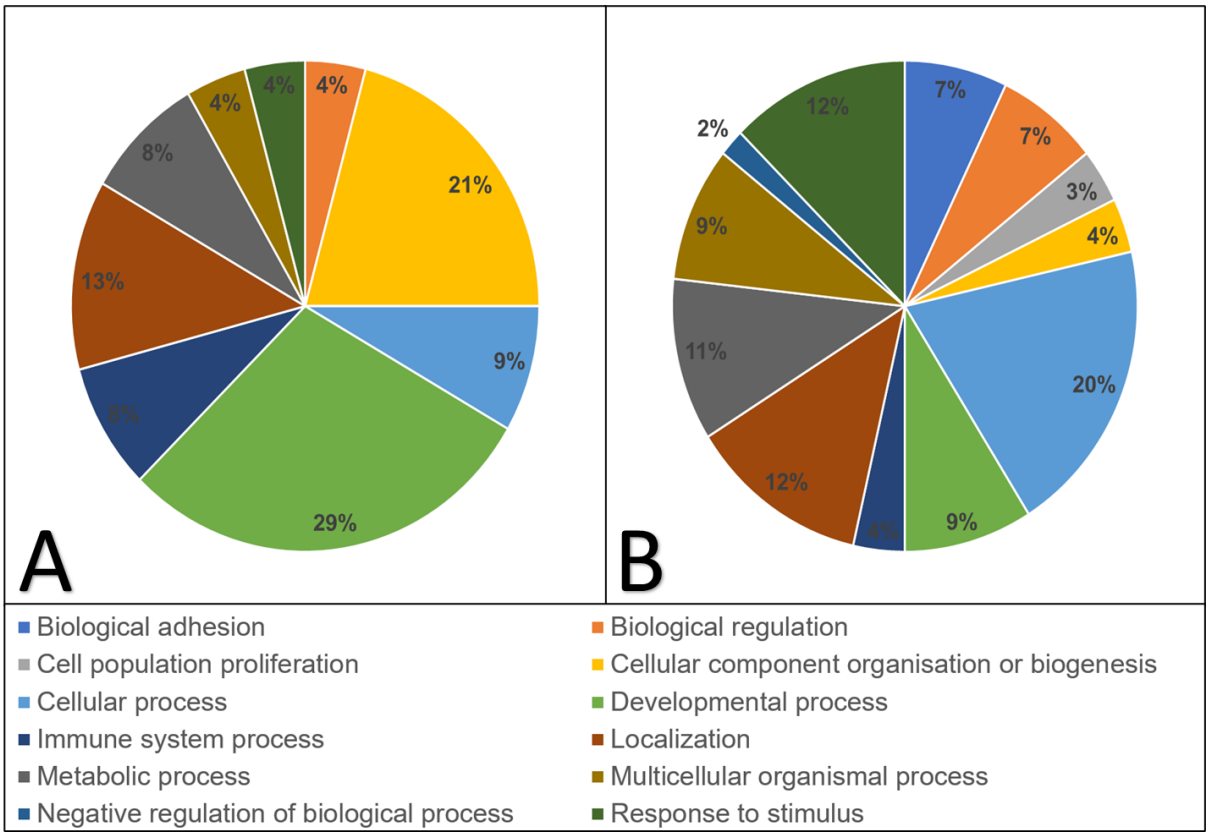

Figure 8.4. Upregulated biological processes in CRS vs healthy mucus.

(A) *CRSsNP vs healthy,* ***(B)*** *CRSwNP vs healthy. (%) of all biological processes.*

Upregulated biological processes in CRSsNP vs CRSwNP mucus

Nine significantly enriched biological processes were stratified into 5 groups (Figure 8.5). They were identified from two differentially expressed proteins between CRSsNP and CRSwNP mucus samples. Cellular processes (23%), developmental processes (22%), immune system processes (22%) and metabolic processes (22%) made up 89% of all upregulated biological processes in CRSsNP compared to CRSwNP. Cellular processes were those involved in intracellular signal transduction (GO:0048017, GO:0048015). Developmental processes included structural development of the skin (GO:0043588) and epidermis (GO:0008544). Immune processes included activation of the innate immune response (GO:0002220) and lectin pathway (GO:0002223). Metabolic processes were composed of carbohydrate metabolism (GO:0006493, GO:0016266). Tissue remodelling pathways were 33% of upregulated pathways

in CRSsNP, consisting of developmental processes (GO:0043588, GO:0008544) and intermediate filament organization (GO:0045109).

Upregulated biological processes in CRSwNP vs CRSsNP mucus

One hundred and forty-six significantly enriched biological processes were stratified into 5 groups (Figure 8.5). They were identified from 11 differentially expressed proteins between CRSwNP and CRSsNP mucus samples. Cellular processes (20%), metabolic processes (17%) and biological regulation (15%) composed 52% of upregulated pathways in CRSwNP compared to CRSsNP. Cellular processes were composed of lipid (GO:0042304, GO:0006641, GO:0010872) and protein metabolic processes (GO:0045861), actin filament-based processes (GO:0033275, GO:0030050, GO:0034314), immune response regulation (GO:0038093, GO:0038095, GO:0038094) and response to oxidative stress (GO:0071451). Metabolic processes included regulation of lipid (GO:0046890), protein (GO:0070613) and carbohydrate (GO:0006094) metabolism. Biological regulation processes included regulation of lipid homeostasis (GO:0055088) and protease function (GO:0052547). Tissue remodelling pathways were 14% of upregulated pathways in CRSwNP, consisting of: biological adhesion processes (GO:0033629, GO:0033628, GO:0007159, GO:0001954, GO:0051894, GO:0051893), cellular component organisation processes (GO:1901890, GO:1903393, GO:0065003, GO:0120033, GO:0010592, GO:0010591, GO:1902745), cellular processes (GO:0045010, GO:0033275, GO:0034314, GO:0030050), localization processes (GO:0099515, GO:0099518) and positive regulation of epithelial to mesenchymal transition (GO:0010718). Tissue remodelling pathways were 14% of upregulated pathways in CRSwNP, consisting of: biological adhesion processes (GO:0033629, GO:0033628, GO:0007159, GO:0001954, GO:0051894, GO:0051893), cellular component organisation processes (GO:1901890, GO:1903393, GO:0065003, GO:0120033, GO:0010592, GO:0010591, GO:1902745), cellular processes (GO:0045010, GO:0033275,

GO:0034314, GO:0030050), localization processes (GO:0099515, GO:0099518) and positive regulation of epithelial to mesenchymal transition (GO:0010718).

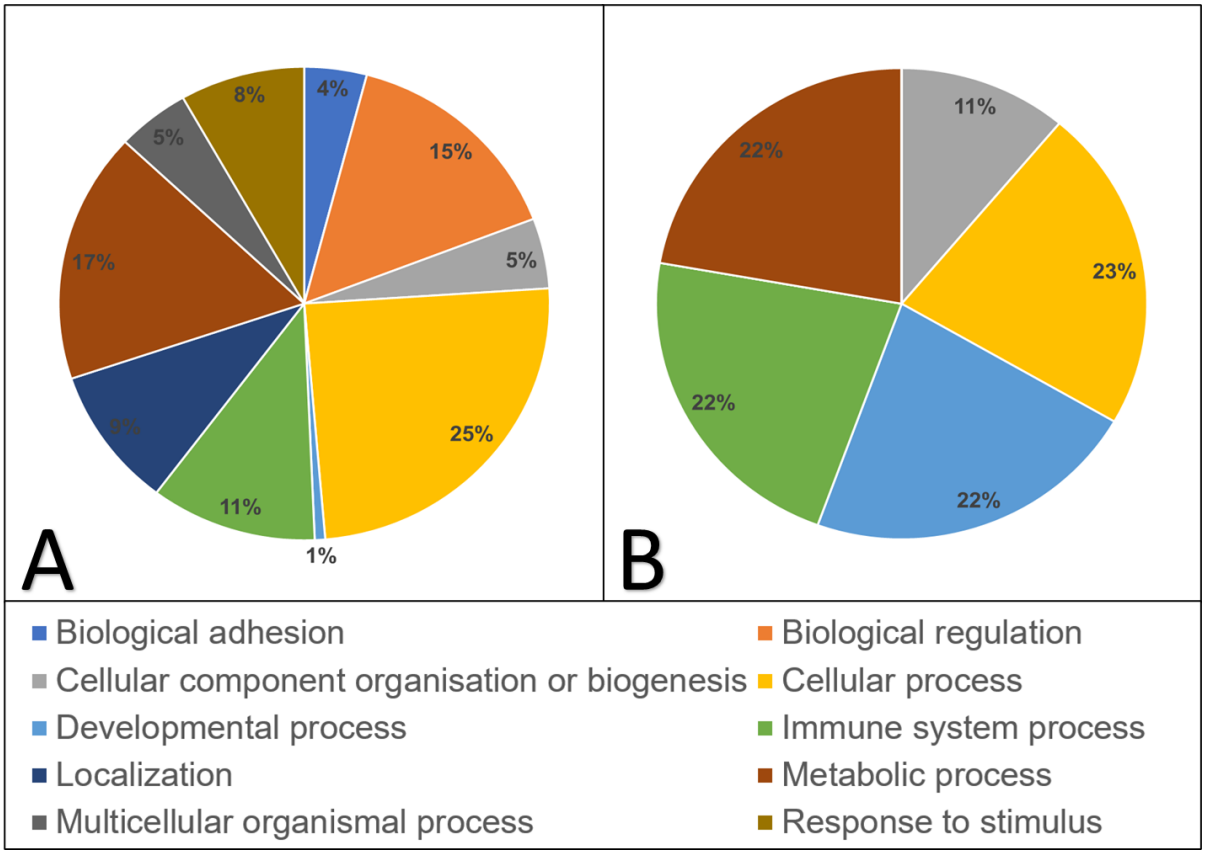

Figure 8.5. Upregulated biological processes between CRS phenotypes.

(A) *CRSsNP vs CRSwNP,* ***(B)*** *CRSwNP vs CRSsNP. (%) of all biological processes.*

DISCUSSION

The pathogenesis of CRS is complex and unclear with no curative treatments currently available. The heterogeneous nature of this disease makes classification, prognostication and management challenging for clinicians. The recent focus on CRS endotypes is an important step in understanding the various different inflammatory profiles present in patients with CRS and may ultimately allow individualised treatment protocols. Proteomic analysis of nasal mucus is capable of providing further insights into the upstream inflammatory processes that lead to the downstream clinical manifestations of CRS. This comprehensive study has utilised recent advances in mass spectrometry technology to build on previous knowledge from studies conducted eight years ago comparing healthy and CRS proteome. In this study we observed that CRS mucus demonstrated dysfunction in immunological pathways, reduced cellular signalling and increased cellular metabolism with associated tissue remodelling pathways. The dysregulation of these biological processes in comparison to healthy mucus may account for the clinical manifestations observed in CRS.

Tissue Remodelling

Barrier dysfunction with increased paracellular permeability is a common feature in CRS. This study identified a greater proportion of biological processes involved in cytoskeletal and barrier organisation and assembly in CRS mucus compared to healthy mucus samples. Additionally, CRSwNP appeared to have a greater number of upregulated tissue remodelling pathways compared to CRSsNP (20 vs 3). The upregulation of these processes may have relevance in the context of epithelial-to-mesenchymal transition (EMT) described as a result of inflammation and remodelling.[218] Furthermore, positive regulation of EMT (GO:0010718) biological process was upregulated in CRSwNP compared to CRSsNP, which may possibly contribute to polyp formation in these patients. This study found reduced expression of cofilin-1 in CRSsNP mucus

compared to healthy mucus. The cofilin protein family and actin depolymerising factor both regulate F-actin dynamics, which is essential in the stability and rearrangement of tight junctions and adherens junctions.[571, 572] Studies have suggested the importance of cofilin in establishing the paracellular barrier, through tight junction and adherens junction reassembly.[573] It has been proposed that loss of the cofilin proteins may lead to barrier dysfunction resulting in increased exposure of submucosa to luminal bacteria with associated mucosal inflammation in murine models.[573] The 40S ribosomal protein SA (RPSA) is expressed in the cell membrane, histones in the nucleus and pre-ribosome in the nucleolus.[574] As a cell surface receptor for laminin, it plays a vital role in cell adhesion to the basement membrane and signal transduction pathways.[574, 575] The reduced expression of these proteins in nasal mucus may account for the barrier function observed in CRS. Together these proteomic findings correlate with the mucosal histopathology findings of epithelial and goblet cell hyperplasia and increased basement membrane thickening.

This study demonstrated increased expression of Kininogen-1 (KNG1) in CRSwNP mucus compared to healthy mucus. KNG1 is the precursor protein to high-molecular-weight kininogen (HMWK), low-molecular-weight kininogen (LMWK) and bradykinin. Physiologically, KNG1 is a vital constituent in the coagulation cascade and kallikrein-kinin system. Coagulation cascade dysfunction has been described in the pathogenesis of many inflammatory conditions.[225] The initiation of the coagulation cascade begins with the activation of factor XII with HMWK, which leads to the liberation of bradykinin.[576] The binding of bradykinin B2 receptor induces neutrophil chemotaxis, vessel dilatation and increased vascular permeability.[577, 578] Studies have demonstrated bradykinin-induced mucosal fibroblast proliferation in nasal and bronchial tissue, indicating a role in mucosal remodelling.[579, 580] These findings are demonstrated by the marked subepithelial fibrosis present in the CRSwNP

histopathology samples. Deleted in brain malignant tumour (DBMT1) protein is a member of the scavenger receptor cysteine-rich superfamily. Elevated expression of DBMT1 in healthy respiratory epithelium has been described, with its deletion or inactivation leading to malignancy.[581, 582] DBMT1 has been demonstrated to be a regulator of nasal epithelial proliferation through apoptosis, where reduced levels of DBMT1 in nasal polyp tissue is associated with reduced apoptosis.[583] The findings from this study support these findings with 2.5 increased fold change in the levels of DBMT1 in healthy mucus compared to CRSwNP.

All keratins identified, were under expressed in CRS mucus compared to healthy, except KRT72. KRT72 has a role in hair follicle formation, and is likely a contaminant in the nasal mucus collection. Keratin presence in proteomic analysis is controversial due to the potential for contamination. Despite this, the downregulation of keratin proteins in CRS mucus may represent constant cytoskeletal reconstruction and remodelling secondary to chronic inflammation. This is further supported by the increased cellular remodelling and squamous metaplasia demonstrated in the CRS histology sections.

Mucociliary dysfunction

Mucociliary dysfunction is a feature present in chronic inflammatory diseases of the upper and lower airways. Effective mucociliary clearance is vital in maintaining a healthy environment in the nasal cavity through the clearance of invading pathogens. Thus, alterations in mucus composition that reflect dysfunction in cilia function may relate to detrimental effects observed in CRS. The major constituents of mucus are mucins, encoded by MUC genes.[389] This study demonstrated elevated mucin 5AC (MUC5AC) expression in CRS mucus compared to healthy mucus samples. MUC5AC is expressed in mucus secreted from goblet cells located within the surface epithelium of the respiratory tract.[239] It is considered a major constituent of airway

mucus vital in protecting the mucosa from inhaled invading pathogens and irritants with consequent removal via the mucociliary system.[584] Studies have found elevated expression of MUC5AC in the mucosal epithelium of CRS patients with associated secretory cell hyperplasia and metaplasia compared to healthy patients.[238, 239] IL-19, identified in several inflammatory diseases with Th2 immunological responses, has been demonstrated to upregulate MUC5AC production through the STAT3 pathway.[585-587] Tropomyosin alpha-3 chains (TPM3) bind to actin filaments stabilising the cytoskeleton and have been found to be a key component in the proteome of cilia.[588] Reduced expression in CRS mucus found in this study may reflect poor cilia function compared to healthy mucus. These changes present in mucus and cilia function may account for the reduced mucosal immunity and consequent barrier dysfunction observed in CRS.

Host Immunity

Host immune system dysregulation is an important disease modifying factor in CRS contributing to disease severity and recalcitrance. Immune system processes, encompassing signalling pathways and chemotaxis of granulocytes and lymphocytes, were largely downregulated in the CRSsNP and CRSwNP mucus groups compared to the healthy mucus group. Furthermore, defence response to gram positive (GO:0050830) and negative bacterium (GO:0050829) pathways were downregulated in CRSwNP mucus compared to healthy mucus. Bitter taste perception biological processes were downregulated in CRSwNP compared to healthy mucus. Studies have found the bitter taste receptor gene family, particularly T2R38, to be associated with activation of the local innate immune response through increased mucociliary clearance and bactericidal activity.[159, 160] Thus polymorphisms and reduced function in bitter taste receptors may play a role in sinonasal immunity in CRS.[167] The reduced

expression of these pathways reflects the bacterial species commonly responsible for recurrent infections in CRS patients.[589]

Impairment in function of immune cells may account for the inadequate immune response against invading pathogens. Macrophage-capping protein (CAPG) is an actin-binding protein of the gelsolin/villin superfamily associated with cell motility.[590] CAPG has exhibited its importance in host immunity through macrophage motility and facilitation of IgG complement phagocytosis.[591] Thus, reduced expression in CRSsNP mucus observed in this study may indicate impaired macrophage mediated inflammatory responses. Additionally, elafin (PI3) an endogenous protein expressed predominately in epithelial tissue has the ability to inhibit neutrophil elastase and proteinase-3.[592] The upregulation of PI3 identified in inflamed sinus mucosa and nasal mucus from this study may account for reduced bacterial killing due to inactivated neutrophil serine proteases.[593]

S100 proteins have a role as intracellular regulators and extracellular signalling proteins secreted to regulate activities of target cells. Intracellularly, they are capable of regulating cell proliferation, differentiation, apoptosis, inflammation and calcium homeostasis. Extracellularly, the S100 proteins act via the activation of surface receptors, G-protein-coupled and scavenger receptors in the regulation of cell proliferation, differentiation, survival, inflammation, tissue repair and antimicrobial activity.[594] S100A7 (psoriasin) is upregulated in inflammatory skin diseases induced by IL-17 and IL-22.[595] Additionally, it has antimicrobial responses through ROS generation from neutrophils and binding to and reducing survival of *E. coli*.[596, 597] The reduced expression of S100A7 in CRSsNP mucus may be associated with decreased mucosal immunity.

A range of proteins involved in immune function was found to be downregulated in CRS compared to healthy patients. Polymeric immunoglobulin receptor (PIR) is a transmembrane protein expressed on the basolateral surface of ciliated epithelial cells in mucosal epithelium, assisting the transportation of IgA and IgM across the epithelial barrier to the mucosal surface in response to viral and bacterial infections.[598] There was a significant fold reduction of PIR in both CRSwNP and CRSsNP mucus compared to healthy mucus, indicating a reduced mucosal immunity present in CRS compared to healthy patients. Proteasome subunit beta type-2 (PSMB2) and proteasome subunit alpha type-1 (PSMA1) are essential subunits of the 20S proteasome complex, which in turn is a component of the immunoproteasome.[599] The immunoproteasome is capable of antigen presentation on MHC class I molecules. Deficiencies identified in mice have been associated with reduced $CD8^+$ cell activation against hepatitis B and influenza virus infections.[600-602] Furthermore, its ability to influence T cell polarisation has been implicated in autoimmune diseases.[603] This study suggests reduction in expression of proteasome subunits to be implicated in the heightened viral invasion in CRSsNP.[604] Increased levels of eosinophil cationic protein and eosinophil peroxidase were identified in CRSwNP mucus, although not statistically significant, it correlates well with the eosinophil inflammatory predominance in these patients.

Altered Cellular Metabolism

The regulation of cellular metabolic function is paramount to tissue homeostasis and survival. CRS mucus appears to have reduced ATP metabolic pathways compared to healthy mucus. Conversely carbohydrate and lipid metabolism pathways were upregulated in CRS patients. These findings may reflect in the increased metabolic demand required to combat the chronic inflammation and pathogen colonisation. Increased glucose has been found in the airway fluid of patients with cystic fibrosis, as cells require constant glucose for cellular function and tissue

integrity. The reduced ATP generation in CRS patients may reflect the inability for these patients to keep up with the increased metabolic demand leading to a build of reactive oxygen species (ROS).

The balance in antioxidant pathways is vital in reducing cellular damage from ROS, the end result of cellular metabolism. The chronic inflammation associated with CRS places host cells at increased risk of oxidative damage and barrier dysfunction. Apolipoprotein A-IV (APOA4) has demonstrated roles in glucose homeostasis, antioxidant and anti-inflammatory properties.[605-607] In asthma, its immunomodulatory properties include improving bronchioalveolar epithelial integrity and reduction of mucin expression.[608] Elevated levels of APOA1 and APOA2 were found in patients with allergic rhinitis compared to healthy controls.[609] Increased expression may reflect the increased inflammation observed in CRSwNP compared to CRSsNP. Alpha-1-microglobulin/bikunin precursor (AMBP) belong to the lipocalin superfamily of transport proteins, and is suggested to play a role in regulation of inflammatory processes. Alpha-1microglobuin (A1M), an acute phase protein, is capable of inhibiting antigen-stimulated proliferation of lymphocytes and IL-2 secretion.[610] Elevated levels of urinary A1M are associated with increased acute phase proteins c-reactive protein and fibrinogen, indicating a role of A1M in the overall inflammatory status in patients.[611] Elevated expression of A1M was found in CRSwNP mucus compared to both CRSsNP and healthy mucus samples. Ribonuclease inhibitor (RNH1) resides within the cytosol with suggested biological roles including protection from invading ribonucleases, regulation or termination of ribonuclease activity with known intracellular functions and monitoring the oxidative stress of the cell.[612] This study found 12 fold reduced expression of RHN1 in CRSsNP compared to healthy indicating a reduced protection against oxidative stressors.

Limitations

Complex protein mixtures, such as nasal mucus, require separation prior to mass spectrometry analysis to improve protein visualisation and identification. Gel electrophoresis is the most commonly employed method for protein separation in mucus proteomic studies.[567] The recovery of proteins from gel is poor for highly glocosylated and sialidated and sulphated proteins. Alternative non-gel-based separation methods include various chromatography techniques. Despite these limitations, we were able to identify a comprehensive catalogue of proteins correlating well with previously published literature.[567] Furthermore, minimal cytokines were identified by MS analysis within nasal mucus. Yoshikawa et al. found MS to be insensitive for cytokines and growth factors due to their small size and low abundance.[613] Multiplex assays of nasal mucus and mucosa are better alternatives for the detection and quantification of cytokines. The mass spectrometry technique employed in our study is a validated and widely recognised as an effective method of shotgun proteomics. In contrast, Müeller et al. al employed ultracentrifugation to isolate exosomes for proteomic analysis via SOMAScan™ as a novel approach in nasal mucus proteomic research.[614, 615] SOMAscan is a novel and validated proteomic analysis method utilising aptamers to affinity purify proteins and the aptamers quantified using array technology. Our technique has the potential to identify more proteins present within the mucus samples providing a more wholistic picture. SOMAscan has demonstrated itself to be an effective alternative to mass spectrometry in proteomic analysis, especially when analysing extracts with very high dynamic range such as serum.[616]

The shotgun proteomics and GSEA performed in this study has generated a vast array of biological processes to aid in understanding and directing future research in the pathophysiology of CRS. The authors acknowledge the statistical method employed in this study may lead to detection of some false positive proteins, however, we do not believe this has

significantly affected the downstream biological analyses and conclusions. An Omnibus test in the form of a one-way ANOVA was performed to determine which proteins were differentially expressed across all 3 groups. Twenty significantly differentially expressed proteins (Supplementary 8.3) were identified after controlling for false discovery rates compared to 94 proteins identified with the pairwise analysis. Subsequently, the reduced numbers of proteins lead to a reduced number of unique biological pathways identified on GSEA in the downstream analysis. Overall, both analyses demonstrated similar trends of increased tissue remodelling and immunological pathways in CRSsNP and CRSwNP compared to healthy mucus samples. We believe as an exploratory study, casting a wider net initially, will aid in directing more focussed studies and research in the future. Ultimately, these findings will direct further targeted analysis of prominent cellular pathways involved in this chronic inflammatory disease.

Conclusion

This study conducted shotgun proteomics on nasal mucus from healthy and CRS patients, followed by GSEA on differentially expressed proteins to identify differences in biological pathway regulation. These findings identified significant downregulation of mucosal immunity processes, antioxidant and metabolic pathways with associated tissue remodelling that may lead to the downstream manifestation in CRS. This study should hopefully guide further focussed proteomic analysis and understanding of different CRS endotypes.

ACKNOWLEDGEMENTS

This project was supported by Adelaide University Research Training Program Scholarship, Bertha Sudholz Scholarship and Garnett Passe Rodney Williams Memorial Foundation Scholarship to SSK.

SUPPLEMENTARY MATERIAL

MATERIALS AND METHODS

Mucus Preparation

Mucus samples were mixed with 500 µL of 1× PBS and centrifuged as 12,000 g for 5 minutes. Supernatant was aspirated and mixed with 10 times volume of acetone (Chem-Supply, SA, Australia) and incubated at -20oC for one hour to allow for protein precipitation. Protein was collected following centrifugation at 10,000 rpm for 10 minutes and resolubilised in 35 µL of 6 M urea (Univar, NSW, Australia) with 5 mM Dithiothreitol (DTT, Sigma-Aldrich, MO, USA). EZQ protein quantification kit (Bio-Rad, CA, USA) was employed to calculate the amount of protein required for a loading concentration of 20 µg per well for gel electrophoresis.

Gel Electrophoresis

20 µg of protein from mucus samples were mixed with 4x sample buffer consisting of DTT, Glycerol, SDS and Bromophenol blue as described previously.[617] 40 µL of sample was loaded into each well of the Mini-PROTEAN TGX 4-20% Stain-Free Gels (Bio-Rad, CA, USA). Electrophoresis was performed for 30 minutes at 200V. Gels were stained with Coomassie blue stain (Coomassie Brilliant Blue R-250) for visualisation and scanned with GelDoc^{TM} EZ Imager (Bio-Rad, CA, USA). Gels were stored in fixative (20% methanol, 7.5% acetic acid) at room temperature prior to mass spectrometry.

Trypsin gel digest

Each lane of the SDS-PAGE gels, were cut into twelve equal sized gel pieces using sterile scalpels and transferred into 1.5 mL maximum recovery tubes (Axygen, CA, USA). Dissected gel pieces were de-stained with 50% methanol (Univar, Vic Australia). This was followed by sequential reduction and alkylation with 100 mM DTT and 400 mM iodoacetamide (Bio-Rad,

MO, USA) and dehydrated in acetonitrile (BDH Laboratory Supplies, Poole, UK). Gel pieces were rehydrated with 100 mM ammonium bicarbonate (Sigma-Aldrich, MO, USA) containing trypsin digest containing trypsin (Promega, WI, USA) and 1 mM calcium chloride (BDH Chemicals, Vic, Australia) for 12 hours. Supernatant was collected and transferred into mass spectrometry vials (Thermo Scientific, TN, USA).

ESI-Q-TOF Mass Spectrometry and Protein Identification

Tryptic digests were analysed with an Ekspert nano-LC 415 µHPLC (Eksigent, CA, USA), coupled online to a quadrupole time-of-flight mass spectrometer (Sciex TripleTOF 5600+; ON, Canada). Samples were loaded onto a Protecol trap column, 3µ 120 Å, C18, 10 mm x 300 µm (Trajan Scientific P/N 2POL-03T30K) and desalted in water with 0.1% formic acid, 2% ACN (v/v) at a flow rate of 20 µL/min for 5 minutes. Peptides were separated on a 15 cm x 75 µm column packed with 5 µm porous silica C18 beads (Nikkyo Technos, Tokyo, Japan) and electrosprayed from columns integrated spray emitter at 2kV. Mobile phases A and B were water with 0.1% formic acid (v/v) and ACN, 0.1% formic acid (v/v). Peptides were eluted at a constant flow rate of 500 nL/min, a binary gradient was ramped from 5% to 25% B within 6 minutes, increased to 40% B within 2 minutes, then further increased to 95% B within 2 minutes for washing. After 3 minutes the organic phase was returned to 5% ACN within 3 minutes and the column re-equilibrated for a further 10 minutes.

Full MS scans in the m/z 350-1500 mass range were acquired with a 100 ms transient time in positive ion mode. Following each MS scan, the 20 most intense multiply charged ions were subjected to collusion-induced dissociation and the MS2 spectra were acquired in high sensitivity mode with an accumulation time of 25 ms, with a mass range of m/z 50-1500. Only precursors with a charge state ≥2 and ≤5 were included and previously fragmented ions were

dynamically excluded for 30 seconds after 3 occurrences. Rolling collision energy and dynamic accumulation were both enabled for all MS2 spectra acquired.

Database Search

Liquid chromatography-tandem mass spectrometry (LC-MS/MS) data was analysed by searching the Uniprot database (Downloaded 15 February 2017) with MASCOT v2.6 (Matrix Science, London, UK). Search parameters included: mass value (Monoisotopic), enzyme (Trypsin); maximum missed cleavage (2), fixed modifications (Carbamidomethyl); variable modifications (methionine oxidation and serine/threonine/tyrosine phosphorylation); peptide charge (2+, 3+, 4+), peptide tolerance (±20 ppm); MS/MS tolerance (±0.05 Da). Acceptance parameters were two or more unique peptides after automatic validation (False discovery rate 1%). Identified proteins were annotated from Uniprot, and emPAI scores were calculated from the MASCOT software v2.6 using the same search parameters.

SUPPLEMENTARY TABLE 8.1. PROTEIN LIST WITH EMPAI VALUES

Uniprot	Gene	CRSsNP	CRSwNP	Healthy
A0A075B6I0	IGLV8-61	0.09000	0.32727	0.30000
A0A075B6I1	IGLV4-60	0.00000	0.08000	0.00000
A0A075B6I9	IGLV7-46	0.00000	0.08364	0.07667
A0A075B6K4	IGLV3-10	0.60700	0.83636	0.88833
A0A075B6P5	IGKV2-28	0.17600	0.16000	0.00000
A0A075B6R2	IGHV4-4	0.08900	0.24273	0.14833
A0A075B6S2	IGKV2D-29	0.76400	0.97818	0.92750
A0A0A0MS15	IGHV3-49	0.08700	0.00000	0.00000
A0A0B4J1U7	IGHV6-1	0.08400	0.00000	0.07000
A0A0B4J1V0	IGHV3-15	0.08800	0.22364	0.07333
A0A0B4J1V1	IGHV3-21	0.08900	0.00000	0.07417
A0A0B4J1V2	IGHV2-26	0.00000	0.07818	0.00000
A0A0B4J1V6	IGHV3-73	0.00000	0.08091	0.00000
A0A0B4J1X5	IGHV3-74	0.58600	0.59818	0.20750
A0A0B4J1Y8	IGLV9-49	0.00000	0.08000	0.22000
A0A0B4J1Y9	IGHV3-72	0.08600	0.14000	0.07167
A0A0C4DH25	IGKV3D-20	1.52000	1.33182	1.22083
A0A0C4DH38	IGHV5-51	0.09000	0.16364	0.00000
A0A0C4DH41	IGHV4-61	0.08700	0.23727	0.14500
A0A0C4DH68	IGKV2-24	0.78300	0.79091	0.65250
A0AVT1	UBA6	0.00000	0.00000	0.00583
A0M8Q6	IGLC7	0.00000	0.17727	0.16250
A2A2Z9	ANKRD18B	0.00000	0.00000	0.00583
A5PKW4	PSD	0.00000	0.00000	0.00667
A6NC98	CCDC88B	0.00000	0.00455	0.00417
A6NCN2	KRT87P	0.00000	1.46182	0.00000
A6NE01	FAM186A	0.00000	0.00000	0.00500
A6NHG4	DDTL	0.00000	0.14091	0.12833
A6NMB1	SIGLEC16	0.00000	0.00000	0.02833
A6NMY6	ANXA2P2	0.07900	0.05727	0.07667
A8MPP1	DDX11L8	0.00000	0.00818	0.00000
A8MTJ3	GNAT3	0.02300	0.02091	0.00000
A8MWD9	SNRPGP15	0.00000	0.00000	0.91917
B2RPK0	HMGB1P1	0.00000	0.03727	0.03417
B5ME19	EIF3CL	0.02200	0.00000	0.00000
B9A064	IGLL5	0.94500	1.10000	0.91000
C9JRZ8	AKR1B15	0.00000	0.07091	0.04833
E9PAV3	NACA	0.00000	0.00545	0.01500
O00148	DDX39A	0.00000	0.00000	0.04917
O00151	PDLIM1	0.00000	0.00000	0.08250
O00154	ACOT7	0.00000	0.02000	0.00000
O00192	ARVCF	0.00800	0.00000	0.00000
O00231	PSMD11	0.00000	0.02727	0.02500
O00232	PSMD12	0.00000	0.01545	0.05083
O00299	CLIC1	0.54600	1.26455	1.18833
O00303	EIF3F	0.00000	0.00000	0.02083
O00391	QSOX1	0.18100	0.12545	0.14250
O00423	EML1	0.00000	0.00909	0.00000
O00483	NDUFA4	0.13800	0.00000	0.00000
O00487	PSMD14	0.05500	0.08000	0.08167
O00560	SDCBP	0.00000	0.02727	0.00000
O00584	RNASET2	0.00000	0.00000	0.02667
O00602	FCN1	0.00000	0.02455	0.00000
O00750	PIK3C2B	0.00000	0.00455	0.00000

O00757	FBP2	0.05200	0.00000	0.02083
O00764	PDXK	0.05400	0.16818	0.17333
O14578	CIT	0.00000	0.00000	0.00333
O14579	COPE	0.00000	0.04000	0.02250
O14618	CCS	0.00000	0.00000	0.04417
O14745	SLC9A3R1	0.00000	0.02182	0.05167
O14791	APOL1	0.03300	0.12364	0.11333
O14818	PSMA7	0.15200	0.42364	0.45500
O14933	UBE2L6	0.00000	0.13818	0.00000
O14950	MYL12B	0.18400	0.17364	0.43667
O15020	SPTBN2	0.00000	0.00455	0.00417
O15078	CEP290	0.00300	0.00273	0.00583
O15119	TBX3	0.02200	0.00000	0.00000
O15143	ARPC1B	0.03600	0.05182	0.10250
O15144	ARPC2	0.10700	0.70727	0.48167
O15145	ARPC3	0.16600	0.39909	0.46000
O15212	PFDN6	0.00000	0.00000	0.06417
O15217	GSTA4	0.00000	0.05727	0.05250
O15305	PMM2	0.00000	0.03091	0.02833
O15372	EIF3H	0.00000	0.06273	0.09333
O15498	YKT6	0.00000	0.00000	0.03750
O15511	ARPC5	0.06700	0.06000	0.30000
O43242	PSMD3	0.00000	0.01364	0.01250
O43324	EEF1E1	0.00000	0.00000	0.04333
O43396	TXNL1	0.00000	0.09727	0.11917
O43399	TPD52L2	0.00000	0.08273	0.19167
O43447	PPIH	0.00000	0.04818	0.11833
O43488	AKR7A2	0.02300	0.03364	0.04333
O43490	PROM1	0.01400	0.00000	0.00000
O43617	TRAPPC3	0.00000	0.00000	0.04167
O43633	CHMP2A	0.00000	0.03636	0.00000
O43681	ASNA1	0.00000	0.03455	0.04000
O43707	ACTN4	0.41900	0.45545	0.55667
O43708	GSTZ1	0.00000	0.00000	0.03417
O43747	AP1G1	0.00000	0.01364	0.01250
O43776	NARS	0.00000	0.00000	0.01167
O43790	KRT86	7.27000	3.14909	0.45583
O43809	NUDT21	0.00000	0.00000	0.06167
O43866	CD5L	0.00000	0.08545	0.19250
O60218	AKR1B10	0.17300	0.68000	0.62833
O60234	GMFG	0.00000	0.21364	0.19917
O60256	PRPSAP2	0.00000	0.00000	0.01917
O60282	KIF5C	0.00800	0.00000	0.00667
O60437	PPL	0.01800	0.02000	0.07833
O60493	SNX3	0.00000	0.21636	0.36333
O60547	GMDS	0.02200	0.00000	0.01833
O60610	DIAPH1	0.00000	0.00000	0.01333
O60635	TSPAN1	0.00000	0.03364	0.00000
O60664	PLIN3	0.00000	0.00000	0.08500
O60701	UGDH	0.00000	0.01455	0.02667
O60763	USO1	0.00800	0.03273	0.01333
O60879	DIAPH2	0.00000	0.00636	0.00000
O60925	PFDN1	0.00000	0.12636	0.24750
O75037	KIF21B	0.00500	0.00000	0.00000
O75083	WDR1	0.04200	0.08909	0.13167
O75116	ROCK2	0.00000	0.00727	0.00000
O75223	GGCT	0.00000	0.26182	0.54583
O75347	TBCA	0.25200	1.27455	1.53417

O75348	ATP6V1G1	0.00000	0.07364	0.06750
O75367	H2AFY	0.03800	0.00000	0.09167
O75368	SH3BGRL	0.00000	0.31364	0.54333
O75369	FLNB	0.00800	0.04636	0.08167
O75376	NCOR1	0.00000	0.00000	0.00250
O75390	CS	0.00000	0.00000	0.01500
O75420	GIGYF1	0.00800	0.00000	0.00000
O75436	VPS26A	0.00000	0.02273	0.00000
O75534	CSDE1	0.00000	0.00000	0.00833
O75556	SCGB2A1	0.62700	0.65364	0.99250
O75608	LYPLA1	0.00000	0.00000	0.08750
O75636	FCN3	0.00000	0.09455	0.00000
O75663	TIPRL	0.00000	0.00000	0.04083
O75821	EIF3G	0.00000	0.00000	0.02167
O75828	CBR3	0.07200	0.15909	0.05917
O75832	PSMD10	0.00000	0.03636	0.05500
O75874	IDH1	0.11900	0.35909	0.61083
O75882	ATRN	0.00000	0.00455	0.01250
O75884	RBBP9	0.00000	0.00000	0.04000
O75891	ALDH1L1	0.00000	0.00818	0.00000
O75964	ATP5MG	0.10500	0.00000	0.00000
O76003	GLRX3	0.00000	0.03636	0.00000
O76009	KRT33A	2.41100	2.53000	0.23750
O76011	KRT34	0.84400	0.98273	0.15833
O76013	KRT36	0.00000	0.24818	0.09250
O76014	KRT37	0.00000	0.05091	0.00000
O76015	KRT38	0.16500	0.21545	0.00000
O76070	SNCG	0.00000	0.13909	0.30833
O94760	DDAH1	0.00000	0.00000	0.02583
O94788	ALDH1A2	0.00000	0.04364	0.02667
O94832	MYO1D	0.00800	0.00000	0.00000
O94915	FRYL	0.00000	0.00273	0.00000
O94991	SLITRK5	0.00000	0.00727	0.00000
O95140	MFN2	0.00000	0.00000	0.00833
O95197	RTN3	0.00800	0.00000	0.00667
O95248	SBF1	0.00000	0.00000	0.00333
O95294	RASAL1	0.00000	0.05909	0.04167
O95336	PGLS	0.03500	0.13455	0.18417
O95433	AHSA1	0.00000	0.00000	0.02000
O95445	APOM	0.00000	0.08545	0.03917
O95568	METTL18	0.00000	0.00000	0.01833
O95678	KRT75	0.00000	0.70545	0.33583
O95716	RAB3D	0.09800	0.00000	0.03417
O95777	LSM8	0.00000	0.10818	0.48417
O95782	AP2A1	0.01200	0.00000	0.00000
O95865	DDAH2	0.00000	0.00000	0.02667
O95968	SCGB1D1	0.46700	1.08364	1.30417
O95969	SCGB1D2	0.49200	1.57909	1.02500
O95994	AGR2	0.52100	0.71909	0.69500
O96017	CHEK2	0.00000	0.01364	0.00000
P00326	ADH1C	0.67800	1.29636	1.75167
P00338	LDHA	0.89600	1.84455	2.02417
P00352	ALDH1A1	1.11100	2.08727	1.86333
P00367	GLUD1	0.02300	0.00000	0.02583
P00390	GSR	0.03200	0.07364	0.14250
P00403	MT-CO2	0.11600	0.00000	0.06333
P00441	SOD1	0.36600	0.60273	0.62750
P00450	CP	0.44100	0.63727	0.51583

P00491	PNP	0.14800	0.19727	0.24583
P00492	HPRT1	0.00000	0.12091	0.19417
P00505	GOT2	0.03000	0.03818	0.08667
P00558	PGK1	0.71300	1.82727	2.15417
P00568	AK1	0.00000	0.07091	0.23000
P00734	F2	0.00000	0.04091	0.00000
P00736	C1R	0.00000	0.00000	0.00917
P00738	HP	3.21500	6.21545	4.02333
P00739	HPR	0.00000	0.31182	0.24917
P00747	PLG	0.19300	0.30545	0.26417
P00748	F12	0.00000	0.04727	0.01083
P00751	CFB	0.32100	0.53545	0.59167
P00915	CA1	0.00000	0.46364	0.06583
P00918	CA2	0.00000	0.07909	0.08667
P00966	ASS1	0.27200	0.26091	0.44417
P01008	SERPINC1	0.94000	1.96182	1.30417
P01009	SERPINA1	3.22700	5.86727	3.40417
P01011	SERPINA3	1.41600	1.61545	1.22167
P01019	AGT	0.04400	0.15364	0.07917
P01023	A2M	1.04100	1.58818	1.23583
P01024	C3	1.79200	2.89455	2.45500
P01031	C5	0.04300	0.12909	0.14083
P01033	TIMP1	0.33600	0.58909	0.31833
P01034	CST3	0.72200	0.93273	0.96583
P01036	CST4	0.06500	0.92364	0.50333
P01037	CST1	0.00000	0.20273	0.09333
P01040	CSTA	3.44400	4.44636	3.74583
P01042	KNG1	0.21900	0.50182	0.28500
P01591	JCHAIN	2.16500	2.17364	2.28167
P01602	IGKV1-5	0.00000	0.00000	0.07417
P01619	IGKV3-20	1.34400	1.25545	1.27333
P01700	IGLV1-47	0.00000	0.17091	0.07833
P01701	IGLV1-51	0.28200	0.83818	0.70500
P01706	IGLV2-11	0.18200	0.41364	0.30333
P01709	IGLV2-8	0.27900	0.59182	0.54250
P01714	IGLV3-19	0.48200	0.96455	0.80333
P01717	IGLV3-25	0.48300	0.79000	0.64167
P01718	IGLV3-27	0.00000	0.08636	0.00000
P01742	IGHV1-69	0.00000	0.16545	0.07583
P01743	IGHV1-46	0.00000	0.00000	0.07333
P01764	IGHV3-23	0.45500	0.16545	0.15167
P01768	IGHV3-30	0.15800	0.43000	0.65667
P01772	IGHV3-33	0.15500	0.56545	0.39000
P01780	IGHV3-7	1.35000	1.83636	1.54500
P01782	IGHV3-9	0.00000	0.08000	0.00000
P01833	PIGR	1.48300	1.34818	1.50833
P01834	IGKC	4.01100	5.47727	4.30333
P01857	IGHG1	2.31300	2.63091	2.53417
P01859	IGHG2	1.73100	1.92545	1.78917
P01860	IGHG3	1.41200	1.74182	1.70667
P01861	IGHG4	0.86300	1.63909	1.32333
P01871	IGHM	1.36100	1.61727	1.64833
P01876	IGHA1	2.33400	2.31273	2.24833
P01877	IGHA2	1.06100	0.97364	0.65000
P01880	IGHD	0.02200	0.03182	0.06750
P01903	HLA-DRA	0.03400	0.00000	0.02833
P01911	HLA-DRB1	0.03200	0.00000	0.00000
P02042	HBD	0.58600	3.62091	0.56167

P02100	HBE1	0.00000	0.06091	0.00000
P02533	KRT14	8.31800	7.90091	6.41417
P02538	KRT6A	6.06900	8.08000	5.48000
P02545	LMNA	0.13900	0.28727	0.37583
P02585	TNNC2	0.00000	0.00000	0.04833
P02647	APOA1	4.78100	10.50091	7.80667
P02649	APOE	0.00000	0.62182	0.22583
P02652	APOA2	2.55400	3.71000	2.92667
P02654	APOC1	0.00000	0.12727	0.23333
P02655	APOC2	0.00000	0.19273	0.00000
P02671	FGA	0.38100	0.67364	0.46083
P02675	FGB	0.91300	1.72545	1.21833
P02679	FGG	1.07500	1.39818	1.25750
P02686	MBP	0.00000	0.00000	0.02417
P02743	APCS	0.35800	0.82818	0.66583
P02746	C1QB	0.22000	0.61364	0.47250
P02747	C1QC	0.21600	0.45909	0.53583
P02748	C9	0.01400	0.03273	0.04167
P02749	APOH	0.00000	0.16455	0.09083
P02750	LRG1	0.12800	0.37636	0.25083
P02751	FN1	0.15700	0.27727	0.29833
P02753	RBP4	0.00000	0.50909	0.15417
P02760	AMBP	0.13700	0.61818	0.25583
P02763	ORM1	0.75900	1.35000	0.80667
P02765	AHSG	0.25600	0.46182	0.32333
P02766	TTR	0.45500	0.97273	0.60500
P02768	ALB	20.55200	31.58182	26.05583
P02774	GC	0.72000	1.75455	1.39167
P02787	TF	2.30500	4.66364	2.98500
P02788	LTF	4.99900	5.40455	5.60000
P02790	HPX	0.50100	1.08727	0.74083
P02792	FTL	0.00000	0.24273	0.07167
P02794	FTH1	0.04800	0.15000	0.20417
P03950	ANG	0.00000	0.05818	0.00000
P03952	KLKB1	0.00000	0.05636	0.02583
P03973	SLPI	3.90400	4.67364	2.78417
P04003	C4BPA	0.08100	0.08545	0.07917
P04004	VTN	0.04300	0.09273	0.04250
P04040	CAT	0.10000	0.25364	0.14167
P04062	GBA	0.01500	0.01364	0.00000
P04066	FUCA1	0.00000	0.00000	0.01417
P04075	ALDOA	1.10200	1.90545	1.99917
P04080	CSTB	0.32400	2.15636	2.43083
P04083	ANXA1	1.72900	1.75091	2.06333
P04114	APOB	0.04300	0.44727	0.37917
P04179	SOD2	0.10600	0.22000	0.16833
P04196	HRG	0.09800	0.37364	0.28250
P04211	IGLV7-43	0.00000	0.08364	0.00000
P04217	A1BG	0.18000	0.41909	0.28417
P04229	HLA-DRB1	0.00000	0.00000	0.02667
P04259	KRT6B	5.29000	7.18273	3.91833
P04264	KRT1	9.71700	10.15818	8.24250
P04279	SEMG1	0.03800	0.04545	0.47250
P04406	GAPDH	0.90600	1.68455	1.17833
P04632	CAPNS1	0.14600	0.34636	0.33917
P04792	HSPB1	1.48100	2.52727	2.61917
P04839	CYBB	0.04700	0.00000	0.00000
P04899	GNAI2	0.03600	0.00000	0.00000

P04908	HIST1H2AB	0.22400	0.00000	0.00000
P04908	HIST1H2AE	0.22400	0.00000	0.00000
P05023	ATP1A1	0.02400	0.00000	0.02333
P05089	ARG1	0.11600	0.05636	0.03667
P05090	APOD	0.79100	1.37727	0.76667
P05091	ALDH2	0.00000	0.00000	0.04667
P05107	ITGB2	0.08100	0.00909	0.00000
P05109	S100A8	8.79300	9.56182	10.57000
P05141	SLC25A5	0.44900	0.02636	0.11917
P05154	SERPINA5	0.00000	0.02909	0.00000
P05155	SERPING1	0.48000	0.86545	0.70333
P05156	CFI	0.02600	0.09273	0.07833
P05161	ISG15	0.00000	0.05364	0.00000
P05164	MPO	0.54100	0.55091	0.30417
P05198	EIF2S1	0.00000	0.05364	0.12083
P05387	RPLP2	0.00000	0.09273	0.17000
P05388	RPLP0	0.06300	0.09818	0.19667
P05452	CLEC3B	0.00000	0.13818	0.31417
P05455	SSB	0.00000	0.01818	0.02583
P05543	SERPINA7	0.00000	0.12636	0.06250
P05546	SERPIND1	0.16400	0.37091	0.26667
P05783	KRT18	0.27600	0.44818	0.67333
P05787	KRT8	2.33100	3.55818	3.67417
P05976	MYL1	0.00000	0.00000	0.06667
P06310	IGKV2-30	0.00000	0.21818	0.00000
P06312	IGKV4-1	0.17000	0.37545	0.33917
P06396	GSN	0.42800	0.51091	0.54083
P06576	ATP5F1B	0.19300	0.02273	0.09250
P06681	C2	0.00000	0.02455	0.02667
P06702	S100A9	10.56600	16.26364	13.55917
P06703	S100A6	4.78100	3.30091	3.21833
P06727	APOA4	0.86100	3.69000	2.38333
P06731	CEACAM5	0.04800	0.03818	0.04000
P06732	CKM	0.00000	0.03091	0.02833
P06733	ENO1	1.67000	2.47273	2.54583
P06737	PYGL	0.07100	0.07909	0.04167
P06744	GPI	0.24700	0.46818	0.46917
P06748	NPM1	0.02900	0.18455	0.23500
P06753	TPM3	0.28600	0.78182	0.92583
P06899	HIST1H2BJ	0.71000	0.00000	0.00000
P07099	EPHX1	0.09900	0.00000	0.02250
P07108	DBI	0.00000	0.11455	0.10500
P07195	LDHB	0.57700	1.47727	1.38667
P07196	NEFL	0.00000	0.00000	0.01250
P07197	NEFM	0.00000	0.00000	0.00750
P07203	GPX1	0.00000	0.04091	0.16750
P07205	PGK2	0.00000	0.02909	0.03750
P07237	P4HB	0.18100	0.18091	0.27333
P07305	H1F0	0.00000	0.00000	0.06833
P07339	CTSD	0.47600	0.88818	0.79917
P07355	ANXA2	2.04800	1.33091	1.48417
P07358	C8B	0.01300	0.00000	0.01083
P07360	C8G	0.12000	0.35000	0.51583
P07384	CAPN1	0.13900	0.21545	0.28917
P07437	TUBB	0.15400	0.51273	0.42750
P07476	IVL	0.02800	0.06000	0.00000
P07477	PRSS1	0.00000	0.03273	0.00000
P07602	PSAP	0.06300	0.17727	0.19250

P07686	HEXB	0.00000	0.01273	0.03000
P07711	CTSL	0.00000	0.00000	0.02083
P07737	PFN1	1.84000	3.23364	3.33750
P07741	APRT	0.05300	0.22273	0.41917
P07814	EPRS	0.01300	0.00909	0.01500
P07858	CTSB	0.06300	0.13455	0.18083
P07864	LDHC	0.00000	0.00000	0.02167
P07900	HSP90AA1	0.28800	0.52545	0.66500
P07910	HNRNPC	0.02800	0.15182	0.22500
P07949	RET	0.00000	0.00636	0.00000
P07951	TPM2	0.00000	0.04273	0.25333
P07954	FH	0.00000	0.01545	0.01417
P07996	THBS1	0.06800	0.01909	0.02583
P07998	RNASE1	0.00000	0.15909	0.09833
P08133	ANXA6	0.09500	0.00000	0.00000
P08174	CD55	0.02200	0.00000	0.00000
P08185	SERPINA6	0.00000	0.07455	0.01667
P08238	HSP90AB1	0.29400	0.43273	0.58083
P08246	ELANE	0.27700	0.37182	0.29250
P08263	GSTA1	0.72700	1.15909	1.05250
P08311	CTSG	0.66500	0.59818	0.33583
P08519	LPA	0.00000	0.00273	0.00417
P08575	PTPRC	0.01200	0.00000	0.00000
P08603	CFH	0.19200	0.43636	0.43750
P08670	VIM	0.67400	1.19818	1.41333
P08697	SERPINF2	0.00000	0.06364	0.06417
P08708	RPS17	0.00000	0.00000	0.05833
P08727	KRT19	5.69000	5.98636	6.57667
P08729	KRT7	0.88100	1.65364	1.58667
P08754	GNAI3	0.02300	0.00000	0.01917
P08758	ANXA5	0.43600	0.20364	0.26750
P08779	KRT16	8.36500	9.62273	5.33833
P08865	RPSA	0.02900	0.10182	0.19667
P08962	CD63	0.00000	0.03364	0.00000
P09012	SNRPA	0.00000	0.02818	0.02583
P09104	ENO2	0.00000	0.01727	0.00000
P09210	GSTA2	0.74900	0.91364	1.21000
P09211	GSTP1	1.55300	2.18273	1.89583
P09382	LGALS1	0.00000	0.11636	0.12167
P09429	HMGB1	0.00000	0.00000	0.05417
P09455	RBP1	0.00000	0.06182	0.15500
P09467	FBP1	0.04100	0.14818	0.22917
P09488	GSTM1	0.00000	0.08182	0.00000
P09496	CLTA	0.00000	0.05364	0.06000
P09497	CLTB	0.00000	0.00000	0.03250
P09525	ANXA4	0.18600	0.02364	0.18333
P09619	PDGFRB	0.00000	0.00000	0.00583
P09651	HNRNPA1	0.11100	0.36636	0.47333
P09668	CTSH	0.00000	0.00000	0.02083
P09669	COX6C	0.15300	0.00000	0.00000
P09758	TACSTD2	0.00000	0.02364	0.00000
P09871	C1S	0.00000	0.01636	0.03833
P09914	IFIT1	0.00000	0.01455	0.00000
P09960	LTA4H	0.00000	0.02545	0.08083
P09972	ALDOC	0.07200	0.12818	0.12917
P0C0L4	C4A	0.11300	0.34091	0.20917
P0C0L5	C4B	0.23400	0.29364	0.38667
P0C0L5	C4B_2	0.23400	0.29364	0.38667

P0C0S5	H2AFZ	0.40200	0.28818	0.47417
P0C7H8	KRTAP2-3	0.07100	0.06455	0.00000
P0C7P4	UQCRFS1P1	0.06200	0.00000	0.02583
P0CF74	IGLC6	0.00000	0.09545	0.16250
P0CG38	POTEI	0.01900	0.00000	0.00000
P0DMM9	SULT1A3	0.00000	0.00000	0.02333
P0DMR1	HNRNPCL4	0.03000	0.00000	0.00000
P0DMV8	HSPA1A	0.33300	0.59909	0.58667
P10153	RNASE2	0.00000	0.08545	0.00000
P10253	GAA	0.00000	0.00000	0.01333
P10412	HIST1H1E	0.09400	0.04182	0.07750
P10599	TXN	1.78600	3.40091	3.61750
P10620	MGST1	0.10300	0.00000	0.00000
P10643	C7	0.01900	0.02091	0.04250
P10809	HSPD1	0.07500	0.00000	0.05500
P10909	CLU	0.55600	0.99455	0.84917
P11021	HSPA5	0.10300	0.07091	0.12083
P11055	MYH3	0.00000	0.00000	0.02083
P11142	HSPA8	0.42200	0.69182	0.67167
P11171	EPB41	0.00000	0.00000	0.00750
P11215	ITGAM	0.07400	0.00000	0.00000
P11216	PYGB	0.08800	0.14364	0.24583
P11217	PYGM	0.00000	0.02727	0.00000
P11233	RALA	0.00000	0.00000	0.03500
P11279	LAMP1	0.05200	0.00000	0.00000
P11413	G6PD	0.14300	0.27091	0.29000
P11441	UBL4A	0.00000	0.00000	0.04917
P11586	MTHFD1	0.00000	0.02091	0.01917
P11678	EPX	0.01100	0.25182	0.00000
P11684	SCGB1A1	0.39600	0.11182	0.10250
P11766	ADH5	0.04600	0.08091	0.10417
P11908	PRPS2	0.00000	0.02455	0.04500
P11940	PABPC1	0.00000	0.03909	0.01083
P12035	KRT3	0.00000	0.46364	0.24250
P12081	HARS	0.00000	0.00000	0.05500
P12236	SLC25A6	0.30600	0.00000	0.00000
P12273	PIP	4.61900	4.09364	3.79417
P12277	CKB	0.00000	0.00000	0.13917
P12429	ANXA3	0.80200	0.70909	0.36583
P12724	RNASE3	0.11100	0.27000	0.15667
P12814	ACTN1	0.19100	0.21364	0.29833
P12830	CDH1	0.02300	0.02909	0.05250
P12882	MYH1	0.00000	0.00000	0.02917
P12883	MYH7	0.00000	0.00000	0.02500
P12955	PEPD	0.00000	0.02364	0.02167
P12956	XRCC6	0.00000	0.01818	0.04417
P13010	XRCC5	0.01100	0.03909	0.10250
P13073	COX4I1	0.05300	0.00000	0.00000
P13473	LAMP2	0.03200	0.00000	0.00000
P13489	RNH1	0.01800	0.09818	0.28083
P13498	CYBA	0.08100	0.00000	0.00000
P13639	EEF2	0.29700	0.54455	0.64583
P13645	KRT10	11.75900	12.82091	8.38083
P13646	KRT13	2.67300	2.19273	1.74500
P13647	KRT5	6.86300	8.63000	5.88333
P13671	C6	0.00000	0.05818	0.05833
P13693	TPT1	0.19500	0.53545	0.97083
P13796	LCP1	0.36100	0.45909	0.43750

P13797	PLS3	0.02000	0.01727	0.05083
P13798	APEH	0.00000	0.01545	0.03917
P13929	ENO3	0.00000	0.00000	0.03583
P14136	GFAP	0.00000	0.00000	0.01500
P14174	MIF	0.09200	0.40091	0.38333
P14222	PRF1	0.00000	0.01364	0.00000
P14314	PRKCSH	0.02300	0.00000	0.03500
P14324	FDPS	0.01900	0.04455	0.04750
P14406	COX7A2	0.13800	0.00000	0.00000
P14550	AKR1A1	0.30400	0.64091	0.88167
P14555	PLA2G2A	0.00000	0.00000	0.05333
P14618	PKM	0.91600	1.66545	1.71083
P14625	HSP90B1	0.11400	0.01818	0.06083
P14649	MYL6B	0.00000	0.08000	0.00000
P14735	IDE	0.00700	0.00636	0.00000
P14780	MMP9	0.34200	0.41182	0.34250
P14866	HNRNPL	0.01400	0.00000	0.01167
P14868	DARS	0.00000	0.05000	0.04583
P14902	IDO1	0.00000	0.05273	0.00000
P14923	JUP	0.70300	0.68909	0.34667
P15104	GLUL	0.08400	0.27091	0.36083
P15121	AKR1B1	0.02600	0.14909	0.18083
P15144	ANPEP	0.03700	0.00000	0.00000
P15153	RAC2	0.20800	0.21455	0.26667
P15170	GSPT1	0.00000	0.00000	0.06667
P15259	PGAM2	0.06800	0.00000	0.00000
P15311	EZR	0.51400	0.55909	0.85500
P15374	UCHL3	0.00000	0.05545	0.10500
P15531	NME1	0.58000	1.74364	1.96750
P15559	NQO1	0.16000	0.20091	0.27167
P15880	RPS2	0.08000	0.13909	0.10667
P15924	DSP	0.42400	0.38091	0.23250
P15941	MUC1	0.02100	0.01000	0.01750
P16050	ALOX15	0.07300	0.19182	0.48083
P16070	CD44	0.00000	0.01000	0.00917
P16152	CBR1	0.33100	0.83182	0.87000
P16402	HIST1H1D	0.04600	0.10091	0.09250
P16435	POR	0.01200	0.00000	0.00000
P16949	STMN1	0.00000	0.05636	0.27333
P17174	GOT1	0.03100	0.25909	0.39833
P17213	BPI	0.02600	0.03091	0.05000
P17612	PRKACA	0.00000	0.00000	0.07917
P17655	CAPN2	0.02200	0.05364	0.08583
P17844	DDX5	0.00000	0.00000	0.01083
P17858	PFKL	0.00000	0.00000	0.01833
P17900	GM2A	0.00000	0.07273	0.26667
P17931	LGALS3	0.30700	0.45000	0.48667
P17980	PSMC3	0.00000	0.00000	0.03417
P17987	TCP1	0.03000	0.02909	0.04333
P18077	RPL35A	0.16900	0.08455	0.22667
P18085	ARF4	0.41300	0.82727	0.89917
P18124	RPL7	0.13200	0.07000	0.10917
P18206	VCL	0.11800	0.39273	0.45333
P18283	GPX2	0.00000	0.00000	0.07667
P18669	PGAM1	0.00000	0.29727	0.29917
P19012	KRT15	0.00000	0.18455	0.15000
P19013	KRT4	1.53200	0.96545	0.73583
P19338	NCL	0.03200	0.08000	0.09833

P19367	HK1	0.07700	0.00000	0.01500
P19623	SRM	0.00000	0.00000	0.02333
P19652	ORM2	0.38400	0.79000	0.43417
P19823	ITIH2	0.21500	0.51545	0.47250
P19827	ITIH1	0.14100	0.34909	0.32250
P19878	NCF2	0.00000	0.00000	0.01917
P19957	PI3	0.00000	0.49636	0.15167
P19971	TYMP	0.08100	0.20273	0.18917
P20020	ATP2B1	0.00000	0.00545	0.00000
P20061	TCN1	0.33900	0.29091	0.33583
P20160	AZU1	0.19300	0.14273	0.06000
P20290	BTF3	0.00000	0.00000	0.07667
P20292	ALOX5AP	0.09900	0.00000	0.00000
P20340	RAB6A	0.00000	0.06364	0.05833
P20591	MX1	0.01200	0.04364	0.02667
P20618	PSMB1	0.00000	0.38273	0.59500
P20674	COX5A	0.06400	0.00000	0.05333
P20700	LMNB1	0.01400	0.05273	0.04250
P20742	PZP	0.02900	0.01545	0.01917
P20930	FLG	0.01500	0.01273	0.00500
P21281	ATP6V1B2	0.00000	0.01455	0.02083
P21283	ATP6V1C1	0.00000	0.01909	0.05083
P21291	CSRP1	0.00000	0.04364	0.04000
P21333	FLNA	0.00000	0.01000	0.05167
P21796	VDAC1	0.10400	0.00000	0.04167
P21860	ERBB3	0.00000	0.00000	0.00500
P21926	CD9	0.03800	0.06909	0.09500
P21964	COMT	0.03200	0.10455	0.16500
P21980	TGM2	0.05600	0.02182	0.07167
P22061	PCMT1	0.00000	0.07273	0.10000
P22079	LPO	0.09500	0.03091	0.10417
P22102	GART	0.00000	0.00000	0.00667
P22234	PAICS	0.00000	0.00000	0.01583
P22307	SCP2	0.00000	0.00000	0.02000
P22314	UBA1	0.06800	0.15727	0.23083
P22352	GPX3	0.03800	0.10455	0.13750
P22392	NME2	0.69300	1.96636	1.79833
P22528	SPRR1B	0.24200	0.77000	0.50417
P22531	SPRR2E	0.00000	0.89182	0.00000
P22532	SPRR2D	0.00000	0.89182	0.00000
P22626	HNRNPA2B1	0.26100	0.65909	0.68500
P22695	UQCRC2	0.01900	0.00000	0.00000
P22735	TGM1	0.00000	0.01364	0.00000
P22792	CPN2	0.00000	0.03455	0.00000
P22894	MMP8	0.03700	0.09364	0.05417
P23141	CES1	0.01400	0.00000	0.00000
P23142	FBLN1	0.00000	0.00000	0.06167
P23246	SFPQ	0.03200	0.01091	0.05917
P23284	PPIB	0.12600	0.26273	0.44833
P23381	WARS	0.06600	0.25636	0.10000
P23396	RPS3	0.39600	0.59818	0.88917
P23490	LOR	0.03700	0.00000	0.00000
P23526	AHCY	0.03000	0.06273	0.22333
P23528	CFL1	0.68400	1.96000	2.51750
P24158	PRTN3	0.05600	0.14727	0.04667
P24534	EEF1B2	0.04000	0.03636	0.10000
P24539	ATP5PB	0.00000	0.00000	0.02833
P24666	ACP1	0.00000	0.05182	0.14250

P24821	TNC	0.00000	0.00818	0.01750
P25311	AZGP1	1.90300	2.60273	2.37417
P25398	RPS12	0.00000	0.11818	0.23167
P25705	ATP5F1A	0.19100	0.00000	0.08500
P25774	CTSS	0.02500	0.11818	0.07417
P25786	PSMA1	0.13400	0.54636	0.78250
P25787	PSMA2	0.00000	0.08182	0.12667
P25788	PSMA3	0.05500	0.29273	0.44333
P25789	PSMA4	0.12900	0.33909	0.31083
P25815	S100P	0.92900	1.71909	1.67500
P26038	MSN	0.32100	0.47364	0.72667
P26373	RPL13	0.00000	0.06091	0.00000
P26447	S100A4	0.87000	2.14273	1.88167
P26583	HMGB2	0.00000	0.00000	0.05667
P26599	PTBP1	0.00000	0.02273	0.01333
P26639	TARS	0.00000	0.01000	0.03750
P26640	VARS	0.00000	0.00545	0.00000
P26641	EEF1G	0.05800	0.18455	0.20250
P27105	STOM	0.28100	0.13545	0.00000
P27169	PON1	0.04700	0.22727	0.12750
P27348	YWHAQ	0.49800	1.11455	1.96167
P27361	MAPK3	0.00000	0.01909	0.02833
P27482	CALML3	0.16600	0.56000	0.27667
P27487	DPP4	0.02100	0.05545	0.00000
P27695	APEX1	0.00000	0.02364	0.04333
P27797	CALR	0.00000	0.00000	0.01583
P27824	CANX	0.01300	0.00000	0.00000
P28062	PSMB8	0.00000	0.14636	0.18667
P28065	PSMB9	0.17700	0.27818	0.32917
P28066	PSMA5	0.24200	0.60636	0.48833
P28070	PSMB4	0.08700	0.18545	0.20750
P28072	PSMB6	0.00000	0.12909	0.24750
P28074	PSMB5	0.00000	0.00000	0.15667
P28482	MAPK1	0.00000	0.00000	0.09500
P28676	GCA	0.29100	0.09000	0.00000
P28838	LAP3	0.10400	0.31364	0.24250
P29034	S100A2	0.10700	0.38636	0.60583
P29218	IMPA1	0.00000	0.07545	0.09583
P29401	TKT	0.45300	0.56818	0.60500
P29508	SERPINB3	1.91700	4.11909	3.79417
P29622	SERPINA4	0.00000	0.14364	0.03167
P29692	EEF1D	0.00000	0.15273	0.16833
P30041	PRDX6	0.83000	1.88455	2.23750
P30043	BLVRB	0.04600	0.32364	0.28833
P30044	PRDX5	0.86000	1.61909	1.41917
P30048	PRDX3	0.00000	0.03182	0.06833
P30049	ATP5F1D	0.06100	0.00000	0.05083
P30050	RPL12	0.00000	0.05364	0.34750
P30084	ECHS1	0.04900	0.00000	0.04000
P30085	CMPK1	0.07500	0.26909	0.36167
P30086	PEBP1	0.31200	0.70545	0.86417
P30101	PDIA3	0.09500	0.09273	0.16917
P30153	PPP2R1A	0.00000	0.02636	0.06083
P30520	ADSS	0.00000	0.00000	0.01500
P30622	CLIP1	0.00000	0.01000	0.00000
P30626	SRI	0.11400	0.04182	0.13167
P30740	SERPINB1	0.66200	1.62364	1.44417
P30838	ALDH3A1	0.85800	1.60727	1.33333

P31025	LCN1	1.48100	2.04091	3.17000
P31146	CORO1A	0.05000	0.15455	0.23333
P31151	S100A7	0.20800	1.27182	1.14917
P31513	FMO3	0.00000	0.00000	0.01250
P31939	ATIC	0.00000	0.00000	0.02500
P31944	CASP14	0.60900	0.66000	0.33833
P31946	YWHAB	1.44700	2.58000	2.19833
P31947	SFN	1.71700	3.48273	2.68917
P31948	STIP1	0.00000	0.00000	0.01833
P31949	S100A11	2.18200	3.41545	3.22917
P31997	CEACAM8	0.02400	0.00000	0.00000
P32119	PRDX2	0.90000	1.37273	1.64750
P32455	GBP1	0.00000	0.02545	0.03750
P32969	RPL9	0.00000	0.07000	0.07667
P32969	RPL9P7	0.00000	0.07000	0.07667
P32969	RPL9P8	0.00000	0.07000	0.07667
P32969	RPL9P9	0.00000	0.07000	0.07667
P33176	KIF5B	0.01700	0.01091	0.04417
P33764	S100A3	0.64400	0.00000	0.00000
P34096	RNASE4	0.22900	0.24818	0.00000
P34932	HSPA4	0.00000	0.03545	0.05417
P35080	PFN2	0.00000	0.12909	0.17750
P35221	CTNNA1	0.02900	0.01182	0.03000
P35228	NOS2	0.00000	0.00909	0.00000
P35232	PHB	0.20900	0.00000	0.08500
P35237	SERPINB6	0.03400	0.04000	0.15083
P35268	RPL22	0.20600	0.25455	0.27833
P35321	SPRR1A	0.00000	0.35455	0.00000
P35527	KRT9	10.85300	6.79727	6.46250
P35542	SAA4	0.00000	0.06727	0.00000
P35573	AGL	0.00000	0.01909	0.04583
P35579	MYH9	0.25500	0.18364	0.25250
P35580	MYH10	0.00000	0.01273	0.00000
P35606	COPB2	0.03300	0.01182	0.02583
P35749	MYH11	0.00000	0.00000	0.01167
P35908	KRT2	8.94800	9.93091	7.30667
P35916	FLT4	0.00000	0.00000	0.00500
P35998	PSMC2	0.00000	0.02636	0.03417
P36542	ATP5F1C	0.08900	0.00000	0.03833
P36543	ATP6V1E1	0.00000	0.14636	0.34167
P36871	PGM1	0.00000	0.00000	0.06083
P36952	SERPINB5	0.21700	0.38818	0.53000
P36955	SERPINF1	0.17200	0.36000	0.32250
P36969	GPX4	0.00000	0.00000	0.06167
P36980	CFHR2	0.00000	0.02727	0.02500
P37802	TAGLN2	0.66300	1.62273	1.71417
P37837	TALDO1	0.70400	1.14000	1.26167
P38159	RBMX	0.00000	0.04455	0.09417
P38405	GNAL	0.00000	0.01909	0.00000
P38606	ATP6V1A	0.01300	0.01182	0.03417
P38646	HSPA9	0.02600	0.00000	0.00000
P39019	RPS19	0.00000	0.06091	0.11167
P39023	RPL3	0.00000	0.00000	0.01667
P39687	ANP32A	0.00000	0.05000	0.25083
P40121	CAPG	0.06300	0.42000	0.49833
P40199	CEACAM6	0.04000	0.02273	0.00000
P40227	CCT6A	0.00000	0.08182	0.13750
P40306	PSMB10	0.05400	0.07091	0.18000

P40394	ADH7	0.26300	0.75636	1.21167
P40429	RPL13A	0.00000	0.03818	0.00000
P40616	ARL1	0.00000	0.04545	0.07000
P40692	MLH1	0.01000	0.00000	0.00000
P40763	STAT3	0.00000	0.00000	0.00833
P40925	MDH1	0.28200	1.05273	0.87250
P40926	MDH2	0.24800	0.37182	0.46833
P41091	EIF2S3	0.00000	0.00000	0.03250
P41218	MNDA	0.04400	0.05818	0.16667
P41250	GARS	0.00000	0.00000	0.01333
P41252	IARS	0.01200	0.02818	0.02000
P42025	ACTR1B	0.00000	0.03182	0.01833
P42224	STAT1	0.02600	0.08000	0.07167
P42330	AKR1C3	0.12100	0.48091	0.44667
P42574	CASP3	0.03000	0.09818	0.09000
P42704	LRPPRC	0.00800	0.00000	0.00417
P43487	RANBP1	0.00000	0.03909	0.13083
P43490	NAMPT	0.06200	0.12636	0.22250
P43652	AFM	0.12900	0.47909	0.37833
P43686	PSMC4	0.00000	0.01727	0.04667
P45880	VDAC2	0.03000	0.00000	0.04000
P45974	USP5	0.00000	0.01727	0.00750
P46100	ATRX	0.00000	0.00273	0.00000
P46779	RPL28	0.07000	0.00000	0.00000
P46781	RPS9	0.22000	0.18364	0.29667
P46782	RPS5	0.00000	0.06545	0.08833
P46783	RPS10	0.00000	0.00000	0.04583
P46926	GNPDA1	0.00000	0.08091	0.13000
P46940	IQGAP1	0.05300	0.05545	0.14667
P46976	GYG1	0.00000	0.02182	0.06167
P47755	CAPZA2	0.02900	0.15818	0.09667
P47756	CAPZB	0.06100	0.24636	0.26167
P47897	QARS	0.01000	0.02455	0.03000
P47929	LGALS7	0.71600	2.27182	1.03500
P47929	LGALS7B	0.71600	2.27182	1.03500
P48047	ATP5PO	0.00000	0.00000	0.05917
P48059	LIMS1	0.00000	0.00000	0.02000
P48444	ARCN1	0.00000	0.06455	0.03667
P48506	GCLC	0.00000	0.00000	0.03417
P48556	PSMD8	0.00000	0.03364	0.05000
P48594	SERPINB4	0.42300	0.95091	1.04667
P48595	SERPINB10	0.00000	0.06818	0.00000
P48637	GSS	0.04500	0.08364	0.12583
P48643	CCT5	0.00000	0.00000	0.01250
P48668	KRT6C	1.14800	5.94273	0.51250
P48735	IDH2	0.05600	0.01636	0.02333
P48741	HSPA7	0.00000	0.30091	0.17583
P49189	ALDH9A1	0.01700	0.03909	0.12083
P49247	RPIA	0.00000	0.02545	0.04667
P49327	FASN	0.01100	0.09636	0.08583
P49368	CCT3	0.05500	0.01364	0.08333
P49411	TUFM	0.01900	0.00000	0.00000
P49419	ALDH7A1	0.00000	0.00000	0.01250
P49441	INPP1	0.00000	0.00000	0.01750
P49458	SRP9	0.00000	0.00000	0.29583
P49720	PSMB3	0.00000	0.17182	0.42500
P49721	PSMB2	0.04400	0.28364	0.46000
P49748	ACADVL	0.02000	0.00000	0.00000

P49755	TMED10	0.04000	0.00000	0.05417
P49773	HINT1	0.00000	0.29545	0.20250
P49788	RARRES1	0.07500	0.00000	0.00000
P49913	CAMP	0.69400	0.30000	0.51750
P50135	HNMT	0.00000	0.06727	0.06083
P50225	SULT1A1	0.00000	0.06545	0.03750
P50395	GDI2	0.17500	0.42727	0.37667
P50452	SERPINB8	0.00000	0.00000	0.08500
P50453	SERPINB9	0.00000	0.00000	0.04000
P50502	ST13	0.00000	0.00000	0.01833
P50583	NUDT2	0.00000	0.00000	0.15583
P50851	LRBA	0.00000	0.00000	0.00333
P50914	RPL14	0.04300	0.00000	0.07167
P50990	CCT8	0.00000	0.08182	0.25250
P50991	CCT4	0.00000	0.05364	0.13833
P50995	ANXA11	0.00000	0.00000	0.04917
P51148	RAB5C	0.00000	0.09364	0.09333
P51149	RAB7A	0.00000	0.28455	0.65250
P51571	SSR4	0.05500	0.00000	0.00000
P51572	BCAP31	0.13900	0.00000	0.06833
P51580	TPMT	0.00000	0.03091	0.02833
P51665	PSMD7	0.00000	0.06909	0.04167
P51795	CLCN5	0.00000	0.01000	0.00000
P51812	RPS6KA3	0.00000	0.00000	0.00917
P51858	HDGF	0.00000	0.03364	0.06167
P51884	LUM	0.00000	0.11818	0.06000
P51991	HNRNPA3	0.04800	0.05545	0.12750
P52209	PGD	0.39700	0.61727	0.85333
P52272	HNRNPM	0.00000	0.02182	0.01833
P52565	ARHGDIA	0.04400	0.22909	0.38500
P52566	ARHGDIB	0.40400	0.81545	1.17583
P52740	ZNF132	0.00000	0.00000	0.02750
P52788	SMS	0.00000	0.00000	0.01833
P52790	HK3	0.00000	0.01182	0.01083
P52895	AKR1C2	0.33500	0.64818	0.63083
P52907	CAPZA1	0.00000	0.04182	0.03833
P53004	BLVRA	0.00000	0.07818	0.16000
P53396	ACLY	0.00000	0.00000	0.00583
P53618	COPB1	0.01700	0.02818	0.01000
P53621	COPA	0.04900	0.03182	0.05917
P53634	CTSC	0.00000	0.00000	0.01417
P53671	LIMK2	0.00000	0.00000	0.01000
P53680	AP2S1	0.00000	0.05636	0.00000
P53990	IST1	0.00000	0.00000	0.01917
P53999	SUB1	0.00000	0.00000	0.06417
P54108	CRISP3	0.12400	0.14364	0.10333
P54136	RARS	0.00000	0.00000	0.01500
P54652	HSPA2	0.00000	0.01818	0.00000
P54727	RAD23B	0.00000	0.00000	0.01833
P54819	AK2	0.00000	0.00000	0.07250
P54920	NAPA	0.00000	0.00000	0.03750
P55058	PLTP	0.21400	0.08727	0.18833
P55060	CSE1L	0.00000	0.01455	0.00000
P55072	VCP	0.18800	0.28909	0.42250
P55210	CASP7	0.00000	0.02455	0.00000
P55259	GP2	0.02300	0.00000	0.00000
P55263	ADK	0.00000	0.00000	0.03833
P55327	TPD52	0.00000	0.00000	0.03417

P55786	NPEPPS	0.05600	0.06364	0.18083
P55854	SUMO3	0.00000	0.00000	0.08500
P55884	EIF3B	0.02000	0.00909	0.01667
P56192	MARS	0.00000	0.00818	0.00000
P56537	EIF6	0.00000	0.19273	0.15833
P56715	RP1	0.00400	0.00000	0.00000
P57735	RAB25	0.00000	0.10182	0.16333
P58107	EPPK1	0.00200	0.01182	0.00000
P58499	FAM3B	0.00000	0.03364	0.00000
P59665	DEFA1	0.91300	1.33727	0.96750
P59665	DEFA1B	0.91300	1.33727	0.96750
P59827	BPIFB4	0.07800	0.00000	0.00000
P59998	ARPC4	0.87300	1.25364	1.02250
P60174	TPI1	1.06600	1.90545	1.78333
P60228	EIF3E	0.01700	0.02455	0.01417
P60660	MYL6	0.63900	0.61818	0.84167
P60709	ACTB	2.01300	3.37727	3.11500
P60763	RAC3	0.11600	0.04273	0.13000
P60842	EIF4A1	0.14600	0.23091	0.41000
P60866	RPS20	0.00000	0.07727	0.14167
P60900	PSMA6	0.12700	0.50182	0.70667
P60903	S100A10	0.10700	0.00000	0.17667
P60953	CDC42	0.07900	0.19273	0.30000
P60981	DSTN	0.09400	0.79909	1.30750
P60983	GMFB	0.00000	0.00000	0.09083
P61006	RAB8A	0.10200	0.12727	0.14167
P61019	RAB2A	0.04200	0.27091	0.44333
P61020	RAB5B	0.00000	0.03818	0.03500
P61026	RAB10	0.20200	0.30364	0.55000
P61081	UBE2M	0.00000	0.00000	0.04000
P61086	UBE2K	0.00000	0.06727	0.13667
P61088	UBE2N	0.00000	0.21273	0.33000
P61106	RAB14	0.11100	0.12545	0.28417
P61158	ACTR3	0.04900	0.17364	0.21583
P61160	ACTR2	0.11100	0.13455	0.17500
P61204	ARF3	0.66300	0.87455	0.89333
P61224	RAP1B	0.12900	0.07364	0.20083
P61247	RPS3A	0.03200	0.12000	0.10500
P61289	PSME3	0.00000	0.04818	0.02750
P61313	RPL15	0.04100	0.03727	0.00000
P61353	RPL27	0.07000	0.06273	0.00000
P61457	PCBD1	0.00000	0.00000	0.30917
P61586	RHOA	0.24500	0.31000	0.35333
P61604	HSPE1	0.56400	0.19000	0.46667
P61626	LYZ	5.96500	7.35000	8.36917
P61758	VBP1	0.00000	0.00000	0.03667
P61769	B2M	0.71700	0.66727	0.80000
P61803	DAD1	0.16600	0.00000	0.00000
P61916	NPC2	0.06400	0.37364	0.42333
P61923	COPZ1	0.00000	0.00000	0.04250
P61956	SUMO2	0.00000	0.20455	0.37333
P61970	NUTF2	0.00000	0.06909	0.12667
P61978	HNRNPK	0.00000	0.07727	0.11083
P61981	YWHAG	0.50600	1.05909	1.18750
P62081	RPS7	0.00000	0.10273	0.17083
P62140	PPP1CB	0.00000	0.03545	0.04167
P62195	PSMC5	0.02000	0.04091	0.04333
P62241	RPS8	0.06800	0.06091	0.09000

P62244	RPS15A	0.13000	0.27091	0.43000
P62249	RPS16	0.25200	0.31818	0.52583
P62258	YWHAE	1.34500	2.89455	3.16000
P62263	RPS14	0.06600	0.06000	0.00000
P62269	RPS18	0.30900	0.14091	0.48500
P62277	RPS13	0.06200	0.05636	0.00000
P62280	RPS11	0.05700	0.08727	0.12750
P62310	LSM3	0.00000	0.09091	0.25000
P62314	SNRPD1	0.00000	0.00000	0.14333
P62316	SNRPD2	0.08300	0.07545	0.31583
P62318	SNRPD3	0.08100	0.14545	0.26750
P62330	ARF6	0.05100	0.04636	0.11417
P62333	PSMC6	0.00000	0.04182	0.03500
P62424	RPL7A	0.00000	0.02909	0.02667
P62495	ETF1	0.01900	0.00000	0.00000
P62701	RPS4X	0.10600	0.06818	0.18000
P62736	ACTA2	0.31600	0.20818	0.29167
P62750	RPL23A	0.06000	0.00000	0.31667
P62753	RPS6	0.03400	0.07182	0.02833
P62805	HIST1H4A	3.97500	3.17727	3.03417
P62805	HIST1H4B	3.97500	3.17727	3.03417
P62805	HIST1H4C	3.97500	3.17727	3.03417
P62805	HIST1H4D	3.97500	3.17727	3.03417
P62805	HIST1H4E	3.97500	3.17727	3.03417
P62805	HIST1H4F	3.97500	3.17727	3.03417
P62805	HIST1H4H	3.97500	3.17727	3.03417
P62805	HIST1H4I	3.97500	3.17727	3.03417
P62805	HIST1H4J	3.97500	3.17727	3.03417
P62805	HIST1H4K	3.97500	3.17727	3.03417
P62805	HIST1H4L	3.97500	3.17727	3.03417
P62805	HIST2H4A	3.97500	3.17727	3.03417
P62805	HIST2H4B	3.97500	3.17727	3.03417
P62805	HIST4H4	3.97500	3.17727	3.03417
P62820	RAB1A	0.20000	0.23545	0.55583
P62826	RAN	0.04100	0.22455	0.30083
P62829	RPL23	0.07400	0.00000	0.06167
P62851	RPS25	0.14700	0.21091	0.43333
P62854	RPS26	0.15400	0.13909	0.00000
P62857	RPS28	0.36000	0.16273	0.59667
P62873	GNB1	0.00000	0.02273	0.02083
P62888	RPL30	0.08900	0.08091	0.07417
P62906	RPL10A	0.04000	0.05909	0.03333
P62913	RPL11	0.05100	0.04545	0.15333
P62917	RPL8	0.00000	0.03182	0.02917
P62937	PPIA	2.82900	3.32273	3.20667
P62979	RPS27A	0.87900	1.11091	1.18417
P62993	GRB2	0.00000	0.00000	0.05333
P63000	RAC1	0.00000	0.14455	0.26500
P63092	GNAS	0.00000	0.00000	0.01667
P63104	YWHAZ	2.36300	3.98364	4.07667
P63165	SUMO1	0.00000	0.00000	0.08500
P63167	DYNLL1	0.00000	0.10636	0.29250
P63173	RPL38	0.00000	0.00000	0.27583
P63208	SKP1	0.00000	0.05000	0.00000
P63220	RPS21	0.28600	0.50182	0.57917
P63241	EIF5A	0.06300	0.56273	0.82500
P63244	RACK1	0.06100	0.26091	0.13583
P67936	TPM4	0.00000	0.22545	0.58417

P68032	ACTC1	0.00000	0.77182	0.00000
P68036	UBE2L3	0.05900	0.23000	0.37667
P68104	EEF1A1	0.00000	0.13636	0.00000
P68366	TUBA4A	0.00000	0.11818	0.24500
P68371	TUBB4B	0.38700	0.55000	0.75833
P68871	HBB	2.29900	7.30727	3.95583
P69891	HBG1	0.00000	0.37273	0.00000
P69905	HBA1	0.94800	6.19091	1.21167
P69905	HBA2	0.94800	6.19091	1.21167
P78371	CCT2	0.00000	0.08455	0.15917
P78385	KRT83	3.96300	2.33727	0.00000
P78386	KRT85	4.22400	3.43091	0.18917
P78417	GSTO1	0.14700	0.48000	0.64917
P78527	PRKDC	0.00300	0.01273	0.01500
P80188	LCN2	1.93600	2.67909	2.20083
P80303	NUCB2	0.12100	0.13091	0.20750
P80511	S100A12	1.15300	1.80000	1.27333
P80748	IGLV3-21	0.00000	0.08364	0.00000
P81605	DCD	1.06100	1.41364	0.97083
P83731	RPL24	0.00000	0.05364	0.00000
P84085	ARF5	0.26000	0.36636	0.50667
P84095	RHOG	0.00000	0.00000	0.03917
P84098	RPL19	0.04300	0.06364	0.03583
P84103	SRSF3	0.05300	0.00000	0.04417
P98088	MUC5AC	0.13600	0.01000	0.00667
P98160	HSPG2	0.00200	0.00000	0.00000
P98161	PKD1	0.00000	0.00000	0.00167
P98171	ARHGAP4	0.00000	0.00727	0.00000
P99999	CYCS	0.00000	0.90636	0.70500
Q00325	SLC25A3	0.12400	0.00000	0.04250
Q00341	HDLBP	0.00600	0.00000	0.00000
Q00610	CLTC	0.13800	0.13091	0.19000
Q00765	REEP5	0.04700	0.04273	0.07833
Q00796	SORD	0.13800	0.39273	0.51667
Q01082	SPTBN1	0.02200	0.03636	0.07333
Q01105	SET	0.02900	0.12091	0.13833
Q01469	FABP5	1.55200	2.97545	3.02667
Q01518	CAP1	0.12200	0.44818	0.55417
Q01546	KRT76	0.11500	0.53909	0.00000
Q01813	PFKP	0.01000	0.05000	0.08250
Q02383	SEMG2	0.02100	0.01909	0.35583
Q02413	DSG1	0.19300	0.20818	0.10000
Q02817	MUC2	0.00600	0.00000	0.00000
Q02818	NUCB1	0.01700	0.00000	0.02250
Q02878	RPL6	0.00000	0.06091	0.00000
Q03252	LMNB2	0.00000	0.00000	0.01083
Q03591	CFHR1	0.00000	0.11455	0.15667
Q04637	EIF4G1	0.00000	0.00636	0.00000
Q04695	KRT17	4.43700	5.15455	2.93000
Q04760	GLO1	0.00000	0.11000	0.35083
Q04828	AKR1C1	0.42400	0.92091	0.93833
Q04837	SSBP1	0.10700	0.00000	0.00000
Q04917	YWHAH	0.22400	0.52273	0.70333
Q05315	CLC	0.00000	0.22091	0.05417
Q06033	ITIH3	0.00000	0.00818	0.00000
Q06210	GFPT1	0.02200	0.02182	0.05750
Q06323	PSME1	0.69400	1.75455	1.56083
Q06830	PRDX1	3.98200	5.72545	6.19333

Q07020	RPL18	0.00000	0.00000	0.07833
Q07654	TFF3	0.00000	0.25818	0.00000
Q07960	ARHGAP1	0.00000	0.02545	0.01500
Q08188	TGM3	0.05100	0.02727	0.03000
Q08211	DHX9	0.02700	0.02455	0.02417
Q08257	CRYZ	0.00000	0.00000	0.03583
Q08380	LGALS3BP	0.37100	0.19000	0.35083
Q08554	DSC1	0.07700	0.04818	0.03750
Q09472	EP300	0.00000	0.00273	0.00000
Q09666	AHNAK	0.00200	0.00818	0.02833
Q0VDD8	DNAH14	0.00000	0.00636	0.00000
Q10567	AP1B1	0.00800	0.00727	0.00000
Q10588	BST1	0.00000	0.02364	0.00000
Q12792	TWF1	0.02300	0.06727	0.06250
Q12905	ILF2	0.00000	0.03091	0.07417
Q12906	ILF3	0.00000	0.02273	0.03667
Q12996	CSTF3	0.01100	0.03000	0.00917
Q13045	FLII	0.00000	0.00000	0.00500
Q13126	MTAP	0.00000	0.04455	0.08167
Q13162	PRDX4	0.00000	0.00000	0.04250
Q13200	PSMD2	0.01800	0.03636	0.04167
Q13201	MMRN1	0.00000	0.00000	0.00500
Q13228	SELENBP1	0.32900	0.75273	0.83750
Q13231	CHIT1	0.00000	0.00000	0.02250
Q13263	TRIM28	0.00000	0.00000	0.00833
Q13347	EIF3I	0.00000	0.02364	0.00000
Q13363	CTBP1	0.00000	0.00000	0.01583
Q13367	AP3B2	0.00700	0.00000	0.00000
Q13404	UBE2V1	0.11200	0.43000	0.47000
Q13409	DYNC1I2	0.00000	0.00000	0.02583
Q13421	MSLN	0.19700	0.21636	0.17500
Q13510	ASAH1	0.16800	0.42091	0.39667
Q13576	IQGAP2	0.00000	0.00000	0.00833
Q13618	CUL3	0.00000	0.00000	0.00833
Q13620	CUL4B	0.00000	0.00000	0.00667
Q13630	TSTA3	0.04200	0.03818	0.12667
Q13740	ALCAM	0.01400	0.06000	0.04083
Q13797	ITGA9	0.00000	0.00000	0.00667
Q13813	SPTAN1	0.01600	0.04636	0.09167
Q13835	PKP1	0.15700	0.11727	0.07833
Q13838	DDX39B	0.00000	0.06091	0.06833
Q13867	BLMH	0.02700	0.01545	0.00000
Q13885	TUBB2A	0.00000	0.17909	0.00000
Q13938	CAPS	0.84200	1.61273	1.89083
Q14011	CIRBP	0.05700	0.05091	0.14000
Q14019	COTL1	0.25200	0.94636	0.82167
Q14103	HNRNPD	0.00000	0.10000	0.18250
Q14116	IL18	0.04500	0.06727	0.24333
Q14134	TRIM29	0.00000	0.01273	0.01167
Q14152	EIF3A	0.03200	0.02091	0.03250
Q14203	DCTN1	0.00600	0.01182	0.01000
Q14204	DYNC1H1	0.02000	0.06364	0.12083
Q14210	LY6D	0.00000	0.07364	0.06750
Q14232	EIF2B1	0.00000	0.02545	0.03750
Q14240	EIF4A2	0.00000	0.08636	0.02583
Q14315	FLNC	0.00000	0.00273	0.00000
Q14376	GALE	0.02400	0.02182	0.04000
Q14508	WFDC2	0.16100	0.14727	0.13500

Q14525	KRT33B	1.80600	1.94091	0.29750
Q14532	KRT32	0.58800	0.49273	0.04167
Q14533	KRT81	3.46100	1.12909	0.00000
Q14624	ITIH4	0.26000	0.58000	0.43250
Q14651	PLS1	0.01300	0.00000	0.03917
Q14686	NCOA6	0.00000	0.00000	0.00333
Q14697	GANAB	0.02500	0.00727	0.00667
Q14739	LBR	0.02000	0.00000	0.00000
Q14764	MVP	0.23700	0.27273	0.33917
Q14847	LASP1	0.03200	0.00000	0.14917
Q14894	CRYM	0.15600	0.50273	0.53000
Q14914	PTGR1	0.04200	0.00000	0.06500
Q14974	KPNB1	0.02400	0.02182	0.02750
Q14CN4	KRT72	0.04500	0.26909	0.11500
Q15008	PSMD6	0.00000	0.04091	0.01667
Q15019	SEPTIN2	0.00000	0.00000	0.06583
Q15046	KARS	0.00000	0.00000	0.01083
Q15063	POSTN	0.00000	0.01273	0.06000
Q15075	EEA1	0.00000	0.01273	0.02167
Q15080	NCF4	0.00000	0.00000	0.03167
Q15102	PAFAH1B3	0.00000	0.03455	0.03167
Q15149	PLEC	0.01900	0.06000	0.08500
Q15181	PPA1	0.07600	0.27909	0.41083
Q15185	PTGES3	0.00000	0.08455	0.12333
Q15233	NONO	0.00000	0.00000	0.03917
Q15257	PTPA	0.00000	0.04636	0.09000
Q15323	KRT31	1.66000	2.21636	0.38917
Q15365	PCBP1	0.02500	0.14455	0.27500
Q15366	PCBP2	0.00000	0.00000	0.04500
Q15370	ELOB	0.00000	0.29909	0.46000
Q15382	RHEB	0.08400	0.07636	0.41417
Q15393	SF3B3	0.00000	0.00545	0.00500
Q15517	CDSN	0.01800	0.00000	0.00000
Q15631	TSN	0.00000	0.14455	0.12500
Q15691	MAPRE1	0.00000	0.00000	0.02667
Q15772	SPEG	0.00000	0.00000	0.00500
Q15819	UBE2V2	0.00000	0.10273	0.24333
Q15907	RAB11B	0.17500	0.52182	0.45667
Q16181	SEPTIN7	0.00000	0.01636	0.02333
Q16204	CCDC6	0.00000	0.00000	0.01417
Q16378	PRR4	0.07300	0.06636	0.06083
Q16478	GRIK5	0.00000	0.00000	0.00667
Q16531	DDB1	0.00000	0.03182	0.03667
Q16629	SRSF7	0.03600	0.00000	0.00000
Q16698	DECR1	0.02600	0.00000	0.03500
Q16719	KYNU	0.01700	0.00000	0.02833
Q16777	HIST2H2AC	0.22700	0.00000	0.00000
Q16836	HADH	0.00000	0.00000	0.02333
Q16851	UGP2	0.02500	0.19636	0.30417
Q16881	TXNRD1	0.00000	0.02909	0.04833
Q16891	IMMT	0.01100	0.00000	0.00000
Q2TAA8	TSNAXIP1	0.01200	0.00000	0.00000
Q2VIQ3	KIF4B	0.00600	0.00000	0.00000
Q2VIR3	EIF2S3B	0.00000	0.01636	0.00000
Q32MZ4	LRRFIP1	0.00000	0.02455	0.07750
Q3SY84	KRT71	0.00000	0.05000	0.00000
Q3V6T2	CCDC88A	0.00000	0.00000	0.00333
Q3ZCM7	TUBB8	0.00000	0.00000	0.01500

Q4G0X9	CCDC40	0.01400	0.01909	0.02000
Q53GD3	SLC44A4	0.00000	0.01545	0.00000
Q53H82	LACTB2	0.00000	0.00000	0.02417
Q562R1	ACTBL2	0.08200	0.00000	0.12500
Q58FG1	HSP90AA4P	0.00000	0.02727	0.00000
Q5CZC0	FSIP2	0.00000	0.00000	0.00083
Q5D862	FLG2	0.03000	0.04545	0.02500
Q5JW98	CALHM4	0.07900	0.00000	0.00000
Q5JXB2	UBE2NL	0.06200	0.11273	0.13917
Q5M775	SPECC1	0.00000	0.00000	0.00583
Q5QNW6	HIST2H2BF	1.66300	1.00182	0.80500
Q5SYB0	FRMPD1	0.00000	0.00455	0.00000
Q5T200	ZC3H13	0.00000	0.00000	0.00333
Q5T749	KPRP	0.01300	0.10818	0.08917
Q5TCS8	AK9	0.00400	0.00000	0.00000
Q5THR3	EFCAB6	0.00000	0.00000	0.00417
Q5TZA2	CROCC	0.01200	0.01455	0.00667
Q5VTE0	EEF1A1P5	0.42200	0.58636	0.68167
Q5VW32	BROX	0.00000	0.01818	0.00000
Q63HK5	TSHZ3	0.00000	0.00000	0.01167
Q63HN8	RNF213	0.00000	0.00182	0.00000
Q63HR2	TNS2	0.00600	0.00000	0.00500
Q68DQ2	CRYBG3	0.00300	0.00000	0.00000
Q6A162	KRT40	0.00000	0.04818	0.02417
Q6A163	KRT39	0.18200	0.03727	0.00000
Q6BCY4	CYB5R2	0.00000	0.02727	0.02500
Q6DN03	HIST2H2BC	0.11400	0.00000	0.00000
Q6EMB2	TTLL5	0.00600	0.00000	0.00000
Q6GMV3	PTRHD1	0.00000	0.06273	0.11500
Q6IS14	EIF5AL1	0.00000	0.05727	0.00000
Q6KB66	KRT80	0.09700	0.03273	0.04500
Q6MZM0	HEPHL1	0.01000	0.00000	0.00000
Q6P4A8	PLBD1	0.00000	0.02818	0.00000
Q6P5S2	LEG1	0.42600	0.49909	0.58083
Q6PRD1	GPR179	0.00000	0.00273	0.00000
Q6S8J3	POTEE	0.05100	0.08818	0.16667
Q6UWP8	SBSN	0.06100	0.07727	0.03167
Q6UWW0	LCN15	0.34100	0.47727	0.54833
Q6UX06	OLFM4	0.00000	0.00000	0.01333
Q6UXB2	CXCL17	0.16000	0.07273	0.06667
Q6VAB6	KSR2	0.00000	0.00727	0.00667
Q6VUC0	TFAP2E	0.00000	0.01818	0.06667
Q6XQN6	NAPRT	0.00000	0.02182	0.06333
Q6ZMW3	EML6	0.00000	0.00000	0.00333
Q6ZU15	SEPTIN14	0.00000	0.00000	0.01500
Q6ZVX7	NCCRP1	0.00000	0.10182	0.06750
Q6ZWH5	NEK10	0.00000	0.00636	0.00000
Q71DI3	HIST2H3A	0.63800	0.61273	0.84167
Q71DI3	HIST2H3C	0.63800	0.61273	0.84167
Q71DI3	HIST2H3D	0.63800	0.61273	0.84167
Q71UM5	RPS27L	0.13100	0.00000	0.10917
Q7KZF4	SND1	0.01300	0.00818	0.01500
Q7L014	DDX46	0.00000	0.00000	0.01167
Q7L1Q6	BZW1	0.00000	0.01727	0.06667
Q7L266	ASRGL1	0.00000	0.14364	0.03917
Q7L576	CYFIP1	0.02600	0.02364	0.01583
Q7L7X3	TAOK1	0.00000	0.00000	0.02000
Q7L9L4	MOB1B	0.00000	0.03545	0.00000

Q7RTS7	KRT74	0.10000	0.07182	0.13917
Q7Z2K8	GPRIN1	0.00000	0.00818	0.00000
Q7Z3E5	ARMC9	0.01000	0.00000	0.00000
Q7Z3Y7	KRT28	0.06400	0.11636	0.19167
Q7Z3Y8	KRT27	0.02900	0.06273	0.03333
Q7Z406	MYH14	0.12600	0.05455	0.06583
Q7Z4W1	DCXR	0.00000	0.05545	0.10167
Q7Z5L0	VMO1	0.09200	0.04182	0.07667
Q7Z6Z7	HUWE1	0.00000	0.00000	0.00167
Q7Z794	KRT77	0.15200	0.63000	0.55250
Q7Z7A1	CNTRL	0.00000	0.00273	0.00000
Q86SJ6	DSG4	0.01600	0.01455	0.00000
Q86UP2	KTN1	0.00000	0.00727	0.00000
Q86VD1	MORC1	0.00000	0.00000	0.00667
Q86VP6	CAND1	0.00600	0.04909	0.04417
Q86WA8	LONP2	0.00900	0.00000	0.00000
Q86WR0	CCDC25	0.00000	0.00000	0.03333
Q86WX3	RPS19BP1	0.00000	0.06364	0.00000
Q86X76	NIT1	0.00000	0.00000	0.02167
Q86XW9	NME9	0.00000	0.02273	0.00000
Q86Y46	KRT73	0.25300	0.24818	0.09917
Q86YZ3	HRNR	0.07500	0.06182	0.04250
Q8IUC1	KRTAP11-1	0.05700	0.05182	0.00000
Q8IV04	TBC1D10C	0.00000	0.04909	0.01500
Q8IVF6	ANKRD18A	0.00000	0.00727	0.00667
Q8IVL1	NAV2	0.00000	0.00000	0.00250
Q8IWN7	RP1L1	0.00000	0.00273	0.00000
Q8IYW2	CFAP46	0.00000	0.00000	0.00250
Q8IZ83	ALDH16A1	0.00000	0.00909	0.00000
Q8IZP2	ST13P4	0.00000	0.00000	0.04833
Q8N1A0	KRT222	0.00000	0.00000	0.04667
Q8N1N4	KRT78	0.31800	0.24273	0.08500
Q8N335	GPD1L	0.02400	0.08364	0.07917
Q8N3K9	CMYA5	0.00400	0.00727	0.00917
Q8N4F0	BPIFB2	0.58700	0.53455	0.49833
Q8N554	ZNF276	0.00000	0.01182	0.00000
Q8N8N7	PTGR2	0.00000	0.00000	0.02000
Q8NAB2	KBTBD3	0.00000	0.00000	0.01083
Q8NBJ4	GOLM1	0.16500	0.08818	0.06000
Q8NE09	RGS22	0.00600	0.00000	0.00000
Q8NEB7	ACRBP	0.00000	0.00000	0.03000
Q8NFU3	TSTD1	0.09300	0.08455	0.15500
Q8TAX7	MUC7	0.13400	0.13091	0.10000
Q8TCA0	LRRC20	0.00000	0.04545	0.00000
Q8TD57	DNAH3	0.00200	0.00182	0.00000
Q8TDB8	SLC2A14	0.01600	0.00000	0.00000
Q8TDL5	BPIFB1	2.12800	1.29636	1.47250
Q8TDQ7	GNPDA2	0.00000	0.00000	0.04083
Q8TE77	SSH3	0.00000	0.00000	0.01000
Q8TF66	LRRC15	0.02100	0.04000	0.00000
Q8WUM4	PDCD6IP	0.06400	0.06818	0.20083
Q8WVQ1	CANT1	0.00000	0.01909	0.01750
Q8WVV4	POF1B	0.02800	0.07909	0.00000
Q8WVY7	UBLCP1	0.00000	0.00000	0.07000
Q8WW52	FAM151A	0.00000	0.00000	0.01167
Q8WWA0	ITLN1	0.08800	0.09818	0.07333
Q8WXG6	MADD	0.01000	0.00000	0.00000
Q8WXG9	ADGRV1	0.00100	0.00000	0.00000

Q8WXQ8	CPA5	0.01900	0.00000	0.01583
Q8WZ42	TTN	0.00000	0.00182	0.00083
Q92499	DDX1	0.00000	0.00000	0.02250
Q92599	SEPTIN8	0.00000	0.00000	0.02083
Q92616	GCN1	0.00000	0.00364	0.00250
Q92688	ANP32B	0.03400	0.09636	0.20333
Q92734	TFG	0.00000	0.01909	0.01750
Q92743	HTRA1	0.02800	0.00000	0.02333
Q92747	ARPC1A	0.00000	0.00000	0.01833
Q92764	KRT35	1.06700	0.91273	0.03833
Q92817	EVPL	0.00800	0.00364	0.01000
Q92820	GGH	0.00000	0.02364	0.02167
Q92841	DDX17	0.00000	0.00000	0.00917
Q92930	RAB8B	0.00000	0.00000	0.05833
Q92945	KHSRP	0.00000	0.01091	0.02000
Q93008	USP9X	0.00300	0.00000	0.00000
Q969N2	PIGT	0.00000	0.01273	0.00000
Q96A72	MAGOHB	0.00000	0.05636	0.15500
Q96BQ1	FAM3D	0.04000	0.08545	0.00000
Q96BW5	PTER	0.00000	0.03455	0.06000
Q96BY7	ATG2B	0.00000	0.00000	0.00333
Q96C19	EFHD2	0.20000	0.49273	0.64333
Q96CN7	ISOC1	0.00000	0.04273	0.03917
Q96DA0	ZG16B	1.24600	1.34000	1.43667
Q96DB5	RMDN1	0.00000	0.02364	0.00000
Q96DR8	MUCL1	0.00000	0.13182	0.00000
Q96DT5	DNAH11	0.00000	0.00182	0.00000
Q96EN8	MOCOS	0.00000	0.00818	0.00000
Q96FC7	PHYHIPL	0.00000	0.02000	0.00000
Q96FJ2	DYNLL2	0.00000	0.10909	0.29750
Q96FQ6	S100A16	0.10000	0.25636	0.38667
Q96FW1	OTUB1	0.00000	0.13636	0.17750
Q96G03	PGM2	0.00000	0.01818	0.03333
Q96GW7	BCAN	0.00000	0.00000	0.01083
Q96HN2	AHCYL2	0.00000	0.01182	0.02167
Q96IU4	ABHD14B	0.04500	0.12273	0.17500
Q96JH7	VCPIP1	0.00600	0.00545	0.00000
Q96KP4	CNDP2	0.11000	0.16636	0.41083
Q96KR1	ZFR	0.02100	0.02545	0.03333
Q96LP2	FAM81B	0.00000	0.01636	0.00000
Q96NG3	TTC25	0.02400	0.01091	0.00000
Q96NL6	SCLT1	0.03300	0.01000	0.00917
Q96P63	SERPINB12	0.15400	0.03636	0.04250
Q96PD5	PGLYRP2	0.00000	0.01273	0.00000
Q96PI1	SPRR4	0.00000	0.13000	0.00000
Q96QA5	GSDMA	0.00000	0.06091	0.00000
Q96QK1	VPS35	0.00000	0.02909	0.03833
Q96QZ7	MAGI1	0.00000	0.00455	0.00000
Q96T68	SETDB2	0.00000	0.00000	0.00917
Q96TA1	NIBAN2	0.02200	0.03182	0.09417
Q99417	MYCBP	0.00000	0.26727	0.00000
Q99436	PSMB7	0.03200	0.02909	0.08000
Q99459	CDC5L	0.00000	0.00909	0.00833
Q99460	PSMD1	0.01700	0.02000	0.02833
Q99471	PFDN5	0.00000	0.05545	0.08667
Q99497	PARK7	0.70200	1.50364	1.69167
Q99536	VAT1	0.00000	0.00000	0.07250
Q99570	PIK3R4	0.00000	0.00000	0.00500

Q99578	RIT2	0.04000	0.00000	0.00000
Q99584	S100A13	0.00000	0.94273	0.69417
Q99598	TSNAX	0.00000	0.00000	0.02417
Q99623	PHB2	0.14300	0.00000	0.09417
Q99714	HSD17B10	0.05900	0.00000	0.00000
Q99728	BARD1	0.00000	0.00000	0.00833
Q99741	CDC6	0.00000	0.01273	0.00000
Q99798	ACO2	0.01600	0.00000	0.00000
Q99832	CCT7	0.00000	0.00000	0.08583
Q99873	PRMT1	0.00000	0.00000	0.02917
Q99933	BAG1	0.00000	0.00000	0.04500
Q99935	OPRPN	0.00000	0.00000	0.03000
Q9BPU6	DPYSL5	0.01500	0.00000	0.01250
Q9BPX5	ARPC5L	0.00000	0.00000	0.05250
Q9BQE3	TUBA1C	0.29400	0.58636	0.68417
Q9BQE5	APOL2	0.00000	0.03636	0.00000
Q9BR76	CORO1B	0.00000	0.01545	0.05000
Q9BRA2	TXNDC17	0.00000	0.07182	0.24750
Q9BRF8	CPPED1	0.05300	0.10091	0.11583
Q9BS26	ERP44	0.00000	0.00000	0.01583
Q9BS40	LXN	0.03800	0.10364	0.09500
Q9BT78	COPS4	0.00000	0.00000	0.01667
Q9BUL8	PDCD10	0.00000	0.06000	0.16167
Q9BUT1	BDH2	0.00000	0.00000	0.09833
Q9BV20	MRI1	0.00000	0.00000	0.02000
Q9BVA1	TUBB2B	0.01800	0.07364	0.04333
Q9BVJ7	DUSP23	0.00000	0.05818	0.00000
Q9BVK6	TMED9	0.07200	0.00000	0.00000
Q9BW30	TPPP3	0.19900	0.59091	0.62667
Q9BWD1	ACAT2	0.00000	0.03182	0.04750
Q9BXL6	CARD14	0.00000	0.00000	0.00667
Q9BXS5	AP1M1	0.00000	0.01727	0.02500
Q9BYE4	SPRR2G	0.00000	0.00000	0.12750
Q9BYP9	KRTAP9-9	0.05500	0.00000	0.00000
Q9BYQ3	KRTAP9-3	0.05300	0.00000	0.00000
Q9BYR4	KRTAP4-3	0.04100	0.03727	0.00000
Q9BYR8	KRTAP3-1	0.19100	0.09455	0.00000
Q9BZQ8	NIBAN1	0.00000	0.00000	0.01500
Q9BZZ5	API5	0.00000	0.00000	0.01250
Q9C099	LRRCC1	0.00700	0.00000	0.00000
Q9GIY3	HLA-DRB1	0.03200	0.00000	0.00000
Q9GZZ8	LACRT	0.00000	0.32636	0.23333
Q9H008	LHPP	0.00000	0.03000	0.00000
Q9H0U4	RAB1B	0.44200	0.77455	0.74250
Q9H299	SH3BGRL3	0.12000	0.31182	0.56000
Q9H2G2	SLK	0.00600	0.00545	0.03833
Q9H2U2	PPA2	0.00000	0.00000	0.04583
Q9H3K6	BOLA2	0.00000	0.00000	0.10083
Q9H3K6	BOLA2B	0.00000	0.00000	0.10083
Q9H444	CHMP4B	0.00000	0.05909	0.16667
Q9H4G4	GLIPR2	0.06200	0.00000	0.00000
Q9H4M9	EHD1	0.00000	0.00000	0.01917
Q9H6K5	PRR36	0.00700	0.00000	0.00000
Q9H6S0	YTHDC2	0.00000	0.00455	0.00000
Q9H892	TTC12	0.00000	0.00000	0.00917
Q9HAB8	PPCS	0.00000	0.14091	0.21167
Q9HAU5	UPF2	0.00000	0.00000	0.00500
Q9HAV0	GNB4	0.00000	0.00000	0.02083

Q9HB40	SCPEP1	0.00000	0.00000	0.07000
Q9HB71	CACYBP	0.00000	0.00000	0.03083
Q9HBL7	PLGRKT	0.06200	0.00000	0.00000
Q9HC38	GLOD4	0.04300	0.37000	0.34417
Q9HC84	MUC5B	0.13500	0.01455	0.02750
Q9HCY8	S100A14	0.46800	0.18182	0.30333
Q9HD89	RETN	0.09800	0.08909	0.08083
Q9HDC9	APMAP	0.07200	0.00000	0.00000
Q9NP55	BPIFA1	0.93300	1.06636	1.06667
Q9NP58	ABCB6	0.00900	0.02455	0.01500
Q9NPJ3	ACOT13	0.07300	0.00000	0.00000
Q9NQR4	NIT2	0.00000	0.02818	0.04167
Q9NQW7	XPNPEP1	0.00000	0.00000	0.01667
Q9NR31	SAR1A	0.00000	0.04091	0.07500
Q9NR45	NANS	0.02300	0.11636	0.32667
Q9NR48	ASH1L	0.00000	0.00545	0.00000
Q9NRW1	RAB6B	0.00000	0.00000	0.03583
Q9NRX2	MRPL17	0.00000	0.04727	0.00000
Q9NSB2	KRT84	0.05700	0.06091	0.12083
Q9NSB4	KRT82	0.30000	0.53818	0.04667
Q9NTK5	OLA1	0.00000	0.00000	0.05500
Q9NU22	MDN1	0.00000	0.00000	0.00083
Q9NUQ9	FAM49B	0.00000	0.00000	0.08167
Q9NVH2	INTS7	0.00000	0.00000	0.00667
Q9NVJ2	ARL8B	0.04700	0.00000	0.03917
Q9NW64	RBM22	0.00000	0.00000	0.01583
Q9NY33	DPP3	0.01100	0.03273	0.08833
Q9NYL9	TMOD3	0.00000	0.00000	0.03083
Q9NYU2	UGGT1	0.00500	0.00000	0.00000
Q9NZD2	GLTP	0.06900	0.20273	0.44583
Q9NZM1	MYOF	0.00400	0.00000	0.00000
Q9NZT1	CALML5	0.49700	0.93364	0.53750
Q9P0W8	SPATA7	0.02600	0.00000	0.00000
Q9P1Z0	ZBTB4	0.00000	0.00000	0.00667
Q9P227	ARHGAP23	0.00500	0.01818	0.00417
Q9P2D1	CHD7	0.00500	0.00000	0.00250
Q9P2E9	RRBP1	0.00600	0.06364	0.04750
Q9P2M7	CGN	0.00000	0.00000	0.00500
Q9P2R3	ANKFY1	0.00000	0.00000	0.00583
Q9P2T1	GMPR2	0.02500	0.04455	0.03250
Q9UBC9	SPRR3	1.29200	0.98818	1.40583
Q9UBQ0	VPS29	0.00000	0.04545	0.08333
Q9UBR2	CTSZ	0.00000	0.00000	0.02333
Q9UBZ9	REV1	0.00000	0.00545	0.00500
Q9UDY2	TJP2	0.00000	0.00000	0.00583
Q9UFH2	DNAH17	0.00000	0.00000	0.00167
Q9UGM3	DMBT1	0.11800	0.08636	0.13417
Q9UHB6	LIMA1	0.00000	0.00000	0.00833
Q9UHQ9	CYB5R1	0.00000	0.00000	0.02333
Q9UHV9	PFDN2	0.00000	0.22455	0.23917
Q9UIV8	SERPINB13	0.00000	0.06000	0.10333
Q9UJ70	NAGK	0.00000	0.02273	0.05417
Q9UJT2	TSKS	0.00000	0.00000	0.03500
Q9UJT9	FBXL7	0.00000	0.00000	0.02083
Q9UKK3	PARP4	0.00000	0.00000	0.01167
Q9UKM9	RALY	0.00000	0.04273	0.13750
Q9UKX2	MYH2	0.00000	0.00000	0.02500
Q9UL25	RAB21	0.00000	0.06000	0.03333

Q9UL46	PSME2	0.35400	0.56455	0.66500
Q9ULA0	DNPEP	0.00000	0.01545	0.03083
Q9ULZ3	PYCARD	0.04700	0.17727	0.46750
Q9UM07	PADI4	0.00000	0.00000	0.01500
Q9UM54	MYO6	0.01500	0.00000	0.00750
Q9UMN6	KMT2B	0.00000	0.00364	0.00250
Q9UMS4	PRPF19	0.00000	0.00000	0.03500
Q9UMY4	SNX12	0.00000	0.00000	0.17333
Q9UNM6	PSMD13	0.02200	0.12727	0.30167
Q9UNX3	RPL26L1	0.06200	0.05636	0.00000
Q9UQ16	DNM3	0.00000	0.00818	0.00000
Q9UQ35	SRRM2	0.00300	0.00273	0.00000
Q9UQ80	PA2G4	0.00000	0.05545	0.16083
Q9Y230	RUVBL2	0.01800	0.00000	0.05750
Q9Y250	LZTS1	0.00000	0.00000	0.01083
Q9Y262	EIF3L	0.02100	0.00000	0.01083
Q9Y265	RUVBL1	0.00000	0.01636	0.05667
Q9Y266	NUDC	0.00000	0.00000	0.04583
Q9Y277	VDAC3	0.03100	0.00000	0.00000
Q9Y2A7	NCKAP1	0.01000	0.00000	0.00583
Q9Y2H9	MAST1	0.00000	0.00000	0.00417
Q9Y2Q3	GSTK1	0.12700	0.08364	0.13750
Q9Y2S2	CRYL1	0.00000	0.02364	0.00000
Q9Y376	CAB39	0.02400	0.03364	0.05000
Q9Y3C8	UFC1	0.05300	0.00000	0.00000
Q9Y3D6	FIS1	0.00000	0.05727	0.00000
Q9Y3E7	CHMP3	0.00000	0.00000	0.03333
Q9Y3I0	RTCB	0.00000	0.00000	0.01333
Q9Y3U8	RPL36	0.00000	0.00000	0.07917
Q9Y3Z3	SAMHD1	0.00000	0.00000	0.06500
Q9Y446	PKP3	0.00000	0.01455	0.00000
Q9Y490	TLN1	0.00800	0.05727	0.06667
Q9Y4C4	MFHAS1	0.00000	0.00636	0.00000
Q9Y4G6	TLN2	0.00000	0.01000	0.00000
Q9Y4I1	MYO5A	0.00400	0.02545	0.02000
Q9Y4L1	HYOU1	0.01200	0.00000	0.00000
Q9Y566	SHANK1	0.00000	0.00000	0.00333
Q9Y5P6	GMPPB	0.00000	0.02091	0.03833
Q9Y5W7	SNX14	0.00000	0.00000	0.01333
Q9Y5Z4	HEBP2	0.11700	0.34273	0.24083
Q9Y623	MYH4	0.01900	0.00000	0.02500
Q9Y678	COPG1	0.00000	0.01273	0.00750
Q9Y6B6	SAR1B	0.00000	0.00000	0.03750
Q9Y6N5	SQOR	0.04000	0.00000	0.00000
Q9Y6R7	FCGBP	0.05300	0.08000	0.05833
Q9Y6V0	PCLO	0.00000	0.00182	0.00000

CRSsNP: Chronic rhinosinusitis without nasal polyps, CRSwNP: Chronic rhinosinusitis with nasal polyps, emPAI: exponentially modified abundance index.

SUPPLEMENTARY TABLE 8.2. UNIQUE PROTEINS

Healthy Proteins						
ACLY	ACRBP	ADK	ADSS	AHSA1	AK2	ALDH2
ALDH7A1	ANKFY1	ANKRD18B	ANXA11	API5	ARPC1A	ARPC5L
ATG2B	ATIC	ATP5PB	ATP5PO	BAG1	BARD1	BCAN
BDH2	BOLA2	BOLA2B	BTF3	C1R	CACYBP	CALR
CARD14	CCDC25	CCDC6	CCDC88A	CCS	CCT5	CCT7
CFAP46	CGN	CHIT1	CHMP3	CIT	CKB	CLTB
COPS4	COPZ1	CRYZ	CS	CSDE1	CTBP1	CTSC
CTSH	CTSL	CTSZ	CUL3	CUL4B	CYB5R1	DDAH1
DDAH2	DDX1	DDX17	DDX39A	DDX46	DDX5	DIAPH1
DNAH17	DYNC1I2	EEF1E1	EFCAB6	EHD1	EIF2S3	EIF3F
EIF3G	EML6	ENO3	EPB41	ERBB3	ERP44	FAM151A
FAM186A	FAM49B	FBLN1	FBXL7	FLII	FLT4	FMO3
FSIP2	FUCA1	GAA	GARS	GART	GCLC	GFAP
GMFB	GNAS	GNB4	GNPDA2	GPX2	GPX4	GRB2
GRIK5	GSPT1	GSTZ1	H1F0	HADH	HARS	HLA-DRB1
HMGB1	HMGB2	HUWE1	IGHV1-46	IGKV1-5	INPP1	INTS7
IQGAP2	IST1	ITGA9	KARS	KBTBD3	KRT222	LACTB2
LDHC	LIMA1	LIMK2	LIMS1	LMNB2	LRBA	LYPLA1
LZTS1	MAPK1	MAPRE1	MAST1	MBP	MDN1	METTL18
MFN2	MMRN1	MORC1	MRI1	MYH1	MYH11	MYH2
MYH3	MYH7	MYL1	NAPA	NARS	NAV2	NCF2
NCF4	NCOA6	NCOR1	NEFL	NEFM	NIBAN1	NIT1
NONO	NUDC	NUDT2	NUDT21	OLA1	OLFM4	OPRPN
PADI4	PAICS	PARP4	PCBD1	PCBP2	PDGFRB	PDLIM1
PFDN6	PFKL	PGM1	PIK3R4	PKD1	PLA2G2A	PLIN3
PPA2	PRDX4	PRKACA	PRMT1	PRPF19	PRPSAP2	PSD
PSMB5	PSMC3	PTGR2	RAB6B	RAB8B	RAD23B	RALA

RARS	RBBP9	RBM22	RHOG	RNASET2	RPL18	RPL3
RPL36	RPL38	RPS10	RPS17	RPS6KA3	RTCB	SAMHD1
SAR1B	SBF1	SCP2	SCPEP1	SEPTIN14	SEPTIN2	SEPTIN8
SERPINB8	SERPINB9	SETDB2	SHANK1	SIGLEC16	SMS	SNRPD1
SNRPGP15	SNX12	SNX14	SPECC1	SPEG	SPRR2G	SRM
SRP9	SSH3	ST13	ST13P4	STAT3	STIP1	SUB1
SULT1A3	SUMO1	SUMO3	TAOK1	TIPRL	TJP2	TMOD3
TNNC2	TPD52	TRAPPC3	TRIM28	TSHZ3	TSKS	TSNAX
TTC12	TUBB8	UBA6	UBE2M	UBL4A	UBLCP1	UPF2
VAT1	VBP1	XPNPEP1	YKT6	ZBTB4	ZC3H13	ZNF132

CRSsNP Proteins						
ACADVL	ACO2	ACOT13	ADGRV1	AK9	ALOX5AP	ANPEP
ANXA6	AP2A1	AP3B2	APMAP	ARMC9	ARVCF	ATP5MG
BPIFB4	CALHM4	CANX	CD55	CDSN	CEACAM8	CES1
COX4I1	COX6C	COX7A2	CRYBG3	CYBA	CYBB	DAD1
EIF3CL	ETF1	GIGYF1	GLIPR2	GNAI2	GP2	HDLBP
HEPHL1	HIST1H2AB	HIST1H2AE	HIST1H2BJ	HIST2H2AC	HIST2H2BC	HLA-DRB1
HLA-DRB1	HNRNPCL4	HSD17B10	HSPA9	HSPG2	HYOU1	IGHV3-49
IMMT	ITGAM	KIF21B	KIF4B	KRTAP9-3	KRTAP9-9	LAMP1
LAMP2	LBR	LONP2	LOR	LRRCC1	MADD	MGST1
MLH1	MUC2	MYO1D	MYOF	NDUFA4	PGAM2	PLGRKT
POR	POTEI	PROM1	PRR36	PTPRC	RARRES1	RGS22
RIT2	RP1	RPL28	S100A3	SLC25A6	SLC2A14	SPATA7
SQOR	SRSF7	SSBP1	SSR4	TBX3	TMED9	TSNAXIP1
TTLL5	TUFM	UFC1	UGGT1	UQCRC2	USP9X	VDAC3

CRSwNP Proteins

ACOT7	ACTC1	ALDH16A1	ALDH1L1	ANG	AP2S1	APOC2
APOL2	ARHGAP4	ASH1L	ATP2B1	ATRX	BROX	BST1
CASP7	CD63	CDC6	CHEK2	CHMP2A	CLCN5	CLIP1
CNTRL	CPN2	CRYL1	CSE1L	DDX11L8	DIAPH2	DNAH11
DNAH14	DNM3	DUSP23	EEF1A1	EIF2S3B	EIF3I	EIF4G1
EIF5AL1	EML1	ENO2	EP300	F2	FAM3B	FAM81B
FCN1	FCN3	FIS1	FLNC	FRMPD1	FRYL	GLRX3
GNAL	GPR179	GPRIN1	GSDMA	GSTM1	HBE1	HBG1
HSP90AA4P	HSPA2	IDO1	IFIT1	IGHV2-26	IGHV3-73	IGHV3-9
IGKV2-30	IGLV3-21	IGLV3-27	IGLV4-60	IGLV7-43	ISG15	ITIH3
KRT37	KRT71	KRT87P	KTN1	LHPP	LRRC20	MAGI1
MARS	MFHAS1	MOB1B	MOCOS	MRPL17	MUCL1	MYCBP
MYH10	MYL6B	NEK10	NME9	NOS2	PCLO	PGLYRP2
PHYHIPL	PIGT	PIK3C2B	PKP3	PLBD1	PRF1	PRSS1
PYGM	RET	RMDN1	RNASE2	RNF213	ROCK2	RP1L1
RPL13	RPL13A	RPL24	RPL6	RPS19BP1	SAA4	SDCBP
SERPINA5	SERPINB10	SKP1	SLC44A4	SLITRK5	SPRR1A	SPRR2D
SPRR2E	SPRR4	TACSTD2	TFF3	TGM1	TLN2	TSPAN1
TUBB2A	UBE2L6	VARS	VPS26A	YTHDC2	ZNF276	

CRSsNP: Chronic rhinosinusitis without nasal polyposis, CRSwNP: Chronic rhinosinusitis with nasal polyposis

SUPPLEMENTARY TABLE 8.3. DIFFERENTIALLY EXPRESSED PROTEINS ACROSS ALL GROUPS DETECTED VIA OMNIBUS TEST

ADH7	CAPG	CFL1	CSTB	GC
GOT1	IDH1	KNG1	KPRP	KRT72
MDH1	MUC5AC	MYO5A	PIGR	PSMA1
PSMB2	S100A7	TPM3	UGP2	YWHAE

CHAPTER 9: DISCUSSION AND CONCLUSIONS

The pathophysiology of CRS remains a highly debated topic amongst the rhinology community with varying hypotheses proposed. The current phenotypical classification of CRS based on polyp presence remains inadequate in disease prognostication and formulating personalised treatment regimes. Various studies have investigated the role of different inflammatory endotypes that may assist in a more accurate classification of CRS. The goal of this thesis was to investigate and understand the complex and intimate relationship between nasal mucus and the mucosal barrier. Various aspects of barrier function were assessed following exposure of HNECs to healthy and CRS mucus. As neutrophils are commonly encountered within the mucus and nasal epithelial cells, the effects of NSPs were tested on the HNECs. A systematic review of nasal mucus and mucosa proteomes was conducted to investigate the current progress within the literature, and to assist in directing future research through identification of deficiencies in our current understanding of CRS. Lastly, the proteome of healthy and CRS patients was investigated to identify important cellular pathways that may contribute to the clinical manifestations of CRS. The main conclusions from all the studies are summarised below.

PROTECTIVE EFFECTS OF HEALTHY NASAL MUCUS ON EPITHELIAL BARRIER FUNCTION

The rheological properties of nasal mucus have been well studied.[232, 357, 359] Our study suggests mucus from healthy controls may have a protective effect on mucosal barrier structure and function as evidenced by an increased TER and CBF compared to PBS-negative controls. In contrast, mucus from CRS patients did not appear to confer this protective effect. CRSwNP mucus samples had cytotoxic effects on HNEC-ALI monolayers and both CRSsNP and

CRSwNP mucus induced increased IL-8 and IL-6 cytokine production by the cells compared to negative controls.

Our study found increased TER and CBF of HNECs following exposure to healthy mucus compared to PBS. Indeed, while PBS did not adversely affect TER and CBF, the absence of protective molecules potentially present in healthy mucus might explain the differences in TER and CBF. The difference in mucus composition between healthy and CRS patients may account for changes in barrier function with increased permeability in CRS mucus.[8, 499, 500] Previously published studies have shown tight junction disruption in HNEC-ALI with the application of cytokines, bacteria and bacterial proteases associated with CRS.[180, 205, 229, 230] Our proteomic analysis of nasal mucus demonstrated the downregulation of various proteins and immune system processes in CRS patients compared to healthy patients. Notably, defence response to Gram positive (GO:0050830) and Gram negative bacterium (GO:0050829) pathways were both downregulated in CRSwNP mucus. Significant reductions in expression of the proteins polymeric immunoglobulin (PIR) and macrophage-capping protein (CAPG) were present CRS mucus. Deficiencies in these proteins may lead to impairment in the transportation of IgA and IgM across the epithelial barrier and deterioration in macrophage motility and phagocytosis, respectively.[591, 598] Thus, we hypothesise that the differing composition of cytokines and bacterial products in CRS mucus compared to healthy control mucus might account for the detrimental effects on mucosal barrier function observed after application of CRS mucus to HNEC. Future studies should focus on these proteomic differences in the mucus composition to aid in the development of directed immunological therapies for CRS.

Interestingly, the application of healthy mucus improved the CBF compared to PBS-treated HNEC-ALI. These findings support the importance of the rheological properties of mucus to

cilia function and mucociliary clearance. The stimulatory effects of ions and cytokines within the mucus may account for the increased CBF seen with the cells exposed to mucus compared to untreated cells.[618] Moreover, mucus contains a complex network of immunoglobulins and glycoproteins that can bind specifically and non-specifically to pathogens or drugs, sequestering them.[357] This process has been shown to trigger increases in mucociliary function that expedites the removal of these pathogens.[360] The bitter perception biological process has demonstrated its importance in the activation of local innate immunity through increased mucociliary clearance.[159] Our study found the downregulation of this biological process in CRSwNP compared to healthy mucus. Tropomyosin alpha-3-chains (TPM3), a vital component of the cilia cytoskeleton, was downregulated in CRS mucus compared to health mucus.[588] These findings suggest the impairment of structural and functional process within cilia activity in CRS patients. Future studies should focus on the proteome differences in CRS and healthy cilia, and correlate these findings with high resolution live-imaging technology.

Conversely, we observed a reduction in CBF with cells treated with the CRS mucus compared to healthy mucus. The CRS mucus demonstrated upregulation of mucin 5AC (MUC5AC) associated with secretory cell hyperplasia in the mucosal epithelium. This overexpression in CRS is a potential source for the increased mucus production and viscosity commonly observed in patients with CRS. Additionally, in the context of chronic inflammation, CRS mucus might be enriched with particular cytokines and bacterial products that may account for the detrimental effects on cell viability and mucosal barrier function when compared with healthy control mucus. These protective properties of healthy mucus require further investigation to assist the overall understanding of CRS pathophysiology.

INCREASED INFLAMMATORY CYTOKINE RELEASE FROM EXPOSURE TO CRS MUCUS

Increased inflammatory processes and cytokines were present in CRS compared to healthy mucus. We found that the application of CRS mucus demonstrated an increase release of IL-8 from HNEC-ALI compared to healthy mucus. IL-8 induces neutrophil migration and activation in sites of inflammation, with elevated levels demonstrated in nasal discharge of CRS patients with associated increased gene expression found in sinus mucosal specimens.[505, 509, 619] Additionally, previous studies have demonstrated the downregulation of tight junction proteins secondary to IL-8 in a dose and time dependent manner in human vascular endothelium.[620] The consequent neutrophil chemotaxis and release of proteases with associated collateral damage is discussed in the following sections.

Elevated levels of IL-6 have been linked to CRS although its role in its pathogenesis is not clearly identified.[8] Increased release of IL-6 from the HNEC-ALI occurred with the application to CRSsNP mucus compared to healthy mucus. As IL-6 is a key stimulator in the production of acute phase proteins present in acute inflammation, this may account for its higher levels in CRSsNP. Studies have demonstrated IL-6 to increase expression of claudin-2 in intestinal epithelial cells, thus resulting in cation channel formation with associated reduction in TER.[621] This selective enhancement of the "leaky" claudins may also contribute to the tight junction disruption observed following the application of CRSsNP mucus. This study demonstrated a trend of increased IL-6 release following application of CRSwNP mucus compared to healthy mucus, however, statistical significance was not achieved. Additional studies are required to investigate the wider cytokine profile of cells following exposure to CRS mucus. This intimate relationship and interactions between the mucosa and mucus require further cytokine and proteomic analysis to assist in formulating an accurate endotyping tool.

IMPROVED BARRIER INTEGRITY OF HEALTHY HUMAN NASAL EPITHELIAL CELLS

Our research found that the type of HNEC treated with nasal mucus also played a significant role in TER reduction. There was a reduction in TER following the application of healthy control mucus on CRS HNEC compared to control HNEC. These results suggest that HNECs obtained from CRS patients are possibly more prone to tight junction disruption and less resilient to external challenges when compared to control patients. Microscopic examination of mucosa and polyp tissue samples from our CRS patient cohort exhibited severe inflammation evidenced by basement membrane thickening, subepithelial oedema and inflammatory cell infiltration, including eosinophils, lymphocytes and plasma cells. Proteomic analysis of CRS patients demonstrated a greater proportion of biological processes involved in cytoskeletal and barrier reorganisation and assembly compared to healthy patients. The biological process *positive regulation of epithelial-to-mesenchymal transition* (GO:0010718) was upregulated in CRSwNP compared to CRSsNP, which may contribute to polyp formation. Furthermore, the reduced expression of cofilin-1 and 40S ribosomal protein SA (PRSA) may account for impairment in TJ and AJ reassembly and adhesion to the basement membrane.[571, 572 574] The reduced resilience and integrity of CRSwNP cells is likely a cumulative effect of chronic inflammation and infection that has been shown to result in a down regulation of TJ proteins.[204]

Patients in the CRS groups were found to have higher rates of asthma and atopy, which are associated with tight junction disruption.[622] In addition, CRS mucus and its known proinflammatory and infective components is also likely to mediate further increases in epithelial permeability. It has been proposed that the disrupted epithelial barrier allows for the invasion of the submucosa and deeper tissues by microbial pathogens resulting in recalcitrant CRS.[204] These findings are supported by previous studies demonstrating increased epithelial

permeability in acute fungal sinusitis and CRSwNP patients compared to healthy control patients. [204, 205] We hypothesise that this perpetual cycle of inflammation and infection may also cause gradual genotypical changes that may result in the development of polyposis. These findings of a lower baseline TER measurements in CRSwNP HNEC compared with control HNECs, adds further support to the proposed mucosal barrier dysfunction hypothesis of CRS.[202] Most importantly, this has implications on future experiments conducted on HNECS in vitro.

COLLATERAL TISSUE DAMAGE FROM NEUTROPHIL SERINE PROTEASES

Neutrophil chemotaxis secondary to acute inflammation is a common histological observation in numerous inflammatory conditions. The accumulation and aberrant activation of neutrophils with associated release of NSPs, such as elastase, cathepsin G and proteinase 3, likely contribute to the increased mucosal permeability.[510] Our findings demonstrated significant barrier disruptive effects following exposure to NSPs evidenced by reduction in TER with increased paracellular permeability of HNECs. Structural disorganisation of TJ proteins was found with reduced ZO-1 immunolocalisation following application of NE and CG to the same HNECs. The barrier dysfunction secondary to NSP-induced disruption of the apical junctional complexes, may allow for the submucosal invasion by pathogens leading to disease severity and recalcitrance. East Asian populations with CRSwNP have exhibited neutrophilic infiltration with Th1/Th17 inflammatory patterns compared to the Th2 eosinophilic inflammatory response with Caucasian CRSwNP patients.[175] This amplified neutrophilia in CRSwNP is associated with poorer prognostic outcomes and is likely a significant disease modifying factor. Interestingly, our study found reduced expression of elafin (PI3), a NE and PR3 inhibitor, in CRS mucus.[592] This may account for reduced bacterial killing secondary to impaired NSP function. Further studies are required to determine differences in levels of NSPs present in the

nasal mucus of CRS and healthy patients. The manipulation of these serine proteases through biological therapy may assist in the future treatments of CRS patients.

LACK OF STANDARDISATION OF MUCUS COLLECTION

Nasal mucus proteomics in CRS is an exciting frontier in improving the understanding of CRS and its endotypes. The gradual improvements in MS instruments have progressed protein identification and quantification in various inflammatory airways diseases. Our scoping review demonstrated substantial heterogeneity in methodology from sample collection and processing to MS techniques. This variability in methodology is a source of bias, but also effects the reproducibility of results. Thus, we suggest standardising sample collection techniques for further research.

Firstly, studies must determine if the proteome of interest is obtained from mucosal tissue or secretions. Mucosal tissue samples have a significantly more complex proteome due to its composition of various cells with associated organelles. We suggest employing microscopy to identify the cells within the tissue sample being tested to accurately determine the cellular origin of the proteome assessed. Furthermore, the cellular contents between healthy and CRS mucosa are likely similar, as all cells require the same organelles to survive. Due to these challenges faced in purifying the cell lysates, we believe the collection of nasal mucus is more advantageous as the secretome is simpler to process and likely more representative of the disease process. Additional research is required to identify differences in the nasal proteome from samples collected from mucosal tissue against mucus from the same patient. This will have implications on the direction of future research.

Secondly, targeted sample collection is vital in reducing heterogeneity in proteomic results. The absorption technique for mucus collection, described in the literature and employed in from our department, has demonstrated itself to be reproducible and effective in identifying various proteins.[411] Concentrations of cytokines and expression of proteins vary for differing subsites of the nasal cavity. Therefore, the same subsite must be utilised for all patients with clear documentation to ensure consistency in the study. Further research is required to determine the various cytokine and protein compositions between various subsites of the nasal cavity.

CONCLUSION

Nasal mucus is of paramount importance in maintaining mucosal barrier function and protection within the nasal cavity and paranasal sinuses. Increasing knowledge of CRS pathophysiology has gradually directed research toward CRS endotyping to better understand and classify this disease process. Advances in proteomic instrumentation and analysis has assisted this evolution in knowledge. Our studies have demonstrated protective properties within healthy mucus improving mucosal barrier function. Conversely, increased barrier dysfunction was observed with exposure to CRS mucus. Furthermore, we found NSPs as a potential source of barrier dysfunction during states of inflammation. Delving further into the differences in composition of nasal mucus between healthy and CRS patients, proteomic analysis was conducted. Initial scoping review found significant heterogeneity in methodology within the literature. These preliminary findings assisted in directing our own proteomic analysis with additional gene set enrichment analysis. Our analysis of CRS mucus exhibited reduced expression of immunological and signalling processes with increased tissue remodelling and cellular metabolism pathways. These findings support the current literature and the proposed CRS barrier hypothesis pathophysiology. The dysregulation of these pathways may account for the downstream clinical manifestation of CRS. We hope our findings

will guide future proteomic research to improve our understanding of CRS pathophysiology and its endotypes. Ultimately, addressing these deficiencies in the literature will guide future treatment paradigms in the management of CRS.

REFERENCES

1. Fokkens WJ, Lund VJ, Hopkins C, Hellings PW, Kern R, Reitsma S, et al. European Position Paper on Rhinosinusitis and Nasal Polyps 2020. Rhinology. 2020;58(Suppl S29):1-464.
2. Stevens WW, Schleimer RP, Kern RC. Chronic Rhinosinusitis with Nasal Polyps. The journal of allergy and clinical immunology In practice. 2016;4(4):565-72.
3. Lund VJ, Kennedy DW. Quantification for staging sinusitis. The Staging and Therapy Group. Ann Otol Rhinol Laryngol Suppl. 1995;167:17-21.
4. Lund VJ, Mackay IS. Staging in rhinosinusitus. Rhinology. 1993;31(4):183-4.
5. Akdis CA, Bachert C, Cingi C, Dykewicz MS, Hellings PW, Naclerio RM, et al. Endotypes and phenotypes of chronic rhinosinusitis: a PRACTALL document of the European Academy of Allergy and Clinical Immunology and the American Academy of Allergy, Asthma & Immunology. J Allergy Clin Immunol. 2013;131(6):1479-90.
6. Bachert C, Al Bahrani N, Al Dousary S, van Crombruggen K, Krysko O, Perez-Novo C, et al. The Pathogenesis of CRS: An Update. Current Otorhinolaryngology Reports. 2013;1(1):25-32.
7. Bachert C, Zhang N, Holtappels G, De Lobel L, van Cauwenberge P, Liu S, et al. Presence of IL-5 protein and IgE antibodies to staphylococcal enterotoxins in nasal polyps is associated with comorbid asthma. J Allergy Clin Immunol. 2010;126(5):962-8, 8.e1-6.
8. Turner JH, Chandra RK, Li P, Bonnet K, Schlundt DG. Identification of clinically relevant chronic rhinosinusitis endotypes using cluster analysis of mucus cytokines. J Allergy Clin Immunol. 2018;141(5):1895-7.e7.
9. Hutcheson PS, Schubert MS, Slavin RG. Distinctions between allergic fungal rhinosinusitis and chronic rhinosinusitis. Am J Rhinol Allergy. 2010;24(6):405-8.
10. Bent JP, 3rd, Kuhn FA. Diagnosis of allergic fungal sinusitis. Otolaryngol Head Neck Surg. 1994;111(5):580-8.
11. Luong A, Davis LS, Marple BF. Peripheral blood mononuclear cells from allergic fungal rhinosinusitis adults express a Th2 cytokine response to fungal antigens. Am J Rhinol Allergy. 2009;23(3):281-7.
12. Collins M, Nair S, Smith W, Kette F, Gillis D, Wormald PJ. Role of local immunoglobulin E production in the pathophysiology of noninvasive fungal sinusitis. Laryngoscope. 2004;114(7):1242-6.
13. Ahn CN, Wise SK, Lathers DM, Mulligan RM, Harvey RJ, Schlosser RJ. Local production of antigen-specific IgE in different anatomic subsites of allergic fungal rhinosinusitis patients. Otolaryngol Head Neck Surg. 2009;141(1):97-103.
14. Laidlaw TM, Boyce JA. Aspirin-Exacerbated Respiratory Disease--New Prime Suspects. N Engl J Med. 2016;374(5):484-8.
15. Settipane GA. Epidemiology of nasal polyps. Allergy Asthma Proc. 1996;17(5):231-6.
16. Szczeklik A. The cyclooxygenase theory of aspirin-induced asthma. Eur Respir J. 1990;3(5):588.
17. Picado C, Fernandez-Morata JC, Juan M, Roca-Ferrer J, Fuentes M, Xaubet A, et al. Cyclooxygenase-2 mRNA is downexpressed in nasal polyps from aspirin-sensitive asthmatics. Am J Respir Crit Care Med. 1999;160(1):291-6.
18. Pierzchalska M, Szabó Z, Sanak M, Soja J, Szczeklik A. Deficient prostaglandin E₂ production by bronchial fibroblasts of asthmatic patients, with special reference to aspirin-induced asthma. J Allergy Clin Immunol. 2003;111(5):1041-8.
19. Chang JE, White A, Simon RA, Stevenson DD. Aspirin-exacerbated respiratory disease: burden of disease. Allergy Asthma Proc. 2012;33(2):117-21.

20. ABS. Australian Health Survey, 2018, http://www.abs.gov.au/AUSSTATS/abs@.nsf/DetailsPage/4364.0.55.0012017-18?OpenDocument.
21. Hamilos DL. Chronic rhinosinusitis: epidemiology and medical management. J Allergy Clin Immunol. 2011;128(4):693-707; quiz 8-9.
22. Hastan D, Fokkens WJ, Bachert C, Newson RB, Bislimovska J, Bockelbrink A, et al. Chronic rhinosinusitis in Europe--an underestimated disease. A GA(2)LEN study. Allergy. 2011;66(9):1216-23.
23. Stevens WW, Peters AT, Suh L, Norton JE, Kern RC, Conley DB, et al. A retrospective, cross-sectional study reveals that women with CRSwNP have more severe disease than men. Immun Inflamm Dis. 2015;3(1):14-22.
24. Bhattacharyya N. Clinical and symptom criteria for the accurate diagnosis of chronic rhinosinusitis. Laryngoscope. 2006;116(7 Pt 2 Suppl 110):1-22.
25. Tomassen P, Newson RB, Hoffmans R, Lotvall J, Cardell LO, Gunnbjornsdottir M, et al. Reliability of EP3OS symptom criteria and nasal endoscopy in the assessment of chronic rhinosinusitis--a GA(2) LEN study. Allergy. 2011;66(4):556-61.
26. Cooke G, Valenti L, Glasziou P, Britt H. Common general practice presentations and publication frequency. Aust Fam Physician. 2013;42(1-2):65-8.
27. Gliklich RE, Metson R. The health impact of chronic sinusitis in patients seeking otolaryngologic care. Otolaryngol Head Neck Surg. 1995;113(1):104-9.
28. Bhattacharyya N. Incremental health care utilization and expenditures for chronic rhinosinusitis in the United States. Ann Otol Rhinol Laryngol. 2011;120(7):423-7.
29. Rudmik L. Economics of Chronic Rhinosinusitis. Curr Allergy Asthma Rep. 2017;17(4):20.
30. Tan BK, Kern RC, Schleimer RP, Schwartz BS. Chronic rhinosinusitis: the unrecognized epidemic. Am J Respir Crit Care Med. 2013;188(11):1275-7.
31. Sasama J, Sherris DA, Shin SH, Kephart GM, Kern EB, Ponikau JU. New paradigm for the roles of fungi and eosinophils in chronic rhinosinusitis. Curr Opin Otolaryngol Head Neck Surg. 2005;13(1):2-8.
32. Davis LJ, Kita H. Pathogenesis of chronic rhinosinusitis: role of airborne fungi and bacteria. Immunol Allergy Clin North Am. 2004;24(1):59-73.
33. Braun H, Buzina W, Freudenschuss K, Beham A, Stammberger H. 'Eosinophilic fungal rhinosinusitis': a common disorder in Europe? Laryngoscope. 2003;113(2):264-9.
34. Ponikau JU, Sherris DA, Kern EB, Homburger HA, Frigas E, Gaffey TA, et al. The diagnosis and incidence of allergic fungal sinusitis. Mayo Clin Proc. 1999;74(9):877-84.
35. Bhushan B, Homma T, Norton JE, Sha Q, Siebert J, Gupta DS, et al. Suppression of epithelial signal transducer and activator of transcription 1 activation by extracts of Aspergillus fumigatus. Am J Respir Cell Mol Biol. 2015;53(1):87-95.
36. Douglas R, Bruhn M, Tan LW, Ooi E, Psaltis A, Wormald PJ. Response of peripheral blood lymphocytes to fungal extracts and staphylococcal superantigen B in chronic rhinosinusitis. Laryngoscope. 2007;117(3):411-4.
37. Inoue Y, Matsuwaki Y, Shin SH, Ponikau JU, Kita H. Nonpathogenic, environmental fungi induce activation and degranulation of human eosinophils. J Immunol. 2005;175(8):5439-47.
38. Wei JL, Kita H, Sherris DA, Kern EB, Weaver A, Ponikau JU. The chemotactic behavior of eosinophils in patients with chronic rhinosinusitis. Laryngoscope. 2003;113(2):303-6.

39. Ponikau JU, Sherris DA, Kephart GM, Kern EB, Congdon DJ, Adolphson CR, et al. Striking deposition of toxic eosinophil major basic protein in mucus: implications for chronic rhinosinusitis. J Allergy Clin Immunol. 2005;116(2):362-9.
40. Orlandi RR, Marple BF, Georgelas A, Durtschi D, Barr L. Immunologic response to fungus is not universally associated with rhinosinusitis. Otolaryngol Head Neck Surg. 2009;141(6):750-6.e1-2.
41. Ebbens FA, Scadding GK, Badia L, Hellings PW, Jorissen M, Mullol J, et al. Amphotericin B nasal lavages: not a solution for patients with chronic rhinosinusitis. J Allergy Clin Immunol. 2006;118(5):1149-56.
42. Bachert C, Zhang N, Patou J, van Zele T, Gevaert P. Role of staphylococcal superantigens in upper airway disease. Curr Opin Allergy Clin Immunol. 2008;8(1):34-8.
43. Seiberling KA, Conley DB, Tripathi A, Grammer LC, Shuh L, Haines GK, 3rd, et al. Superantigens and chronic rhinosinusitis: detection of staphylococcal exotoxins in nasal polyps. Laryngoscope. 2005;115(9):1580-5.
44. Seiberling KA, Grammer L, Kern RC. Chronic rhinosinusitis and superantigens. Otolaryngol Clin North Am. 2005;38(6):1215-36, ix.
45. Wang M, Shi P, Yue Z, Chen B, Zhang H, Zhang D, et al. Superantigens and the expression of T-cell receptor repertoire in chronic rhinosinusitis with nasal polyps. Acta Otolaryngol. 2008;128(8):901-8.
46. Van Zele T, Vaneechoutte M, Holtappels G, Gevaert P, van Cauwenberge P, Bachert C. Detection of enterotoxin DNA in Staphylococcus aureus strains obtained from the middle meatus in controls and nasal polyp patients. Am J Rhinol. 2008;22(3):223-7.
47. Costerton JW, Stewart PS, Greenberg EP. Bacterial biofilms: a common cause of persistent infections. Science. 1999;284(5418):1318-22.
48. Foreman A, Holtappels G, Psaltis AJ, Jervis-Bardy J, Field J, Wormald PJ, et al. Adaptive immune responses in Staphylococcus aureus biofilm-associated chronic rhinosinusitis. Allergy. 2011;66(11):1449-56.
49. Cantero D, Cooksley C, Bassiouni A, Tran HB, Roscioli E, Wormald PJ, et al. Staphylococcus aureus biofilms induce apoptosis and expression of interferon-gamma, interleukin-10, and interleukin-17A on human sinonasal explants. Am J Rhinol Allergy. 2015;29(1):23-8.
50. Psaltis AJ, Ha KR, Beule AG, Tan LW, Wormald PJ. Confocal scanning laser microscopy evidence of biofilms in patients with chronic rhinosinusitis. Laryngoscope. 2007;117(7):1302-6.
51. Zhang Z, Han D, Zhang S, Han Y, Dai W, Fan E, et al. Biofilms and mucosal healing in postsurgical patients with chronic rhinosinusitis. Am J Rhinol Allergy. 2009;23(5):506-11.
52. Singhal D, Psaltis AJ, Foreman A, Wormald PJ. The impact of biofilms on outcomes after endoscopic sinus surgery. Am J Rhinol Allergy. 2010;24(3):169-74.
53. Psaltis AJ, Wormald PJ, Ha KR, Tan LW. Reduced levels of lactoferrin in biofilm-associated chronic rhinosinusitis. Laryngoscope. 2008;118(5):895-901.
54. Tan NC, Foreman A, Jardeleza C, Douglas R, Tran H, Wormald PJ. The multiplicity of Staphylococcus aureus in chronic rhinosinusitis: correlating surface biofilm and intracellular residence. Laryngoscope. 2012;122(8):1655-60.
55. Nomura K, Obata K, Keira T, Miyata R, Hirakawa S, Takano K, et al. Pseudomonas aeruginosa elastase causes transient disruption of tight junctions and downregulation of PAR-2 in human nasal epithelial cells. Respir Res. 2014;15:21.

56. van der Plas MJ, Bhongir RK, Kjellstrom S, Siller H, Kasetty G, Morgelin M, et al. Pseudomonas aeruginosa elastase cleaves a C-terminal peptide from human thrombin that inhibits host inflammatory responses. Nat Commun. 2016;7:11567.
57. Li J, Ramezanpour M, Fong SA, Cooksley C, Murphy J, Suzuki M, et al. Pseudomonas aeruginosa Exoprotein-Induced Barrier Disruption Correlates With Elastase Activity and Marks Chronic Rhinosinusitis Severity. Frontiers in Cellular and Infection Microbiology. 2019;9(38).
58. Funk CD. Prostaglandins and leukotrienes: advances in eicosanoid biology. Science. 2001;294(5548):1871-5.
59. Simmons DL, Botting RM, Hla T. Cyclooxygenase isozymes: the biology of prostaglandin synthesis and inhibition. Pharmacol Rev. 2004;56(3):387-437.
60. Roca-Ferrer J, Garcia-Garcia FJ, Pereda J, Perez-Gonzalez M, Pujols L, Alobid I, et al. Reduced expression of COXs and production of prostaglandin E(2) in patients with nasal polyps with or without aspirin-intolerant asthma. J Allergy Clin Immunol. 2011;128(1):66-72.e1.
61. Van Crombruggen K, Van Bruaene N, Holtappels G, Bachert C. Chronic sinusitis and rhinitis: clinical terminology "Chronic Rhinosinusitis" further supported. Rhinology. 2010;48(1):54-8.
62. Tomassen P, Van Zele T, Zhang N, Perez-Novo C, Van Bruaene N, Gevaert P, et al. Pathophysiology of chronic rhinosinusitis. Proc Am Thorac Soc. 2011;8(1):115-20.
63. Van Crombruggen K, Zhang N, Gevaert P, Tomassen P, Bachert C. Pathogenesis of chronic rhinosinusitis: inflammation. J Allergy Clin Immunol. 2011;128(4):728-32.
64. Leung RM, Kern RC, Conley DB, Tan BK, Chandra RK. Osteomeatal complex obstruction is not associated with adjacent sinus disease in chronic rhinosinusitis with polyps. Am J Rhinol Allergy. 2011;25(6):401-3.
65. Steinke JW, Bradley D, Arango P, Crouse CD, Frierson H, Kountakis SE, et al. Cysteinyl leukotriene expression in chronic hyperplastic sinusitis-nasal polyposis: importance to eosinophilia and asthma. J Allergy Clin Immunol. 2003;111(2):342-9.
66. Pérez-Novo CA, Claeys C, Van Cauwenberge P, Bachert C. Expression of eicosanoid receptors subtypes and eosinophilic inflammation: implication on chronic rhinosinusitis. Respir Res. 2006;7(1):75-.
67. Perez-Novo CA, Watelet JB, Claeys C, Van Cauwenberge P, Bachert C. Prostaglandin, leukotriene, and lipoxin balance in chronic rhinosinusitis with and without nasal polyposis. J Allergy Clin Immunol. 2005;115(6):1189-96.
68. Laidlaw TM, Kidder MS, Bhattacharyya N, Xing W, Shen S, Milne GL, et al. Cysteinyl leukotriene overproduction in aspirin-exacerbated respiratory disease is driven by platelet-adherent leukocytes. Blood. 2012;119(16):3790-8.
69. Gervais FG, Cruz RP, Chateauneuf A, Gale S, Sawyer N, Nantel F, et al. Selective modulation of chemokinesis, degranulation, and apoptosis in eosinophils through the PGD2 receptors CRTH2 and DP. J Allergy Clin Immunol. 2001;108(6):982-8.
70. Schratl P, Royer JF, Kostenis E, Ulven T, Sturm EM, Waldhoer M, et al. The Role of the Prostaglandin D₂ Receptor, DP, in Eosinophil Trafficking. The Journal of Immunology. 2007;179(7):4792.
71. Nantel F, Fong C, Lamontagne S, Wright DH, Giaid A, Desrosiers M, et al. Expression of prostaglandin D synthase and the prostaglandin D2 receptors DP and CRTH2 in human nasal mucosa. Prostaglandins Other Lipid Mediat. 2004;73(1-2):87-101.
72. Perez-Novo CA, Holtappels G, Vinall SL, Xue L, Zhang N, Bachert C, et al. CRTH2 mediates the activation of human Th2 cells in response to PGD(2) released from IgE/anti-IgE treated nasal polyp tissue. Allergy. 2010;65(3):304-10.

73. Okano M, Fujiwara T, Yamamoto M, Sugata Y, Matsumoto R, Fukushima K, et al. Role of prostaglandin D2 and E2 terminal synthases in chronic rhinosinusitis. Clin Exp Allergy. 2006;36(8):1028-38.
74. Mullol J, Fernàndez-Morata JC, Roca-Ferrer J, Pujols L, Xaubet A, Benitez P, et al. Cyclooxygenase 1 and cyclooxygenase 2 expression is abnormally regulated in human nasal polyps. J Allergy Clin Immunol. 2002;109(5):824-30.
75. Perez-Novo CA, Waeytens A, Claeys C, Cauwenberge PV, Bachert C. Staphylococcus aureus enterotoxin B regulates prostaglandin E2 synthesis, growth, and migration in nasal tissue fibroblasts. J Infect Dis. 2008;197(7):1036-43.
76. Okano M, Fujiwara T, Haruna T, Kariya S, Makihara S, Higaki T, et al. Prostaglandin E(2) suppresses staphylococcal enterotoxin-induced eosinophilia-associated cellular responses dominantly through an E-prostanoid 2-mediated pathway in nasal polyps. J Allergy Clin Immunol. 2009;123(4):868-74.e13.
77. Lawley TD, Clare S, Walker AW, Goulding D, Stabler RA, Croucher N, et al. Antibiotic treatment of clostridium difficile carrier mice triggers a supershedder state, spore-mediated transmission, and severe disease in immunocompromised hosts. Infect Immun. 2009;77(9):3661-9.
78. Dorrestein PC, Mazmanian SK, Knight R. Finding the missing links among metabolites, microbes, and the host. Immunity. 2014;40(6):824-32.
79. Gallo RL. S. epidermidis influence on host immunity: more than skin deep. Cell host & microbe. 2015;17(2):143-4.
80. Lee JT, Frank DN, Ramakrishnan V. Microbiome of the paranasal sinuses: Update and literature review. Am J Rhinol Allergy. 2016;30(1):3-16.
81. Schwartz JS, Peres AG, Mfuna Endam L, Cousineau B, Madrenas J, Desrosiers M. Topical probiotics as a therapeutic alternative for chronic rhinosinusitis: A preclinical proof of concept. Am J Rhinol Allergy. 2016;30(6):202-5.
82. Psaltis AJ, Wormald PJ. Therapy of Sinonasal Microbiome in CRS: A Critical Approach. Curr Allergy Asthma Rep. 2017;17(9):59.
83. Wagner Mackenzie B, Waite DW, Hoggard M, Douglas RG, Taylor MW, Biswas K. Bacterial community collapse: a meta-analysis of the sinonasal microbiota in chronic rhinosinusitis. Environ Microbiol. 2017;19(1):381-92.
84. Hoggard M, Biswas K, Zoing M, Wagner Mackenzie B, Taylor MW, Douglas RG. Evidence of microbiota dysbiosis in chronic rhinosinusitis. Int Forum Allergy Rhinol. 2017;7(3):230-9.
85. Cleland EJ, Bassiouni A, Boase S, Dowd S, Vreugde S, Wormald PJ. The fungal microbiome in chronic rhinosinusitis: richness, diversity, postoperative changes and patient outcomes. Int Forum Allergy Rhinol. 2014;4(4):259-65.
86. Zhao YC, Bassiouni A, Tanjararak K, Vreugde S, Wormald PJ, Psaltis AJ. Role of fungi in chronic rhinosinusitis through ITS sequencing. Laryngoscope. 2018;128(1):16-22.
87. Aurora R, Chatterjee D, Hentzleman J, Prasad G, Sindwani R, Sanford T. Contrasting the microbiomes from healthy volunteers and patients with chronic rhinosinusitis. JAMA Otolaryngol Head Neck Surg. 2013;139(12):1328-38.
88. Wylie KM, Mihindukulasuriya KA, Zhou Y, Sodergren E, Storch GA, Weinstock GM. Metagenomic analysis of double-stranded DNA viruses in healthy adults. BMC Biol. 2014;12:71.
89. Goggin RK, Bennett CA, Bialasiewicz S, Vediappan RS, Vreugde S, Wormald PJ, et al. The presence of virus significantly associates with chronic rhinosinusitis disease severity. Allergy. 2019;74(8):1569-72.
90. Sivasubramaniam R, Douglas R. The microbiome and chronic rhinosinusitis. World journal of otorhinolaryngology - head and neck surgery. 2018;4(3):216-21.

91. Van Roey GA, Vanison CC, Wu J, Huang JH, Suh LA, Carter RG, et al. Classical complement pathway activation in the nasal tissue of patients with chronic rhinosinusitis. The Journal of allergy and clinical immunology. 2017;140(1):89-100.e2.
92. Schlosser RJ, Mulligan RM, Casey SE, Varela JC, Harvey RJ, Atkinson C. Alterations in gene expression of complement components in chronic rhinosinusitis. American journal of rhinology & allergy. 2010;24(1):21-5.
93. Pothoven KL, Norton JE, Hulse KE, Suh LA, Carter RG, Rocci E, et al. Oncostatin M promotes mucosal epithelial barrier dysfunction, and its expression is increased in patients with eosinophilic mucosal disease. The Journal of allergy and clinical immunology. 2015;136(3):737-46.e4.
94. Korkmaz B, Horwitz MS, Jenne DE, Gauthier F. Neutrophil elastase, proteinase 3, and cathepsin G as therapeutic targets in human diseases. Pharmacol Rev. 2010;62(4):726-59.
95. Garwicz D, Lennartsson A, Jacobsen SE, Gullberg U, Lindmark A. Biosynthetic profiles of neutrophil serine proteases in a human bone marrow-derived cellular myeloid differentiation model. Haematologica. 2005;90(1):38-44.
96. Pham CT. Neutrophil serine proteases: specific regulators of inflammation. Nat Rev Immunol. 2006;6(7):541-50.
97. Benson KF, Li FQ, Person RE, Albani D, Duan Z, Wechsler J, et al. Mutations associated with neutropenia in dogs and humans disrupt intracellular transport of neutrophil elastase. Nat Genet. 2003;35(1):90-6.
98. Witko-Sarsat V, Cramer EM, Hieblot C, Guichard J, Nusbaum P, Lopez S, et al. Presence of proteinase 3 in secretory vesicles: evidence of a novel, highly mobilizable intracellular pool distinct from azurophil granules. Blood. 1999;94(7):2487-96.
99. Kobayashi SD, Voyich JM, Burlak C, DeLeo FR. Neutrophils in the innate immune response. Arch Immunol Ther Exp (Warsz). 2005;53(6):505-17.
100. Papayannopoulos V, Zychlinsky A. NETs: a new strategy for using old weapons. Trends Immunol. 2009;30(11):513-21.
101. Zasloff M. Antimicrobial peptides of multicellular organisms. Nature. 2002;415(6870):389-95.
102. Reeves EP, Lu H, Jacobs HL, Messina CG, Bolsover S, Gabella G, et al. Killing activity of neutrophils is mediated through activation of proteases by K+ flux. Nature. 2002;416(6878):291-7.
103. Black RA, Rauch CT, Kozlosky CJ, Peschon JJ, Slack JL, Wolfson MF, et al. A metalloproteinase disintegrin that releases tumour-necrosis factor-alpha from cells. Nature. 1997;385(6618):729-33.
104. Weber A, Wasiliew P, Kracht M. Interleukin-1beta (IL-1beta) processing pathway. Sci Signal. 2010;3(105):cm2.
105. Baggiolini M, Clark-Lewis I. Interleukin-8, a chemotactic and inflammatory cytokine. FEBS Lett. 1992;307(1):97-101.
106. Lomas DA, Carrell RW. Serpinopathies and the conformational dementias. Nat Rev Genet. 2002;3(10):759-68.
107. Jiang D, Wenzel SE, Wu Q, Bowler RP, Schnell C, Chu HW. Human neutrophil elastase degrades SPLUNC1 and impairs airway epithelial defense against bacteria. PLoS One. 2013;8(5):e64689.
108. Boxio R, Wartelle J, Nawrocki-Raby B, Lagrange B, Malleret L, Hirche T, et al. Neutrophil elastase cleaves epithelial cadherin in acutely injured lung epithelium. Respir Res. 2016;17(1):129.
109. Stevens WW, Lee RJ, Schleimer RP, Cohen NA. Chronic rhinosinusitis pathogenesis. The Journal of allergy and clinical immunology. 2015;136(6):1442-53.

110. Mjosberg JM, Trifari S, Crellin NK, Peters CP, van Drunen CM, Piet B, et al. Human IL-25- and IL-33-responsive type 2 innate lymphoid cells are defined by expression of CRTH2 and CD161. Nat Immunol. 2011;12(11):1055-62.
111. Walford HH, Lund SJ, Baum RE, White AA, Bergeron CM, Husseman J, et al. Increased ILC2s in the eosinophilic nasal polyp endotype are associated with corticosteroid responsiveness. Clin Immunol. 2014;155(1):126-35.
112. Takabayashi T, Kato A, Peters AT, Suh LA, Carter R, Norton J, et al. Glandular mast cells with distinct phenotype are highly elevated in chronic rhinosinusitis with nasal polyps. J Allergy Clin Immunol. 2012;130(2):410-20.e5.
113. Mahdavinia M, Carter RG, Ocampo CJ, Stevens W, Kato A, Tan BK, et al. Basophils are elevated in nasal polyps of patients with chronic rhinosinusitis without aspirin sensitivity. J Allergy Clin Immunol. 2014;133(6):1759-63.
114. Areschoug T, Gordon S. Pattern recognition receptors and their role in innate immunity: focus on microbial protein ligands. Contrib Microbiol. 2008;15:45-60.
115. Parker D, Prince A. Innate immunity in the respiratory epithelium. Am J Respir Cell Mol Biol. 2011;45(2):189-201.
116. Lane AP, Truong-Tran QA, Schleimer RP. Altered expression of genes associated with innate immunity and inflammation in recalcitrant rhinosinusitis with polyps. Am J Rhinol. 2006;20(2):138-44.
117. Vareille M, Kieninger E, Edwards MR, Regamey N. The airway epithelium: soldier in the fight against respiratory viruses. Clin Microbiol Rev. 2011;24(1):210-29.
118. Seshadri S, Rosati M, Lin DC, Carter RG, Norton JE, Choi AW, et al. Regional differences in the expression of innate host defense molecules in sinonasal mucosa. J Allergy Clin Immunol. 2013;132(5):1227-30.e5.
119. Yan M, Pamp SJ, Fukuyama J, Hwang PH, Cho DY, Holmes S, et al. Nasal microenvironments and interspecific interactions influence nasal microbiota complexity and S. aureus carriage. Cell Host Microbe. 2013;14(6):631-40.
120. Clamp JR, Creeth JM. Some non-mucin components of mucus and their possible biological roles. Ciba Found Symp. 1984;109:121-36.
121. Legrand D. Lactoferrin, a key molecule in immune and inflammatory processes. Biochem Cell Biol. 2012;90(3):252-68.
122. Sano H, Nagai K, Tsutsumi H, Kuroki Y. Lactoferrin and surfactant protein A exhibit distinct binding specificity to F protein and differently modulate respiratory syncytial virus infection. Eur J Immunol. 2003;33(10):2894-902.
123. Psaltis AJ, Bruhn MA, Ooi EH, Tan LW, Wormald PJ. Nasal mucosa expression of lactoferrin in patients with chronic rhinosinusitis. Laryngoscope. 2007;117(11):2030-5.
124. Klockars M, Reitamo S. Tissue distribution of lysozyme in man. J Histochem Cytochem. 1975;23(12):932-40.
125. Ellison RT, 3rd, Giehl TJ. Killing of gram-negative bacteria by lactoferrin and lysozyme. The Journal of clinical investigation. 1991;88(4):1080-91.
126. Nash JA, Ballard TN, Weaver TE, Akinbi HT. The peptidoglycan-degrading property of lysozyme is not required for bactericidal activity in vivo. J Immunol. 2006;177(1):519-26.
127. Woods CM, Hooper DN, Ooi EH, Tan LW, Carney AS. Human lysozyme has fungicidal activity against nasal fungi. Am J Rhinol Allergy. 2011;25(4):236-40.
128. Prokhorenko IR, Zubova SV, Ivanov AY, Grachev SV. Interaction of Gram-negative bacteria with cationic proteins: Dependence on the surface characteristics of the bacterial cell. Int J Gen Med. 2009;2:33-8.

129. Seshadri S, Lin DC, Rosati M, Carter RG, Norton JE, Suh L, et al. Reduced expression of antimicrobial PLUNC proteins in nasal polyp tissues of patients with chronic rhinosinusitis. Allergy. 2012;67(7):920-8.
130. Wijkstrom-Frei C, El-Chemaly S, Ali-Rachedi R, Gerson C, Cobas MA, Forteza R, et al. Lactoperoxidase and human airway host defense. Am J Respir Cell Mol Biol. 2003;29(2):206-12.
131. Fischer H. Mechanisms and function of DUOX in epithelia of the lung. Antioxid Redox Signal. 2009;11(10):2453-65.
132. Moskwa P, Lorentzen D, Excoffon KJ, Zabner J, McCray PB, Jr., Nauseef WM, et al. A novel host defense system of airways is defective in cystic fibrosis. Am J Respir Crit Care Med. 2007;175(2):174-83.
133. Stoeckelhuber M, Feuerhake F, Schmitz C, Wolff K-D, Kesting MR. Immunolocalization of Surfactant Proteins SP-A, SP-B, SP-C, and SP-D in Infantile Labial Glands and Mucosa. The journal of histochemistry and cytochemistry : official journal of the Histochemistry Society. 2018;66(7):531-8.
134. Chen PH, Fang SY. The expression of human antimicrobial peptide LL-37 in the human nasal mucosa. Am J Rhinol. 2004;18(6):381-5.
135. Golec M. Cathelicidin LL-37: LPS-neutralizing, pleiotropic peptide. Ann Agric Environ Med. 2007;14(1):1-4.
136. Sorensen OE, Follin P, Johnsen AH, Calafat J, Tjabringa GS, Hiemstra PS, et al. Human cathelicidin, hCAP-18, is processed to the antimicrobial peptide LL-37 by extracellular cleavage with proteinase 3. Blood. 2001;97(12):3951-9.
137. Chennupati SK, Chiu AG, Tamashiro E, Banks CA, Cohen MB, Bleier BS, et al. Effects of an LL-37-derived antimicrobial peptide in an animal model of biofilm Pseudomonas sinusitis. Am J Rhinol Allergy. 2009;23(1):46-51.
138. Sultan B, Ramanathan M, Jr., Lee J, May L, Lane AP. Sinonasal epithelial cells synthesize active vitamin D, augmenting host innate immune function. Int Forum Allergy Rhinol. 2013;3(1):26-30.
139. Hansdottir S, Monick MM. Vitamin D effects on lung immunity and respiratory diseases. Vitam Horm. 2011;86:217-37.
140. Chen PH, Fang SY. Expression of human beta-defensin 2 in human nasal mucosa. Eur Arch Otorhinolaryngol. 2004;261(5):238-41.
141. Lee SH, Kim JE, Lim HH, Lee HM, Choi JO. Antimicrobial defensin peptides of the human nasal mucosa. Ann Otol Rhinol Laryngol. 2002;111(2):135-41.
142. Harder J, Meyer-Hoffert U, Teran LM, Schwichtenberg L, Bartels J, Maune S, et al. Mucoid Pseudomonas aeruginosa, TNF-alpha, and IL-1beta, but not IL-6, induce human beta-defensin-2 in respiratory epithelia. Am J Respir Cell Mol Biol. 2000;22(6):714-21.
143. Proud D, Sanders SP, Wiehler S. Human rhinovirus infection induces airway epithelial cell production of human beta-defensin 2 both in vitro and in vivo. J Immunol. 2004;172(7):4637-45.
144. Schutte BC, McCray PB, Jr. [beta]-defensins in lung host defense. Annu Rev Physiol. 2002;64:709-48.
145. Singh PK, Jia HP, Wiles K, Hesselberth J, Liu L, Conway BA, et al. Production of beta-defensins by human airway epithelia. Proc Natl Acad Sci U S A. 1998;95(25):14961-6.
146. Bingle CD, Craven CJ. PLUNC: a novel family of candidate host defence proteins expressed in the upper airways and nasopharynx. Hum Mol Genet. 2002;11(8):937-43.
147. Tieu DD, Peters AT, Carter RG, Suh L, Conley DB, Chandra R, et al. Evidence for diminished levels of epithelial psoriasin and calprotectin in chronic rhinosinusitis. J Allergy Clin Immunol. 2010;125(3):667-75.

148. Wolk K, Kunz S, Witte E, Friedrich M, Asadullah K, Sabat R. IL-22 increases the innate immunity of tissues. Immunity. 2004;21(2):241-54.
149. Wolk K, Witte E, Wallace E, Docke WD, Kunz S, Asadullah K, et al. IL-22 regulates the expression of genes responsible for antimicrobial defense, cellular differentiation, and mobility in keratinocytes: a potential role in psoriasis. Eur J Immunol. 2006;36(5):1309-23.
150. Pickert G, Neufert C, Leppkes M, Zheng Y, Wittkopf N, Warntjen M, et al. STAT3 links IL-22 signaling in intestinal epithelial cells to mucosal wound healing. J Exp Med. 2009;206(7):1465-72.
151. Aujla SJ, Chan YR, Zheng M, Fei M, Askew DJ, Pociask DA, et al. IL-22 mediates mucosal host defense against Gram-negative bacterial pneumonia. Nat Med. 2008;14(3):275-81.
152. Hulse K, Norton J, Harris K, Conley D, Chandra R, Kern R, et al. Epithelial STAT3 activation is associated with expression of the antimicrobial peptide S100A7 (89.14). The Journal of Immunology. 2010;184(1 Supplement):89.14.
153. Ramanathan M, Jr., Spannhake EW, Lane AP. Chronic rhinosinusitis with nasal polyps is associated with decreased expression of mucosal interleukin 22 receptor. Laryngoscope. 2007;117(10):1839-43.
154. Peters AT, Kato A, Zhang N, Conley DB, Suh L, Tancowny B, et al. Evidence for altered activity of the IL-6 pathway in chronic rhinosinusitis with nasal polyps. J Allergy Clin Immunol. 2010;125(2):397-403.e10.
155. Yoon SS, Coakley R, Lau GW, Lymar SV, Gaston B, Karabulut AC, et al. Anaerobic killing of mucoid Pseudomonas aeruginosa by acidified nitrite derivatives under cystic fibrosis airway conditions. J Clin Invest. 2006;116(2):436-46.
156. Maniscalco M, Sofia M, Pelaia G. Nitric oxide in upper airways inflammatory diseases. Inflamm Res. 2007;56(2):58-69.
157. Deja M, Busch T, Bachmann S, Riskowski K, Campean V, Wiedmann B, et al. Reduced nitric oxide in sinus epithelium of patients with radiologic maxillary sinusitis and sepsis. Am J Respir Crit Care Med. 2003;168(3):281-6.
158. Phillips PS, Sacks R, Marcells GN, Cohen NA, Harvey RJ. Nasal nitric oxide and sinonasal disease: a systematic review of published evidence. Otolaryngol Head Neck Surg. 2011;144(2):159-69.
159. Cohen NA. The genetics of the bitter taste receptor T2R38 in upper airway innate immunity and implications for chronic rhinosinusitis. The Laryngoscope. 2017;127(1):44-51.
160. Lee RJ, Cohen NA. Sinonasal solitary chemosensory cells "taste" the upper respiratory environment to regulate innate immunity. American journal of rhinology & allergy. 2014;28(5):366-73.
161. Braun T, Mack B, Kramer MF. Solitary chemosensory cells in the respiratory and vomeronasal epithelium of the human nose: a pilot study. Rhinology. 2011;49(5):507-12.
162. Lee RJ, Cohen NA. Taste receptors in innate immunity. Cell Mol Life Sci. 2015;72(2):217-36.
163. Lee RJ, Cohen NA. Bitter and sweet taste receptors in the respiratory epithelium in health and disease. J Mol Med (Berl). 2014;92(12):1235-44.
164. Zhang Z, Adappa ND, Lautenbach E, Chiu AG, Doghramji L, Howland TJ, et al. The effect of diabetes mellitus on chronic rhinosinusitis and sinus surgery outcome. Int Forum Allergy Rhinol. 2014;4(4):315-20.

165. Pezzulo AA, Gutierrez J, Duschner KS, McConnell KS, Taft PJ, Ernst SE, et al. Glucose depletion in the airway surface liquid is essential for sterility of the airways. PLoS One. 2011;6(1):e16166.
166. Brennan AL, Gyi KM, Wood DM, Johnson J, Holliman R, Baines DL, et al. Airway glucose concentrations and effect on growth of respiratory pathogens in cystic fibrosis. J Cyst Fibros. 2007;6(2):101-9.
167. Maina IW, Workman AD, Cohen NA. The role of bitter and sweet taste receptors in upper airway innate immunity: Recent advances and future directions. World Journal of Otorhinolaryngology - Head and Neck Surgery. 2018;4(3):200-8.
168. Spellberg B, Edwards JE, Jr. Type 1/Type 2 immunity in infectious diseases. Clin Infect Dis. 2001;32(1):76-102.
169. Shen Y, Tang XY, Yang YC, Ke X, Kou W, Pan CK, et al. Impaired balance of Th17/Treg in patients with nasal polyposis. Scand J Immunol. 2011;74(2):176-85.
170. Dubin PJ, Kolls JK. Th17 cytokines and mucosal immunity. Immunol Rev. 2008;226:160-71.
171. Nagarkar DR, Poposki JA, Tan BK, Comeau MR, Peters AT, Hulse KE, et al. Thymic stromal lymphopoietin activity is increased in nasal polyps of patients with chronic rhinosinusitis. J Allergy Clin Immunol. 2013;132(3):593-600.e12.
172. Olze H, Forster U, Zuberbier T, Morawietz L, Luger EO. Eosinophilic nasal polyps are a rich source of eotaxin, eotaxin-2 and eotaxin-3. Rhinology. 2006;44(2):145-50.
173. Yao T, Kojima Y, Koyanagi A, Yokoi H, Saito T, Kawano K, et al. Eotaxin-1, -2, and -3 immunoreactivity and protein concentration in the nasal polyps of eosinophilic chronic rhinosinusitis patients. Laryngoscope. 2009;119(6):1053-9.
174. Van Zele T, Claeys S, Gevaert P, Van Maele G, Holtappels G, Van Cauwenberge P, et al. Differentiation of chronic sinus diseases by measurement of inflammatory mediators. Allergy. 2006;61(11):1280-9.
175. Zhang N, Van Zele T, Perez-Novo C, Van Bruaene N, Holtappels G, DeRuyck N, et al. Different types of T-effector cells orchestrate mucosal inflammation in chronic sinus disease. J Allergy Clin Immunol. 2008;122(5):961-8.
176. Mahdavinia M, Suh LA, Carter RG, Stevens WW, Norton JE, Kato A, et al. Increased noneosinophilic nasal polyps in chronic rhinosinusitis in US second-generation Asians suggest genetic regulation of eosinophilia. J Allergy Clin Immunol. 2015;135(2):576-9.
177. Van Bruaene N, Perez-Novo CA, Basinski TM, Van Zele T, Holtappels G, De Ruyck N, et al. T-cell regulation in chronic paranasal sinus disease. J Allergy Clin Immunol. 2008;121(6):1435-41, 41.e1-3.
178. Zhao J, Lloyd CM, Noble A. Th17 responses in chronic allergic airway inflammation abrogate regulatory T-cell-mediated tolerance and contribute to airway remodeling. Mucosal Immunol. 2013;6(2):335-46.
179. Jiang XD, Li GY, Li L, Dong Z, Zhu DD. The characterization of IL-17A expression in patients with chronic rhinosinusitis with nasal polyps. Am J Rhinol Allergy. 2011;25(5):e171-5.
180. Ramezanpour M, Moraitis S, Smith JLP, Wormald PJ, Vreugde S. Th17 Cytokines Disrupt the Airway Mucosal Barrier in Chronic Rhinosinusitis. Mediators Inflamm. 2016;2016:9798206-.
181. Lan F, Zhang N, Zhang J, Krysko O, Zhang Q, Xian J, et al. Forkhead box protein 3 in human nasal polyp regulatory T cells is regulated by the protein suppressor of cytokine signaling 3. J Allergy Clin Immunol. 2013;132(6):1314-21.
182. Pesenacker AM, Cook L, Levings MK. The role of FOXP3 in autoimmunity. Curr Opin Immunol. 2016;43:16-23.

183. Pant H, Hughes A, Schembri M, Miljkovic D, Krumbiegel D. CD4(+) and CD8(+) regulatory T cells in chronic rhinosinusitis mucosa. Am J Rhinol Allergy. 2014;28(2):e83-9.
184. Bacchetta R, Gambineri E, Roncarolo MG. Role of regulatory T cells and FOXP3 in human diseases. J Allergy Clin Immunol. 2007;120(2):227-35; quiz 36-7.
185. Mauri C, Bosma A. Immune regulatory function of B cells. Annu Rev Immunol. 2012;30:221-41.
186. Gatto D, Brink R. The germinal center reaction. J Allergy Clin Immunol. 2010;126(5):898-907; quiz 8-9.
187. Tan BK, Peters AT, Schleimer RP, Hulse KE. Pathogenic and protective roles of B cells and antibodies in patients with chronic rhinosinusitis. J Allergy Clin Immunol. 2018;141(5):1553-60.
188. Waffarn EE, Baumgarth N. Protective B cell responses to flu--no fluke! J Immunol. 2011;186(7):3823-9.
189. Germain C, Gnjatic S, Dieu-Nosjean MC. Tertiary Lymphoid Structure-Associated B Cells are Key Players in Anti-Tumor Immunity. Front Immunol. 2015;6:67.
190. Kato A, Hulse KE, Tan BK, Schleimer RP. B-lymphocyte lineage cells and the respiratory system. J Allergy Clin Immunol. 2013;131(4):933-57; quiz 58.
191. Carragher DM, Rangel-Moreno J, Randall TD. Ectopic lymphoid tissues and local immunity. Semin Immunol. 2008;20(1):26-42.
192. Aloisi F, Pujol-Borrell R. Lymphoid neogenesis in chronic inflammatory diseases. Nat Rev Immunol. 2006;6(3):205-17.
193. Gevaert P, Holtappels G, Johansson SG, Cuvelier C, Cauwenberge P, Bachert C. Organization of secondary lymphoid tissue and local IgE formation to Staphylococcus aureus enterotoxins in nasal polyp tissue. Allergy. 2005;60(1):71-9.
194. Feldman S, Kasjanski R, Poposki J, Hernandez D, Chen JN, Norton JE, et al. Chronic airway inflammation provides a unique environment for B cell activation and antibody production. Clin Exp Allergy. 2017;47(4):457-66.
195. Lau A, Lester S, Moraitis S, Ou J, Psaltis AJ, McColl S, et al. Tertiary lymphoid organs in recalcitrant chronic rhinosinusitis. J Allergy Clin Immunol. 2017;139(4):1371-3.e6.
196. Van Zele T, Gevaert P, Holtappels G, van Cauwenberge P, Bachert C. Local immunoglobulin production in nasal polyposis is modulated by superantigens. Clin Exp Allergy. 2007;37(12):1840-7.
197. Hulse KE, Norton JE, Suh L, Zhong Q, Mahdavinia M, Simon P, et al. Chronic rhinosinusitis with nasal polyps is characterized by B-cell inflammation and EBV-induced protein 2 expression. J Allergy Clin Immunol. 2013;131(4):1075-83, 83.e1-7.
198. Gevaert P, Nouri-Aria KT, Wu H, Harper CE, Takhar P, Fear DJ, et al. Local receptor revision and class switching to IgE in chronic rhinosinusitis with nasal polyps. Allergy. 2013;68(1):55-63.
199. Cameron L, Hamid Q, Wright E, Nakamura Y, Christodoulopoulos P, Muro S, et al. Local synthesis of epsilon germline gene transcripts, IL-4, and IL-13 in allergic nasal mucosa after ex vivo allergen exposure. J Allergy Clin Immunol. 2000;106(1 Pt 1):46-52.
200. De Schryver E, Devuyst L, Derycke L, Dullaers M, Van Zele T, Bachert C, et al. Local immunoglobulin e in the nasal mucosa: clinical implications. Allergy Asthma Immunol Res. 2015;7(4):321-31.
201. Zhang N, Holtappels G, Gevaert P, Patou J, Dhaliwal B, Gould H, et al. Mucosal tissue polyclonal IgE is functional in response to allergen and SEB. Allergy. 2011;66(1):141-8.

202. Lam K, Schleimer R, Kern RC. The Etiology and Pathogenesis of Chronic Rhinosinusitis: a Review of Current Hypotheses. Current allergy and asthma reports. 2015;15(7):41-.
203. Wang X, Kim J, McWilliams R, Cutting GR. Increased prevalence of chronic rhinosinusitis in carriers of a cystic fibrosis mutation. Arch Otolaryngol Head Neck Surg. 2005;131(3):237-40.
204. Soyka MB, Wawrzyniak P, Eiwegger T, Holzmann D, Treis A, Wanke K, et al. Defective epithelial barrier in chronic rhinosinusitis: the regulation of tight junctions by IFN-gamma and IL-4. J Allergy Clin Immunol. 2012;130(5):1087-96.e10.
205. Den Beste KA, Hoddeson EK, Parkos CA, Nusrat A, Wise SK. Epithelial permeability alterations in an in vitro air-liquid interface model of allergic fungal rhinosinusitis. Int Forum Allergy Rhinol. 2013;3(1):19-25.
206. De Benedetto A, Rafaels NM, McGirt LY, Ivanov AI, Georas SN, Cheadle C, et al. Tight junction defects in patients with atopic dermatitis. J Allergy Clin Immunol. 2011;127(3):773-86.e1-7.
207. Barmeyer C, Schulzke JD, Fromm M. Claudin-related intestinal diseases. Semin Cell Dev Biol. 2015;42:30-8.
208. Holgate ST. The sentinel role of the airway epithelium in asthma pathogenesis. Immunol Rev. 2011;242(1):205-19.
209. Hackett TL. Epithelial-mesenchymal transition in the pathophysiology of airway remodelling in asthma. Curr Opin Allergy Clin Immunol. 2012;12(1):53-9.
210. Heilingoetter AL, Tajudeen B, Kuhar HN, Gattuso P, Ghai R, Mahdavinia M, et al. Histopathology in Chronic Rhinosinusitis Varies With Sinus Culture. Am J Rhinol Allergy. 2018;32(2):112-8.
211. Shay AD, Tajudeen BA. Histopathologic analysis in the diagnosis and management of chronic rhinosinusitis. Curr Opin Otolaryngol Head Neck Surg. 2019;27(1):20-4.
212. Al-Muhsen S, Johnson JR, Hamid Q. Remodeling in asthma. J Allergy Clin Immunol. 2011;128(3):451-62; quiz 63-4.
213. Halwani R, Al-Muhsen S, Al-Jahdali H, Hamid Q. Role of transforming growth factor-beta in airway remodeling in asthma. Am J Respir Cell Mol Biol. 2011;44(2):127-33.
214. Van Bruaene N, Derycke L, Perez-Novo CA, Gevaert P, Holtappels G, De Ruyck N, et al. TGF-beta signaling and collagen deposition in chronic rhinosinusitis. J Allergy Clin Immunol. 2009;124(2):253-9, 9.e1-2.
215. Li X, Meng J, Qiao X, Liu Y, Liu F, Zhang N, et al. Expression of TGF, matrix metalloproteinases, and tissue inhibitors in Chinese chronic rhinosinusitis. J Allergy Clin Immunol. 2010;125(5):1061-8.
216. Pain M, Bermudez O, Lacoste P, Royer P-J, Botturi K, Tissot A, et al. Tissue remodelling in chronic bronchial diseases: from the epithelial to mesenchymal phenotype. European Respiratory Review. 2014;23(131):118.
217. Kalluri R, Weinberg RA. The basics of epithelial-mesenchymal transition. J Clin Invest. 2009;119(6):1420-8.
218. Zhang N, Van Crombruggen K, Gevaert E, Bachert C. Barrier function of the nasal mucosa in health and type-2 biased airway diseases. Allergy. 2016;71(3):295-307.
219. Hupin C, Gohy S, Bouzin C, Lecocq M, Polette M, Pilette C. Features of mesenchymal transition in the airway epithelium from chronic rhinosinusitis. Allergy. 2014;69(11):1540-9.
220. Rogers GA, Den Beste K, Parkos CA, Nusrat A, Delgaudio JM, Wise SK. Epithelial tight junction alterations in nasal polyposis. International forum of allergy & rhinology. 2011;1(1):50-4.

221. Tang Z, Lu B, Hatch E, Sacks SH, Sheerin NS. C3a mediates epithelial-to-mesenchymal transition in proteinuric nephropathy. Journal of the American Society of Nephrology : JASN. 2009;20(3):593-603.
222. Shin HW, Cho K, Kim DW, Han DH, Khalmuratova R, Kim SW, et al. Hypoxia-inducible factor 1 mediates nasal polypogenesis by inducing epithelial-to-mesenchymal transition. Am J Respir Crit Care Med. 2012;185(9):944-54.
223. Sidhu SS, Yuan S, Innes AL, Kerr S, Woodruff PG, Hou L, et al. Roles of epithelial cell-derived periostin in TGF-beta activation, collagen production, and collagen gel elasticity in asthma. Proc Natl Acad Sci U S A. 2010;107(32):14170-5.
224. Lee SN, Lee DH, Sohn MH, Yoon JH. Overexpressed proprotein convertase 1/3 induces an epithelial-mesenchymal transition in airway epithelium. Eur Respir J. 2013;42(5):1379-90.
225. Kim DY, Cho SH, Takabayashi T, Schleimer RP. Chronic Rhinosinusitis and the Coagulation System. Allergy Asthma Immunol Res. 2015;7(5):421-30.
226. Muszbek L, Bereczky Z, Bagoly Z, Komaromi I, Katona E. Factor XIII: a coagulation factor with multiple plasmatic and cellular functions. Physiological reviews. 2011;91(3):931-72.
227. Coste A, Wang Q-P, Roudot-Thoraval F, Chapelin C, Bedbeder P, Poron F, et al. Epithelial Cell Proliferation in Nasal Polyps Could Be Up-Regulated by Platelet-Derived Growth Factor. The Laryngoscope. 1996;106(5):578-83.
228. Antoniades HN, Bravo MA, Avila RE, Galanopoulos T, Neville-Golden J, Maxwell M, et al. Platelet-derived growth factor in idiopathic pulmonary fibrosis. The Journal of clinical investigation. 1990;86(4):1055-64.
229. Malik Z, Roscioli E, Murphy J, Ou J, Bassiouni A, Wormald PJ, et al. Staphylococcus aureus impairs the airway epithelial barrier in vitro. Int Forum Allergy Rhinol. 2015;5(6):551-6.
230. Murphy J, Ramezanpour M, Stach N, Dubin G, Psaltis AJ, Wormald PJ, et al. Staphylococcus Aureus V8 protease disrupts the integrity of the airway epithelial barrier and impairs IL-6 production in vitro. The Laryngoscope. 2018;128(1):E8-e15.
231. Chen B, Antunes MB, Claire SE, Palmer JN, Chiu AG, Kennedy DW, et al. Reversal of chronic rhinosinusitis-associated sinonasal ciliary dysfunction. Am J Rhinol. 2007;21(3):346-53.
232. Antunes MB, Gudis DA, Cohen NA. Epithelium, cilia, and mucus: their importance in chronic rhinosinusitis. Immunology and allergy clinics of North America. 2009;29(4):631-43.
233. Wang X, Moylan B, Leopold DA, Kim J, Rubenstein RC, Togias A, et al. Mutation in the gene responsible for cystic fibrosis and predisposition to chronic rhinosinusitis in the general population. Jama. 2000;284(14):1814-9.
234. Li YY, Li CW, Chao SS, Yu FG, Yu XM, Liu J, et al. Impairment of cilia architecture and ciliogenesis in hyperplastic nasal epithelium from nasal polyps. J Allergy Clin Immunol. 2014;134(6):1282-92.
235. Martínez-Antón A, DeBolós C, Garrido M, Roca-Ferrer J, Barranco C, Alobid I, et al. Mucin genes have different expression patterns in healthy and diseased upper airway mucosa. Clin Exp Allergy. 2006;36(4):448-57.
236. Martinez-Anton A, Roca-Ferrer J, Mullol J. Mucin gene expression in rhinitis syndromes. Curr Allergy Asthma Rep. 2006;6(3):189-97.
237. Kanoh S, Tanabe T, Rubin BK. IL-13-induced MUC5AC production and goblet cell differentiation is steroid resistant in human airway cells. Clin Exp Allergy. 2011;41(12):1747-56.

238. Ding GQ, Zheng CQ. The expression of MUC5AC and MUC5B mucin genes in the mucosa of chronic rhinosinusitis and nasal polyposis. Am J Rhinol. 2007;21(3):359-66.
239. Kim DH, Chu HS, Lee JY, Hwang SJ, Lee SH, Lee HM. Up-regulation of MUC5AC and MUC5B mucin genes in chronic rhinosinusitis. Arch Otolaryngol Head Neck Surg. 2004;130(6):747-52.
240. Ferguson JL, McCaffrey TV, Kern EB, Martin WJ, 2nd. The effects of sinus bacteria on human ciliated nasal epithelium in vitro. Otolaryngology--head and neck surgery : official journal of American Academy of Otolaryngology-Head and Neck Surgery. 1988;98(4):299-304.
241. Allen-Gipson DS, Romberger DJ, Forget MA, May KL, Sisson JH, Wyatt TA. IL-8 inhibits isoproterenol-stimulated ciliary beat frequency in bovine bronchial epithelial cells. Journal of aerosol medicine : the official journal of the International Society for Aerosols in Medicine. 2004;17(2):107-15.
242. Papathanasiou A, Djahanbakhch O, Saridogan E, Lyons RA. The effect of interleukin-6 on ciliary beat frequency in the human fallopian tube. Fertility and sterility. 2008;90(2):391-4.
243. DeMarcantonio MA, Han JK. Nasal polyps: pathogenesis and treatment implications. Otolaryngol Clin North Am. 2011;44(3):685-95, ix.
244. Anderson JM, Van Itallie CM. Physiology and Function of the Tight Junction. Cold Spring Harb Perspect Biol. 2009;1(2):a002584.
245. Vogelmann R, Nelson WJ. Fractionation of the epithelial apical junctional complex: reassessment of protein distributions in different substructures. Mol Biol Cell. 2005;16(2):701-16.
246. Hartsock A, Nelson WJ. Adherens and tight junctions: structure, function and connections to the actin cytoskeleton. Biochim Biophys Acta. 2008;1778(3):660-9.
247. Raleigh DR, Marchiando AM, Zhang Y, Shen L, Sasaki H, Wang Y, et al. Tight junction-associated MARVEL proteins marveld3, tricellulin, and occludin have distinct but overlapping functions. Mol Biol Cell. 2010;21(7):1200-13.
248. Chiba H, Osanai M, Murata M, Kojima T, Sawada N. Transmembrane proteins of tight junctions. Biochim Biophys Acta. 2008;1778(3):588-600.
249. Colegio OR, Van Itallie CM, McCrea HJ, Rahner C, Anderson JM. Claudins create charge-selective channels in the paracellular pathway between epithelial cells. Am J Physiol Cell Physiol. 2002;283(1):C142-7.
250. Angelow S, Ahlstrom R, Yu ASL. Biology of claudins. American journal of physiology Renal physiology. 2008;295(4):F867-F76.
251. Lal-Nag M, Morin PJ. The claudins. Genome Biol. 2009;10(8):235-.
252. Furuse M, Fujita K, Hiiragi T, Fujimoto K, Tsukita S. Claudin-1 and -2: novel integral membrane proteins localizing at tight junctions with no sequence similarity to occludin. J Cell Biol. 1998;141(7):1539-50.
253. Gunzel D, Yu AS. Claudins and the modulation of tight junction permeability. Physiol Rev. 2013;93(2):525-69.
254. Weber CR. Dynamic properties of the tight junction barrier. Ann N Y Acad Sci. 2012;1257:77-84.
255. Steed E, Balda MS, Matter K. Dynamics and functions of tight junctions. Trends Cell Biol. 2010;20(3):142-9.
256. Shen L, Weber CR, Raleigh DR, Yu D, Turner JR. Tight junction pore and leak pathways: a dynamic duo. Annu Rev Physiol. 2011;73:283-309.
257. Sanchez-Pulido L, Martin-Belmonte F, Valencia A, Alonso MA. MARVEL: a conserved domain involved in membrane apposition events. Trends Biochem Sci. 2002;27(12):599-601.

258. Vacca B, Sanchez-Heras E, Steed E, Busson SL, Balda MS, Ohnuma SI, et al. Control of neural crest induction by MarvelD3-mediated attenuation of JNK signalling. Sci Rep. 2018;8(1):1204.
259. Balda MS, Flores-Maldonado C, Cereijido M, Matter K. Multiple domains of occludin are involved in the regulation of paracellular permeability. J Cell Biochem. 2000;78(1):85-96.
260. Sakakibara A, Furuse M, Saitou M, Ando-Akatsuka Y, Tsukita S. Possible involvement of phosphorylation of occludin in tight junction formation. J Cell Biol. 1997;137(6):1393-401.
261. Chen Y-H, Lu Q, Goodenough DA, Jeansonne B. Nonreceptor Tyrosine Kinase c-Yes Interacts with Occludin during Tight Junction Formation in Canine Kidney Epithelial Cells. Mol Biol Cell. 2002;13(4):1227-37.
262. Andreeva AY, Krause E, Muller EC, Blasig IE, Utepbergenov DI. Protein kinase C regulates the phosphorylation and cellular localization of occludin. J Biol Chem. 2001;276(42):38480-6.
263. Nunbhakdi-Craig V, Schuechner S, Sontag JM, Montgomery L, Pallas DC, Juno C, et al. Expression of protein phosphatase 2A mutants and silencing of the regulatory B alpha subunit induce a selective loss of acetylated and detyrosinated microtubules. J Neurochem. 2007;101(4):959-71.
264. Wong V, Gumbiner BM. A synthetic peptide corresponding to the extracellular domain of occludin perturbs the tight junction permeability barrier. J Cell Biol. 1997;136(2):399-409.
265. Krug SM, Amasheh S, Richter JF, Milatz S, Gunzel D, Westphal JK, et al. Tricellulin forms a barrier to macromolecules in tricellular tight junctions without affecting ion permeability. Mol Biol Cell. 2009;20(16):3713-24.
266. Ikenouchi J, Furuse M, Furuse K, Sasaki H, Tsukita S, Tsukita S. Tricellulin constitutes a novel barrier at tricellular contacts of epithelial cells. J Cell Biol. 2005;171(6):939-45.
267. Cording J, Berg J, Kading N, Bellmann C, Tscheik C, Westphal JK, et al. In tight junctions, claudins regulate the interactions between occludin, tricellulin and marvelD3, which, inversely, modulate claudin oligomerization. J Cell Sci. 2013;126(Pt 2):554-64.
268. Krug SM, Bojarski C, Fromm A, Lee IM, Dames P, Richter JF, et al. Tricellulin is regulated via interleukin-13-receptor α2, affects macromolecule uptake, and is decreased in ulcerative colitis. Mucosal Immunol. 2018;11(2):345-56.
269. Steed E, Rodrigues NT, Balda MS, Matter K. Identification of MarvelD3 as a tight junction-associated transmembrane protein of the occludin family. BMC Cell Biol. 2009;10:95.
270. Steed E, Elbediwy A, Vacca B, Dupasquier S, Hemkemeyer SA, Suddason T, et al. MarvelD3 couples tight junctions to the MEKK1–JNK pathway to regulate cell behavior and survival. J Cell Biol. 2014;204(5):821-38.
271. Garrido-Urbani S, Bradfield PF, Imhof BA. Tight junction dynamics: the role of junctional adhesion molecules (JAMs). Cell Tissue Res. 2014;355(3):701-15.
272. Bazzoni G. The JAM family of junctional adhesion molecules. Curr Opin Cell Biol. 2003;15(5):525-30.
273. Hamazaki Y, Itoh M, Sasaki H, Furuse M, Tsukita S. Multi-PDZ domain protein 1 (MUPP1) is concentrated at tight junctions through its possible interaction with claudin-1 and junctional adhesion molecule. J Biol Chem. 2002;277(1):455-61.
274. Ebnet K, Suzuki A, Ohno S, Vestweber D. Junctional adhesion molecules (JAMs): more molecules with dual functions? J Cell Sci. 2004;117(1):19-29.
275. Joberty G, Petersen C, Gao L, Macara IG. The cell-polarity protein Par6 links Par3 and atypical protein kinase C to Cdc42. Nat Cell Biol. 2000;2(8):531-9.

276. Ebnet K. Junctional Adhesion Molecules (JAMs): Cell Adhesion Receptors With Pleiotropic Functions in Cell Physiology and Development. Physiol Rev. 2017;97(4):1529-54.
277. Ebnet K, Aurrand-Lions M, Kuhn A, Kiefer F, Butz S, Zander K, et al. The junctional adhesion molecule (JAM) family members JAM-2 and JAM-3 associate with the cell polarity protein PAR-3: a possible role for JAMs in endothelial cell polarity. J Cell Sci. 2003;116(Pt 19):3879-91.
278. Ebnet K, Suzuki A, Horikoshi Y, Hirose T, Meyer Zu Brickwedde MK, Ohno S, et al. The cell polarity protein ASIP/PAR-3 directly associates with junctional adhesion molecule (JAM). EMBO J. 2001;20(14):3738-48.
279. Itoh M, Sasaki H, Furuse M, Ozaki H, Kita T, Tsukita S. Junctional adhesion molecule (JAM) binds to PAR-3: a possible mechanism for the recruitment of PAR-3 to tight junctions. J Cell Biol. 2001;154(3):491-7.
280. Tsukita S, Furuse M, Itoh M. Multifunctional strands in tight junctions. Nat Rev Mol Cell Biol. 2001;2(4):285-93.
281. Iden S, Misselwitz S, Peddibhotla SS, Tuncay H, Rehder D, Gerke V, et al. aPKC phosphorylates JAM-A at Ser285 to promote cell contact maturation and tight junction formation. J Cell Biol. 2012;196(5):623-39.
282. Laukoetter MG, Nava P, Lee WY, Severson EA, Capaldo CT, Babbin BA, et al. JAM-A regulates permeability and inflammation in the intestine in vivo. J Exp Med. 2007;204(13):3067-76.
283. Vetrano S, Rescigno M, Cera MR, Correale C, Rumio C, Doni A, et al. Unique role of junctional adhesion molecule-a in maintaining mucosal homeostasis in inflammatory bowel disease. Gastroenterology. 2008;135(1):173-84.
284. Guillemot L, Paschoud S, Pulimeno P, Foglia A, Citi S. The cytoplasmic plaque of tight junctions: a scaffolding and signalling center. Biochim Biophys Acta. 2008;1778(3):601-13.
285. Lee H-J, Zheng JJ. PDZ domains and their binding partners: structure, specificity, and modification. Cell Communication and Signaling. 2010;8(1):8.
286. Willott E, Balda MS, Fanning AS, Jameson B, Van Itallie C, Anderson JM. The tight junction protein ZO-1 is homologous to the Drosophila discs-large tumor suppressor protein of septate junctions. Proc Natl Acad Sci U S A. 1993;90(16):7834-8.
287. Umeda K, Ikenouchi J, Katahira-Tayama S, Furuse K, Sasaki H, Nakayama M, et al. ZO-1 and ZO-2 independently determine where claudins are polymerized in tight-junction strand formation. Cell. 2006;126(4):741-54.
288. Utepbergenov DI, Fanning AS, Anderson JM. Dimerization of the scaffolding protein ZO-1 through the second PDZ domain. J Biol Chem. 2006;281(34):24671-7.
289. Giepmans BN, Moolenaar WH. The gap junction protein connexin43 interacts with the second PDZ domain of the zona occludens-1 protein. Curr Biol. 1998;8(16):931-4.
290. Fanning AS, Little BP, Rahner C, Utepbergenov D, Walther Z, Anderson JM. The unique-5 and -6 motifs of ZO-1 regulate tight junction strand localization and scaffolding properties. Mol Biol Cell. 2007;18(3):721-31.
291. Itoh M, Morita K, Tsukita S. Characterization of ZO-2 as a MAGUK family member associated with tight as well as adherens junctions with a binding affinity to occludin and alpha catenin. J Biol Chem. 1999;274(9):5981-6.
292. Itoh M, Nagafuchi A, Moroi S, Tsukita S. Involvement of ZO-1 in cadherin-based cell adhesion through its direct binding to alpha catenin and actin filaments. J Cell Biol. 1997;138(1):181-92.

293. Fanning AS, Jameson BJ, Jesaitis LA, Anderson JM. The tight junction protein ZO-1 establishes a link between the transmembrane protein occludin and the actin cytoskeleton. J Biol Chem. 1998;273(45):29745-53.
294. Wittchen ES, Haskins J, Stevenson BR. NZO-3 expression causes global changes to actin cytoskeleton in Madin-Darby canine kidney cells: linking a tight junction protein to Rho GTPases. Mol Biol Cell. 2003;14(5):1757-68.
295. Laura RP, Ross S, Koeppen H, Lasky LA. MAGI-1: a widely expressed, alternatively spliced tight junction protein. Exp Cell Res. 2002;275(2):155-70.
296. Hirabayashi S, Tajima M, Yao I, Nishimura W, Mori H, Hata Y. JAM4, a junctional cell adhesion molecule interacting with a tight junction protein, MAGI-1. Mol Cell Biol. 2003;23(12):4267-82.
297. Dobrosotskaya IY, James GL. MAGI-1 interacts with beta-catenin and is associated with cell-cell adhesion structures. Biochem Biophys Res Commun. 2000;270(3):903-9.
298. Sakurai A, Fukuhara S, Yamagishi A, Sako K, Kamioka Y, Masuda M, et al. MAGI-1 is required for Rap1 activation upon cell-cell contact and for enhancement of vascular endothelial cadherin-mediated cell adhesion. Mol Biol Cell. 2006;17(2):966-76.
299. Assemat E, Crost E, Ponserre M, Wijnholds J, Le Bivic A, Massey-Harroche D. The multi-PDZ domain protein-1 (MUPP-1) expression regulates cellular levels of the PALS-1/PATJ polarity complex. Exp Cell Res. 2013;319(17):2514-25.
300. Zhang J, Yang X, Wang Z, Zhou H, Xie X, Shen Y, et al. Structure of an L27 domain heterotrimer from cell polarity complex Patj/Pals1/Mals2 reveals mutually independent L27 domain assembly mode. J Biol Chem. 2012;287(14):11132-40.
301. Shin K, Straight S, Margolis B. PATJ regulates tight junction formation and polarity in mammalian epithelial cells. The Journal of cell biology. 2005;168(5):705-11.
302. Cordenonsi M, D'Atri F, Hammar E, Parry DA, Kendrick-Jones J, Shore D, et al. Cingulin contains globular and coiled-coil domains and interacts with ZO-1, ZO-2, ZO-3, and myosin. The Journal of cell biology. 1999;147(7):1569-82.
303. Guillemot L, Schneider Y, Brun P, Castagliuolo I, Pizzuti D, Martines D, et al. Cingulin is dispensable for epithelial barrier function and tight junction structure, and plays a role in the control of claudin-2 expression and response to duodenal mucosa injury. J Cell Sci. 2012;125(Pt 21):5005-14.
304. Guillemot L, Paschoud S, Jond L, Foglia A, Citi S. Paracingulin Regulates the Activity of Rac1 and RhoA GTPases by Recruiting Tiam1 and GEF-H1 to Epithelial Junctions. Mol Biol Cell. 2008;19(10):4442-53.
305. Farquhar MG, Palade GE. Junctional complexes in various epithelia. J Cell Biol. 1963;17:375-412.
306. Hirokawa N, Heuser JE. Quick-freeze, deep-etch visualization of the cytoskeleton beneath surface differentiations of intestinal epithelial cells. J Cell Biol. 1981;91(2 Pt 1):399-409.
307. Niessen CM, Gottardi CJ. Molecular components of the adherens junction. Biochimica et Biophysica Acta (BBA) - Biomembranes. 2008;1778(3):562-71.
308. Rudini N, Dejana E. Adherens junctions. Curr Biol. 2008;18(23):R1080-2.
309. Overduin M, Harvey TS, Bagby S, Tong KI, Yau P, Takeichi M, et al. Solution structure of the epithelial cadherin domain responsible for selective cell adhesion. Science. 1995;267(5196):386-9.
310. Pokutta S, Herrenknecht K, Kemler R, Engel J. Conformational changes of the recombinant extracellular domain of E-cadherin upon calcium binding. Eur J Biochem. 1994;223(3):1019-26.
311. Meng W, Takeichi M. Adherens junction: molecular architecture and regulation. Cold Spring Harb Perspect Biol. 2009;1(6):a002899-a.

312. Van Aken E, De Wever O, Correia da Rocha AS, Mareel M. Defective E-cadherin/catenin complexes in human cancer. Virchows Arch. 2001;439(6):725-51.
313. Yap AS, Niessen CM, Gumbiner BM. The juxtamembrane region of the cadherin cytoplasmic tail supports lateral clustering, adhesive strengthening, and interaction with p120ctn. J Cell Biol. 1998;141(3):779-89.
314. Piedra J, Miravet S, Castano J, Palmer HG, Heisterkamp N, Garcia de Herreros A, et al. p120 Catenin-associated Fer and Fyn tyrosine kinases regulate beta-catenin Tyr-142 phosphorylation and beta-catenin-alpha-catenin Interaction. Mol Cell Biol. 2003;23(7):2287-97.
315. Noren NK, Liu BP, Burridge K, Kreft B. p120 catenin regulates the actin cytoskeleton via Rho family GTPases. J Cell Biol. 2000;150(3):567-80.
316. Knudsen KA, Wheelock MJ. Plakoglobin, or an 83-kD homologue distinct from beta-catenin, interacts with E-cadherin and N-cadherin. J Cell Biol. 1992;118(3):671-9.
317. Huber AH, Stewart DB, Laurents DV, Nelson WJ, Weis WI. The cadherin cytoplasmic domain is unstructured in the absence of beta-catenin. A possible mechanism for regulating cadherin turnover. J Biol Chem. 2001;276(15):12301-9.
318. Chen YT, Stewart DB, Nelson WJ. Coupling assembly of the E-cadherin/beta-catenin complex to efficient endoplasmic reticulum exit and basal-lateral membrane targeting of E-cadherin in polarized MDCK cells. J Cell Biol. 1999;144(4):687-99.
319. Yamada S, Pokutta S, Drees F, Weis WI, Nelson WJ. Deconstructing the cadherin-catenin-actin complex. Cell. 2005;123(5):889-901.
320. Kobielak A, Pasolli HA, Fuchs E. Mammalian formin-1 participates in adherens junctions and polymerization of linear actin cables. Nat Cell Biol. 2004;6(1):21-30.
321. Watabe-Uchida M, Uchida N, Imamura Y, Nagafuchi A, Fujimoto K, Uemura T, et al. alpha-Catenin-vinculin interaction functions to organize the apical junctional complex in epithelial cells. J Cell Biol. 1998;142(3):847-57.
322. Maul RS, Song Y, Amann KJ, Gerbin SC, Pollard TD, Chang DD. EPLIN regulates actin dynamics by cross-linking and stabilizing filaments. The Journal of cell biology. 2003;160(3):399-407.
323. Fukuhara A, Irie K, Nakanishi H, Takekuni K, Kawakatsu T, Ikeda W, et al. Involvement of nectin in the localization of junctional adhesion molecule at tight junctions. Oncogene. 2002;21(50):7642-55.
324. Fukuhara A, Irie K, Yamada A, Katata T, Honda T, Shimizu K, et al. Role of nectin in organization of tight junctions in epithelial cells. Genes Cells. 2002;7(10):1059-72.
325. Mandai K, Nakanishi H, Satoh A, Obaishi H, Wada M, Nishioka H, et al. Afadin: A novel actin filament-binding protein with one PDZ domain localized at cadherin-based cell-to-cell adherens junction. J Cell Biol. 1997;139(2):517-28.
326. Yamamoto T, Harada N, Kano K, Taya S, Canaani E, Matsuura Y, et al. The Ras target AF-6 interacts with ZO-1 and serves as a peripheral component of tight junctions in epithelial cells. J Cell Biol. 1997;139(3):785-95.
327. Ebnet K, Schulz CU, Meyer Zu Brickwedde MK, Pendl GG, Vestweber D. Junctional adhesion molecule interacts with the PDZ domain-containing proteins AF-6 and ZO-1. J Biol Chem. 2000;275(36):27979-88.
328. Zhadanov AB, Provance DW, Jr., Speer CA, Coffin JD, Goss D, Blixt JA, et al. Absence of the tight junctional protein AF-6 disrupts epithelial cell-cell junctions and cell polarity during mouse development. Curr Biol. 1999;9(16):880-8.
329. Mese G, Richard G, White TW. Gap junctions: basic structure and function. J Invest Dermatol. 2007;127(11):2516-24.
330. Giepmans BN, van Ijzendoorn SC. Epithelial cell-cell junctions and plasma membrane domains. Biochim Biophys Acta. 2009;1788(4):820-31.

331. Krutovskikh V, Yamasaki H. Connexin gene mutations in human genetic diseases. Mutation Research/Reviews in Mutation Research. 2000;462(2):197-207.
332. Cruciani V, Mikalsen SO. Connexins, gap junctional intercellular communication and kinases. Biol Cell. 2002;94(7-8):433-43.
333. Lampe PD, Lau AF. The effects of connexin phosphorylation on gap junctional communication. Int J Biochem Cell Biol. 2004;36(7):1171-86.
334. Goodenough DA, Paul DL. Gap junctions. Cold Spring Harb Perspect Biol. 2009;1(1):a002576.
335. Hama T, Oyamada M, Dejima K, Takenaka H, Takamatsu T. Expression of Gap Junctional Protein Connexins in Human Nasal Epithelium, and Its Contribution to Intercellular Calcium Signalling. ACTA HISTOCHEMICA ET CYTOCHEMICA. 2000;33(1):23-30.
336. Kojima T, Sawada N, Chiba H, Kokai Y, Yamamoto M, Urban M, et al. Induction of tight junctions in human connexin 32 (hCx32)-transfected mouse hepatocytes: connexin 32 interacts with occludin. Biochem Biophys Res Commun. 1999;266(1):222-9.
337. Ai Z, Fischer A, Spray DC, Brown AM, Fishman GI. Wnt-1 regulation of connexin43 in cardiac myocytes. J Clin Invest. 2000;105(2):161-71.
338. Thomason HA, Scothern A, McHarg S, Garrod DR. Desmosomes: adhesive strength and signalling in health and disease. Biochem J. 2010;429(3):419-33.
339. Amagai M, Stanley JR. Desmoglein as a target in skin disease and beyond. J Invest Dermatol. 2012;132(3 Pt 2):776-84.
340. Delmar M, McKenna WJ. The cardiac desmosome and arrhythmogenic cardiomyopathies: from gene to disease. Circ Res. 2010;107(6):700-14.
341. Delva E, Tucker DK, Kowalczyk AP. The desmosome. Cold Spring Harb Perspect Biol. 2009;1(2):a002543.
342. Pokutta S, Weis WI. Structure and mechanism of cadherins and catenins in cell-cell contacts. Annu Rev Cell Dev Biol. 2007;23:237-61.
343. Kowalczyk AP, Bornslaeger EA, Norvell SM, Palka HL, Green KJ. Desmosomes: intercellular adhesive junctions specialized for attachment of intermediate filaments. Int Rev Cytol. 1999;185:237-302.
344. Mathur M, Goodwin L, Cowin P. Interactions of the cytoplasmic domain of the desmosomal cadherin Dsg1 with plakoglobin. J Biol Chem. 1994;269(19):14075-80.
345. Garrod D, Chidgey M. Desmosome structure, composition and function. Biochim Biophys Acta. 2008;1778(3):572-87.
346. Holthofer B, Windoffer R, Troyanovsky S, Leube RE. Structure and function of desmosomes. Int Rev Cytol. 2007;264:65-163.
347. Peifer M, McCrea PD, Green KJ, Wieschaus E, Gumbiner BM. The vertebrate adhesive junction proteins beta-catenin and plakoglobin and the Drosophila segment polarity gene armadillo form a multigene family with similar properties. J Cell Biol. 1992;118(3):681-91.
348. Chitaev NA, Leube RE, Troyanovsky RB, Eshkind LG, Franke WW, Troyanovsky SM. The binding of plakoglobin to desmosomal cadherins: patterns of binding sites and topogenic potential. J Cell Biol. 1996;133(2):359-69.
349. Bierkamp C, McLaughlin KJ, Schwarz H, Huber O, Kemler R. Embryonic heart and skin defects in mice lacking plakoglobin. Dev Biol. 1996;180(2):780-5.
350. Hatzfeld M, Haffner C, Schulze K, Vinzens U. The function of plakophilin 1 in desmosome assembly and actin filament organization. J Cell Biol. 2000;149(1):209-22.
351. Wahl JK, 3rd. A role for plakophilin-1 in the initiation of desmosome assembly. J Cell Biochem. 2005;96(2):390-403.

352. Yin T, Green KJ. Regulation of desmosome assembly and adhesion. Semin Cell Dev Biol. 2004;15(6):665-77.
353. Bornslaeger EA, Corcoran CM, Stappenbeck TS, Green KJ. Breaking the connection: displacement of the desmosomal plaque protein desmoplakin from cell-cell interfaces disrupts anchorage of intermediate filament bundles and alters intercellular junction assembly. J Cell Biol. 1996;134(4):985-1001.
354. Gallicano GI, Kouklis P, Bauer C, Yin M, Vasioukhin V, Degenstein L, et al. Desmoplakin is required early in development for assembly of desmosomes and cytoskeletal linkage. J Cell Biol. 1998;143(7):2009-22.
355. Vasioukhin V, Bowers E, Bauer C, Degenstein L, Fuchs E. Desmoplakin is essential in epidermal sheet formation. Nat Cell Biol. 2001;3(12):1076-85.
356. Gallicano GI, Bauer C, Fuchs E. Rescuing desmoplakin function in extra-embryonic ectoderm reveals the importance of this protein in embryonic heart, neuroepithelium, skin and vasculature. Development. 2001;128(6):929-41.
357. Beule AG. Physiology and pathophysiology of respiratory mucosa of the nose and the paranasal sinuses. GMS current topics in otorhinolaryngology, head and neck surgery. 2011;9:Doc07-Doc.
358. Munkholm M, Mortensen J. Mucociliary clearance: pathophysiological aspects. Clin Physiol Funct Imaging. 2014;34(3):171-7.
359. Fahy JV, Dickey BF. Airway mucus function and dysfunction. N Engl J Med. 2010;363(23):2233-47.
360. Bustamante-Marin XM, Ostrowski LE. Cilia and Mucociliary Clearance. Cold Spring Harb Perspect Biol. 2017;9(4):a028241.
361. Hays SR, Fahy JV. Characterizing mucous cell remodeling in cystic fibrosis: relationship to neutrophils. Am J Respir Crit Care Med. 2006;174(9):1018-24.
362. Rawlins EL, Ostrowski LE, Randell SH, Hogan BL. Lung development and repair: contribution of the ciliated lineage. Proc Natl Acad Sci U S A. 2007;104(2):410-7.
363. Breeze RG, Wheeldon EB. The cells of the pulmonary airways. Am Rev Respir Dis. 1977;116(4):705-77.
364. Rock JR, Randell SH, Hogan BLM. Airway basal stem cells: a perspective on their roles in epithelial homeostasis and remodeling. Disease Models & Mechanisms. 2010;3(9-10):545-56.
365. Didon L, Zwick RK, Chao IW, Walters MS, Wang R, Hackett NR, et al. RFX3 modulation of FOXJ1 regulation of cilia genes in the human airway epithelium. Respir Res. 2013;14:70.
366. Kikkawa M. Big steps toward understanding dynein. J Cell Biol. 2013;202(1):15-23.
367. Tilley AE, Walters MS, Shaykhiev R, Crystal RG. Cilia dysfunction in lung disease. Annu Rev Physiol. 2015;77:379-406.
368. Brekman A, Walters MS, Tilley AE, Crystal RG. FOXJ1 prevents cilia growth inhibition by cigarette smoke in human airway epithelium in vitro. Am J Respir Cell Mol Biol. 2014;51(5):688-700.
369. Ishikawa H, Marshall WF. Ciliogenesis: building the cell's antenna. Nat Rev Mol Cell Biol. 2011;12(4):222-34.
370. Singla V, Reiter JF. The primary cilium as the cell's antenna: signaling at a sensory organelle. Science. 2006;313(5787):629-33.
371. Brokaw CJ, Kamiya R. Bending patterns of Chlamydomonas flagella: IV. Mutants with defects in inner and outer dynein arms indicate differences in dynein arm function. Cell Motil Cytoskeleton. 1987;8(1):68-75.

372. Ostrowski LE, Blackburn K, Radde KM, Moyer MB, Schlatzer DM, Moseley A, et al. A proteomic analysis of human cilia: identification of novel components. Mol Cell Proteomics. 2002;1(6):451-65.
373. Brooks ER, Wallingford JB. Multiciliated cells. Current biology : CB. 2014;24(19):R973-R82.
374. Wallingford JB. Planar cell polarity signaling, cilia and polarized ciliary beating. Curr Opin Cell Biol. 2010;22(5):597-604.
375. Mitchell B, Jacobs R, Li J, Chien S, Kintner C. A positive feedback mechanism governs the polarity and motion of motile cilia. Nature. 2007;447(7140):97-101.
376. Satir P, Christensen ST. Overview of structure and function of mammalian cilia. Annu Rev Physiol. 2007;69:377-400.
377. Hofmann W, Asgharian B. The Effect of Lung Structure on Mucociliary Clearance and Particle Retention in Human and Rat Lungs. Toxicol Sci. 2003;73(2):448-56.
378. Morse DM, Smullen JL, Davis CW. Differential effects of UTP, ATP, and adenosine on ciliary activity of human nasal epithelial cells. Am J Physiol Cell Physiol. 2001;280(6):C1485-97.
379. Clary-Meinesz CF, Cosson J, Huitorel P, Blaive B. Temperature effect on the ciliary beat frequency of human nasal and tracheal ciliated cells. Biol Cell. 1992;76(3):335-8.
380. Clary-Meinesz C, Mouroux J, Cosson J, Huitorel P, Blaive B. Influence of external pH on ciliary beat frequency in human bronchi and bronchioles. Eur Respir J. 1998;11(2):330-3.
381. Shah AS, Ben-Shahar Y, Moninger TO, Kline JN, Welsh MJ. Motile cilia of human airway epithelia are chemosensory. Science (New York, NY). 2009;325(5944):1131-4.
382. Elliott MK, Sisson JH, Wyatt TA. Effects of cigarette smoke and alcohol on ciliated tracheal epithelium and inflammatory cell recruitment. Am J Respir Cell Mol Biol. 2007;36(4):452-9.
383. Milara J, Armengot M, Banuls P, Tenor H, Beume R, Artigues E, et al. Roflumilast N-oxide, a PDE4 inhibitor, improves cilia motility and ciliated human bronchial epithelial cells compromised by cigarette smoke in vitro. Br J Pharmacol. 2012;166(8):2243-62.
384. Davis CW, Lazarowski E. Coupling of airway ciliary activity and mucin secretion to mechanical stresses by purinergic signaling. Respir Physiol Neurobiol. 2008;163(1-3):208-13.
385. Lazarowski ER, Boucher RC. Purinergic receptors in airway epithelia. Curr Opin Pharmacol. 2009;9(3):262-7.
386. Tarran R, Button B, Boucher RC. Regulation of normal and cystic fibrosis airway surface liquid volume by phasic shear stress. Annu Rev Physiol. 2006;68:543-61.
387. Raphael GD, Druce HM, Baraniuk JN, Kaliner MA. Pathophysiology of rhinitis. 1. Assessment of the sources of protein in methacholine-induced nasal secretions. Am Rev Respir Dis. 1988;138(2):413-20.
388. Raphael GD, Meredith SD, Baraniuk JN, Druce HM, Banks SM, Kaliner MA. The pathophysiology of rhinitis. II. Assessment of the sources of protein in histamine-induced nasal secretions. Am Rev Respir Dis. 1989;139(3):791-800.
389. Thornton DJ, Rousseau K, McGuckin MA. Structure and function of the polymeric mucins in airways mucus. Annu Rev Physiol. 2008;70:459-86.
390. Rose MC, Voynow JA. Respiratory tract mucin genes and mucin glycoproteins in health and disease. Physiol Rev. 2006;86(1):245-78.
391. Evans CM, Koo JS. Airway mucus: the good, the bad, the sticky. Pharmacol Ther. 2009;121(3):332-48.

392. Buisine MP, Devisme L, Copin MC, Durand-Reville M, Gosselin B, Aubert JP, et al. Developmental mucin gene expression in the human respiratory tract. Am J Respir Cell Mol Biol. 1999;20(2):209-18.
393. Groneberg DA, Eynott PR, Oates T, Lim S, Wu R, Carlstedt I, et al. Expression of MUC5AC and MUC5B mucins in normal and cystic fibrosis lung. Respir Med. 2002;96(2):81-6.
394. Holtzman MJ, Byers DE, Benoit LA, Battaile JT, You Y, Agapov E, et al. Immune pathways for translating viral infection into chronic airway disease. Adv Immunol. 2009;102:245-76.
395. Curran DR, Cohn L. Advances in mucous cell metaplasia: a plug for mucus as a therapeutic focus in chronic airway disease. Am J Respir Cell Mol Biol. 2010;42(3):268-75.
396. Hung LY, Velichko S, Huang F, Thai P, Wu R. Regulation of airway innate and adaptive immune responses: the IL-17 paradigm. Crit Rev Immunol. 2008;28(4):269-79.
397. Deshmukh HS, Shaver C, Case LM, Dietsch M, Wesselkamper SC, Hardie WD, et al. Acrolein-activated matrix metalloproteinase 9 contributes to persistent mucin production. Am J Respir Cell Mol Biol. 2008;38(4):446-54.
398. Davis CW, Dickey BF. Regulated airway goblet cell mucin secretion. Annu Rev Physiol. 2008;70:487-512.
399. Kim KC, Hisatsune A, Kim DJ, Miyata T. Pharmacology of airway goblet cell mucin release. J Pharmacol Sci. 2003;92(4):301-7.
400. Wine JJ, Joo NS. Submucosal glands and airway defense. Proc Am Thorac Soc. 2004;1(1):47-53.
401. Hayashi T, Ishii A, Nakai S, Hasegawa K. Ultrastructure of goblet-cell metaplasia from Clara cell in the allergic asthmatic airway inflammation in a mouse model of asthma in vivo. Virchows Arch. 2004;444(1):66-73.
402. Verdugo P. Goblet cells secretion and mucogenesis. Annu Rev Physiol. 1990;52:157-76.
403. Kesimer M, Makhov AM, Griffith JD, Verdugo P, Sheehan JK. Unpacking a gel-forming mucin: a view of MUC5B organization after granular release. Am J Physiol Lung Cell Mol Physiol. 2010;298(1):L15-22.
404. Thornton DJ, Sheehan JK. From mucins to mucus: toward a more coherent understanding of this essential barrier. Proc Am Thorac Soc. 2004;1(1):54-61.
405. Cone RA. Barrier properties of mucus. Adv Drug Deliv Rev. 2009;61(2):75-85.
406. Knowles MR, Boucher RC. Mucus clearance as a primary innate defense mechanism for mammalian airways. J Clin Invest. 2002;109(5):571-7.
407. Lai SK, Wang YY, Wirtz D, Hanes J. Micro- and macrorheology of mucus. Adv Drug Deliv Rev. 2009;61(2):86-100.
408. Swart SJ, van der Baan S, Steenbergen JJ, Nauta JJ, van Kamp GJ, Biewenga J. Immunoglobulin concentrations in nasal secretions differ between patients with an IgE-mediated rhinopathy and a non-IgE-mediated rhinopathy. J Allergy Clin Immunol. 1991;88(4):612-9.
409. Meredith SD, Raphael GD, Baraniuk JN, Banks SM, Kaliner MA. The pathophysiology of rhinitis: III. The control of IgG secretion. J Allergy Clin Immunol. 1989;84(6, Part 1):920-30.
410. Russell MW, Mestecky J. Induction of the mucosal immune response. Rev Infect Dis. 1988;10 Suppl 2:S440-6.
411. Castelli S, Arasi S, Pawankar R, Matricardi PM. Collection of nasal secretions and tears and their use in allergology. Curr Opin Allergy Clin Immunol. 2018;18(1):1-9.

412. Niehaus MD, Gwaltney JM, Jr., Hendley JO, Newman MJ, Heymann PW, Rakes GP, et al. Lactoferrin and eosinophilic cationic protein in nasal secretions of patients with experimental rhinovirus colds, natural colds, and presumed acute community-acquired bacterial sinusitis. J Clin Microbiol. 2000;38(8):3100-2.
413. Tomazic PV, Birner-Gruenberger R, Leitner A, Obrist B, Spoerk S, Lang-Loidolt D. Nasal mucus proteomic changes reflect altered immune responses and epithelial permeability in patients with allergic rhinitis. Journal of Allergy and Clinical Immunology. 2014;133(3):741-50.
414. Watelet JB, Gevaert P, Holtappels G, Van Cauwenberge P, Bachert C. Collection of nasal secretions for immunological analysis. Eur Arch Otorhinolaryngol. 2004;261(5):242-6.
415. Casado B, Iadarola P, Pannell LK. Preparation of nasal secretions for proteome analysis. Methods in molecular biology (Clifton, NJ). 2008;425:77-87.
416. Mathews KP. Calculation of secretory antibodies and immunoglobulins. J Allergy Clin Immunol 1981; 68:46–50.
417. Lu FX, Esch RE. Novel nasal secretion collection method for the analysis of allergen specific antibodies and inflammatory biomarkers. J Immunol Methods. 2010;356(1-2):6-17.
418. Klimek L, Rasp G. Norm values for eosinophil cationic protein in nasal secretions: influence of specimen collection. Clin Exp Allergy. 1999;29(3):367-74.
419. Zegers MM, O'Brien LE, Yu W, Datta A, Mostov KE. Epithelial polarity and tubulogenesis in vitro. Trends Cell Biol. 2003;13(4):169-76.
420. Srinivasan B, Kolli AR, Esch MB, Abaci HE, Shuler ML, Hickman JJ. TEER measurement techniques for in vitro barrier model systems. Journal of laboratory automation. 2015;20(2):107-26.
421. Powell DW. Barrier function of epithelia. Am J Physiol. 1981;241(4):G275-88.
422. Lo CM, Keese CR, Giaever I. Cell-substrate contact: another factor may influence transepithelial electrical resistance of cell layers cultured on permeable filters. Exp Cell Res. 1999;250(2):576-80.
423. Ramezanpour M, Murphy J, Smith JLP, Vreugde S, Psaltis AJ. In vitro safety evaluation of human nasal epithelial cell monolayers exposed to carrageenan sinus wash. Int Forum Allergy Rhinol. 2017;7(12):1170-7.
424. Sheller RA, Cuevas ME, Todd MC. Comparison of transepithelial resistance measurement techniques: Chopsticks vs. Endohm. Biol Proced Online. 2017;19:4.
425. Sambuy Y, De Angelis I, Ranaldi G, Scarino ML, Stammati A, Zucco F. The Caco-2 cell line as a model of the intestinal barrier: influence of cell and culture-related factors on Caco-2 cell functional characteristics. Cell Biol Toxicol. 2005;21(1):1-26.
426. Briske-Anderson MJ, Finley JW, Newman SM. The influence of culture time and passage number on the morphological and physiological development of Caco-2 cells. Proc Soc Exp Biol Med. 1997;214(3):248-57.
427. Horibe Y, Hosoya K, Kim KJ, Ogiso T, Lee VH. Polar solute transport across the pigmented rabbit conjunctiva: size dependence and the influence of 8-bromo cyclic adenosine monophosphate. Pharm Res. 1997;14(9):1246-51.
428. Audus KL, Borchardt RT. Characterization of an in vitro blood-brain barrier model system for studying drug transport and metabolism. Pharm Res. 1986;3(2):81-7.
429. Yoo JW, Kim YS, Lee SH, Lee MK, Roh HJ, Jhun BH, et al. Serially passaged human nasal epithelial cell monolayer for in vitro drug transport studies. Pharm Res. 2003;20(10):1690-6.

430. Neuhaus W, Trzeciak J, Lauer R, Lachmann B, Noe CR. APTS-labeled dextran ladder: A novel tool to characterize cell layer tightness. J Pharm Biomed Anal. 2006;40(4):1035-9.
431. Johnson LG. Applications of imaging techniques to studies of epithelial tight junctions. Adv Drug Deliv Rev. 2005;57(1):111-21.
432. Buckley AG, Looi K, Iosifidis T, Ling KM, Sutanto EN, Martinovich KM, et al. Visualisation of Multiple Tight Junctional Complexes in Human Airway Epithelial Cells. Biol Proced Online. 2018;20:3.
433. Hirst RA, Jackson CL, Coles JL, Williams G, Rutman A, Goggin PM, et al. Culture of primary ciliary dyskinesia epithelial cells at air-liquid interface can alter ciliary phenotype but remains a robust and informative diagnostic aid. PLoS One. 2014;9(2):e89675-e.
434. Feriani L, Juenet M, Fowler CJ, Bruot N, Chioccioli M, Holland SM, et al. Assessing the Collective Dynamics of Motile Cilia in Cultures of Human Airway Cells by Multiscale DDM. Biophys J. 2017;113(1):109-19.
435. Graves PR, Haystead TA. Molecular biologist's guide to proteomics. Microbiol Mol Biol Rev. 2002;66(1):39-63; table of contents.
436. O'Farrell PH. High resolution two-dimensional electrophoresis of proteins. J Biol Chem. 1975;250(10):4007-21.
437. Scheele GA. Two-dimensional gel analysis of soluble proteins. Charaterization of guinea pig exocrine pancreatic proteins. J Biol Chem. 1975;250(14):5375-85.
438. Edman P. A method for the determination of amino acid sequence in peptides. Arch Biochem. 1949;22(3):475.
439. Aebersold RH, Leavitt J, Saavedra RA, Hood LE, Kent SB. Internal amino acid sequence analysis of proteins separated by one- or two-dimensional gel electrophoresis after in situ protease digestion on nitrocellulose. Proc Natl Acad Sci U S A. 1987;84(20):6970-4.
440. Aebersold RH, Pipes G, Hood LE, Kent SB. N-terminal and internal sequence determination of microgram amounts of proteins separated by isoelectric focusing in immobilized pH gradients. Electrophoresis. 1988;9(9):520-30.
441. Andersen JS, Mann M. Functional genomics by mass spectrometry. FEBS Lett. 2000;480(1):25-31.
442. Pandey A, Mann M. Proteomics to study genes and genomes. Nature. 2000;405(6788):837-46.
443. Fleischmann RD, Adams MD, White O, Clayton RA, Kirkness EF, Kerlavage AR, et al. Whole-genome random sequencing and assembly of Haemophilus influenzae Rd. Science. 1995;269(5223):496-512.
444. Finishing the euchromatic sequence of the human genome. Nature. 2004;431(7011):931-45.
445. Pandey A, Lewitter F. Nucleotide sequence databases: a gold mine for biologists. Trends Biochem Sci. 1999;24(7):276-80.
446. Shevchenko A, Jensen ON, Podtelejnikov AV, Sagliocco F, Wilm M, Vorm O, et al. Linking genome and proteome by mass spectrometry: large-scale identification of yeast proteins from two dimensional gels. Proc Natl Acad Sci U S A. 1996;93(25):14440-5.
447. Velculescu VE, Zhang L, Vogelstein B, Kinzler KW. Serial analysis of gene expression. Science. 1995;270(5235):484-7.
448. Schena M, Shalon D, Davis RW, Brown PO. Quantitative monitoring of gene expression patterns with a complementary DNA microarray. Science. 1995;270(5235):467-70.
449. Newman, A. 1998. RNA splicing. Curr. Biol. 8:R903–R905.

450. Jansen M, de Moor CH, Sussenbach JS, van den Brande JL. Translational control of gene expression. Pediatr Res. 1995;37(6):681-6.
451. Krishna RG, Wold F. Post-translational modification of proteins. Adv Enzymol Relat Areas Mol Biol. 1993;67:265-98.
452. Hunter T. Protein kinases and phosphatases: the yin and yang of protein phosphorylation and signaling. Cell. 1995;80(2):225-36.
453. Colledge M, Scott JD. AKAPs: from structure to function. Trends Cell Biol. 1999;9(6):216-21.
454. Pawson T, Nash P. Protein-protein interactions define specificity in signal transduction. Genes Dev. 2000;14(9):1027-47.
455. Blackstock WP, Weir MP. Proteomics: quantitative and physical mapping of cellular proteins. Trends Biotechnol. 1999;17(3):121-7.
456. Edmondson RD, Vondriska TM, Biederman KJ, Zhang J, Jones RC, Zheng Y, et al. Protein kinase C epsilon signaling complexes include metabolism- and transcription/translation-related proteins: complimentary separation techniques with LC/MS/MS. Mol Cell Proteomics. 2002;1(6):421-33.
457. Jung E, Heller M, Sanchez JC, Hochstrasser DF. Proteomics meets cell biology: the establishment of subcellular proteomes. Electrophoresis. 2000;21(16):3369-77.
458. Cordwell SJ, Nouwens AS, Verrills NM, Basseal DJ, Walsh BJ. Subproteomics based upon protein cellular location and relative solubilities in conjunction with composite two-dimensional electrophoresis gels. Electrophoresis. 2000;21(6):1094-103.
459. Lewis TS, Hunt JB, Aveline LD, Jonscher KR, Louie DF, Yeh JM, et al. Identification of Novel MAP Kinase Pathway Signaling Targets by Functional Proteomics and Mass Spectrometry. Mol Cell. 2000;6(6):1343-54.
460. Dunn MJ. Studying heart disease using the proteomic approach. Drug Discov Today. 2000;5(2):76-84.
461. Farajzadeh Deroee A, Oweinah J, Naraghi M, Hosemann W, Athari B, Volker U, et al. Regression of polypoid nasal mucosa after systemic corticosteroid therapy: a proteomics study. American journal of rhinology & allergy. 2009;23(5):480-5.
462. Bjellqvist B, Pasquali C, Ravier F, Sanchez JC, Hochstrasser D. A nonlinear wide-range immobilized pH gradient for two-dimensional electrophoresis and its definition in a relevant pH scale. Electrophoresis. 1993;14(12):1357-65.
463. Gorg A, Obermaier C, Boguth G, Harder A, Scheibe B, Wildgruber R, et al. The current state of two-dimensional electrophoresis with immobilized pH gradients. Electrophoresis. 2000;21(6):1037-53.
464. Binz PA, Muller M, Walther D, Bienvenut WV, Gras R, Hoogland C, et al. A molecular scanner to automate proteomic research and to display proteome images. Anal Chem. 1999;71(21):4981-8.
465. Yan JX, Sanchez JC, Tonella L, Williams KL, Hochstrasser DF. Studies of quantitative analysis of protein expression in Saccharomyces cerevisiae. Electrophoresis. 1999;20(4-5):738-42.
466. Unlu M, Morgan ME, Minden JS. Difference gel electrophoresis: a single gel method for detecting changes in protein extracts. Electrophoresis. 1997;18(11):2071-7.
467. Tonge R, Shaw J, Middleton B, Rowlinson R, Rayner S, Young J, et al. Validation and development of fluorescence two-dimensional differential gel electrophoresis proteomics technology. Proteomics. 2001;1(3):377-96.
468. Gygi SP, Rochon Y, Franza BR, Aebersold R. Correlation between protein and mRNA abundance in yeast. Mol Cell Biol. 1999;19(3):1720-30.
469. Aslam B, Basit M, Nisar MA, Khurshid M, Rasool MH. Proteomics: Technologies and Their Applications. J Chromatogr Sci. 2017;55(2):182-96.

470. Gulcicek EE, Colangelo CM, McMurray W, Stone K, Williams K, Wu T, et al. Proteomics and the analysis of proteomic data: an overview of current protein-profiling technologies. Curr Protoc Bioinformatics. 2005;Chapter 13:Unit 13.1.
471. Banks JF, Gulcicek EE. Rapid peptide mapping by reversed-phase liquid chromatography on nonporous silica with on-line electrospray time-of-flight mass spectrometry. Anal Chem. 1997;69(19):3973-8.
472. Vandekerckhove J, Bauw G, Puype M, Van Damme J, Van Montagu M. Protein-blotting on Polybrene-coated glass-fiber sheets. A basis for acid hydrolysis and gas-phase sequencing of picomole quantities of protein previously separated on sodium dodecyl sulfate/polyacrylamide gel. Eur J Biochem. 1985;152(1):9-19.
473. Aebersold RH, Teplow DB, Hood LE, Kent SB. Electroblotting onto activated glass. High efficiency preparation of proteins from analytical sodium dodecyl sulfate-polyacrylamide gels for direct sequence analysis. J Biol Chem. 1986;261(9):4229-38.
474. Quadroni M, James P. Proteomics and automation. ELECTROPHORESIS. 1999;20(4-5):664-77.
475. Shevchenko A, Wilm M, Vorm O, Mann M. Mass spectrometric sequencing of proteins silver-stained polyacrylamide gels. Anal Chem. 1996;68(5):850-8.
476. Yates JR, 3rd. Mass spectrometry and the age of the proteome. J Mass Spectrom. 1998;33(1):1-19.
477. Fenn JB, Mann M, Meng CK, Wong SF, Whitehouse CM. Electrospray ionization for mass spectrometry of large biomolecules. Science. 1989;246(4926):64-71.
478. Wilm M, Shevchenko A, Houthaeve T, Breit S, Schweigerer L, Fotsis T, et al. Femtomole sequencing of proteins from polyacrylamide gels by nano-electrospray mass spectrometry. Nature. 1996;379(6564):466-9.
479. Konermann L, Ahadi E, Rodriguez AD, Vahidi S. Unraveling the mechanism of electrospray ionization. Anal Chem. 2013;85(1):2-9.
480. Karas M, Hillenkamp F. Laser desorption ionization of proteins with molecular masses exceeding 10,000 daltons. Anal Chem. 1988;60(20):2299-301.
481. Qin J, Fenyo D, Zhao Y, Hall WW, Chao DM, Wilson CJ, et al. A strategy for rapid, high-confidence protein identification. Anal Chem. 1997;69(19):3995-4001.
482. Singhal N, Kumar M, Kanaujia PK, Virdi JS. MALDI-TOF mass spectrometry: an emerging technology for microbial identification and diagnosis. Front Microbiol. 2015;6(791).
483. Haag AM. Mass Analyzers and Mass Spectrometers. Adv Exp Med Biol. 2016;919:157-69.
484. Amster IJ. Fourier Transform Mass Spectrometry. J Mass Spectrom. 1996;31(12):1325-37.
485. Hunt DF, Yates JR, 3rd, Shabanowitz J, Winston S, Hauer CR. Protein sequencing by tandem mass spectrometry. Proc Natl Acad Sci U S A. 1986;83(17):6233-7.
486. Hunt DF, Buko AM, Ballard JM, Shabanowitz J, Giordani AB. Sequence analysis of polypeptides by collision activated dissociation on a triple quadrupole mass spectrometer. Biomed Mass Spectrom. 1981;8(9):397-408.
487. Roepstorff P, Fohlman J. Proposal for a common nomenclature for sequence ions in mass spectra of peptides. Biomed Mass Spectrom. 1984;11(11):601.
488. Biemann K. Contributions of mass spectrometry to peptide and protein structure. Biomed Environ Mass Spectrom. 1988;16(1-12):99-111.
489. Yates JR. Protein structure analysis by mass spectrometry. Methods Enzymol. 1996;271:351-77.
490. Jonscher KR, Yates JR, 3rd. The quadrupole ion trap mass spectrometer--a small solution to a big challenge. Anal Biochem. 1997;244(1):1-15.

491. Ekstrom S, Onnerfjord P, Nilsson J, Bengtsson M, Laurell T, Marko-Varga G. Integrated microanalytical technology enabling rapid and automated protein identification. Anal Chem. 2000;72(2):286-93.
492. Jensen ON, Podtelejnikov AV, Mann M. Identification of the components of simple protein mixtures by high-accuracy peptide mass mapping and database searching. Anal Chem. 1997;69(23):4741-50.
493. Yates JR, 3rd, Speicher S, Griffin PR, Hunkapiller T. Peptide mass maps: a highly informative approach to protein identification. Anal Biochem. 1993;214(2):397-408.
494. Green MK, Johnston MV, Larsen BS. Mass accuracy and sequence requirements for protein database searching. Anal Biochem. 1999;275(1):39-46.
495. Eng JK, McCormack AL, Yates JR. An approach to correlate tandem mass spectral data of peptides with amino acid sequences in a protein database. J Am Soc Mass Spectrom. 1994;5(11):976-89.
496. Mann M, Wilm M. Error-tolerant identification of peptides in sequence databases by peptide sequence tags. Anal Chem. 1994;66(24):4390-9.
497. Reimand J, Isserlin R, Voisin V, Kucera M, Tannus-Lopes C, Rostamianfar A, et al. Pathway enrichment analysis and visualization of omics data using g:Profiler, GSEA, Cytoscape and EnrichmentMap. Nat Protoc. 2019;14(2):482-517.
498. Min-Man W, Hong S, Zhi-Qiang X, Xue-Ping F, Chang-Qi L, Dan L. Differential proteomic analysis of nasal polyps, chronic sinusitis, and normal nasal mucosa tissues. Otolaryngology-Head & Neck Surgery. 2009;141(3):364-8.
499. Upton DC, Welham NV, Kuo JS, Walker JW, Pasic TR. Chronic rhinosinusitis with nasal polyps: a proteomic analysis. Ann Otol Rhinol Laryngol. 2011;120(12):780-6.
500. Tewfik MA, Latterich M, DiFalco MR, Samaha M. Proteomics of nasal mucus in chronic rhinosinusitis. Am J Rhinol. 2007;21(6):680-5.
501. Woods CM, Tan S, Ullah S, Frauenfelder C, Ooi EH, Carney AS. The effect of nasal irrigation formulation on the antimicrobial activity of nasal secretions. Int Forum Allergy Rhinol. 2015;5(12):1104-10.
502. Ramezanpour M, Bolt H, Psaltis A, Wormald PJ, Vreugde S. Inducing a Mucosal Barrier-Sparing Inflammatory Response in Laboratory-Grown Primary Human Nasal Epithelial Cells. Curr Protoc Toxicol. 2019:e69.
503. R. Development Core Team. R: A Language and Environment for Statistical Computing [Internet]. Vienna AAhwR-po.
504. Kojima T, Go M, Takano K, Kurose M, Ohkuni T, Koizumi J, et al. Regulation of tight junctions in upper airway epithelium. Biomed Res Int. 2013;2013:947072.
505. Suzuki H, Takahashi Y, Wataya H, Ikeda K, Nakabayashi S, Shimomura A, et al. Mechanism of neutrophil recruitment induced by IL-8 in chronic sinusitis. The Journal of allergy and clinical immunology. 1996;98(3):659-70.
506. Twigg MS, Brockbank S, Lowry P, FitzGerald SP, Taggart C, Weldon S. The Role of Serine Proteases and Antiproteases in the Cystic Fibrosis Lung. Mediators Inflamm. 2015;2015:293053.
507. Stockley RA. Neutrophils and protease/antiprotease imbalance. Am J Respir Crit Care Med. 1999;160(5 Pt 2):S49-52.
508. Cho S-W, Kim DW, Kim J-W, Lee CH, Rhee C-S. Classification of chronic rhinosinusitis according to a nasal polyp and tissue eosinophilia: limitation of current classification system for Asian population. Asia Pacific allergy. 2017;7(3):121-30.
509. Rhyoo C, Sanders SP, Leopold DA, Proud D. Sinus mucosal IL-8 gene expression in chronic rhinosinusitis. J Allergy Clin Immunol. 1999;103(3 Pt 1):395-400.
510. Pothoven KL, Norton JE, Suh LA, Carter RG, Harris KE, Biyasheva A, et al. Neutrophils are a major source of the epithelial barrier disrupting cytokine oncostatin

M in patients with mucosal airways disease. J Allergy Clin Immunol. 2017;139(6):1966-78.e9.
511. Kong IG, Kim DW. Pathogenesis of Recalcitrant Chronic Rhinosinusitis: The Emerging Role of Innate Immune Cells. Immune network. 2018;18(2):e6-e.
512. Voynow JA, Fischer BM, Zheng S. Proteases and cystic fibrosis. The international journal of biochemistry & cell biology. 2008;40(6-7):1238-45.
513. McMahon DB, Workman AD, Kohanski MA, Carey RM, Freund JR, Hariri BM, et al. Protease-activated receptor 2 activates airway apical membrane chloride permeability and increases ciliary beating. FASEB J. 2018;32(1):155-67.
514. Sommerhoff CP, Nadel JA, Basbaum CB, Caughey GH. Neutrophil elastase and cathepsin G stimulate secretion from cultured bovine airway gland serous cells. The Journal of clinical investigation. 1990;85(3):682-9.
515. Park JA, He F, Martin LD, Li Y, Chorley BN, Adler KB. Human neutrophil elastase induces hypersecretion of mucin from well-differentiated human bronchial epithelial cells in vitro via a protein kinase C{delta}-mediated mechanism. The American journal of pathology. 2005;167(3):651-61.
516. Azghani AO, Bedinghaus T, Klein R. Detection of elastase from Pseudomonas aeruginosa in sputum and its potential role in epithelial cell permeability. Lung. 2000;178(3):181-9.
517. van Meer G, Simons K. The function of tight junctions in maintaining differences in lipid composition between the apical and the basolateral cell surface domains of MDCK cells. The EMBO journal. 1986;5(7):1455-64.
518. Cereijido M, Valdes J, Shoshani L, Contreras RG. Role of tight junctions in establishing and maintaining cell polarity. Annu Rev Physiol. 1998;60:161-77.
519. Tieu DD, Kern RC, Schleimer RP. Alterations in epithelial barrier function and host defense responses in chronic rhinosinusitis. J Allergy Clin Immunol. 2009;124(1):37-42.
520. Kao SS, Ramezanpour M, Bassiouni A, Finnie J, Wormald PJ, Vreugde S, et al. Barrier disruptive effects of mucus isolated from chronic rhinosinusitis patients. Allergy. 2020;75(1):200-3.
521. Yip J, Monteiro E, Chan Y. Endotypes of chronic rhinosinusitis. Current opinion in otolaryngology & head and neck surgery. 2019;27(1):14-9.
522. Kim DK, Jin HR, Eun KM, Mo JH, Cho SH, Oh S, et al. The role of interleukin-33 in chronic rhinosinusitis. Thorax. 2017;72(7):635-45.
523. Song W, Wang C, Zhou J, Pan S, Lin S. IL-33 Expression in Chronic Rhinosinusitis with Nasal Polyps and Its Relationship with Clinical Severity. ORL; journal for oto-rhino-laryngology and its related specialties. 2017;79(6):323-30.
524. Mahdavinia M, Keshavarzian A, Tobin MC, Landay AL, Schleimer RP. A comprehensive review of the nasal microbiome in chronic rhinosinusitis (CRS). Clinical and experimental allergy : journal of the British Society for Allergy and Clinical Immunology. 2016;46(1):21-41.
525. Stressmann FA, Rogers GB, Chan SW, Howarth PH, Harries PG, Bruce KD, et al. Characterization of bacterial community diversity in chronic rhinosinusitis infections using novel culture-independent techniques. Am J Rhinol Allergy. 2011;25(4):e133-40.
526. Bucher S, Schmid-Grendelmeier P, Soyka MB. Altered Viscosity of Nasal Secretions in Postnasal Drip. Chest. 2019;156(4):659-66.
527. Kuleshov MV, Jones MR, Rouillard AD, Fernandez NF, Duan Q, Wang Z, et al. Enrichr: a comprehensive gene set enrichment analysis web server 2016 update. Nucleic acids research. 2016;44(W1):W90-7.

528. Chen EY, Tan CM, Kou Y, Duan Q, Wang Z, Meirelles GV, et al. Enrichr: interactive and collaborative HTML5 gene list enrichment analysis tool. BMC bioinformatics. 2013;14:128.
529. Tomazic PV, Birner-Gruenberger R, Leitner A, Spoerk S, Lang-Loidolt D. Seasonal proteome changes of nasal mucus reflect perennial inflammatory response and reduced defence mechanisms and plasticity in allergic rhinitis. Journal of proteomics. 2016;133:153-60.
530. Suojalehto H, Lindström I, Wolff H, Puustinen A. Nasal protein profiles in work-related asthma caused by different exposures. Allergy: European Journal of Allergy and Clinical Immunology. 2018;73(3):653-63.
531. Debat H, Eloit C, Blon F, Sarazin B, Henry C, Huet JC, et al. Identification of human olfactory cleft mucus proteins using proteomic analysis. Journal of proteome research. 2007;6(5):1985-96.
532. Schoenebeck B, May C, Guldner C, Respondek G, Mollenhauer B, Hoeglinger G, et al. Improved preparation of nasal lavage fluid (NLF) as a noninvasive sample for proteomic biomarker discovery. Biochimica et biophysica acta. 2015;1854(7):741-5.
533. Gelardi M, Siciliano RA, Papa F, Mazzeo MF, De Nitto E, Quaranta N, et al. Proteomic analysis of human nasal mucosa: different expression profile in rhino-pathologic states. European annals of allergy and clinical immunology. 2014;46(5):164-71.
534. Roxo-Rosa M, da Costa G, Luider TM, Scholte BJ, Coelho AV, Amaral MD, et al. Proteomic analysis of nasal cells from cystic fibrosis patients and non-cystic fibrosis control individuals: search for novel biomarkers of cystic fibrosis lung disease. Proteomics. 2006;6(7):2314-25.
535. Simões T, Charro N, Blonder J, Faria D, Couto FM, Chan KC, et al. Molecular profiling of the human nasal epithelium: A proteomics approach. Journal of proteomics. 2011;75(1):56-69.
536. Kim T, Lee S, Park J, Park S, Jang A, Lee J, et al. Fatty acid binding protein 1 is related with development of aspirin-exacerbated respiratory disease. Allergy: European Journal of Allergy and Clinical Immunology. 2011;66:466-7.
537. Lee JY, Byun JY, Lee SH. Proteomic analysis of normal human nasal mucosa: Establishment of a two-dimensional electrophoresis reference map. Clinical biochemistry. 2009;42(7-8):692-700.
538. Ghafouri B, Irander K, Lindbom J, Tagesson C, Lindahl M. Comparative proteomics of nasal fluid in seasonal allergic rhinitis. Journal of proteome research. 2006;5(2):330-8.
539. Lindahl M, Irander K, Tagesson C, Stahlbom B. Nasal lavage fluid and proteomics as means to identify the effects of the irritating epoxy chemical dimethylbenzylamine. Biomarkers : biochemical indicators of exposure, response, and susceptibility to chemicals. 2004;9(1):56-70.
540. Mortstedt H, Karedal MH, Jonsson BA, Lindh CH. Screening method using selected reaction monitoring for targeted proteomics studies of nasal lavage fluid. Journal of proteome research. 2013;12(1):234-47.
541. Ndika J, Airaksinen L, Suojalehto H, Karisola P, Fyhrquist N, Puustinen A, et al. Epithelial proteome profiling suggests the essential role of interferon-inducible proteins in patients with allergic rhinitis. Journal of Allergy and Clinical Immunology. 2017;140(5):1288-98.
542. Wahlen K, Fornander L, Olausson P, Ydreborg K, Flodin U, Graff P, et al. Protein profiles of nasal lavage fluid from individuals with work-related upper airway symptoms associated with moldy and damp buildings. Indoor air. 2016;26(5):743-54.

543. Benson LM, Mason CJ, Friedman O, Kita H, Bergen HR, 3rd, Plager DA. Extensive fractionation and identification of proteins within nasal lavage fluids from allergic rhinitis and asthmatic chronic rhinosinusitis patients. J Sep Sci. 2009;32(1):44-56.
544. Casado B, Pannell LK, Iadarola P, Baraniuk JN. Identification of human nasal mucous proteins using proteomics. Proteomics. 2005;5(11):2949-59.
545. Lane AP. The role of innate immunity in the pathogenesis of chronic rhinosinusitis. Current allergy and asthma reports. 2009;9(3):205-12.
546. Schleimer RP. Immunopathogenesis of Chronic Rhinosinusitis and Nasal Polyposis. Annual review of pathology. 2017;12:331-57.
547. Van Drunen CM, Mjösberg JM, Segboer CL, Cornet ME, Fokkens WJ. Role of innate immunity in the pathogenesis of chronic rhinosinusitis: Progress and new avenues. Current allergy and asthma reports. 2012;12(2):120-6.
548. Kao SS, Ramezanpour M, Bassiouni A, Wormald PJ, Psaltis AJ, Vreugde S. The effect of neutrophil serine proteases on human nasal epithelial cell barrier function. Int Forum Allergy Rhinol. 2019;9(10):1220-6.
549. Kouzaki H, Matsumoto K, Kikuoka H, Kato T, Tojima I, Shimizu S, et al. Endogenous Protease Inhibitors in Airway Epithelial Cells Contribute to Eosinophilic Chronic Rhinosinusitis. Am J Respir Crit Care Med. 2017;195(6):737-47.
550. Pfeffer PE, Corrigan CJ. An Imbalance between Proteases and Endogenous Protease Inhibitors in Eosinophilic Airway Disease. Am J Respir Crit Care Med. 2017;195(6):707-8.
551. Stoop AE, van der Heijden HA, Biewenga J, van der Baan S. Lymphocytes and nonlymphoid cells in human nasal polyps. The Journal of allergy and clinical immunology. 1991;87(2):470-5.
552. Psaltis AJ, Schlosser RJ, Yawn JR, Henriquez O, Mulligan JK. Characterization of B-cell subpopulations in patients with chronic rhinosinusitis. International forum of allergy & rhinology. 2013;3(8):621-9.
553. Miljkovic D, Psaltis A, Wormald P-J, Vreugde S. Naive and effector B-cell subtypes are increased in chronic rhinosinusitis with polyps. American journal of rhinology & allergy. 2018;32(1):3-6.
554. Paramasivan S, Lester S, Lau A, Ou J, Psaltis AJ, Wormald P-J, et al. Tertiary lymphoid organs: A novel target in patients with chronic rhinosinusitis. Journal of Allergy and Clinical Immunology. 2018;142(5):1673-6.
555. Vickery TW, Ramakrishnan VR. Bacterial Pathogens and the Microbiome. Otolaryngol Clin North Am. 2017;50(1):29-47.
556. Van Bruaene N, Bachert C. Tissue remodeling in chronic rhinosinusitis. Current opinion in allergy and clinical immunology. 2011;11(1):8-11.
557. Abreu MT, Palladino AA, Arnold ET, Kwon RS, McRoberts JA. Modulation of barrier function during Fas-mediated apoptosis in human intestinal epithelial cells. Gastroenterology. 2000;119(6):1524-36.
558. Weiske J, Schoneberg T, Schroder W, Hatzfeld M, Tauber R, Huber O. The fate of desmosomal proteins in apoptotic cells. The Journal of biological chemistry. 2001;276(44):41175-81.
559. Colgan SP, Resnick MB, Parkos CA, Delp-Archer C, McGuirk D, Bacarra AE, et al. IL-4 directly modulates function of a model human intestinal epithelium. Journal of immunology (Baltimore, Md : 1950). 1994;153(5):2122-9.
560. Schmitz H, Fromm M, Bentzel CJ, Scholz P, Detjen K, Mankertz J, et al. Tumor necrosis factor-alpha (TNFalpha) regulates the epithelial barrier in the human intestinal cell line HT-29/B6. Journal of cell science. 1999;112 (Pt 1):137-46.

561. Youakim A, Ahdieh M. Interferon-gamma decreases barrier function in T84 cells by reducing ZO-1 levels and disrupting apical actin. The American journal of physiology. 1999;276(5):G1279-88.
562. Kirkham P, Rahman I. Oxidative stress in asthma and COPD: antioxidants as a therapeutic strategy. Pharmacology & therapeutics. 2006;111(2):476-94.
563. Westerveld GJ, Dekker I, Voss HP, Bast A, Scheeren RA. Antioxidant levels in the nasal mucosa of patients with chronic sinusitis and healthy controls. Archives of otolaryngology--head & neck surgery. 1997;123(2):201-4.
564. Kassim SK, Elbeigermy M, Nasr GF, Khalil R, Nassar M. The role of interleukin-12, and tissue antioxidants in chronic sinusitis. Clinical biochemistry. 2002;35(5):369-75.
565. Baker EH, Clark N, Brennan AL, Fisher DA, Gyi KM, Hodson ME, et al. Hyperglycemia and cystic fibrosis alter respiratory fluid glucose concentrations estimated by breath condensate analysis. Journal of Applied Physiology. 2007;102(5):1969-75.
566. Fordham MT, Mulligan JK, Casey SE, Mulligan RM, Wang EW, Sansoni ER, et al. Reactive oxygen species in chronic rhinosinusitis and secondhand smoke exposure. Otolaryngology--head and neck surgery : official journal of American Academy of Otolaryngology-Head and Neck Surgery. 2013;149(4):633-8.
567. Kao SS, Bassiouni A, Ramezanpour M, Chegeni N, Colella AD, Chataway TK, et al. Scoping review of chronic rhinosinusitis proteomics. Rhinology. 2020.
568. Ishihama Y, Oda Y, Tabata T, Sato T, Nagasu T, Rappsilber J, et al. Exponentially modified protein abundance index (emPAI) for estimation of absolute protein amount in proteomics by the number of sequenced peptides per protein. Mol Cell Proteomics. 2005;4(9):1265-72.
569. Dowle AA, Wilson J, Thomas JR. Comparing the Diagnostic Classification Accuracy of iTRAQ, Peak-Area, Spectral-Counting, and emPAI Methods for Relative Quantification in Expression Proteomics. J Proteome Res. 2016;15(10):3550-62.
570. Hennebert E, Leroy B, Wattiez R, Ladurner P. An integrated transcriptomic and proteomic analysis of sea star epidermal secretions identifies proteins involved in defense and adhesion. J Proteomics. 2015;128:83-91.
571. Mege RM, Gavard J, Lambert M. Regulation of cell-cell junctions by the cytoskeleton. Curr Opin Cell Biol. 2006;18(5):541-8.
572. Garcia-Ponce A, Citalan-Madrid AF, Velazquez-Avila M, Vargas-Robles H, Schnoor M. The role of actin-binding proteins in the control of endothelial barrier integrity. Thromb Haemost. 2015;113(1):20-36.
573. Wang D, Naydenov NG, Feygin A, Baranwal S, Kuemmerle JF, Ivanov AI. Actin-Depolymerizing Factor and Cofilin-1 Have Unique and Overlapping Functions in Regulating Intestinal Epithelial Junctions and Mucosal Inflammation. The American journal of pathology. 2016;186(4):844-58.
574. Ould-Abeih MB, Petit-Topin I, Zidane N, Baron B, Bedouelle H. Multiple folding states and disorder of ribosomal protein SA, a membrane receptor for laminin, anticarcinogens, and pathogens. Biochemistry. 2012;51(24):4807-21.
575. Timpl R, Rohde H, Robey PG, Rennard SI, Foidart JM, Martin GR. Laminin--a glycoprotein from basement membranes. J Biol Chem. 1979;254(19):9933-7.
576. Schmaier AH. The contact activation and kallikrein/kinin systems: pathophysiologic and physiologic activities. J Thromb Haemost. 2016;14(1):28-39.
577. Gailani D, Renne T. Intrinsic pathway of coagulation and arterial thrombosis. Arterioscler Thromb Vasc Biol. 2007;27(12):2507-13.
578. Leeb-Lundberg LM, Marceau F, Muller-Esterl W, Pettibone DJ, Zuraw BL. International union of pharmacology. XLV. Classification of the kinin receptor family:

from molecular mechanisms to pathophysiological consequences. Pharmacol Rev. 2005;57(1):27-77.
579. Sabatini F, Luppi F, Petecchia L, Stefano AD, Longo AM, Eva A, et al. Bradykinin-induced asthmatic fibroblast/myofibroblast activities via bradykinin B2 receptor and different MAPK pathways. Eur J Pharmacol. 2013;710(1-3):100-9.
580. Tsai Y-J, Hao S-P, Chen C-L, Lin BJ, Wu W-B. Involvement of B2 receptor in bradykinin-induced proliferation and proinflammatory effects in human nasal mucosa-derived fibroblasts isolated from chronic rhinosinusitis patients. PLoS One. 2015;10(5):e0126853-e.
581. Liu Z, Kim J, Sypek JP, Wang IM, Horton H, Oppenheim FG, et al. Gene expression profiles in human nasal polyp tissues studied by means of DNA microarray. J Allergy Clin Immunol. 2004;114(4):783-90.
582. Mollenhauer J, End C, Renner M, Lyer S, Poustka A. DMBT1 as an archetypal link between infection, inflammation, and cancer. Inmunología. 2007;26(4):193-209.
583. Lu X, Xu Y, Zhao Y, Tao Q, Wu J. Silenced DMBT1 promotes nasal mucosa epithelial cell growth. Ann Hum Genet. 2018;82(2):102-8.
584. Hovenberg HW, Davies JR, Herrmann A, Linden CJ, Carlstedt I. MUC5AC, but not MUC2, is a prominent mucin in respiratory secretions. Glycoconj J. 1996;13(5):839-47.
585. Lai X, Li X, Chang L, Chen X, Huang Z, Bao H, et al. IL-19 Up-Regulates Mucin 5AC Production in Patients With Chronic Rhinosinusitis via STAT3 Pathway. Front Immunol. 2019;10:1682-.
586. Azuma YT, Nakajima H, Takeuchi T. IL-19 as a potential therapeutic in autoimmune and inflammatory diseases. Current pharmaceutical design. 2011;17(34):3776-80.
587. Liao SC, Cheng YC, Wang YC, Wang CW, Yang SM, Yu CK, et al. IL-19 induced Th2 cytokines and was up-regulated in asthma patients. Journal of immunology (Baltimore, Md : 1950). 2004;173(11):6712-8.
588. Kohli P, Höhne M, Jüngst C, Bertsch S, Ebert LK, Schauss AC, et al. The ciliary membrane-associated proteome reveals actin-binding proteins as key components of cilia. EMBO Rep. 2017;18(9):1521-35.
589. Brook I. Microbiology of chronic rhinosinusitis. European journal of clinical microbiology & infectious diseases : official publication of the European Society of Clinical Microbiology. 2016;35(7):1059-68.
590. Wu W, Chen J, Ding Q, Yang S, Wang J, Yu H, et al. Function of the macrophage-capping protein in colorectal carcinoma. Oncol Lett. 2017;14(5):5549-55.
591. Witke W, Li W, Kwiatkowski DJ, Southwick FS. Comparisons of CapG and gelsolin-null macrophages: demonstration of a unique role for CapG in receptor-mediated ruffling, phagocytosis, and vesicle rocketing. The Journal of cell biology. 2001;154(4):775-84.
592. Shaw L, Wiedow O. Therapeutic potential of human elafin. Biochem Soc Trans. 2011;39(5):1450-4.
593. Lee CW, Kim TH, Lee HM, Lee SH, Lee SH, Yoo JH, et al. Upregulation of elafin and cystatin C in the ethmoid sinus mucosa of patients with chronic sinusitis. Arch Otolaryngol Head Neck Surg. 2009;135(8):771-5.
594. Donato R, Cannon BR, Sorci G, Riuzzi F, Hsu K, Weber DJ, et al. Functions of S100 proteins. Curr Mol Med. 2013;13(1):24-57.
595. Glaser R, Meyer-Hoffert U, Harder J, Cordes J, Wittersheim M, Kobliakova J, et al. The antimicrobial protein psoriasin (S100A7) is upregulated in atopic dermatitis and after experimental skin barrier disruption. J Invest Dermatol. 2009;129(3):641-9.

596. Glaser R, Harder J, Lange H, Bartels J, Christophers E, Schroder JM. Antimicrobial psoriasin (S100A7) protects human skin from Escherichia coli infection. Nat Immunol. 2005;6(1):57-64.
597. Zheng Y, Niyonsaba F, Ushio H, Ikeda S, Nagaoka I, Okumura K, et al. Microbicidal protein psoriasin is a multifunctional modulator of neutrophil activation. Immunology. 2008;124(3):357-67.
598. Turula H, Wobus CE. The Role of the Polymeric Immunoglobulin Receptor and Secretory Immunoglobulins during Mucosal Infection and Immunity. Viruses. 2018;10(5):237.
599. McCarthy MK, Weinberg JB. The immunoproteasome and viral infection: a complex regulator of inflammation. Front Microbiol. 2015;6:21-.
600. Chen W, Norbury CC, Cho Y, Yewdell JW, Bennink JR. Immunoproteasomes shape immunodominance hierarchies of antiviral CD8(+) T cells at the levels of T cell repertoire and presentation of viral antigens. J Exp Med. 2001;193(11):1319-26.
601. Robek MD, Garcia ML, Boyd BS, Chisari FV. Role of immunoproteasome catalytic subunits in the immune response to hepatitis B virus. J Virol. 2007;81(2):483-91.
602. Kincaid EZ, Che JW, York I, Escobar H, Reyes-Vargas E, Delgado JC, et al. Mice completely lacking immunoproteasomes show major changes in antigen presentation. Nat Immunol. 2011;13(2):129-35.
603. Kimura H, Caturegli P, Takahashi M, Suzuki K. New Insights into the Function of the Immunoproteasome in Immune and Nonimmune Cells. Journal of Immunology Research. 2015;2015:8.
604. Kammerl IE, Meiners S. Proteasome function shapes innate and adaptive immune responses. Am J Physiol Lung Cell Mol Physiol. 2016;311(2):L328-36.
605. Vowinkel T, Mori M, Krieglstein CF, Russell J, Saijo F, Bharwani S, et al. Apolipoprotein A-IV inhibits experimental colitis. The Journal of clinical investigation. 2004;114(2):260-9.
606. Ostos MA, Conconi M, Vergnes L, Baroukh N, Ribalta J, Girona J, et al. Antioxidative and Antiatherosclerotic Effects of Human Apolipoprotein A-IV in Apolipoprotein E–Deficient Mice. Arteriosclerosis, thrombosis, and vascular biology. 2001;21(6):1023-8.
607. Wang F, Kohan AB, Kindel TL, Corbin KL, Nunemaker CS, Obici S, et al. Apolipoprotein A-IV improves glucose homeostasis by enhancing insulin secretion. Proceedings of the National Academy of Sciences. 2012;109(24):9641.
608. Park SW, Lee EH, Lee EJ, Kim HJ, Bae DJ, Han S, et al. Apolipoprotein A1 potentiates lipoxin A4 synthesis and recovery of allergen-induced disrupted tight junctions in the airway epithelium. Clinical and experimental allergy : journal of the British Society for Allergy and Clinical Immunology. 2013;43(8):914-27.
609. Tomazic PV, Birner-Gruenberger R, Leitner A, Darnhofer B, Spoerk S, Lang-Loidolt D. Apolipoproteins have a potential role in nasal mucus of allergic rhinitis patients: a proteomic study. The Laryngoscope. 2015;125(3):E91-6.
610. Logdberg L, Wester L. Immunocalins: a lipocalin subfamily that modulates immune and inflammatory responses. Biochim Biophys Acta. 2000;1482(1-2):284-97.
611. Vyssoulis GP, Tousoulis D, Antoniades C, Dimitrakopoulos S, Zervoudaki A, Stefanadis C. Alpha-1 microglobulin as a new inflammatory marker in newly diagnosed hypertensive patients. Am J Hypertens. 2007;20(9):1016-21.
612. Dickson KA, Haigis MC, Raines RT. Ribonuclease inhibitor: structure and function. Prog Nucleic Acid Res Mol Biol. 2005;80:349-74.
613. Yoshikawa K, Wang H, Jaen C, Haneoka M, Saito N, Nakamura J, et al. The human olfactory cleft mucus proteome and its age-related changes. Sci Rep. 2018;8(1):17170.

614. Mueller SK, Nocera AL, Dillon ST, Wu D, Libermann TA, Bleier BS. Highly multiplexed proteomic analysis reveals significant tissue and exosomal coagulation pathway derangement in chronic rhinosinusitis with nasal polyps. Int Forum Allergy Rhinol. 2018;8(12):1438-44.
615. Mueller SK, Nocera AL, Dillon ST, Gu X, Wendler O, Otu HH, et al. Noninvasive exosomal proteomic biosignatures, including cystatin SN, peroxiredoxin-5, and glycoprotein VI, accurately predict chronic rhinosinusitis with nasal polyps. Int Forum Allergy Rhinol. 2019;9(2):177-86.
616. Candia J, Cheung F, Kotliarov Y, Fantoni G, Sellers B, Griesman T, et al. Assessment of Variability in the SOMAscan Assay. Sci Rep. 2017;7(1):14248.
617. Mackenzie KD, Lim Y, Duffield MD, Chataway T, Zhou XF, Keating DJ. Huntingtin-associated protein-1 (HAP1) regulates endocytosis and interacts with multiple trafficking-related proteins. Cell Signal. 2017;35:176-87.
618. Gudis D, Zhao K-q, Cohen NA. Acquired cilia dysfunction in chronic rhinosinusitis. American journal of rhinology & allergy. 2012;26(1):1-6.
619. Miller MD, Krangel MS. Biology and biochemistry of the chemokines: a family of chemotactic and inflammatory cytokines. Critical reviews in immunology. 1992;12(1-2):17-46.
620. Yu H, Huang X, Ma Y, Gao M, Wang O, Gao T, et al. Interleukin-8 regulates endothelial permeability by down-regulation of tight junction but not dependent on integrins induced focal adhesions. Int J Biol Sci. 2013;9(9):966-79.
621. Suzuki T, Yoshinaga N, Tanabe S. Interleukin-6 (IL-6) regulates claudin-2 expression and tight junction permeability in intestinal epithelium. The Journal of biological chemistry. 2011;286(36):31263-71.
622. Davies DE. Epithelial barrier function and immunity in asthma. Ann Am Thorac Soc. 2014;11 Suppl 5:S244-51.